

**MCR-CLICK SYNTHETIC STRATEGIES FOR THE
DEVELOPMENT OF PRIVILEGED SCAFFOLDS
BASED FLUORESCENT INHIBITORS AND
MULTI-FUNCTIONAL PEPTIDOMIMETICS**

*Thesis submitted to the University of Calicut in
Partial fulfillment of the requirements for the degree of*

**DOCTOR OF PHILOSOPHY
IN
CHEMISTRY**

By

JENCY MOHAN .T



**DEPARTMENT OF CHEMISTRY
UNIVERSITY OF CALICUT
KERALA
OCTOBER 2017**

DEPARTMENT OF CHEMISTRY
University of Calicut

Dr. D. Bahulayan
Professor

Calicut University campus,
Malappuram, Kerala,
Tel. (o) 0494 2401144*414
E-mail: bahulayan@yahoo.com

CERTIFICATE

This is to certify that this thesis entitled "*MCR-CLICK synthetic strategies for the development of privileged scaffolds based fluorescent inhibitors and multifunctional peptidomimetics*" submitted by Jency Mohan T. to the University of Calicut for the award of the degree of Doctor of Philosophy in Chemistry, is the result of the bonafide research work carried out at the Department of Chemistry, University of Calicut under my guidance and supervision. The contents of the thesis have been checked for plagiarism using the software 'Urkund' and the similarity index falls under permissible limit. I further certify that the topic discussed in this thesis has not been previously formed the basis of the award of any degree, diploma or associateship of any other University or Institute.

October 2017

D. Bahulayan

DEPARTMENT OF CHEMISTRY
University of Calicut

Dr. D. Bahulayan
Professor

Calicut University campus,
Malappuram, Kerala,
Tel. (o) 0494 2401144*414
E-mail: bahulayan@yahoo.com

CERTIFICATE

This is to certify that the corrections/suggestions from the adjudicators has been addressed and are incorporated in the appropriate sections of the revised thesis entitled "*MCR-CLICK synthetic strategies for the development of privileged scaffolds based fluorescent inhibitors and multifunctional peptidomimetics*" submitted by Jency Mohan. T to the University of Calicut for the award of the degree of Doctor of Philosophy in Chemistry.

October 2018

D. Bahulayan

DECLARATION

I, Jency Mohan T hereby declare that the thesis entitled “**MCR-CLICK SYNTHETIC STRATEGIES FOR THE DEVELOPMENT OF PRIVILEGED SCAFFOLDS BASED FLUORESCENT INHIBITORS AND MULTI-FUNCTIONAL PEPTIDOMIMETICS**” is the report of the original research work carried out by me under the supervision of Dr. D. Bahulayan, Professor, Department of Chemistry, University of Calicut for the award of the degree of Doctor of Philosophy in Chemistry of the University of Calicut and further that this thesis contains no material previously submitted for a degree, diploma, associateship, fellowship or other similar title of any other University or Society.

University of Calicut
October, 2017

Jency Mohan T

Acknowledgement

First of all, I thank "Almighty God" for being kind to me throughout this difficult journey and also for enabling me to finish this research work successfully.

This thesis could not have been completed without the generous support that I have received from so many people over these years, and I owe my gratitude to all of them.

I express my profound gratitude to my supervisor Dr.D. Bahulayan, Professor Department of chemistry, University of Calicut, for his inspiring guidance, constant encouragement and support and patience throughout the course of this study. Under your guidance, I successfully overcame many difficulties and learned a lot. Thank you for being a good mentor to me and I consider you as a blessing in my life.

I wish to express my sincere gratitude to the former Head of the department Prof. T. Ganga Devi, Prof. V.M. Abdul Mujeeb, Prof. K. Muraleedaran and the present Head of the Department Prof. P Raveendran for providing me the necessary facilities for the successful completion of this research work.

I extend my sincere gratitude to all my beloved teachers and other faculty members in the chemistry department.

I also extend my thanks to all the non-teaching staff, especially Mr. Krishnan Kutty T A, former section officer. Mohanan A, Librarian, and Mrs. Beena for their assistance in every possible way.

I also express my sincere thanks to Dr. Arun Kumar C, Dr. Lakshmi, faculty members, NIT Calicut for providing the necessary facilities to do fluorescence measurements.

I would also like to express my sincere thanks to my friends from other institutions such as Ms. Dijo Prasannan, Ms. Jiji A C, Ms. Anju R S and Ms. Anjali Jacob for their valuable support during the course of my research work.

I am also grateful to STIC Cochin University, IIT Madras, NIIST Trivandrum, and IISER Trivandrum for NMR analysis and Nanyang Technical University, Singapore for recording Mass spectra.

I am grateful to Dr. Vimala K, Women postdoctoral fellow, Periyar University for helping me to do anticancer studies.

I thank the research scholars Ms. Vijisha K, Mrs. Shameera for helping me do DFT studies.

I delightfully acknowledge my dear and respected senior research scholars Dr. Pramitha P, Dr. Biny Balan and Dr. Arun S from my research group for their genuine support for the completion of this research work.

I deeply extend my heartfelt gratitude to friends from my research group including Mr. Jithin Raj P, Mrs. Soumya T.V, Mr. Muhammad Ajmal C, Mrs. Rajeena Pathoor, Mrs. Thasnim P, Mr. Shyam Shankar E. P., Mr. Muhammad Salim, Mrs. Shamsiya A for making this journey a delightful , joyous and the most memorable one full of fun, parties, gatherings and chilling moments. I thank them for their constant help and absolutely genuine support in all professional and personal problems and being with me at my best and worst times. I thank them for understanding me and supporting me in all possible ways at all stages of the work.

It is also a pleasure to acknowledge the enthusiastic support and assistance given to me by all research scholars from our department and other departments.

I wish to express my sincere thanks to my friend Mr. Sivanandan C.K for his valuable friendship making each moment a memorable one, and for always being ready to help me.

I wish to express my sincere thanks to my family friends Mr. Shabeeb Marakkat, Mr. Upendran P, Mrs. Jeeja K and their family for the joyful gatherings and all their supports.

I would also like to thank my best friend Mr. Mithun Raj—we became friends in one of my more difficult times of my life. He always took time to listen to me whenever I wanted. He helped prevent me from slipping through the cracks- Thank you for being there as a great friend and a rock of support.

I also thank the Kerala State Govt. for supporting me financially with E-grants Scholarship as research fellowship.

Last but not the least, I wish to express my deep sense of gratitude to my parents: I have no words to express my gratitude to my brother and my sisters for their love, care and support.

Jency Mohan T.

This thesis is dedicated to the memory of my beloved Grand Mother Mrs. Parvathi Raman. I would not be who I am today without her love and support.

PREFACE

Privileged structure based design of molecular scaffolds have been widely used as an effective strategy in medicinal chemistry for drug discovery. It involves the introduction of diversity to a single bioactive core with suitable functionalities. Such functionalized scaffolds can provide ligands for diverse receptors and can be able to interact with unrelated and undruggable targets. Numerous heterocycles have been identified and reinvestigated as privileged scaffolds and their synthesis and applications in medicinal chemistry has been well documented. A lion share of such synthesis are based on multistep synthetic protocols with the involvement of large amount of resources, infrastructure and manpower and have a direct impact on the escalated prize of life saving medicines. Hence the investigations to develop an alternative to such costly synthesis is essential. Skilful use of step economic synthesis such as multicomponent coupling reactions (MCR) and close to natural synthetic methodologies such as click chemistry can contribute a lot to achieve this goal. Motivated with these ideas, two privileged heterocycles such as chromene and furan were selected for scaffold modification based on Click-with MCR methodology to obtain triazole linked peptidomimetics of these scaffolds and that constitutes the topic discussed in this thesis.

The thesis has been divided into five chapters. The first chapter presents an overview of the importance of privileged scaffolds in drug discovery and their biological and material applications with a special emphasis to benzopyrans and furans. Various aspects of these two

privileged structures has been summarized in this chapter, including the applications of new synthetic methodologies for their functionalization and the evaluation of biological properties.

The chapter 2 describes the chemistry and chemical biology of two new series of chromene peptidomimetics with carboxamide and acetamide peptide residues based on Click with MCR synthetic strategy. The fluorescence and anticancer properties of the molecules were evaluated and the molecules showed 2-in-1 properties such as anticancer activity as well as the fluorescence properties suitable for developing bioimaging probes.

Chapter 3 is on the peptidomimetic modifications of another benzopyran (chromene) system such as pyranocoumarin. The pyranocoumarin core scaffold was functionalised with chemical equivalents of α and β -amino acid residues such as α -aminoacylcarboxamide and β -acetamide scaffolds through a triazole linker. The highlight of this chapter is the detailed discussion on the photophysical and biological properties of 24 such new pyranocoumarin derivatives suitable for the development of fluorescent probes or anticancer agents.

Chapter 4 presents the progress of the work from linear peptidomimetics to macrocyclic peptidomimetics by replacing the chromene scaffold with a furan core scaffold using an intra molecular MCR-Click strategy. A discussion on the biological properties of the molecules as well as a brief rationale for the exceptionally high Stokes shifted emission showed by the macrocycles were also presented.

Chapter 5 presents the conclusion and future aspects of the work presented in the thesis. As highlighted in chapters 2-4, this study have made significant advancement in the chemistry, chemical biology and photophysics of large number of chromene and furan peptidomimetics. However further in-depth study based on computational techniques and in vitro and in vivo biological assay is necessary to push this field further ahead to achieve the goal of cost effective and green synthesis of therapeutic agents.

CONTENTS

	<i>Page No.</i>
Preface	i-iii
Chapter 1	1-36
Privileged scaffolds, Multicomponent reactions (MCRs), Click chemistry and Peptidomimetics: a perspective on their medicinal chemistry aspects.	
1.1: Privileged scaffolds	1
1.1.1: Sulfur-Nitrogen heterocycles in general as privileged scaffolds.	2
1.1.2: Quinolines as privileged scaffolds	4
1.1.3: Isoquinoline as privileged scaffolds	5
1.1.4: Rhodanine as privileged scaffolds	6
1.2. Oxygen heterocycles as privileged scaffolds	8
1.2.1. Coumarin	8
1.2.2. Benzopyran or chromene as privileged scaffold	9
1.2.3. Chromenes in material applications	17
1.3 Peptidomimetics as privileged scaffolds: General aspects and synthetic methodologies	18
1.4 Privileged scaffolds based peptidomimetics from multicomponent reactions	22
1.5. 1,2,3-Triazole as a privileged scaffold: The applications of click chemistry in privileged scaffold based drug discovery.	26
1.5.1 .Triazole functionalized Macrocycles as privileged scaffolds	29
1.6 1, 2, 3-Triazoles as privileged scaffolds in linear peptidomimetics	31
1.7 Furan as privileged scaffold	31
References	37

Chapter 2	45-133
Design and synthesis of 1, 2, 3-triazole linked privileged benzopyran based peptidomimetics as blue emitting fluorescent inhibitors	
2.1 Introduction	45
2.2 Result and Discussion	49
2.2.1 Synthesis of alkyne functionalized 2-Amino-3-cyano-4H-chromene scaffolds	50
2.2.2. Synthesis of α -acyl amino carboxamide azides 2.2a-d	51
2.2.3. Click chemistry of chromene alkynes 2.1a-c with α -acyl amino carboxamide azides 2.2a-d.	52
2.2.4. Regioselectivity of the triazole formation.	53
2.3. Photophysical properties of Type 1 peptidomimetics	55
2.4 Evaluation of drug property descriptors	57
2.5 Biological study: The in vitro anti-cancer activity evaluation	58
2.6 synthesis of type 2 peptidomimetics: β -amino acid motifs functionalized chrome peptidomimetics	61
2.7 Photophysical property evaluation	66
2.8 Evaluation of drug property descriptors	67
2.9 Biological study: The in vitro anti-cancer activity evaluation.	68
2.10 Conclusion:	70
2.11 Structural characterization	71
2.12. Experimental Section	89
References	102
Supplementary data	105

Chapter 3	134-172
Design, synthesis and anticancer activity of Pyranocoumarin peptidomimetic fluorophores	
3.1 Introduction	134
3.2 Result and discussion	136
3.2.1 Synthetic strategy pyranocoumarin peptidomimetics	137
3.3 Photophysical properties	142
3.4: Biological property evaluation	145
3.4.1: Evaluation of drug-likeness	145
3.4.2 The in vitro anti-cancer study against MCF-7 Cell lines	146
3.5. Structural characterization	150
3.6. Experimental section	159
References	170
Supplementary data	172
Chapter 4	188-219
Furan tagged Bifunctional Macrocyclic Peptidomimetic Fluorescent inhibitors via Sequential Multicomponent reaction and Click chemistry	
4.1 Introduction	188
4.2 Result and discussion	190
4.2.1. Synthesis of furan macrocycles	190
4.3 Photophysical properties	195
4.4 Biological studies	201
4.4.1 Primary drug property evaluation	201
4.4.2 Invitro anti cancer activity against MCF-7 cells	204
4.5 Structure identification	207
4.6 Experimental section	213
References	216
Supplementary data	218
Chapter 5	221-237
Conclusion and Future Perspectives	

Chapter 1

Privileged scaffolds, Multicomponent reactions (MCRs), Click chemistry and Peptidomimetics: A perspective on their medicinal chemistry aspects.

1.1. Privileged scaffolds	1
1.2. Oxygen heterocycles as privileged scaffolds	8
1.3 Peptidomimetics as privileged scaffolds: General aspects and synthetic methodologies	18
1.4 Privileged scaffolds based peptidomimetics from multicomponent reactions	22
1.5. 1,2,3-Triazole as a privileged scaffold: The applications of click chemistry in privileged scaffold based drug discovery.	26
1.6 1, 2, 3-Triazoles as privileged scaffolds in linear peptidomimetics	31
1.7 Furan as privileged scaffold	31

1.1 Privileged scaffolds

A rapidly emerging theme in drug discovery is the exploration of privileged scaffolds.¹ A privileged scaffold should consist of “a single molecular framework able to provide ligands for diverse receptors”. These molecules have an inherent capacity for biological activity and are capable of interacting with various proteinaceous receptors with high affinity.² The suitable modification of these scaffolds resulting in the formation of ligands for a number of functionally and structurally diverse biological receptors as agonist and antagonist.³ The term privileged scaffold is initially introduced by Evans et.al in the Merck research group in 1988 during the synthesis of benzodiazepines, a non-peptidal antagonist of cholecystokinin receptors.⁴ The benzodiazepines are proven as privileged scaffold because it is present in many drugs that have been used for decades for anticonvulsant, sedative, and anxiolytic purposes.⁵ The privileged benzodiazepine molecule structurally mimics the β -turn of the peptide.⁶ These scaffolds are capable of interacting with proteins having unknown three dimensional structures like G-protein coupled receptors, ion channels and can be able to interact with unrelated and undruggable targets.⁷

In chemical sense, privileged scaffolds have inherent capacity for flexibility and rigidity and also they are able to interact with various functional groups in a favorable arrangement. In biological sense it can be able to mimic a naturally existing molecule which has an inherent capacity to interact with different proteins.⁷ Many natural products are considered as privileged structures because they have high diversity and also have an inherent capacity to interact with a plethora of proteins

receptors.⁸This is the major reason for the half of commercial pharmaceuticals are either natural products or their synthetic analogues.⁹

Most of the privileged scaffolds commonly consist of a rigid heterocyclic ring with appended residues suitable for the bioactivity.¹⁰The compound libraries designed on the basis of privileged scaffolds should exhibit enhanced drug like properties and hence resulting in the generation of high quality lead molecules.¹¹ Several compounds such as nitrogen and sulfur containing heterocycles, biphenyls, diphenylmethane, 1,4-dihydropyridines, chromones, 2-benzoxazolones, indoles, benzimidazoles, benzofurans, quinoline, isoquinoline, purine, benzoxazole, benzopyran, coumarin, carbohydrate and steroids etc are identified as privileged scaffolds.¹²These scaffolds are used for building chemical libraries with relevant pharmaceutical applications.¹³This review will discuss some of the selected privileged scaffolds belonging to sulfur-nitrogen heterocycles and oxygen heterocycles with a special emphasis to medicinally active chromene scaffolds since the research work presented in the subsequent chapters of this thesis are mainly on the structural modifications of chrome scaffolds to obtain potential anticancer agents and multipurpose fluorescent probes.

1.1.1 Sulfur-Nitrogen heterocycles in general as privileged scaffolds.

Sulfur and nitrogen containing heterocycles occupies a prominent place among the various privileged scaffolds with biological activity.

Heteroaromatic rings have the ability to mimic the natural conformations of many of the peptide substrates with increased pharmacological or target binding activity with increased ADME (adsorption, distribution, metabolism and excretion) properties in a preferred biological environment.¹⁴ Consequently, >10% of the diverse ring systems present in drug molecules that are commercially available have six and five membered rings with nitrogen and sulfur as hetero atoms (fig.1 and fig.2).¹⁵

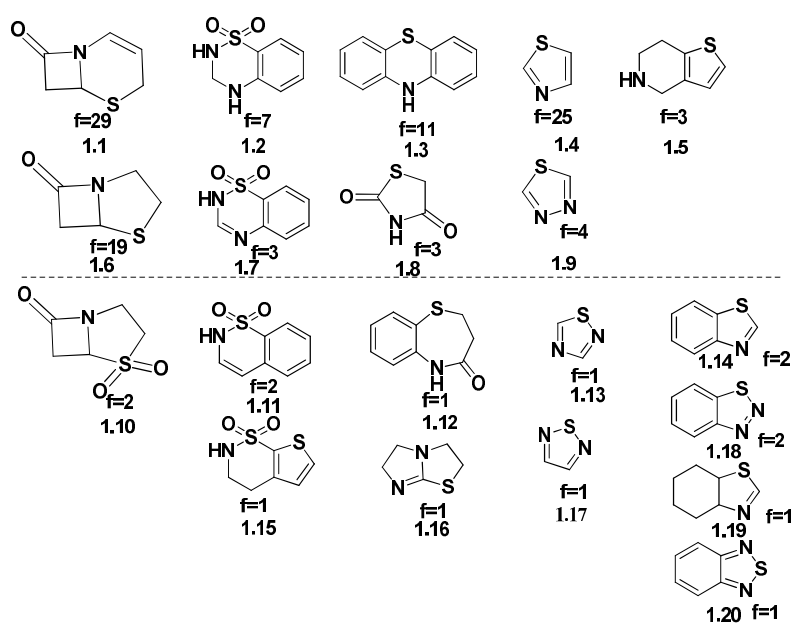


Fig. 1: Typical examples of sulfur-nitrogen heterocycles present in commercial drug molecules and their frequency (f).

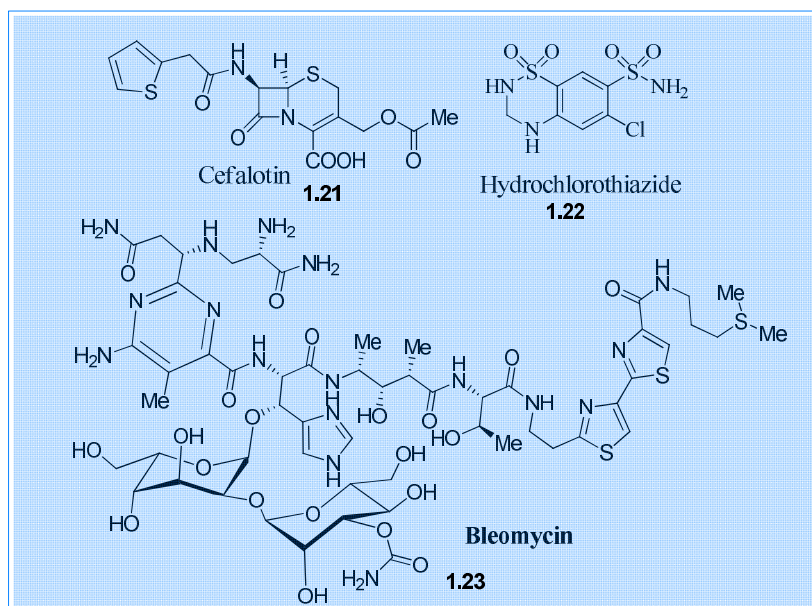


Fig.2: Typical examples of commercial drugs with sulfur-nitrogen heterocyclic ring systems as core bioactive component. Hydrochlorothiazide and bleomycin are included in WHO's list of essential medicines.

1.1.2: Quinolines as privileged scaffold

Quinoline is another frequently occurring privileged scaffolds in medicinally active natural molecules and synthetic drugs¹⁶ with biological profile such as antimalarial,¹⁷ antitubercular,¹⁸ antiviral,¹⁹ anti-inflammatory,²⁰ antibiotic,²¹ antifungal,²² antidepressant²³ and anti-cancer activities.²⁴ Selected examples of semi synthetic and synthetic quinolone based drugs are listed in fig. 3 and 4

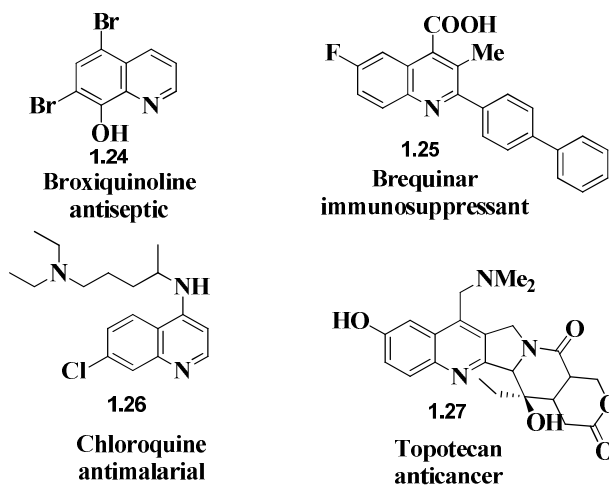


Fig.3: Selected examples of quinolone based semi synthetic drug molecules.

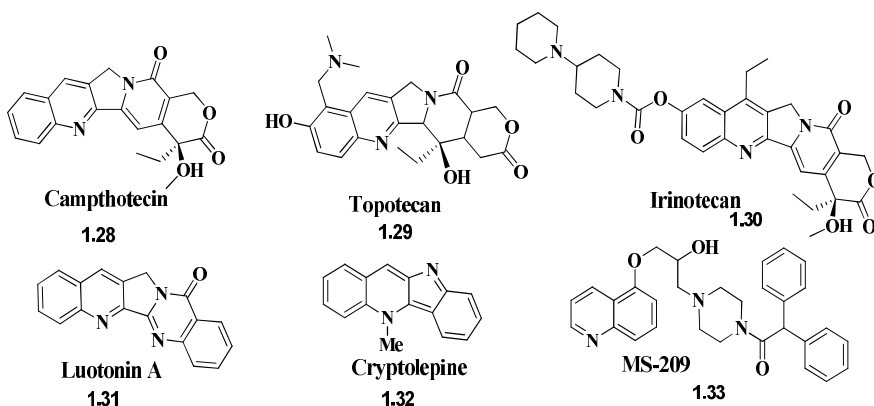


Fig. 4: Selected examples of quinolone based synthetic anticancer agents

1.1.3: Isoquinolines privileged scaffold

Isoquinoline represent another privileged core structure with expandable potential for drug candidates.²⁵ Although isoquinoline alkaloids are one of the best known alkaloids with proven therapeutic potential, currently, only few drugs or drug candidates have isoquinoline core because of the difficulties associated with the

modification of natural product bioactive components due to the occurrence of multiple stereo geniccenters present in them.²⁶ Careful literature survey reveals that isoquinolines have not yet fully exploited and a systematic effort would be necessary for bringing out more potential drug candidates with isoquinoline core structure. The best known isoquinoline drug candidates are listed in fig.5

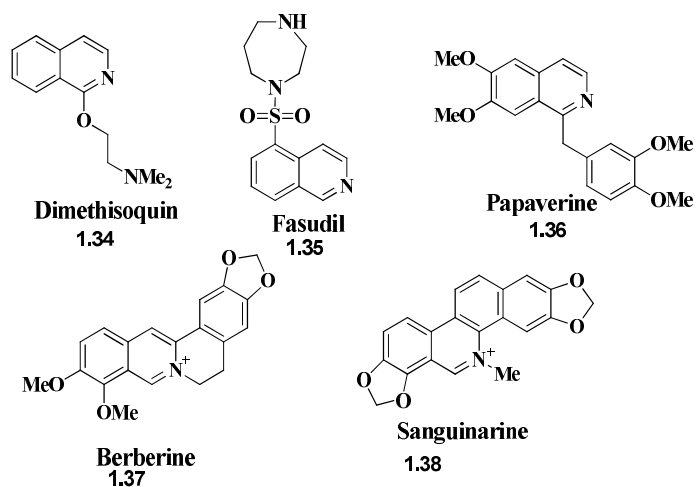
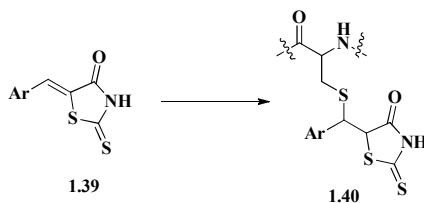


Fig.5: Selected examples of isoquinoline based drugs

1.1.4: Rhodanine as privileged scaffolds

Rhodanine is a five-membered heterocycle containing thioether and amino groups at positions 1 and 3, respectively. Large number of reports are available describing a wide variety of biological activities of rhodanine-based compounds.²⁷ The rhodanine ring is capable to interact with the amino acid residues in ligand binding sites of proteins via hydrogen bonding, hydrophobic interactions, π - π and cation- π interactions with amino acids with aromatic or charged side chains. The significant number of these spatially defined interactions of

rhodanine scaffolds are due to the marked propensity for the formation of polar interactions that can be attributed to the exocyclic double bonded sulphur and the carbonyl group. However, the exocyclic double bond, which is conjugated to the carbonyl group at position 4 of the rhodanine moiety, is a potentially reactive site. It can react as an electrophilic Michael acceptor, with nucleophilic amino acid side chains of the target proteins, such as cysteine with the reactive thiol group, to form a covalent adduct. Additive interaction of a reactive cysteine thiol group to the exocyclic double bond of 5-arylmethylidenerhodanines **1.39** is shown in scheme 1. Rhodanines are also capable to interact with intercellular metal ions for example, 5-benzylidenerhodanine, which is known to be specific towards Zn ions.²⁸ Consequently, large number of compounds possessing biological activity are reported. Selected examples of commercial rhodanines for cancer therapy are presented in fig.6.



Scheme 1: additive interaction of a cysteine thiol group to the exocyclic double bond of 5-arylmethylidenerhodanines

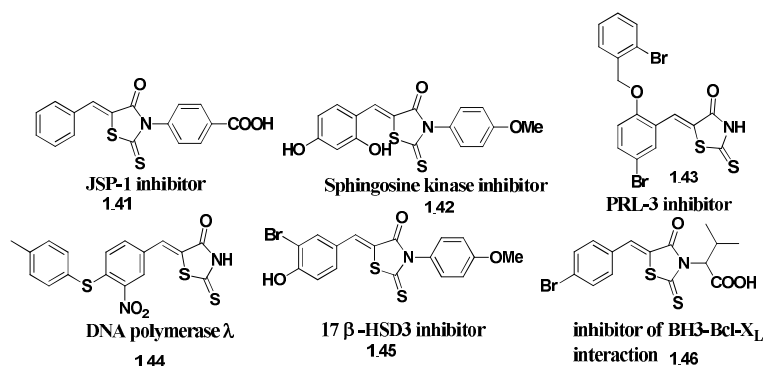


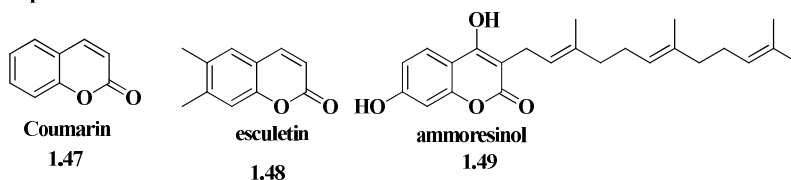
Fig.6: Selected examples of commercial anticancer drugs with rhodanine core scaffold

1.2. Oxygen heterocycles as privileged scaffolds

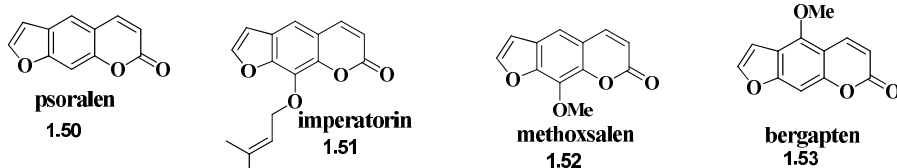
1.2.1. Coumarin

Coumarin constitutes a highly interesting privileged scaffold to access a broad variety of biologically active compounds.²⁹ There are mainly six types of coumarin scaffolds such as furanocoumarins, dihydrofuranocoumarins, linear type pyranocoumarins, angular type pyranocoumarins, phenyl coumarins, and biscoumarins.³⁰ All these are useful for deriving biologically active molecules or fluorescent probes.³¹ Selected examples are shown in fig.7.

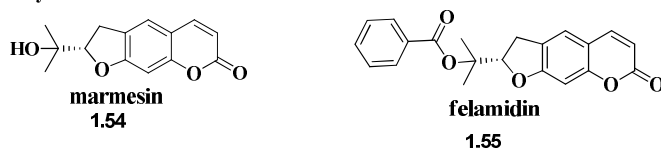
Simple Coumarins



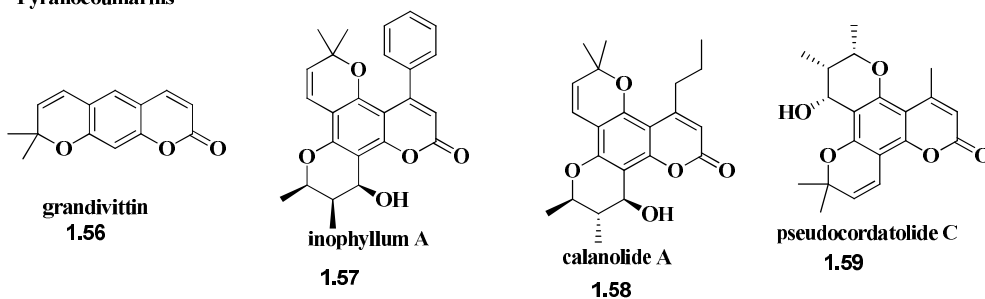
Furano coumarins



Dihydrofurano coumarins



Pyranocoumarins



Biscoumarins

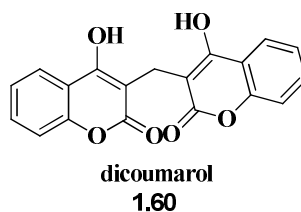


Fig.7: Selected examples of coumarin privileged scaffolds

1.2.2. Benzopyran or chromene as privileged scaffold

Among the various oxygen heterocyclic scaffolds, chromene or benzopyran was one of the privileged scaffolds widely distributed in biologically active natural and synthetic compounds and in a variety

ofknown inhibitors for a broad range of receptors. Chromene constitute the back bone of several naturally occurring alkaloids, flavonoids, anthocyanins and tocopherols.³² Chromene is a bicyclic molecule in which benzene is fused to a pyran ring. Based on the position of double bond in pyran ring chromene is divided into 2H-chromene or 2H-1-benzopyran and 4H-chromene or 4H-1-benzopyranas shown in figure 8. In addition to this, the chromene containing double bonded oxygen in the second position known as oxochromenesare widely distributed in nature and shows potent biological and pharmacological applications.

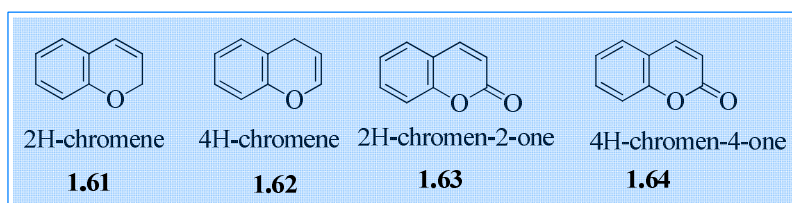


Fig.8: general structure of 2H-chromene, 4H-chromene and its oxochromene

Futher, several fused chromenes are isolated from various plant sources such as furochromenes, bezofurochromenes, pyranochromenes, benzochromenes and naphthochromenes.³³ Some of these compounds are now used as potent drugs against various diseases and more are in clinical trials. Naturally occurring chromene scaffolds possess huge skeletal diversity through the conjunction of the privileged benzopyran motif in their core which allows discrete biological activities such as anti-microbial,antibacterial,cytotoxic, antioxidant,anti-HIV, and antivascular,antiviraland anti-proliferativeactivity against various carcinoma cells.³⁴ The low

toxicity, good lipophilicity and broad spectrum of pharmacological activities have inspired chemists to develop novel therapeutic agents and the generation of lead like or drug like molecules by using chromene as one of the core scaffold. A key feature is that the lipophilic nature of the benzopyran derivatives helps to cross the cell membrane easily.³⁵ Synthetic chromene analogues have been developed over the years, and some of them have been employed as pharmaceuticals fig.9.³⁶

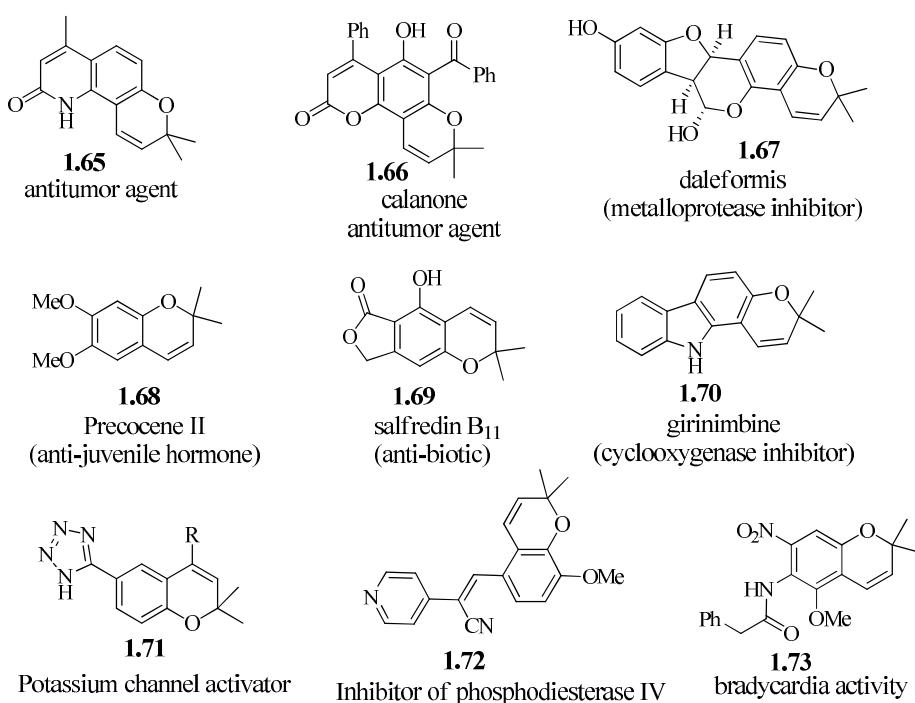


Fig.9: pharmaceutical agents containing benzopyran structural moiety³⁸

Cromakalim 1.75 is the first reported benzopyran derived antihypertensive agent act solely via potassium channel modulation.

The diverse synthetic analogues of cromakalim were reported subsequently as shown in fig.10.³⁷

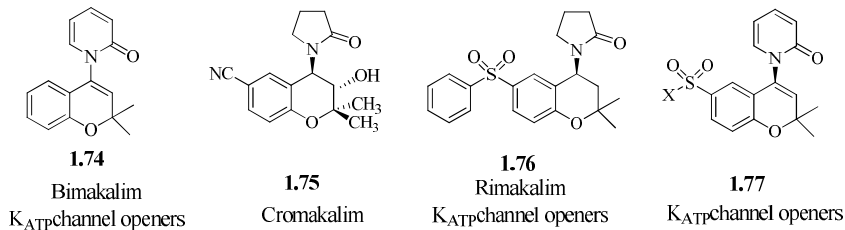


Fig.10: anti-hypertensive cromakalim and its analogues.

Chromene based small molecular agents are also used for developing various chemotherapeutics.³⁸ Chromene also showed excellent cytotoxic activity against various human cancer cell lines through various mechanism such as microtubule depolymerization, apoptotic cell death etc. Crolibulin, EPC 2407 (1.79) is a 4-aryl-4H-chromene derivative under phase I/II clinical trials for the treatment of anaplastic thyroid cancer with acceptable side effect profile.³⁹ Similarly several analogues of 4-aryl or 4-heteroaryl 4H-chromene derivatives show potent activity against various cancer cell lines.⁴⁰ The structures of some pharmacologically active chromene based anticancer agents are summarized in the fig.11.

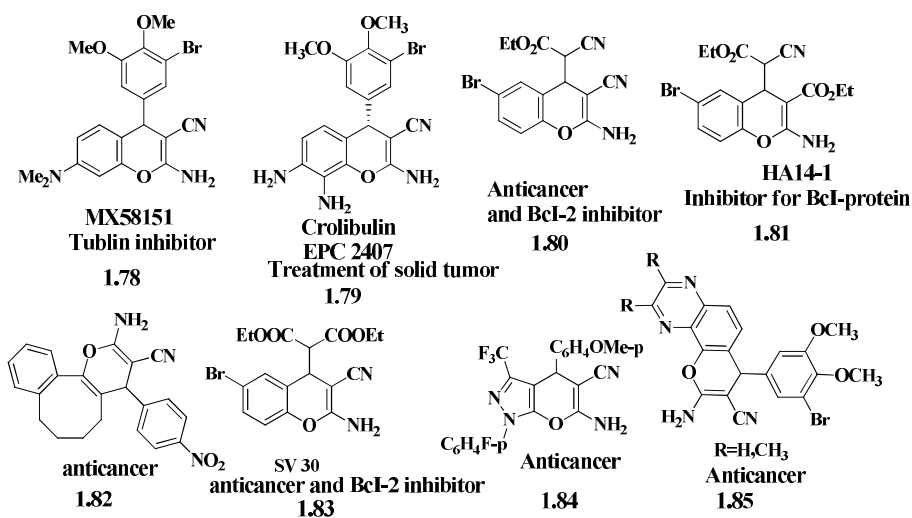


Fig.11:some bioactive anti-cancer chromene analogues⁴⁵

Multidrug resistance, the principal mechanism by which many cancers develop resistance to chemotherapy drugs. It is a major factor in the failure of many forms of chemotherapy.⁴¹ This can affect the persons with different types of cancers such as blood cancer, solid tumours, breast, lungs, ovarian and colonic cancers. Recent studies identified that benzopyran derivatives are potent modulators of multidrug resistance in cancer acting via various mechanisms.⁴² The representative examples are shown in fig.12.

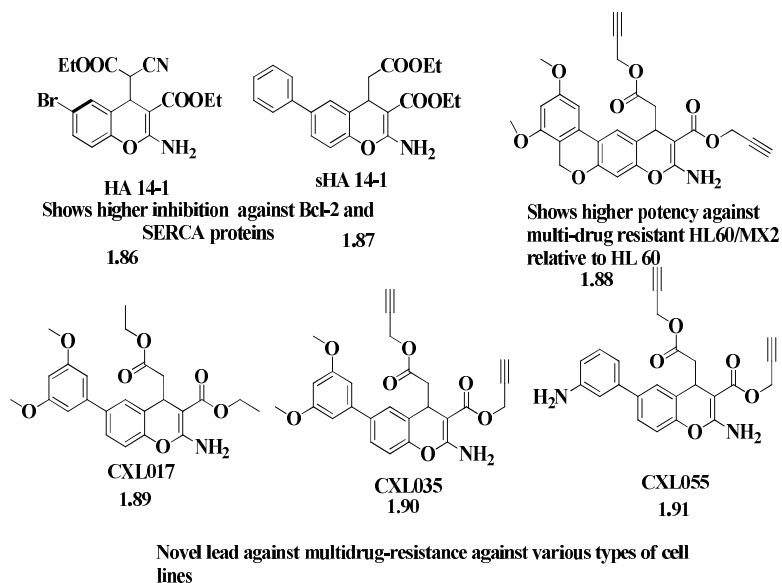
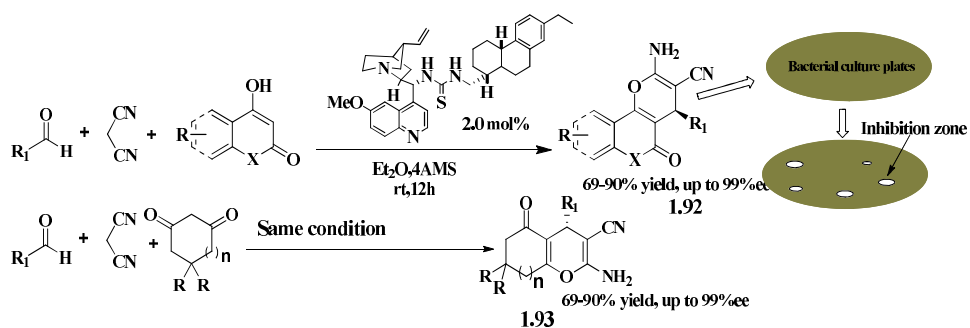


Fig.12: recently reported lead compounds for multi-drug resistance in cancer therapy

Several natural and synthetic chromene scaffolds are active against the microorganisms like bacteria, fungi etc. Zhang et.al reported the Enantioselective synthesis of pyranocoumarin **1.92** and 2-Amino-4H-chromene **1.93** with potential antibacterial activity against *S. aureus* with a minimum inhibitory concentration 6.25 $\mu\text{g/mL}$ as shown in scheme 2.⁴³



Scheme 2: Enantioselective asymmetric organocatalytic synthesis of chromene scaffolds

The search for antibacterial and antimicrobial agents are still very important due to the presence of drug resistance bacterial infections. Chromene derivatives show potent antibacterial or antimicrobial activity against Gram positive *Staphylococcus aureus*, MRSA, *Bacillus subtilis* and *Micrococcus luteus* and gram negative *Escherichia coli* *Pseudomonas aeruginosa* bacterial stains. They show moderate activity when compared to Streptomycin and Ampicillin. Calanolide A and B were the first natural chromene extracted from the leaves of plant *Calophyllum lanigerum* identified to show anti-HIV activity. Some other active antiviral agents are shown in fig. 13.⁴⁴

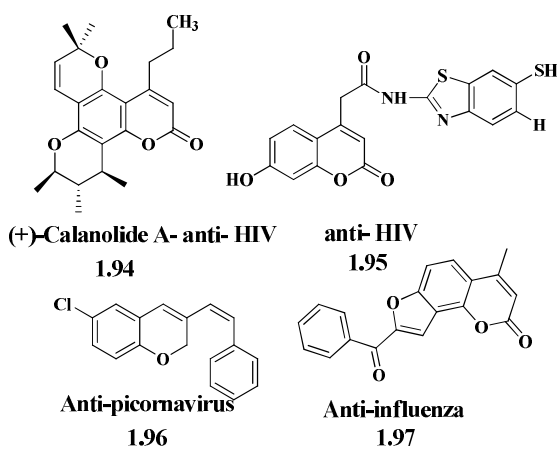


Fig.13: chromene based antiviral agents

Alzheimer's disease is one of the main reasons for dementia in older persons. This neurodegenerative disease is characterized by the gradual loss of the normal cognitive and non-cognitive functions of the body. The factors causing this disease include cholinergic system disorders, accelerated aggregation of β -amyloid peptides, and the dysregulation of metals etc. It was reported that the main reason for Alzheimer's

disease is the cholinergic dysfunction and AD severity provided a rationale for the therapeutic use of acetylcholinesterase inhibitors. There for the recent pharmacological treatment of Alzheimer's disease is based on the use of acetylcholine esterase inhibitors. Taspine, a chromene containing alkaloid extracted from the leaves of *Mangnolia x soulangiana* identified as a potent Acetylcholy inhibitor. Similarly several naturally occurring chromene derivatives are proved to have acetyl choline and butyryl choline inhibitory activities.⁴⁵

Synthetic chromene derivatives are effective Acetylcholy inhibitors compared to the commercial drugs Dopamine, rivastigmine etc. and therefore widely used for the treatment of Alzheimer's disease and Schizophrenia. A novel series of 1,2,3-triazole-chromene hybrid scaffold showed mild to improved AChE inhibitory activity compared to, other drug used for the treatment of dementia due to Alzheimer's and Parkinson's disease.⁴⁶

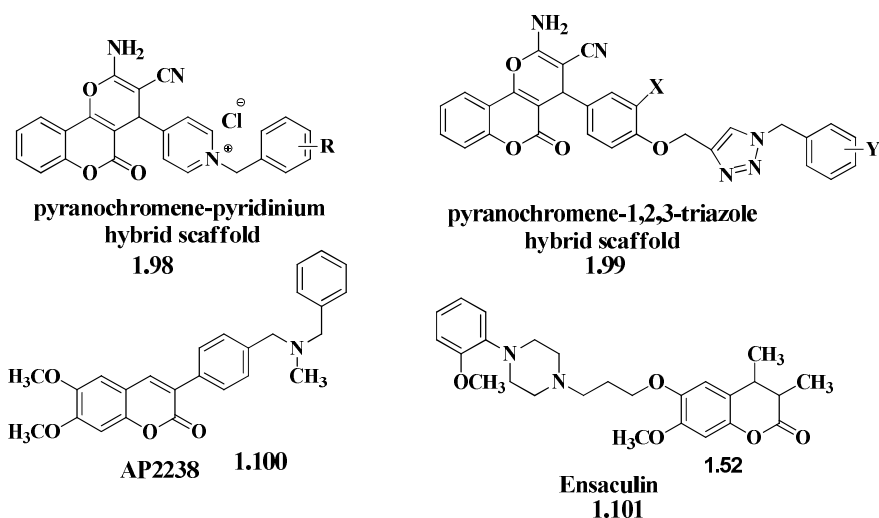


Fig.14: Chromene-heterocycle hybrid scaffold as anti-Alzheimer's agent.

1.2.3. Chromenes in material applications

In addition to the wide range of biological and pharmacological applications molecule having chromene core structures find applications in pigments, cosmetics, agrochemicals, laser dyes, optical brighteners and fluorescence markers. Due to the excellent photochromic properties it find applications in optical transmission materials, optical switches, light modulators, organic light emitting diodes (OLEDs) and memory devices. Pyran or chromenecontaining compounds have been used as a red fluorescent material for the emissive layer of OLEDs. Yoon et al. have reported two series of di-*tert*-butyl chromene-containing red fluorescent materials suitable for OLEDs (fig. 15).⁴⁷

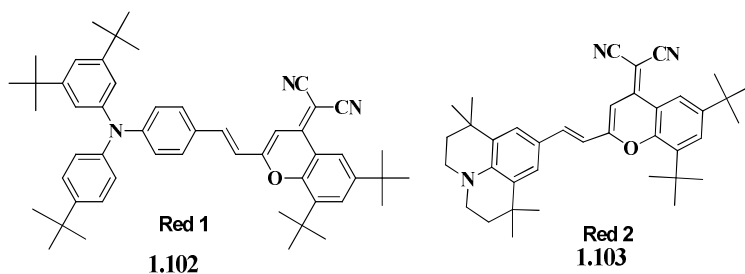
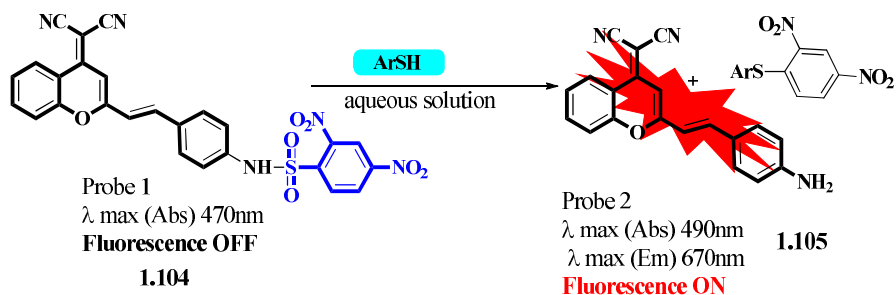


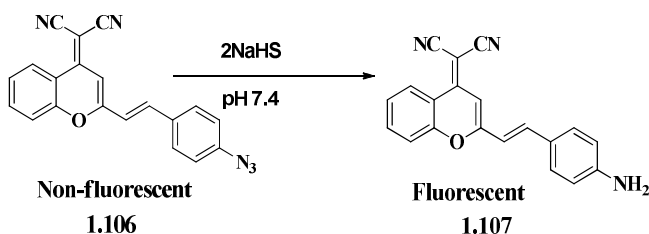
Fig.15: red emitting chromene emissive layer of OLEDs

Chromene scaffolds act as a rapid, selective and sensitive fluorescent probe for the detection of thiols, hydrogen sulfide etc. in the living cells. Feng et al. developed a conjugated dicyanomethylene-benzopyran molecule near IR (NIR) fluorescent probe for the detection of thiophenols in living cells. Similarly 2, 4-dinitrobenzene-1-sulfonamide used as the reaction site for the turn-on fluorescence detection of thiols as shown in scheme 3.⁴⁸



Scheme 3: On and off fluorescent detection of thiols using chromene scaffold

Similarly, a dicyanomethylene-4H-chromene-derived fluorescent probe was reported for detecting hydrogen sulfide based on the reduction of azide with H_2S to amine compound⁴⁹ as shown in scheme 4.



Scheme 4: On and off fluorescent detection of thiols using chromene scaffold

1.3 Peptidomimetics as privileged scaffolds: General aspects and synthetic methodologies

Peptides and proteins are absolutely essential components of organisms in many ways. Peptides play an important role in organisms as hormones, neurotransmitters and neuromodulators.⁵⁰ Peptides and their analogues have long been used in medicinal chemistry as therapeutic agents for pathological conditions generally characterized by a disruption of the interplay between messenger molecules or enzyme substrates and their targets.⁵¹ For various biochemical and

biophysical reasons there is an increasing tendency towards the use of peptidomimetics because such agents generally increase the magnitude of the deceptive effect in proportion to the degree of conversion of a peptide into a nonpeptide.⁵² The concept of rational design has been applied frequently to the development of peptidomimetics with the aid of new computer programs in such design processes. The new developments in peptidomimetics have given a great boost to peptide chemistry as a whole and this trend will be expected to continue with the incorporation of privileged scaffolds to peptidomimetic backbones to increase the selective biological activity of such inhibitors in many fold.⁵³

During the past few decades' great effort has been made to develop more efficient methods for synthesis of linear and cyclic peptidomimetics, as potential drug leads.⁵⁴ The general approach for the development of peptidomimetics is the modification of an existing peptide sequence without altering the biological activity.⁵⁵ Several straight forward synthetic strategies have been introduced for the synthesis of peptidomimetics from the readily and commercially available reagents.⁵⁶ For e.g. asymmetric synthesis using amino acids and sugar derivatives, solid-phase synthesis of peptidomimetics from non-peptide libraries, combinatorial synthesis etc. In the classical combinatorial approach, libraries of synthesized peptidomimetics are reported as modified peptides taking the advantage of chemical diversity of the amino acids and the sequence diversity.⁵⁷

In expanding the molecular diversity along with the improvement in biological and physico chemical properties of the compound libraries

Schreiber and coworkers introduced the concept of diversity-oriented synthesis (DOS) in 2010.⁵⁸ The DOS strategy aims to populate the new chemical space with novel drug-like scaffolds with a high degree of molecular diversity and biological applicability.⁵⁹ The libraries generated based on DOS are helpful for the development of potential therapeutic agents based on the small molecules and therefore DOS emerged as an essential tool in drug discovery and chemical biology.⁶⁰ The screening of DOS libraries provides hits for several non-traditional undruggable targets and protein-protein interactions. In DOS the structurally diverse drug-like scaffolds are usually generated from a common intermediate as represented in the figure. These scaffolds on screening could be able to provide potential lead compounds with enhanced affinity towards targets.⁶¹

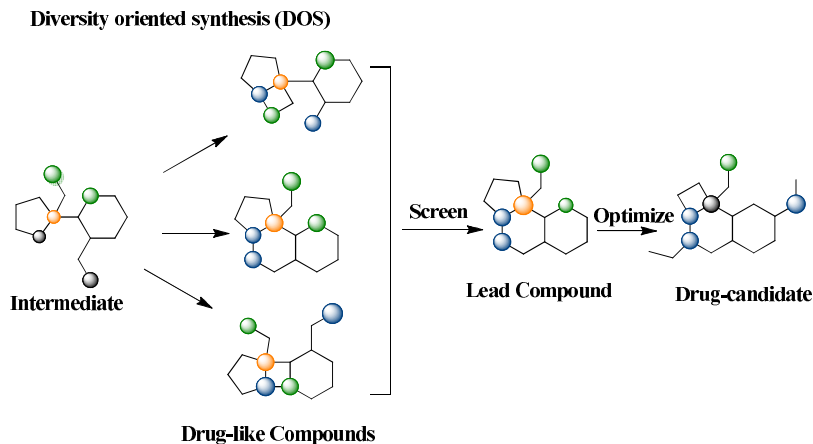
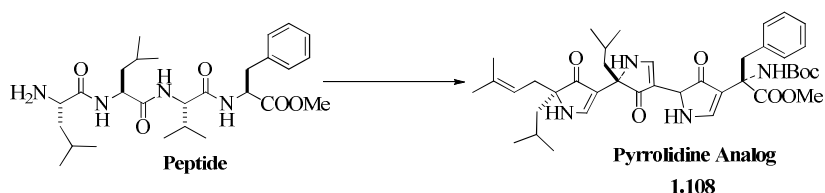


Fig. 16: DOS strategy to drug leads

To achieve privileged scaffold based peptidomimetics with suitable molecular diversity especially skeletal diversity, two distinct diversity oriented strategies such as reagent based approaches and substrate

based approaches were reported.⁶² Both approaches involves multiple stepwise reaction sequences for introducing diversity. These traditional multi step synthetic schemes are time consuming, requires more time and often expensive.



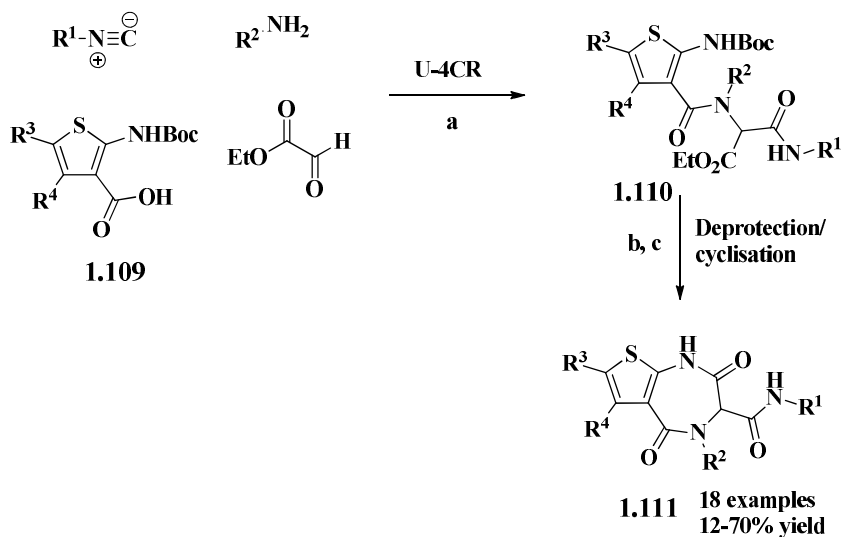
Scheme 5: Synthesis of pyrrolidine (privileged scaffold) based Peptidomimetic from parent peptide⁶³

The most promising method for the economic and green generation of collection of drug-like small molecules by diversity oriented synthesis include the sequencing of the multicomponent reaction followed by post modification methods for achieving complexity and diversity.⁶⁴ The post modification methods include cyclization, refunctionalizations etc. This advanced synthetic methodology is known as Build/Couple/Pair strategy.⁶⁵ In the initial build stage the core chiral building blocks were synthesized. In the couple phase these chiral building blocks were coupled together to obtain skeletally diverse scaffolds. In this phase, multicomponent reactions can be used to produce skeletally diverse core scaffolds. The pair phase involves intra or inter molecular reactions between the typical functional group present in the core scaffolds obtained in the couple phase.

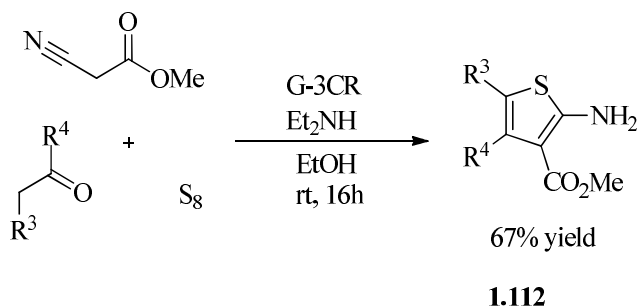
1.4 Privileged scaffolds based peptidomimetics from multicomponent reactions

Multicomponent reactions (MCRs) are considered as an advanced synthetic strategy for the step-economic and cost effective synthesis of potential scaffolds suitable to populate the large drug-like chemical space.⁶⁶ It helps to overcome the problems associated with the classical linear multi-step reactions and helps to provide a straight forward method for the synthesis of bioactive heterocycles, natural product-like molecules etc. Therefore, recently MCRs emerged as highly valuable tool in the drug discovery.⁶⁶ Multicomponent reactions are familiar to synthetic chemists for over 150 years. The first documented reaction in this category is the Strecker synthesis of α -aminonitriles (1850) by the condensation of an aldehyde, ammonia and hydrogen cyanide.⁶⁷ Subsequently, many MCRs were reported for the synthesis of heterocyclic or non-heterocyclic scaffolds (privileged) for e.g. Hantzsch synthesis) of dihydropyrimidine as well as pyrroles,⁶⁸ The Biginelli reaction for the synthesis of 3, 4- dihydropyrimidin-2(1H)-ones,⁶⁹ Debus-Radziszewski of imidazoles,⁷⁰ Mannich reaction for β -amino carbonyl compounds,⁷¹ etc are another brilliant examples of MCR synthesis of privileged scaffolds. Followed by these synthesis, Isocyanide base Multicomponent reaction (IMCRs)⁷¹ such as Ugi reaction for the Synthesis of α -N-acylamino amides,⁷² Passerini reaction for the synthesis of α -acyloxy amides,⁷³ Van Leusen reaction,⁷⁴ Bucherer–Bergs for Synthesis of hydantoins and α -amino acids etc.⁷⁵ were emerged as classical examples of multicomponent synthesis of medicinally active scaffolds.

Isocyanide based multicomponent reactions (IMCRs) are particularly versatile for the synthesis of privileged scaffold based peptidomimetics with drug properties.⁷⁶ Domling et al. reported the synthesis and evaluation of 1,4-thienodiazepine-2,5-diones **1.108** (an interesting privileged scaffold) obtained by an Ugi-Deprotection-Cyclization (UDC) approach.⁷⁷ These compounds were evaluated as inhibitors of p53-MDM2 interaction.⁷⁸ The key step in this synthesis is an U-4CR as depicted in Scheme 6. Interestingly, the carboxylic acid input **1.110** is generated by another MCR known as the Gewald-3CR (G-3CR).⁷⁹ The reaction, depicted in Scheme 6, is a multicomponent reaction between an enolizable ketone or aldehyde, a cyanoacetate and elemental sulfur to obtain substituted aminothiophenes (privileged scaffold) **1.111** which after Boc-protection and saponification are used as input for the Ugi reaction (Scheme 7).

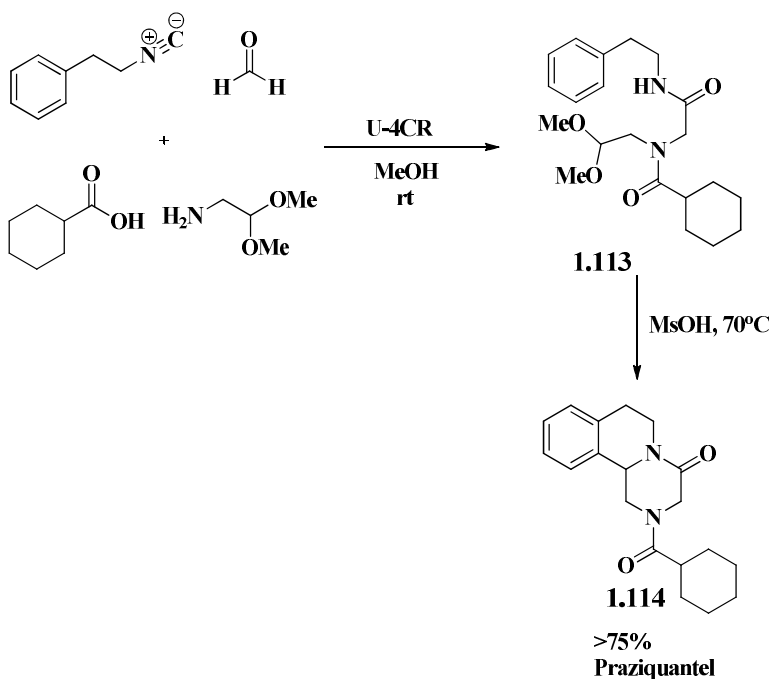


Scheme 6: Synthesis of 1,4-thienodiazepine-2,5-diones by UDC strategy; Reagents and conditions; (a) MeOH, rt, 2 days; (b) TFA, CH₂Cl₂, rt, 16 h and (c) TBD, Et₃N, THF, 40^o C, 16 h.



Scheme 7: G-3CR towards aminothiophene

Domling et al. also reported a very short multicomponent synthesis of praziquantel which is a privileged scaffold based commercial drug for the treatment of schistosomiasis by employing an Ugi reaction followed by Pictet–Spengler cyclization (Scheme 8) to give **1.114** in 75% overall yield.⁸⁰



Scheme 8: Synthesis of Praziquantel employing a U-4CR followed by a Pictet–Spengler cyclization.

Ross and co-workers showed that multicomponent reaction can be used to prepare already marketed therapeutic compounds quite simply.⁸¹ They showed two examples of this concept by preparing clopidogrel (Plavix) **1.115** and bicalutamide (Casodex) **1.116** using MCR chemistry (Fig. 17). Both these synthesis served as brilliant examples of the application of MCRs in privileged scaffold based drug discovery.

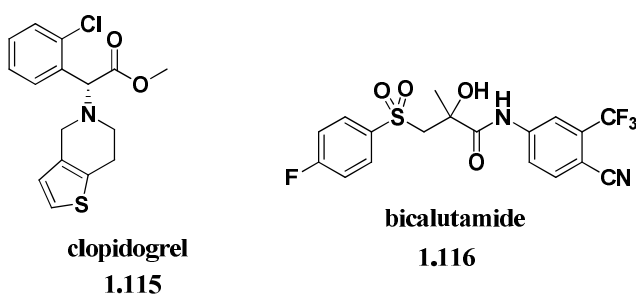
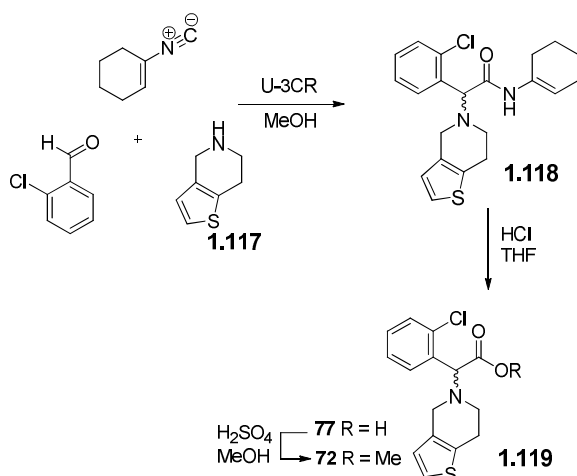


Fig. 17: Structures of clopidogrel (Plavix[®]) and bicalutamide (Casodex[®]).

Ross et al. also reported the synthesis of racemic clopidogrel in 3 steps from commercially available starting materials employing U-3CR as the key step (Scheme 9). After acidic hydrolysis of the enamide and subsequent methyl ester formation, rac-clopidogrel **1.118** is obtained in 73% yield (3 steps).⁸²



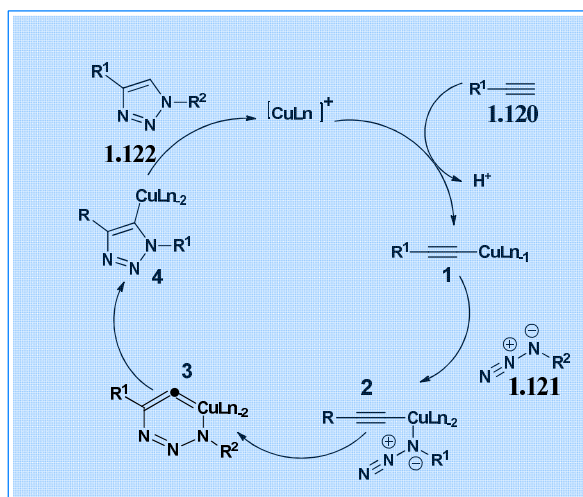
Scheme 9: Synthesis of rac-clopidogrel.

1.5. 1,2,3-Triazole as a privileged scaffold: The applications of click chemistry in privileged scaffold based drug discovery.

Among the various methods that has been used for the identification of new privileged scaffold based therapeutics, fragment-based assembly is versatile and enables the high-throughput identification of small molecule inhibitors using a minimal number of building blocks.⁸³ It typically involves a two-step process including fragment identification and fragment assembly. This approach is powerful especially against protein targets that possess multiple binding pockets in their active sites, and for targets for which structural information is lacking for the rational design of protein ligands.⁸⁴ Among different methods proposed to assemble the fragments, ‘click chemistry’, pioneered by Sharpless *et al.* is highly versatile for the near perfect assembly of structural scaffolds for generating new chemical entities for drug discovery and for multipurpose materials development.⁸⁵

Click reactions as defined by Sharpless is “those reactions which are modular, wide in scope, high yielding, create only inoffensive by-

products (that can be removed without chromatography), are stereospecific, simple to perform and that require benign or easily removable solvent".⁸⁵ A handful of such reactions are now available for chemists use and among them, the Huisgen 1,3-dipolar cycloaddition of alkynes and azides, also called Cu-catalysed azide-alkyne (CuAAC) cycloaddition to form a 1,2,3-triazoles in-between the reacting partners is the most versatile one for fragment assembly.⁸⁶ This reaction often proceeds under mild conditions with high yield and allows achieving complete regioselectivity towards the 1,4-disubstituted adduct without the involvement of any purification efforts. The mechanism of the CuAAC reaction involves the formation of a copper acetylide, **1** followed by the azide binding to the copper through the displacement of another ligand **2**. Subsequently, a six-membered copper (III) metallacycle **3** followed by the ring contraction to a triazolyl-copper derivative **4** will be formed and **4** undergoes protonolysis to afford the triazole derivative as shown in the scheme 10.



Scheme 10: Typical CuAAC reaction

An important feature of the triazole ring is its intrinsic capability to act as a peptidomimetic scaffold.⁸⁷ Triazole ring is considered as a good non-classical bioisostere of the peptidic bond bearing an improved stability in biological systems. The triazole ring is planar and displays similar electronic content and dipole moment as the amide bond. It possesses an analogous hydrogen-bonding profile, too, with the C2 atom acting as a hydrogen-bond donor, and nitrogen atoms at 4 and 5 positions as hydrogen-bonding acceptors with their lone pairs, in the same way to the nitrogen and oxygen atoms of the amide bond, respectively.⁸⁸

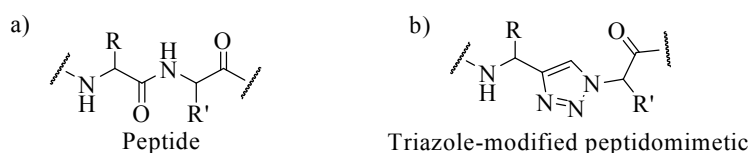
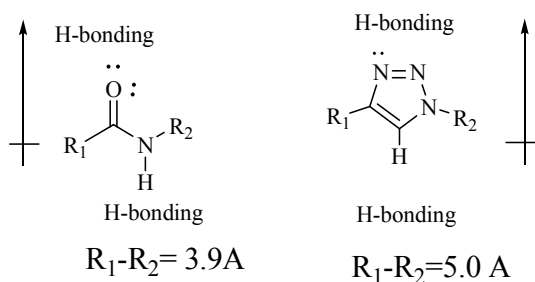


Fig. 18: General structures of a) a peptide and b) a 1H-1,2,3-triazole-modified peptidomimetics



Scheme 11: amide-1,2,3-triazole isosterism

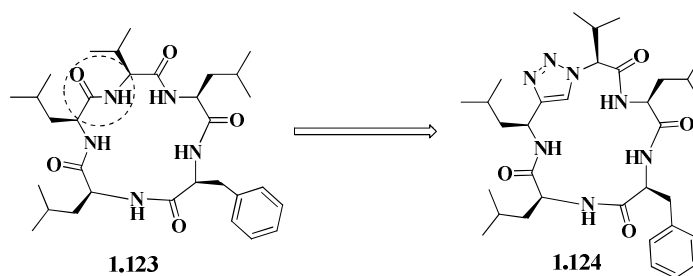
CuAAC has several attributes in peptidomimetic chemistry due to the following reasons. The 1,2,3-triazole ring itself is a privileged scaffold which is a likely candidate for small molecule drug and it is

compatible with the side-chains of all the amino acids, in the protected form. CuAAC is an orthogonal reaction and the triazole unit is resistant to enzymatic degradation, hydrolysis and oxidation, making it an attractive moiety to replace more labile linkers in biologically active compounds.⁸⁹ Thereby establish 1,2,3-triazole as an efficient pharmacophore and are not occurring in natural molecules, yet they are gifted numerous biological activities. Several reports demonstrated that CuAAC reaction can be used to generate potent biological active compounds via 1, 2, 3-triazoles ligation and the triazole unit can be used as surrogates for biologically relevant amide bonds.

1.5.1. Triazole functionalized Macrocycles as privileged scaffolds

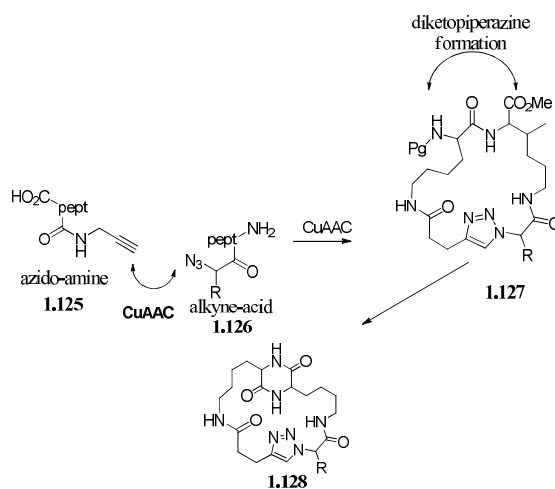
Macrocycles occupy a unique place in various chemical spaces.⁹⁰ These scaffolds are considered as privileged structures with the ring structures containing 12 or more atoms with a wide range of biological activities.⁹¹ Compared to linear scaffolds, macrocycles are conformationally restricted molecules with high affinity, selectivity bioavailability towards biological targets.⁹² Macrocyclic peptidomimetics are a subclass of macrocycles. Macrocycles are designed to mimic cyclic peptides or proteins to exhibit more desirable properties and improved pharmacokinetic and physicochemical properties.⁹³ Many synthetic methods are reported in literature for the synthesis of macrocycles such as macrolactomization, macrolactonization, transition metal catalyzed cross coupling reactions, ring closing metathesis etc.⁹⁴ Compared to these cyclization techniques, CuAAC reaction is unique for the efficient cyclization of peptide scaffolds in close to natural mode or for the triazole modification of a peptide macrocycle to the corresponding

peptidomimetic version with increased biological profile.⁹⁵ An example of such triazole modification is the synthesis of triazole containing Sansalvamide A, **1.123** a cyclic pentapeptide with potential anticancer activities. The replacement of the amide bond with 1,2,3-triazole improved the pharmacological activity compared to the parent peptide **1.124**.⁹⁶



Scheme 12: Sansalvamide A and its 1,2,3-triazole containing Macrocyclic peptidomimetic

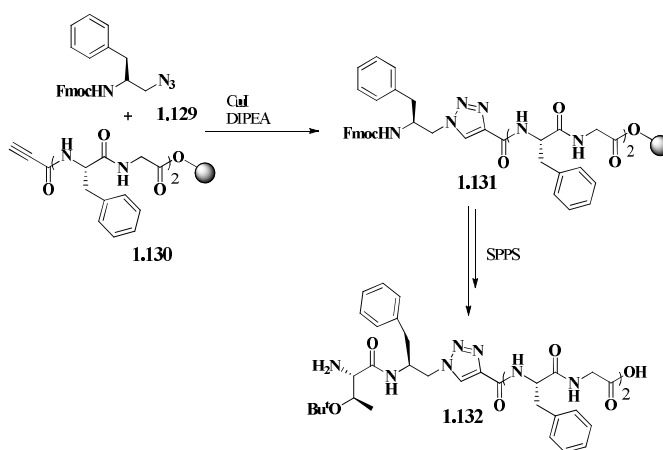
Another recently reported example of the use of CuAAC for the synthesis of macrocyclic peptidomimetics is the synthesis of foldamers, and the triazole ring has been applied as a peptide bond surrogate for folding of the molecule to obtain the cyclic structures as shown in scheme 13 given below.⁹⁷



Scheme 13: DOS approach to macrocyclic peptidomimetics via triazole and diketopiperazine Tethering.

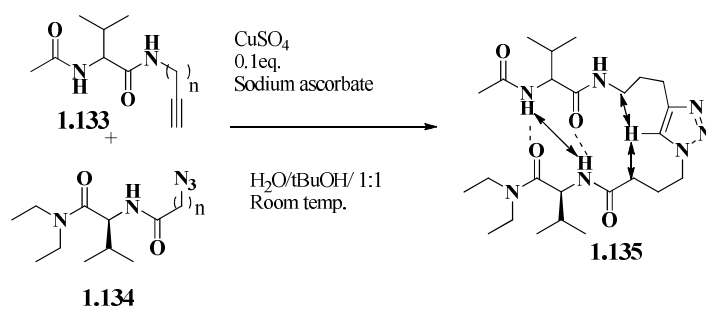
1.6 1, 2, 3-Triazoles as privileged scaffolds in linear peptidomimetics

Similar to macrocyclic peptidomimetics, several 1,2,3-triazole containing linear peptidomimetics were also reported. A pioneering example is the solid phase synthesis reported by Meldel group as shown in scheme 14 below.⁹⁸



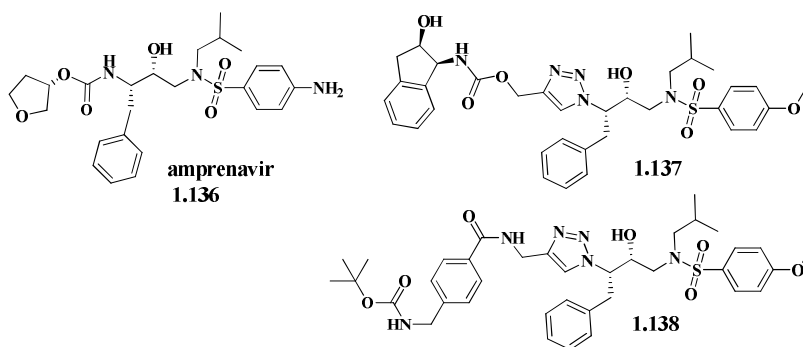
Scheme 14 : 1,2,3-triazole peptidomimetic first reported by Meldel group.

Similarly, 1,2,3-triazole peptidomimetic that mimic β -hairpin structure were synthesized by sharpless et.al via CuAAC by using insitu formation of Cu(I) from Cu (II) SO₄ and sodium ascorbate in a mixed solvent system containing water, tertiary butanol and DMSO as shown in scheme 15.⁹⁹



Scheme 15: 1,2,3-triazole peptidomimetic first reported by Sharples et al.

Another interesting example in this category is the triazole modification of the HIV I protease inhibitor amprenavir to obtain its more stable and bioactive version as shown in scheme 16 below.¹⁰⁰



Scheme 16: Synthesis of triazole modified amprenavir.

1.7 Furan as privileged scaffold

Furan is a five-membered oxygen heterocycle widely distributed in natural and synthetic products and also abundantly available plant secondary metabolites.¹⁰¹ Due to their wide range of biological and therapeutic applications furan is considered as privileged medicinal scaffold in drug discovery process.¹⁰² Furan derivatives exhibit excellent pharmacological activities such as antidepressant, anti-anxiolytic, anti-inflammatory, analgesic, antihypertensive, antiglaucoma, antimicrobial, anticancer activities.¹⁰³ The high therapeutic properties of the furan related drugs encouraged medicinal chemist to synthesize large number of novel chemotherapeutic agents. Furan moiety is an integral part of many drugs available in the market. Ranitidine (Zantac®, GSK) is a commercially available furan containing drug which act as Histamine H₂-receptor antagonist and lowers stomach acid levels and therefore used to treat stomach ulcers.¹⁰⁴ Nitrofurantoin is an antibiotic used in the treatment of urinary tract infections.¹⁰⁵ In addition to the biological properties furan incorporated molecules having conjugated double bonds and fused ring systems have been used in electronic devices such as semiconductors,¹⁰⁶ OLEDs,¹⁰⁷ dye sensitized solar cells (DSSC).¹⁰⁸

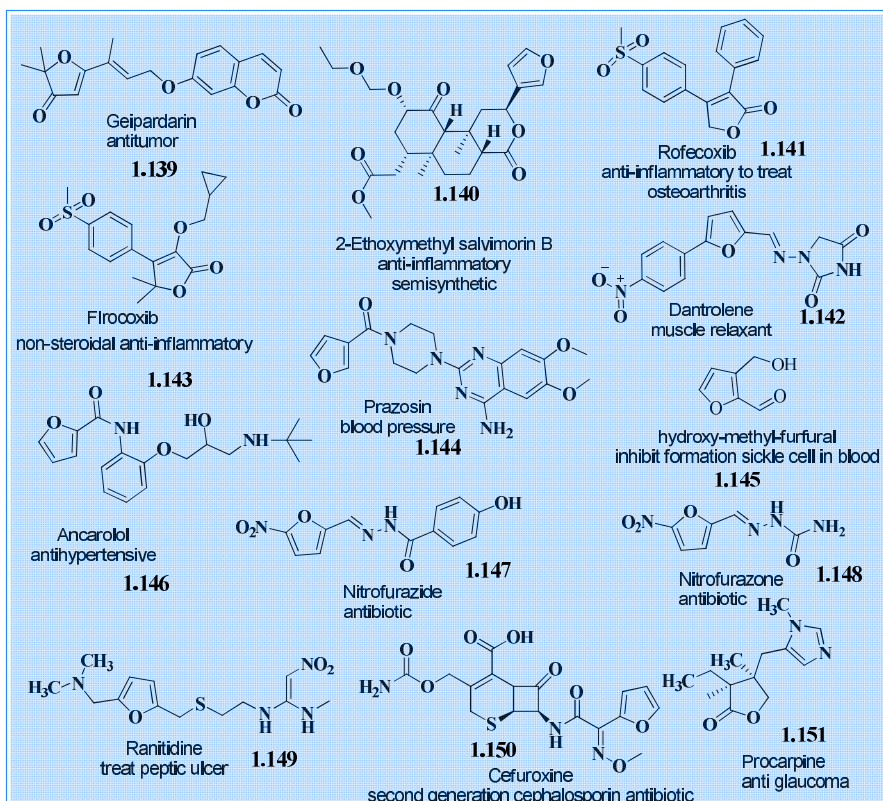


Fig.19: furan based drugs available in market.

Furan easily undergo oxidation under chemical and physiological conditions. The furan photo oxidation based click reactions is an important strategy in biological labelling. The incorporation of furan moiety into the biomolecules such as peptide, proteins and nucleic acids is an important method in site specific labelling. This site-specific chemical modification of proteins and nucleic acids is helpful to understand structure and interactions protein and nucleic acids and also it provides an insights into cellular events. The furan incorporated peptides and nucleic acids (for e.g DNA) can be subjected to direct oxidation reaction with N-Bromosuccinimide (NBS), air, light or photosensitizers in order to generate electrophiles. These reactive

intermediates can be intercepted by various nucleophiles to form stable conjugates.¹⁰⁹

The furan is also useful for peptide labelling through selective oxidation in aqueous solution to form stable conjugates. The incorporation of nucleophilic fluorophores through a cascade reaction sequence, leads to the efficient construction of site-selectively labeled fluorescent peptides. This reaction can be used for the site specific labeling of peptides and proteins and can be carried out in aqueous solution.

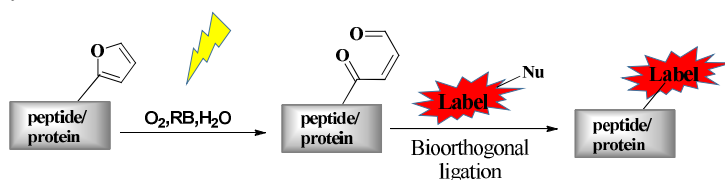


Fig.20: furan based peptide labelling

The furan tagged nucleic acid and a photosensitizer on visible light irradiation can crosslinks through the formation of covalent bond by the reaction of exocyclic amino functionalities at the corresponding position in the complementary strand. Both DNA as well as RNA targets can be covalently trapped in this way using furan-modified oligonucleotide probes.

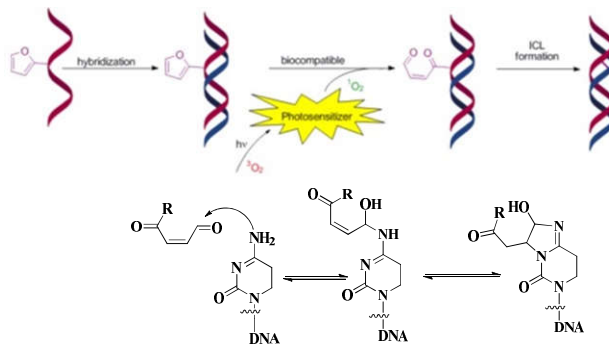
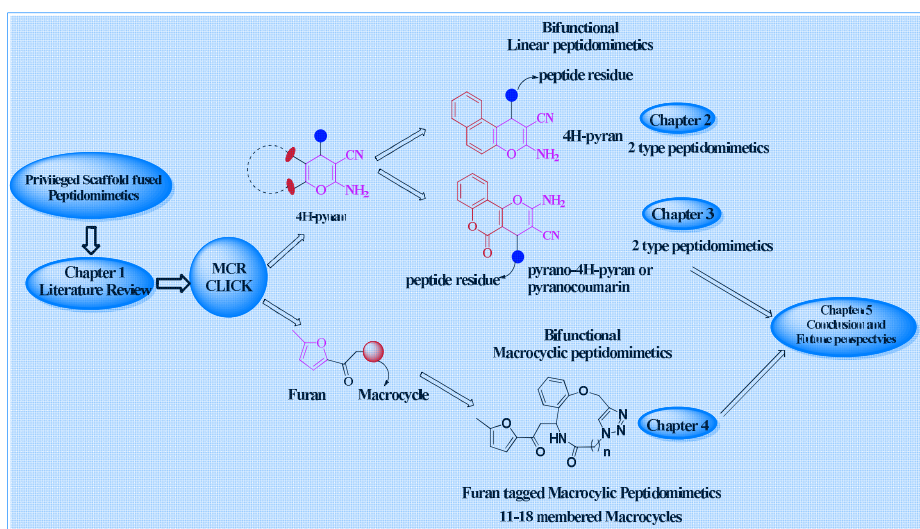


Fig.21: Furan mediated interstrand crosslinking in DNA

In conclusion, this introductory chapter provides a brief perspective about the emergence of the concept of privileged scaffolds in medicinal chemistry. Even though there are more than 100 linear, cyclic and heterocyclic entities are identified as privileged scaffolds, this review described only selected examples in brief with a special emphasis to chromene and 1,2,3-triazoles because the peptidomimetic modification of these two scaffolds are the theme of the research work presented in the coming chapters. More examples of privileged scaffolds and their functions in drug discovery process can be seen in the references listed at the end of this chapter. A schematic representation of the summary of the work presented in chapters 2-5 are shown in the scheme below



Scheme 17: Summary of the work

References

1. Horton, D.A.; Bourne, G.T.; Smythe, M.L. *Chem. Rev.* **2003**, 103, 3, 893-930.
2. (a) Evans, B.E.; Rittle, K.E.; Bock, M.G.; DiPardo, R. M.; Freidinger, R. M.; Whitter, W. L.; Lundell, G. F.; Veber, D. F.; Anderson, P. S.; Chang, R. S. L.; Lotti, V. J.; Cerino, D. J.; Chen, T. B.; Kling, P. J.; Kunkel, K. A.; Springer, J. P.; Hirshfield, J. *J. Med. Chem.* **1988**, 31, 12, 2235-2248. (b) Nicolaou, K. C.; Pfefferkorn, J. A.; Roecker, A. J.; Cao, G.Q.; Barluenga, S.; Mitchell, H. J. *J. Am. Chem. Soc.* **2000**, 122, 41, 9939-9953.
3. Bemis, G. W.; Murcko, M. A. *J. Med. Chem.* **1996**, 39, 15, 2887-2893.
4. Evans, B. E.; et al. *J. Med. Chem.* **1988**, 31, 12, 2235-2246.
5. (a) Patchett, A. A.; Nargund, R. P. *Annu. Rep. Med. Chem.* **2000**, 35, 289-298. (b) Marsters, J. C., McDowell, R. S.; Reynolds, M. E.; Oare, D.A.; Somers, T. C.; Stanley, M. S.; Rawson, T. E.; Struble, M. E.; Burdick, D. J.; Chan, K. S.; Duarte, C. M.; Paris, K. J.; Tom, J.Y. K.; Wan, D. T.; Xue, Y.; Bumier, J. P. *Bioorg. Med. Chem.* **1994**, 2, 9, 949-957.
6. (a) Blomberg, D., Hedenstrom, M., Kreye, P. et al. *J. Org. Chem.* **2004**, 69, 10, 3500-3508. (b) Blomberg, D., Kreye, P., Fowler, C. *Org. Biomol. Chem.* **2006**, 4, 3, 416-423.
7. Kamal, A.; Reddy, K. L.; Devaiah, V.; Shankaraiah, N.; Reddy, D. R. *Mini-Rev. Med. Chem.* **2006**, 6, 1, 53-69.
8. Balamurugan, R.; Dekkerab, F.J.; Waldmann, H.; *Mol. BioSyst.* **2005**, 1, 1, 36-45.
9. (a) Newman, D. J.; Cragg, G. M.; Snader, K. M. *J. Nat. Prod.* **2003**, 66, 7, 1022-1037. (b) Newman, D. J.; Cragg, G. M.; Snader, K. M. *Nat. Prod. Rep.* **2000**, 17, 215-234.
10. Welsch, M.E.; Snyder, S.A.; Stockwell, B.R. *Curr. Opin. Chem. Biol.* **2010**, 14, 3, 347-361.
11. (a) Mason, J. S.; Morize, I.; Menard, P. R.; Cheney, D. L.; Hulme, C.; Labaudiniere, R. F. *J. Med. Chem.* **1999**, 42, 17, 3251-3264. (b) Newman, D. J. *J. Med. Chem.* **2008**, 51, 9, 2589-2599.
12. Stefan Bräse, *Privileged Scaffolds in Medicinal Chemistry: Design, Synthesis, Evaluation*, RSC Drug Discovery, **2016**, The Royal Society of Chemistry, ISBN-13: 978-1782620303.

13. Douglas, A. H.; Gregory T. B.; Mark L. S. *Chem. Rev.* **2003**, 103,3, 893-930.
14. (a) DeSimone, R. W.; Currie, K. S.; Mitchell, S. A.; Darrow, J. W.; Pippin, D. A. *Comb. Chem. High Throughput Screening*, **2004**,7,5,473-494.(b) Dalvie, D.; Kang, P.; Loi, C.M.; Goulet, L.; Nair, S. *Metabolism, Pharmacokinetics and Toxicity of Functional Groups*, ed. D. A. Smith, Royal Society of Chemistry, Cambridge, **2010**, 328.
15. Taylor, R. D.; MacCoss, M.; Lawson, A. D. *J. Med. Chem.*, **2014**,57,14, 5845- 5859.
16. (a) Manske, R.H. *Chem. Rev.* **1942**, 30,1,113-144. (b) G. Jones, *Chemistry of Heterocyclic Compounds: Quinolines, Part I*, John Wiley & Sons, Inc. **2008**, 32, 93–318.
17. (a) Kaur, K.; Jain, M.; Reddy, R. P.; Jain, R. *Eur. J. Med. Chem.* **2010**, 45,8, 3245-3268.(b) Lu, W.J.; Wicht, K. J. ; Wang, L.; Imai, K.; Mei, Z.W.; Kaise, M.; Sayeda, I. E. T. E. ; Eganb, T. J. ; Inokuchia, T. *Eur. J. Med. Chem.* **2013**, 64, 498-511.
18. Lilienkamp, A.; Mao, J.; Wan, B.; Wang, Y.; Franzblau, S.G.; Kozikowski, A.P. *J. Med. Chem.* **2009**, 52, 7, 2109-2118.
19. Guo, R.H., Zhang, Q.; Ma, Y.B.; Huang, X.Y.; Luo, J.; Wang, L.J.; Geng, C.A.; Zhang, X.M.; Zhou, J.; Jiang, Z.Y.; Chen, J.J. *Bioorg. Med. Chem.* **2011**, 19, 4, 1400-1408.
20. Mukherjee, S.; Pal, M. *Curr. Med. Chem.* **2013**, 20, 35, 4386-4410.
21. Mahamoud, A.; Chevalier, J.; Davin-Regli, A.; Barbe, J.; Pages, J.M. *Curr. Drug Targets*, **2006**, 7, 7, 843-847.
22. Vandekerckhove, S.; Tran, H. G.; Desmet T.; Hooghe, M. D. *Bioorg. Med. Chem. Lett.* **2013**, 23,16, 4641-4643.
23. Tran, M.; Stack, G. P. US Pat. 0165245 A1, **2002**.
24. Denny, W. A.; Wilson, W. R.; Ware, D. C.; Atwell, G. J. ; Milbank, J. B. ; Stevenson, R. J. U.S. Pat. 7064117, **2006**.
25. Welsch, M. E. ; Snyder, S. A.; Stockwell, B. R. *Curr. Opin. Chem. Biol.* **2010**, 14, 3, 347–361.
26. Bhadra, K.; Kumar, G. S. *Med. Res. Rev.* **2011**, 31, 6, 821–862.
27. Tomasic, T.; Masic, L. P. *Curr Med Chem.* **2009**, 16, 13, 1596–1629.
28. Forino, M.; Johnson, S.; Wong, T.Y.; Rozanov, D.V.; Savinov, A. Y.; Li, W. ; Fattorusso, R.; Becattini, B.; Orry, A. J. ; Jung, D.; Abagyan, R. A.; Smith, J. W. ; Alibek, K. ; Liddington,

- R. C. ; Strongin, A. Y. ; Pellecchia, M. *Proc. Natl. Acad. Sci. U. S. A.* **2005**, 102,27, 9499–9504
29. Gaudino, C.E.; Tagliapietra, S.; Martina, K.; Palmisano, G.; Cravotto, G. *RSC Adv.***2016**, 6, 46394–46405.
 30. Pratap,R.; Ram,V. J .*Chem Rev* .**2014**, 114, 20, 10476–10526.
 31. Sednev, M.V.; Belov, V.N.; Hell, S.W. *Methods ApplFluoresc.* **2015**,3, 042004.
 32. Thomas,N.; Zachariah, S. M. *Asian J. Pharm. Clin. Res.***2013**, 6, 11-15.
 33. Pratap, R.; Ram,V.J. *Chem Rev.* **2014**, 114,20,10476–10526.
 34. Costantino,L.; Barloccob,D.; *Curr. Med. Chem.* **2006**, 13,1, 65-85
 35. Laskar, S.; Brahmachari, G. *Org. Biomol. Chem.***2014**, 2, 1-50.
 36. Thomas,N.; Zachariah, S. M. *Asian J. Pharm. Clin. Res.***2013**, 6, 2, 11-15.
 37. Soll,R.M.;Qualigato,D.A.;Delninger,D.D.;Dollings,P.J.;Joslyn, B.L.;Dolak,M.T.;Lee,S.J.;Bohan,C.;Wojdan,A.;Morin,M.E.;Os hiro,G.*Bioorg.med. chem.lett.***1991**,1,11,591-594.
 38. Patil, S.A.; Patil,R.; Pfeffer, L.M.; Miller, D.D.; *Future Med. Chem.* **2013**, 5,14, 1647–1660
 39. ClinicalTrials.gov Identifier: NCT01240590.
 40. Anthony, S. P.; Von Hoff, D.; Whisnant, J.K.; Tseng, B.Y. *J. Clin. Oncol.* **2007**, 25, 18, 14043.
 41. (a) Tomas, P.R. *Curr. Med. Chem.* **2006**, 13, 16, 1859-1876.
(b) Gottesman, M. M. *Annual Review of Medicine.* **2002**, 53, 615-627.(c) Holohan, C.; Van Schaeybroeck, S.; Longley, D. B.; Johnston, P. G., *Nature Reviews Cancer*, **2013**, 13 ,10, 714-726.
 42. (a) Das,S.G.; Srinivasan,B.; Hermanson,D.L.; Bleeker,N.P.; Doshi,J.M.; Tang,R.; Beck,W.T.; Xing,C. *J. Med. Chem.* **2011**, 54,16, 5937–5948. (b) Das, S.G.; Doshi,J.M.; Tian,D.; Addo, S.N.; Srinivasan,B.; Hermanson,D.L.; Xing,C.; *J. Med. Chem.***2009**, 52,19,5937–5949.(c)Puppala, M.; Zhao,X.;Casemore,D.; Bo Zhou , Aridoss,G.; Narayanapillai,S.; Xing,C.*Bioorg. Med. Chem.* **2016**, 24, 6, 1292–1297.
 43. Zhang,G.; Zhang,Y.; Yan, J.; Chen,R.; Wang,S.; Ma,Y.; Wang,R. *J. Org. Chem.* **2012**, 77,2, 878–888.
 44. (a) Galinis,D.;Fuller,R.; McKee, T.; Cardellin,J.; Gulakowski, R.; McMahan,J.; Boyd,M. *J. Med. Chem.***1996**, 39, 22, 4507-

4510. (b) Garino,C.; Bihel,F.; Pietrancosta,N.; Laras,Y.; Quělēver, G.; Woo,I.; Klein,P.; Bain,J.; Boucher,J.; Kraus,J. *Bioorg. Med. Chem.***2005**,15,1,135-138.(c) Costantino,L.; Barloccob,D.; *Curr MedChem*,**2006**, 13,1, 65-85. (d) Lee, Y.R.; XinLi. *Bull. Korean Chem. Soc.***2007**, 28, 10, 1739-1745.
45. Lu, Z.; Lin,Z.; Wang, W.; Du,L.; Zhu,T.; Fang, Y.; Gu,Q.; Zhu, W. *J. Nat. Prod*, **2008**, 71,4,543-546.
46. (a) Saeedi ,M.; Safavi ,M.; Razkenari,E.K.; Edraki,M.M.N.; Moghadam, F,H.; Khanavi,M.M; Akbarzadeh,T. *Bioorganic Chemistry*.**2017**,70,86–93.(b) Saeedi,M.; Ansari,S.; Mahdavi,M.; Sabourian,R. ; Akbarzadeh,T.; Foroumadi,A.; Shafiee,A. *Synth.Commun.* **2015**, 45, 2311–2318. (c) Khoobi , M.; Alipour,M.; Sakhteman.M.; Nadri,H.; Moradi,A.; Ghandi,M.; Emami , S.; Foroumadi ,A.; Shafiee, A. *Eur. J. Med. Chem.***2013**, 68 , 260-269.
47. Eun Jae Na, Lee,K.H.; Han,H.; Kim,Y.K.; Yoon,S.S.J. *Nanosci. Nanotechnol.* **2013**,13, 554–557.
48. Yu,D.; Huang,F.; Ding,S.H.; Feng,G. *Anal. Chem.* **2014**, 86, 8835–8841.
49. Zheng,Y.;Zhao,M.; Qiao,Q.; Liu,H.; Lang ,H.; Xu, Z.*Dyes. Pigm.* **2013**, 98, 367-371.
50. Bernd Groner, *peptides as drugs: discovery and development*, Wiley, **2009**, ISBN: 978-3-527-32205-3.
- 51.** Abell, A.; *Advances in Amino Acid Mimetics and Peptidomimetics,1, Elsevier academic press, 1997*
52. Costantino,L.; Barloccob,D.*Curr. Med. Chem.* **2006**, 13, 65-85.
53. (a)William Lubell, *Peptidomimetics I, Springer*,**2017**. (b) William Lubell, *Peptidomimetics II, Springer*, **2017**.
54. (a)Abell, A. *Advances in Amino Acid Mimetics and Peptidomimetics, JAI Press, Greenwich*,**1997**,1.(b) Abell, A. *Advances in Amino Acid Mimetics and Peptidomimetics,JAI Press, Greenwich*,**1999**(c) Vagner, J; Qu, H; Hruby, V.J; *CurrOpinChem Biol.***2008** , 12, 3, 292–296.
55. Trabocchi,A.; Guarna,A.; *Peptidomimetics in Organic and Medicinal Chemistry,Wiley*,**2014**,ISBN: 9781119950608
56. (a) Roger M. Freidinger, *J.Med. Chem.* **2003**, 46, 26, 5553-5561. (b) Cerminara,I.; Chiumminto,I.; Funicello,M.; Guarnaccio,A.; Lupattelli,P. *Pharmaceuticals*, **2012**, 5, 297-316.

57. (a)Trabocchi,A.;Guarna,A.; *Peptidomimetics in Organic and Medicinal Chemistry,Wiley.2014* ISBN: 9781119950608.(b) Freidinger, R.M.*J.Med. Chem.* **2003**, 46, 26, 5553-5561. (c) Cerminara,I.; Chiummiento,I.; Funicello,M.; Guarnaccio,A.; Lupattelli,P. *Pharmaceuticals*, **2012**, 5, 297-316.
58. (a)Spandl, R. J.; Bender, A.; Spring, D. R. *Org. Biomol. Chem.***2008**, 6, 1149–1158. (b) Nielsen, T. E.; Schreiber, S. L. *Angew. Chem., Int. Ed.***2008**, 4748–4756.(c) Schreiber, S. L.*Science*, **2000**, 287, 1964–1969. (d)Spandl, R. J.; Bender, A.; Spring, D. R. *Org. Biomol. Chem.***2008**, 6, 1149–1158. (e) Galloway, W. R. J. D.; Isidro-Llobet, A.; Spring, D. R. *Nat. Commun.* **2010**, 1,80–92. (f) Eckert, H.; *Molecules*,**2012**, 17, 1074-1102.
59. Schreiber, S. L.; Burke, M.D. *Angew.Chem.Int.Ed.***2004**,43,46-58.
60. Trabocch,A.*Diversity-oriented synthesis: basics and applications in organic synthesis, drug discovery, and chemical biology*,**2013**, Wiley, ISBN 978-1-118-14565-4.
61. Galloway, W. R. J.D, Spring, D.R.; *Nature*, **2011**, 470, 42-43.
62. (a)Lee, D.; Sello, J.; Schreiber, S. L, *J.Chem.Soc.* **1999**, 121,45, 10648-10649.(b)Micalizio,G.C.; Schreiber, S. L.*Science*, **2003**,302,613-618.
63. (a) Bradbury, A. F.; Smyth, D. G.; Snell, C. R.; *Nature*, **1976**, 260,165-166.(b)Smith, A.B.; Charnley, A.K.;Hirschmann, R. *Acc. Chem. Res.* **2011**, 44, 3,180–193.
64. (a) Kumaravel, K.; Vasuki, G. *Curr. Org. Chem.* **2009**, 13, 1820–1841. (b) Syamala, M. *Org. Prep. Proced. Int.***2009**, 41, 1–68.(c) Heiner Eckert, *Molecules.* **2012**, 17, 1074-1102.
65. Nielsen,T.E.; Schreiber, S. L.; *Angew. Chem. Int. Ed. Engl.* **2007**, 17,47, 1, 48–56.
66. (a) Jiang, H.;Yang, J.;Tang, X.; Li, J.; Wu, W. *J Org Chem.***2015**,80,17,8763-8771.(b) Tzitzikas, Z. T.; Chandgude, A.L, Dömling, A. *Chem Rec.* **2015**, 15,5,981-996. (c) Zhu, J.; Bienaymé, H. *Multicomponent Reactions; Wiley-VCH: Weinheim, Germany*, **2005** (d) Dömling, A.; Ugi, I. *Angew. Chem., Int. Ed.* **2000**, 39, 3168–3210. (e) Dömling, A. *Chem. Rev.* **2006**, 106, 17–89; (f) Dömling, A.; Wang, W.; Wang, K. *Chem. Rev.***2012**, 112, 3083–3135.
67. Strecker,A.; Liebig,J. *Ann. Chem.* **1850**, 75, 27–45.
68. Hantzsch,A.; Ber. Dtsch. Chem. Ges. **1890**, 23, 1474–1476.

69. (a) Biginelli, P.; Ber. Dtsch. Chem. Ges. **1891**, 24, 1317–1319.
 (b) P. Biginelli, Ber. Dtsch. Chem. Ges. **1891**, 24, 2962–2967.
70. Domling, A. *Chem. Rev.* **2006**, 106, 1, 17–89
71. (a) Mannich, C. *J. Chem. Soc. Abstracts*, **1917**, 112, 634–635. (b) Mannich, C. *Arch. Pharm.* **1917**, 255, 261–276.
72. Dömling, A.; Wang, W.; Wang, K. *Chem. Rev.* **2012**, 112, 6, 3083–3135.
73. Passerini, M.; Gazz. Chim. et. al. **1921**, 51, 126–129.
74. Leusen, D. V.; Leusen, A. M. V. *Organic Reactions*, **2004** - *Wiley Online Library*
75. (a) H. Bergs, Ger. Pat. **1929**, DE566094 (b) Bucherer, H. T.; Steiner, W. *J. Prakt. Chem.* 1934, 140, 291–316. (c) H. T. Bucherer, V. A. Lieb, *J. Prakt. Chem.* **1934**, 141, 5–43.
76. Dömling, A.; Wang, W.; Wang, K. *Chem. Rev.* **2012**, 112, 6, 3083–3135
77. Huang, Y.; Dömling, A. *Chem Biol Drug Des.* **2010**, 76, 2, 130–141.
78. Huang, Y.; Wolf, S.; Bista, M.; Meireles, L.; Camacho, C.; Holak, T. A.; Domling, A. *Chem. Biol. Drug. Des.* **2010**, 76, 116–129.
79. Huang, Y.; Dömling, A. *Mol Divers*, **2011**, 15, 3–33.
80. Sinha, M. K.; Khoury, K.; Herdtweck, E.; Domling, A. *Chemistry*. **2013**, 19, 25, 8048–8052.
81. Kalinski, C.; Umkehrer, M.; Weber, L.; Kolb, J.; Burdack, C.; Ross, G. *Mol Divers*, **2010**, 14, 513–522.
82. (a) Dömling, A.; Ugi, I. *Angew Chem*, **2000**, 112, 3300–3344. (b) Ugi, I.; Meyer, R.; Fetzer, U.; Steinbrückner, C. *Angew Chem*, **1959**, 71, 386–392.
83. Erlanson, D. A. *Curr. Opin. Biotechnol.* **2006**, 17, 643.
84. Rees, D. C.; Congreve, M.; Murray, W. C.; Robin Carr. *Nat Rev Drug Discov.* **2004**, 3, 660–672.
85. Kolb, H. C.; Finn, M. G.; Sharpless, K. B.; *Angew Chem Int Ed.* **2001**, 40, 2004–2021.
86. Tornøe, C. W.; Christensen, C.; Meldel, M. *J. Org. Chem.* **2002**, 67, 9, 3057–3064. (b) Meldel, M., Tornøe, C. W. *Chem. Rev.* **2008**, 108, 2952–3015.
87. (a) Abell, A.; Pedersen, D. S. *Eur. J. Org. Chem.* **2011**, 2399–2411. (b) Valverde, I. E.; Mindt, T. L. *Chimia (Aarau)*, **2013**, 67, 4, 262–266.

88. (a) Brik, A.; Alexandratos, J.; Lin, Y.C.; Elder, J. H.; Olson, A. J.; Wlodawer, A.; Goodsell, D. S.; Wong, C.H. *Chem. Bio. Chem.* **2005**, 6,7, 1167-1169 (b) Bock, V. D.; Hiemstra, H.; van Maarseveen, J. H. *Eur. J. Org. Chem.* **2006**,1, 51-68.
89. Dehaen, W.; Bakulev, V.A. *Chemistry of 1,2,3-triazoles, Springer*, **2014** .(b) Agalave, S.G.; Maujan, S.R.; Pore, V.S. *Chem. Asian J.* **2011**, 6, 2696 – 2718.
90. Driggers, E. M.; Hale, S. P.; Lee, J.; Terrett, N. K. *Nat. Rev. Drug Discovery*, 2008, 7, 608–624.
91. (a) James A. Wisner, *Nature chemistry*, **2013**, **5**,646. (b) Yu, X.; Sun, D. *Molecules*, 2013, 18, 6230-6268.
92. Mallinson, J.; Collins, I. *Future Med. Chem.* **2012**, 4, 11, 1409–1438.
93. Galindo, F.; Burguete, M. I.; Vigarra, L.; Luis, S. V.; Kabir, N.; Gavrilovic, J.; Russell, D. A. *Angew. Chem.* **2005**,117, 6662-6666.
94. Yudin, A.K. *Chem. Sci.* **2015**, 6, 30-49. (b) Maier, M. E., *Org Biomol Chem.* **2015**, 13, 5302-5343.
95. (a) Isidro-Llobet, A., Murillo, T., Bello, P. *Proc. Natl. Acad. Sci. U.S.A.* **2011**, 108, 6793. (b) Nielsen, T.E. and Schreiber, S.L. *Angew. Chem., Int. Ed.* **2008**, 47,1, 48-56.
96. Davis, M.R., Singh, E.K., Wahyudi, H. *Tetrahedron*, **2012**, 68,4, 1029-1051.
97. Guarna, A.; Trabocchi, A. *Peptidomimetics in Organic and Medicinal Chemistry, Wiley*, **2014**.
98. Tornøe, C.W.; Christensen, C.; Meldal, M. *J. Org. Chem.* **2002**, 67, 3057-3064.
99. Kolb, H.C.; Finn, M.G.; Sharpless, K. B. *Angew Chem Int Ed.* **2001**, 40, 2004–2021.
100. Brik, A.; Alexandratos, J.; Lin, Y.C.; Elder, J.H.; Olson, J.; Wlodawer, A.; Goodsell, D.S.; Wong, C.H. *Chem. Bio. Chem.* **2005**, 6, 7, 1167-1169.
101. Truscheit, E.; Frommer, W.; Junge, B.; Müller, L.; Schmidt, D. D.; Wingender, W. *Angew. Chem. Int. Ed. Engl.* **1981**, 20, 744–761.
102. (a) Keay, B.A.; Dibble, P.W.; Katritzky, A.R., Rees, C.W., Scriven, E.F.V., Eds.; Elsevier: New York, NY, USA, **1996**, 2, 395–436. (b) Mortensen, D.S.; Rodriguez, A.L.; Carlson, K.E.; Sun, J.; Katzenellenbogen, B.S.; Katzenellenbogen, J.A. *J. Med. Chem.* **2001**, 44, 3838–3848. (c) Lipshutz, B.H. *Chem.*

- Rev.* **1986**, 86, 795–819.(d)Hou, X.L.; Cheung, H.Y.; Hon, T.Y.; Kwan, P.L.; Lo, T.H.; Tong, S.Y.; Wong, H.N.C. *Tetrahedron*, **1998**, 54, 1955–2020.
103. Banerjee, R.; Kumar,H.K.S.;Banerjee,M.*Int.J.Rev.Life.Sci.* **2012**,2,1, 7-16.
104. L. B. Hough et al. *Bioorg. Med. Chem. Lett.***2007**, 17, 5715–5719.
105. Boyd, M. R.;Stiko, A. W.; Sasame, H. A. *Biochem. Pharmacol.* **1979**, 28, 601- 606.
106. (a) Anthony, J. E. *Chem. Rev.* **2006**, 106, 22, 5028-5048. (b) Jiang, W.; Li, Y.; Wang, Z. H. *Chem. Soc. Rev.***2013**, 42, 6113-6127
107. (a) Xiong,Y.;Wang,M.;Qiao,X.;Li,J.;Li,H.*Tetrahedron*, **2015**, 71, 852-856.
108. Jiann T. Lin, Pin-Cheng Chen, Yung-Sheng Yen, Ying-Chan Hsu, Hsien-Hsin Chou, and Ming-Chang P. Yeh. *Org. Lett.***2009**, 11, 1, 97-100.
109. (a) Carrette, L.L.G.; Gyssels, E.; Madder ,A. *Curr. Prot. Nucl. Acid Chem.* **2013**, 54. (b) Stevens,K.; Madder, A. *Nucleic Acids Research*, **2009**, 1555-1565. (c) Op de Beeck, M., Madder, A., *JACS***2011**, 133, 79 (d) Op de Beeck, M.; Madder A. *JACS***2012**, 10737.(d) Carrette, L.L.G.; Gyssels, E.; Loncke, J. ; Madder, A. *Org. Biomol. Chem.* **2014**, 12, 6, 931-935.(e) Carrette, L.L.G. ;Morii, T.;Madder,A. *Bioconj. Chem.* **2013**, 24, 12, 2008-2014. (f) Deceuninck, A.; Madder, A. *Chem. Comm.***2009**, 340-342. (g) Hoogewijs; K. ; Buyst, D. .; Winne, J.M. ; Martins, J.C. ;Madder,A. *Chem. Comm.* **2012**, 49 ,28, 2927. (h) Antonatou, E.; Hoogewijs, K. ; Baudot, A. ; Kalaitzakis, D.; Vassilikogiannakis, G.; Madder, A. **2016**, 22, 8574-8461.

Chapter 2

**Design and synthesis of 1, 2, 3-triazole linked
privileged benzopyran based peptidomimetics
as blue emitting fluorescent inhibitors**

2.1 Introduction	45
2.2 Result and Discussion	49
2.3. Photophysical properties of Type 1 peptidomimetics	55
2.4 Evaluation of drug property descriptors	57
2.5 Biological study: The in vitro anti-cancer activity evaluation	58
2.6 synthesis of type 2 peptidomimetics: β -amino acid motifs functionalized chrome peptidomimetics	61
2.7 Photophysical property evaluation	66
2.8 Evaluation of drug property descriptors	67
2.9 Biological study: The in vitro anti-cancer activity evaluation.	68
2.10 Conclusion:	70
2.11 Structural characterization	71
2.12. Experimental Section	89
References	102
Supplementary data	105

2.1 Introduction

The design and synthesis of novel small molecular scaffolds targeting various biological receptors is one of main goals in the development of new therapeutics in drug discovery.¹ The Diversity oriented synthesis is the most promising protocol to create collections of small molecules with diverse functionality and capable to interact with different targeted proteins.² In the first chapter we discussed the medicinal chemistry applications of a collection of privileged heterocycles including chromene derivatives and also the short and efficient MCR-Click synthetic strategies to achieve drug leads based on them. As discussed in the first chapter, chromene has been a subject of several kinds of chemical and biological investigations to bring out its medicinal and materials properties. Among various chromene derivatives, the 4H-chromenes and pyran annulated 4H-chromenes are well distributed in various natural and synthetic products.³ Particularly, 2-Amino-3-cyano-4H-chromenes are versatile for the synthesis of ligands with excellent spasmolytic, antibacterial, anticoagulant and diuretic activities.⁴ Currently these scaffolds are used for the treatment of human inflammatory TNF α -mediated diseases like rheumatoid and psoriatic arthritis and in cancer therapy.⁵ Fig. 2.1 shows some of the selected examples of 2-Amino-3-cyano-4H-chromene based therapeutic agents.

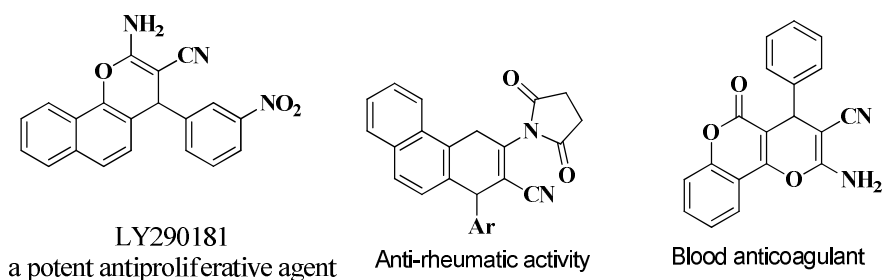


Fig.2.1: therapeutic agents based on 2-Amino-3-cyano-4H-chromenes.

Similarly, various similar scaffolds have been synthesized and tested for their invitro anticancer activity against various cancer cell lines. Crolibulin (EPC2407) is one such compounds which is under phase I/II clinical trials against anaplastic thyroid cancer with optimal side effects⁶. Typical examples of 2-amino-4H-chromenes with anticancer activity⁷ are presented in fig. 2.2.

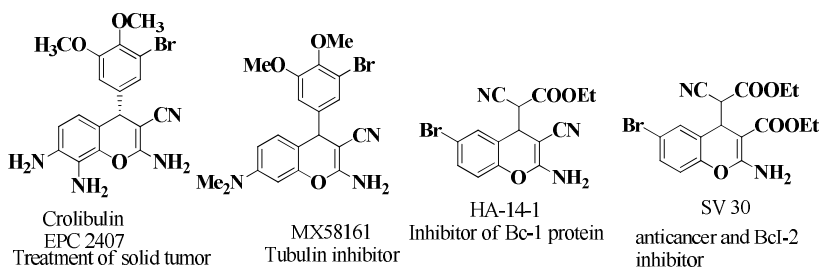


Fig. 2.2: 2-amino-4H-chromenes with anticancer activity.

Similar to drug discovery, an equally important field in medicinal chemistry is the development of small molecule based fluorescent probes to locate the malignant cells.⁸ Fluorescent labels are specially designed molecules for interacting with biological targets. The in-vivo and in-vitro interaction of fluorescent probes with targets causes changes in the spectroscopic properties of the probe molecule in terms

of its fluorescence intensity, emission, excitation wavelengths and fluorescence life time etc. and these changes can be used for the identification of biological targets.⁹ A broad spectrum of privileged scaffold based fluorescent dyes are available in the market for labelling applications. For example, scaffolds such as benzopyrans, rhodamine, cyanine, and squaraine etc. are used as signaling units in commercial fluorescent probes, such as Alexa Fluor®, AMCA and DyLight Fluors.¹⁰ If the labeling agent itself is a drug, it is possible to detect the components of the biological assemblies and imaging and flow cytometry at the same time without the need of washout (cell washing) of the leftover imaging agent to avoid background fluorescence. The development of such 2-in-1 therapeutics are the recent attraction in this field.

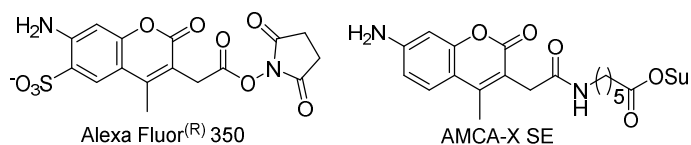
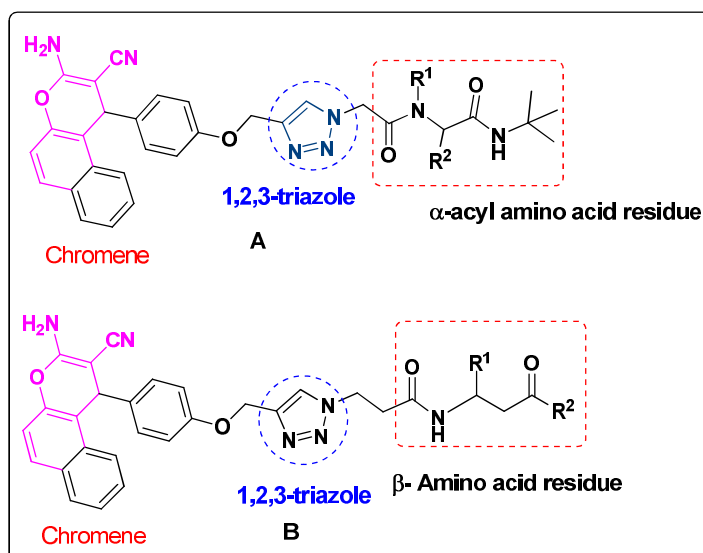


Fig. 2. 3: Commercially available benzopyran based fluorescent dyes

A careful literature survey revealed that although chromene scaffolds has been subjected to a plethora of skeletal modifications to enhance their biological properties, chromene cores functionalized with unnatural amino acid moieties has not been reported. Since unnatural amino acid scaffolds are another potential privileged scaffold structures, we decided to undertake a detailed examination on the fusion of chromene core with unnatural amino acid derivatives such as carboxamide and acetamide derivatives to obtain peptidomimetic

structures to study their photophysical and biological properties. This chapter presents the detailed description on the “Click with MCR” synthesis of two types of peptidomimetics **A** and **B** as shown in the scheme below, their fluorescence property evaluation, imaging studies to explore their probe properties and finally the cytotoxicity evaluation against human breast cancer cell lines MCF-7 to explore their anticancer properties.



Scheme 2.1: Two types of chromene peptidomimetics **A** and **B** presented in chapter 2

The rationale to develop such triazole functionalized compounds is already mentioned in chapter 1. As mentioned in chapter 1, 1,2,3-Triazole moiety is an attractive connecting unit in medicinally active scaffolds because they are stable to metabolic degradation and capable to form hydrogen bonds with biomolecular targets and can also improve the metabolic stability of the drugs. The 1,2,3-triazole moiety does not occur in nature, although the synthetic molecules that contain 1,2,3-triazole units show diverse biological activities. The importance of triazole compounds in medicinal chemistry is undeniable. Click processes can be used for the integration and/or linkage of biomolecules (polyamines, amino acids, and carbohydrates), drugs, and other functional molecules with each other through 1,2,3-triazole ligation leading to the overall improvement in pharmacological activities. Finally, 1,2,3-triazole cores may form the basis of small-molecule pharmaceutical leads.

2.2 Result and Discussion

Synthesis of Type 1 peptidomimetics

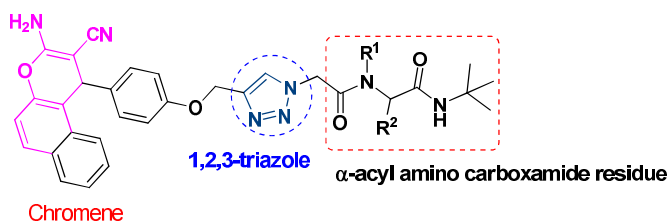
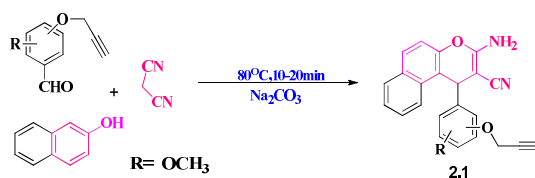


Fig. 2.4: General structure of type1 chromene peptidomimetics

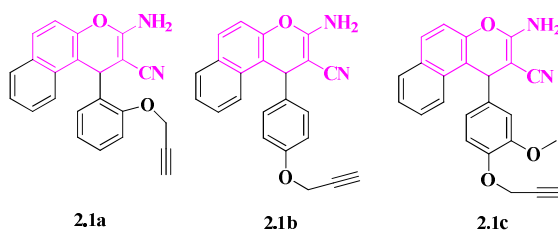
Chemistry

2.2.1 Synthesis of alkyne functionalized 2-Amino-3-cyano-4H-chromene scaffolds

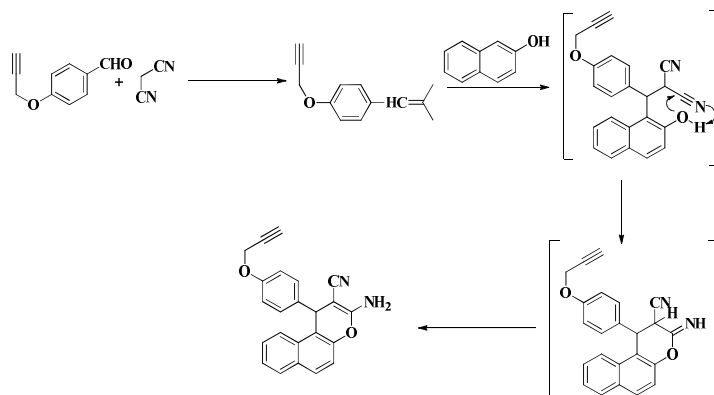
The most straight forward method for the synthesis of 2-Amino-3-cyano-4H-chromene is a one-pot multicomponent reaction involving the condensation of malononitrile, an aldehyde and a phenolic compound in presence of a base catalyst under various reaction conditions.¹¹ A variety of catalysts such as triethyl amine, ionic liquids, hexadecyltrimethyl ammonium bromide, metal oxides, nanoparticles, cetyltrimethyl ammonium bromide, organic bases, DBU etc. were employed to effectively catalyze the reaction.¹² in the present work we have adopted sodium carbonate catalyzed solvent free method¹³ for the synthesis of alkyne functionalized chromene derivative as shown in scheme 2.2.



Scheme 2.2: Synthesis of alkyne functionalized 2-amino-4H-chromene



Scheme 2.3: Alkyne functionalized chromene scaffolds.



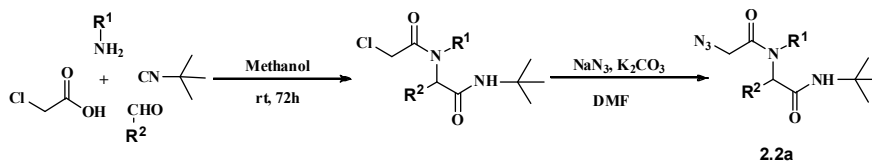
Scheme 2.4: A possible mechanism for the formation of chromene

The synthesis of chromene **2.1** involves grinding equimolar quantities of β -naphthol, malononitrile and a propargylated aldehyde in a mortar using 10 mol % sodium carbonate as catalyst under solvent free condition. The grinded mixture was then heated in an oven at 80^oC for 20 minutes and subsequently washed with hot water and crystallized from ethanol to obtain the chromene alkyne and were characterized by spectroscopic techniques.

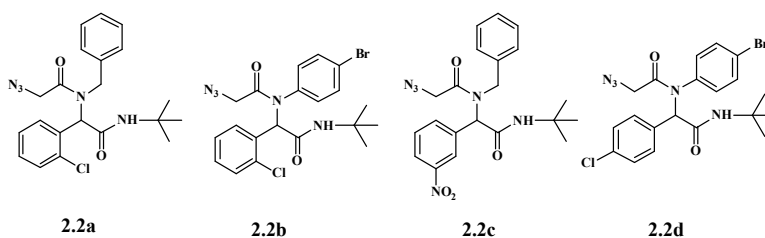
2.2.2. Synthesis of α -acyl amino carboxamide azides **2.2a-d**

The α -amino acid residues for the synthesis of type 1 peptidomimetics were synthesised in the form a carboxamide azide **2.2a-d** from an Ugi four component reaction as shown in scheme 2.5.¹⁴ The reaction between a substituted aldehyde, butyl amine, tertiary butyl isocyanide and chloroacetic acid in methanol solvent as shown in scheme 2.5 afforded the chloro derivative of the carboxamide. The chloro derivatives were then treated with NaN₃ in Dimethyl formamide

(DMF) at room temperature to afford the α -acyl amino carboxamide azides designated as “Ugi azides” **2.2a-2.2l**. (scheme 2.6)



Scheme 2.5: Ugi-4CR to Ugi-type α -amino acyl amide azides

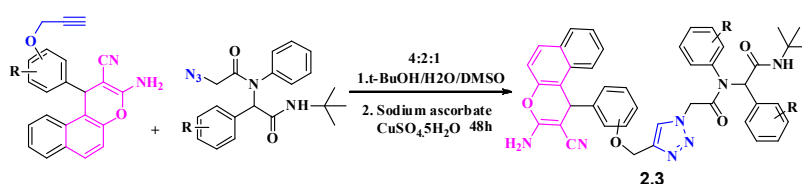


Scheme 2.6: List of azides **2.2a-d** prepared by following an Ugi 4CR

2.2.3. Click chemistry of chromene alkynes **2.1a-c** with α -acyl amino carboxamide azides **2.2a-d**.

The chromene alkynes **2.1a-c** were then ligated to Ugi-azides **2.2a-d**. via Cu (I) catalyzed (3+2) azide-alkyne click cycloaddition (CuAAC) reaction at Sharpless condition using a catalytic system comprising of $\text{CuSO}_4 \cdot 5\text{H}_2\text{O}$ /Sodium ascorbate in *t*-butanol/water/DMSO.¹⁵ In a typical reaction the scaffolds **2.1a** and **2.2c** were mixed with 0.2 equivalent of CuSO_4 and 0.4 equivalent of sodium ascorbate in a mixed solvent system containing *t*-butanol, water and DMSO in 4:2:1 ratio at room temperature for 12 hours as shown in scheme 2.7. The reaction mixture was then diluted with cold

water to afford the click product **2.3a** in solid form. The cycloaddition reactions took place with the near quantitative formation of the 1,2,3-triazole derivatives and the precipitated product was collected and purified by simple washing with solvents. The click products were obtained in 70-81% yield without the aid of any accelerating ligands or post reaction purification techniques. We have successfully synthesized 12 such chromene peptidomimetics **2.3a-2.3l** are presented in table 2.1.



Scheme 2.7: General scheme for the synthesis of 1, 4-disubstituted triazolyl 2-Amino-4H-chromene scaffolds.

2.2.4. Regioselectivity of the triazole formation.

The regioselectivity of the products were assigned by comparing the NMR spectral details of the peptidomimetics with the literature values and also from HPLC analysis. By comparing the J value of the triazole CH proton with reported value and also by comparing the retention time obtained from the HPLC profile with literature values, we confirmed the selective formation of cis-1,4-substituted 1,2,3-triazoles in our click reactions. The representative HPLC profile of the sample **2.3a** is shown in figure 2.5.

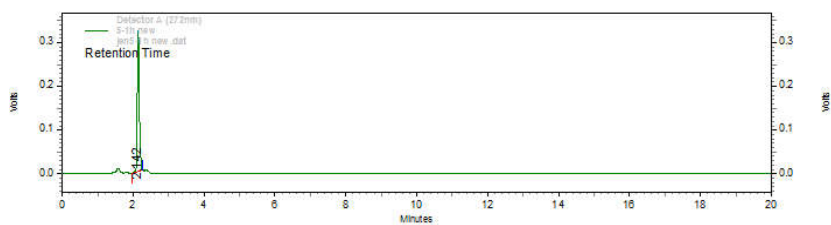
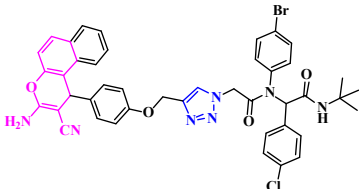
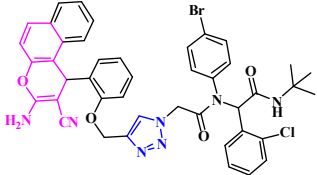
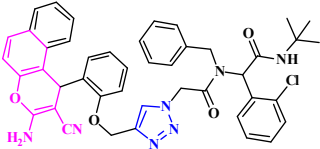
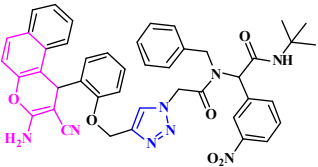
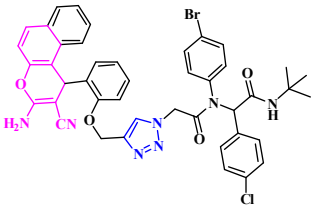


Fig. 2. 5: HPLC profile of the representative sample 2.3a

Table 2.1: List of Type 1 peptidomimetics

Entry	Peptidomimetic	% yield	Abs _{max} (nm)	Em _{max} (nm)	Stokes shift (nm)
2.3a		80%	341	451	110
2.3b		76%	373	432	59
2.3c		82%	372	439	67
2.3d		75%	371	444	73
2.3e		73%	350	419	69
2.3f		76%	350	433	83
2.3g		81%	352	416	64

Table 2.1 cont.....

Entry	Peptidomimetic	% yield	Abs _{max} (nm)	Em _{max} (nm)	Stokes shift (nm)
2.3h		77%	305	444	139
2.3i		75%	306	444	138
2.3j		82%	303	441	138
2.3k		75%	307	442	135
2.3l		73%	361	438	77

2.3. Photophysical properties of Type 1 peptidomimetics

The photophysical properties of the type 1 peptidomimetics **2.3a-l** were studied by measuring its absorption and emission in DMSO at varying pH from 0-10. As a representative example, the compound **2.3a** showed an absorption maxima centered at 341 nm and an

emission maxima centered at 451 nm with a Stokes shift of 110 nm which is significantly larger than some of the commercial fluorophores. These values are found to be intact to the changes in pH. The normalized absorption and emission spectra of the sample **2.3a** is shown in fig.2. 6. The fluorescent probes with high specificity and large stokes shift values are free spectral overlap between absorption and emission wavelengths and allows the sensitive detection of targets. Among the 12 peptidomimetics examined, the fluorescence properties of **2.3b**, **2.3c** and **2.3d** are comparable with the photophysical properties reported for commercial fluorophores such as Alexa Fluor® 405 (Abs/Em: 405 /421nm) and eFluor® 450 (Abs/Em: 405/450 nm). Compound **2.3h** showed Maximum absorption maxima centered at 305 nm and an emission maxima centered at 444 nm with a Stokes shift value of 139 nm.

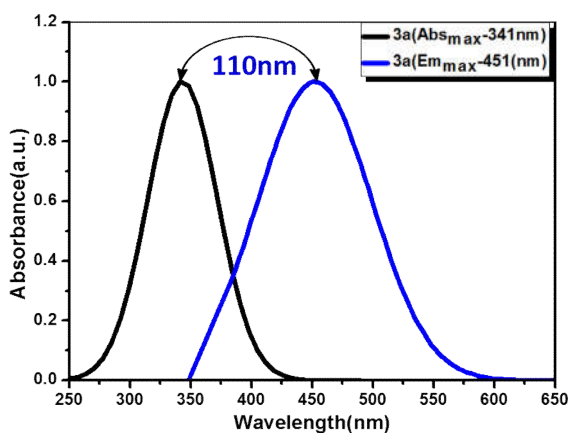


Fig. 2.6: The normalized absorption and emission spectra of the compound **2.3a**

2.4 Evaluation of drug property descriptors

The drug property descriptors of the peptidomimetics were calculated using an online service, www.molinspiration.com.¹⁶ According to the Lipinski's rule of five, the drug-likeness of the molecules were assessed mainly based on their molecular size, lipophilicity as well as polarity (topological polar surface area; tPSA). Drug like molecules usually have log P values between -0.4 and 5.6 and a molecular weight of <500. An orally bioavailable drug will have tPSA between 75 and 160 Å.¹⁷ The strict reliance on the Ro5 may have resulted in lost opportunities, particularly for difficult targets. A recent report by Kihlberg et al revealed that beyond rule of 5 (bRo5) molecules are better candidates for modulating difficult and emerging target classes especially when binding sites are large and flat or groove-shaped. Such bRo5 molecules typically possess descriptor values such as $MW \leq 1000$ Da, $-2 \leq \text{ClogP} \leq 10$, $\text{HBD} \leq 6$, $\text{HBA} \leq 15$, and $\text{NRotB} \leq 20$. In the case of these new peptidomimetics the drug property descriptors are not within the Lipinski's rule of five (Ro5) and they are more suitable for classified as beyond rule of 5 (bRo5) molecules.¹⁸ This suggests our new peptidomimetics could serve as lead compounds for drug discovery related to difficult and emerging target classes. The drug property descriptors of the compound **2.3a-1** are listed in table 2.2.

Table 2.2: Drug property descriptors of type 1 peptidomimetics

Entry	Number of violations	Number of atoms	Log p <5	Molecular weight <500	Number of ON <10	Number of OH NH <5	Number of rotatable of bonds <10
2.3a	3	57	8.75	845.20	11	3	11
2.3b	3	57	8.07	780.33	11	3	12
2.3c	3	59	7.31	790.80	14	3	13
2.3d	3	57	8.77	845.20	11	3	11
2.3e	2	55	8.76	815.17	10	3	10
2.3f	2	55	8.02	750.30	10	3	11
2.3g	3	57	7.33	760.86	13	3	12
2.3h	2	55	8.78	815.17	10	3	10
2.3i	3	56	8.02	831.17	11	3	11
2.3j	3	56	6.91	766.30	11	3	12
2.3k	3	58	6.22	776.85	14	3	13
2.3l	3	56	8.06	831.17	11	3	11

2.5 Biological study: The in vitro anti-cancer activity evaluation.

Out of various disease classes, cancer is a major global problem due to the uncontrolled growth of abnormal cells. Among various cancerous varieties, breast cancer is the most common form of cancer present in women and is the second leading cause of death after lung cancer. According to literature reports, one in every eight women develops metastatic breast cancer in her lifetime. Therefore, there is a tremendous need for safe, potent and selective anticancer drugs. Since chromenes shows excellent cytotoxic activity against various human cancer cell lines we decided to screen our molecules against human breast cancer cell line MCF-7

2.5.1. (A): Cell culture and maintenance

Human breast cancer MCF-7 cells purchased from National Centre for Cell Science (NCCS), Pune, India cells were maintained in RPMI medium 1640 supplemented with 10% fetal bovine serum as well as 100 µg/mL streptomycin, 100 U/mL penicillin, 2 mM L-glutamine and Earle's BSS adjusted to contain 1.5 g/l Na bicarbonate, 0.1 mM nonessential amino acids, and 1.0 mM of Na pyruvate in a humidified atmosphere containing 5% CO₂ at 37 °C.

2.5.1 (B): In vitro cytotoxicity of synthesized **2.3 a**

Cell viability was determined by MTT assay. MCF-7 cells were seeded in 96-well plates at a concentration of 1.0x10⁴ cells/well and incubated overnight at 37°C in a 5% CO₂ humidified environment. Then the cells were treated with different concentrations of the sample **2.1f** like 10, 20, 30, 40, 50, 60, 70, 80, 90, and 100µM/mL (dissolved with RPMI medium 1640), respectively. Controls were cultivated under the same conditions without addition of **2.3a**. The treated cells were incubated for 48 h for cytotoxicity analysis. The cells were then subjected for MTT assay. The stock concentration (5 mg/mL) of MTT-(3-(4,5-Dimethylthiazol-2-yl)-2,5-diphenyltetrazolium bromide, a yellow tetrazole) was prepared and 100 µL of MTT was added in each wells and incubated for 4 h. Purple colour formazan crystals were observed and these crystals were dissolved with 100 µL of dimethyl sulphoxide (DMSO), and read at 620 nm in a multi well ELISA plate reader (Thermo, Multiskan). The dose dependent cytotoxicity was observed in the case of **2.3a** treated MCF-7 cells. Fifty percentage of cell death, which determines the inhibitory

concentration (IC₅₀) value of 2.3a against MCF-7 cells holds at 60 μ M in 48 h (Fig. 2.7). Which indicates that these molecules exhibit increased bioavailability and have tremendous anticancer potential.

Bioimaging studies

2.5.1 (C): DAPI (4, 6-Diamidino-2-phenylindole, dihydrochloride) staining

MCF-7 cells were treated with **2.3a** at its IC₅₀ concentration (60 μ M) for 48 h, and then fixed with methanol: acetic acid (3:1, v/v) prior to washing with PBS. The washed cells were then stained with 1 mg/mL DAPI (4, 6-diamidino-2-phenylindole, dihydrochloride) for 20 min in the dark atmosphere. Stained images were recorded with fluorescent microscope with appropriate excitation filter. The bright field and fluorescence microscopic images are shown in Fig. 2.8. As shown in Fig. 2.8. The strong bluish fluorescence and cellular uptake observed in the imaging studies with **2.3a** reveals that these molecules can act as a torch for locating malignant cell lines.

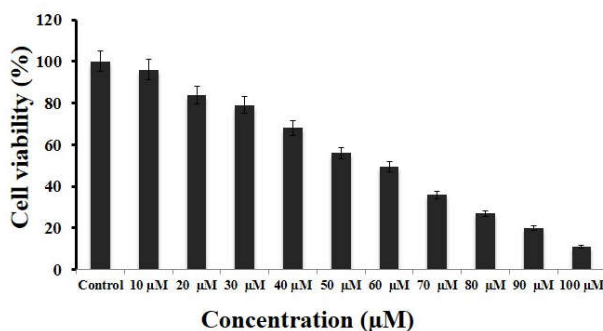


Fig. 2.7: MTT assay results confirming the in vitro cytotoxicity effect of 2.3a against the MCF-7 cells. The detected IC₅₀ concentration was 60 μ M.

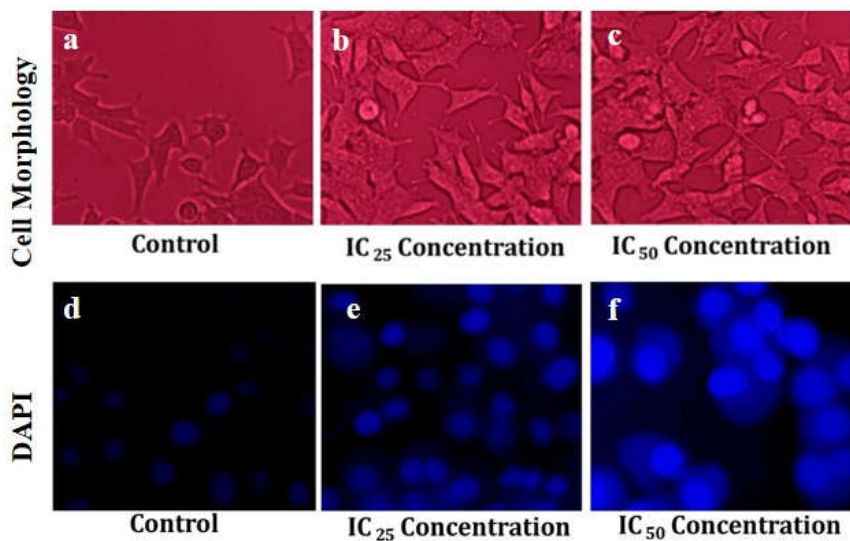


Fig. 2. 8: Bright field inverted light microscopy images (a, b, c) and the DAPI nuclear staining (d, e, f) of control cells and **2.3a** treated cells. The DAPI images exhibits condensed form of nuclear materials in apoptotic cells.

2.6 Synthesis of type 2 peptidomimetics: β -amino acid motifs functionalized chrome peptidomimetics

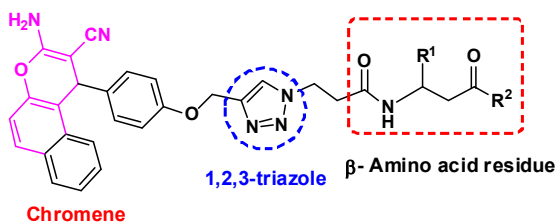
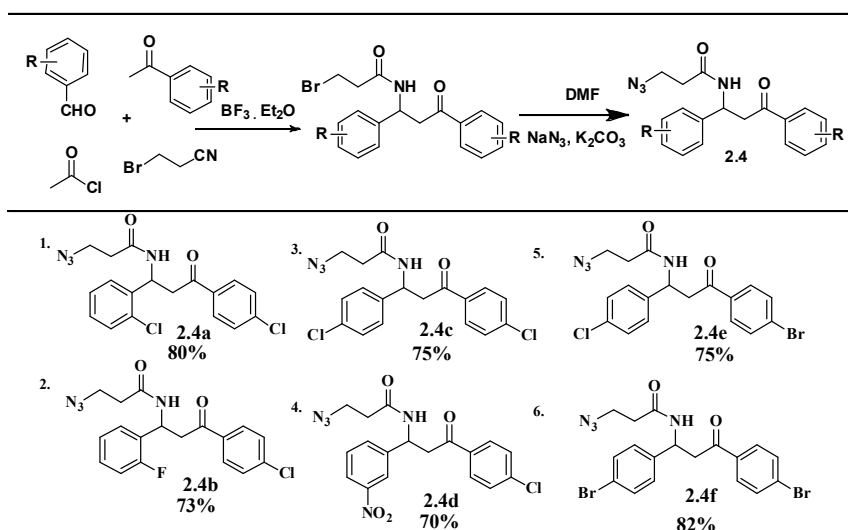


Fig.2.9: General structure of β -amino acid motifs functionalized peptidomimetics

The studies were extended to the randomization of alkynes **1** with β -amino acid residues to obtain the Type 2 peptidomimetics. The β -amino acid residues were synthesized in the form of an acetamide from an alternative Mannich type reaction. These keto acetamides are the

key components/intermediates of various pharmaceuticals and natural products such as β -amino acids, β -lactams, β -amino alcohols etc.¹⁹ In this reaction a bromo propionitrile react with a pair of enolizable (usually a ketone) and a non enolizable (aldehyde) oxo compounds in presence of an acid chloride and CuSO_4 as catalyst resulted in the formation of a bromo derivative of β -keto amides. These bromo derivatives were then converted to corresponding azide derivative by treating with sodium azide in presence of potassium carbonate in DMF at room temperature. The azide-functionalized β -amino acid type peptide residues **2.4a–f** were obtained from these two-step process are shown in Scheme 2.8.



Scheme 2.8: Synthesis of acetamide azides (β -amino acid equivalents) from an alternate Mannich type reaction

The chromene alkyne **2.1a–c** and the acetamide azides **2.4a–f** were then subjected to click cycloaddition reactions as shown in Scheme 2.9 to obtain the Type 2 peptidomimetics **2.5a–l**. As shown in Table 2.3,

Table 2.3: List of type 2 peptidomimetics

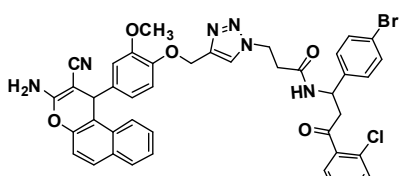
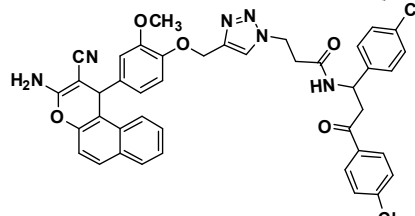
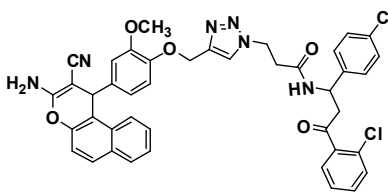
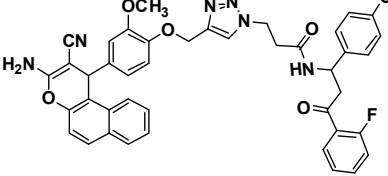
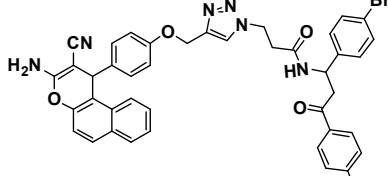
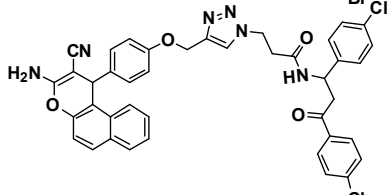
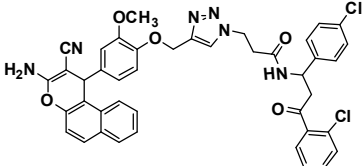
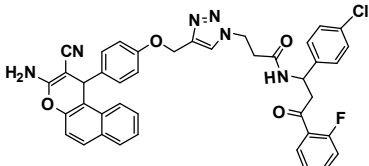
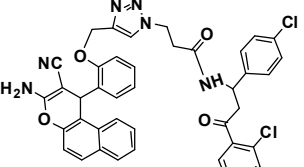
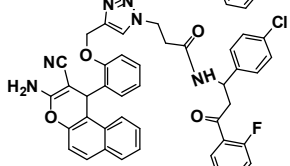
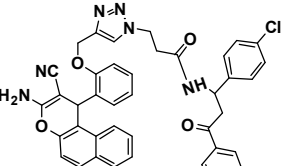
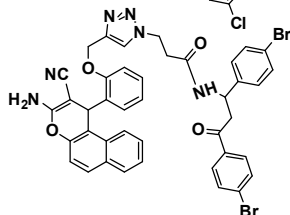
Entry	Peptidomimetic	% yield	Abs _{max} (nm)	Em _{max} (nm)	Stokes shift (nm)
2.5a		80%	352	434	82
2.5b		73%	372	434	62
2.5c		72%	375	434	59
2.5d		76%	370	434	64
2.5e		73%	351	409	58
2.5f		74%	350	419	69

Table 2.3 cont....

Entry	Peptidomimetic	% yield	Abs _{max} (nm)	Em _{max} (nm)	Stokes shift (nm)
2.5g		77%	349	434	85
2.5h		80%	374	434	60
2.5i		70%	379	436	63
2.5j		76%	373	434	64
2.5k		76%	348	434	86
2.5l		78%	346	409	63

2.7 Photophysical property evaluation

Similar to type 1 peptidomimetics, the photophysical properties of type 2 peptidomimetics **2.5a-l** were also evaluated under the same conditions mentioned in the previous case and the absorption, emission and Stokes shift values are listed in the table 2.3. The normalized absorption and emission spectra of the representative sample **2.5a** is shown in fig.2.11 Compound **2.5a** showed an absorption maxima centered at 352 nm and an emission maxima centered at 434 nm with a Stokes shift value of 82 nm. Fluorophores with large Stokes shifts are valuable tools for multicolour experiments to reduce the number of detection channels, to overcome cross-talk and simplifying the imaging scheme. In the case of compounds listed in table 2.3 they exhibit large Stokes shift values compared to the commercially available fluorophores. Compound 2.5g showed Maximum absorption maxima centered at 349 nm and an emission maxima centered at 434 nm with a Stokes shift value of 85nm which is comparable with commercial fluorophores. Also all molecules exhibit large Stokes shift values which is comparable with commercial fluorophores. Generally, the type 2 peptidomimetics, **2.5a-d** and **2.5h-j** were showed absorption maxima around 370 nm and emission maxima close to 450 nm which are comparable with the photophysical properties reported for commercial fluorophores such as Alexa Fluor® 405 (Abs/Em: 405 /421nm) and eFluor® 450 (Abs/Em: 405/450 nm).

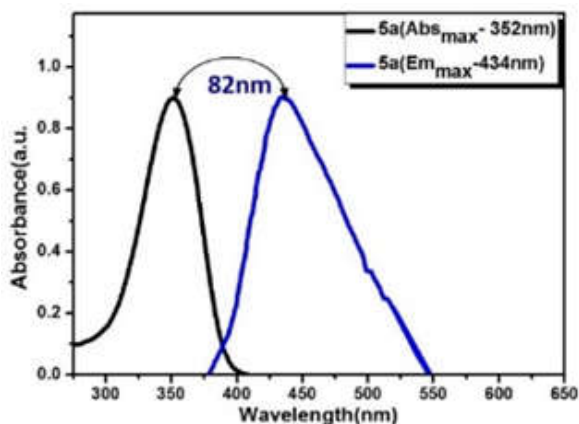


Fig. 2.11: Normalized absorption and emission spectra of 2.5a.

2.8 Evaluation of drug property descriptors

The drug property descriptors of type 2 peptidomimetics were also calculated and are also best fit for the beyond rule of five (bRo5) molecules. The drug property descriptor values are listed in the table 2.4.

Table 2.4: The drug property descriptors of type 2 peptidomimetics

Entry	Number of violations	Number of atoms	Log p <5	Molecular weight <500	Number of ON <10	Number of OH NH <5	Number of rotatable of bonds
2.5a	3	55	6.96	818.13	11	3	13
2.5b	3	55	6.88	773.68	11	3	13
2.5c	3	55	6.83	773.68	11	3	13
2.5d	3	55	6.32	757.22	11	3	13
2.5e	2	53	7.55	832.55	10	3	12
2.5f	2	53	7.29	743.65	10	3	12
2.5g	2	53	7.24	743.65	10	3	12
2.5h	2	53	6.73	727.20	10	3	12
2.5i	2	53	6.44	743.65	10	3	12
2.5j	2	53	5.93	727.20	10	3	12
2.5k	2	53	6.49	743.65	10	3	12
2.5l	2	53	6.75	832.55	10	3	12

2.9 Biological study: The in vitro anti-cancer activity evaluation.

The representative sample **2.5a** was analysed for its invitro cytotoxicity against human breast cancer cell lines based on the same procedure as in the case of type 1 peptidomimetics

2.9.1. (A): Cell culture and maintenance

Human breast cancer MCF-7 cells were maintained in RPMI medium 1640 supplemented with 10% fetal bovine serum as well as 100 µg/mL streptomycin, 100 U/mL penicillin, 2 mM L-glutamine and Earle's BSS adjusted to contain 1.5 g/l Na bicarbonate, 0.1 mM nonessential amino acids, and 1.0 mM of Na pyruate in a humidified atmosphere containing 5% CO₂ at 37 °C.

2.9.1 (B): In vitro cytotoxicity of **2.5a against MCF-7 cells**

Cell viability was determined by MTT assay. MCF-7 cells were seeded in 96-well plates at a concentration of 1.0x10⁴ cells/well and incubated overnight at 37°C in a 5% CO₂ humidified environment. Then the cells were treated with different concentrations of the sample **2.5a** such as 10, 20, 30, 40, 50, 60, 70, 80, 90, and 100µM/mL (dissolved with RPMI medium 1640), respectively. Controls were cultivated under the same conditions without addition of **2.5a**. The treated cells were incubated for 48 h for cytotoxicity analysis and then subjected for MTT assay. The stock concentration (5 mg/mL) of MTT-(3-(4,5-dimethylthiazol-2-yl)-2,5-diphenyltetrazolium bromide, a yellow tetrazole) was prepared and 100 µL of MTT was added in each

wells and incubated for 4 h. Purple color formazan crystals were observed and these crystals were dissolved with 100 μ L of dimethyl sulphoxide (DMSO), and read at 620 nm in a multi well ELISA plate reader (Thermo, Multiskan). The dose dependent cytotoxicity was observed in the case of **2.5a** treated MCF-7 cells. Fifty percentage of cell death, which determines the inhibitory concentration (IC₅₀) value of **2.5a** against MCF-7 cells holds at 50 μ M/mL in 48 h (Fig. 2.12). Which indicates that these molecules exhibit increased bioavailability and have tremendous anticancer potential.

2.9.1 (C): DAPI (4, 6-diamidino-2-phenylindole, dihydrochloride) staining

MCF-7 cells were treated with **2.5a** at its IC₅₀ concentration (50M/mL) for 48 h, and then fixed with methanol: acetic acid (3:1, v/v) prior to washing with PBS. The washed cells were then stained with 1 mg/mL DAPI (4, 6-Diamidino-2-phenylindole, dihydrochloride) for 20 min in the dark atmosphere. Stained images were recorded with fluorescent microscope with appropriate excitation filter. The bright field and fluorescence microscopic images are shown in Fig. 2.13. As shown in this the strong bluish fluorescence and cellular uptake observed in the imaging studies with **2.5a** reveals that these molecules have shown activity against breast cancer cell lines (MCF-7).

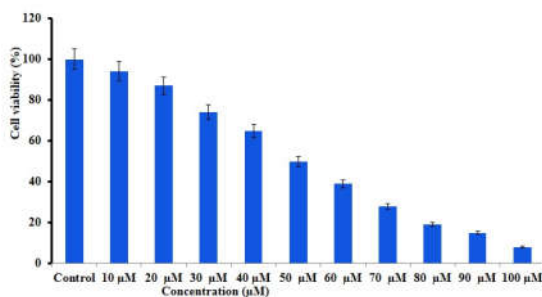


Fig.2. 12: MTT assay results confirming the in vitro cytotoxicity effect of 2.5a against the MCF-7 cells. The detected IC₅₀ concentration was 50 µM.

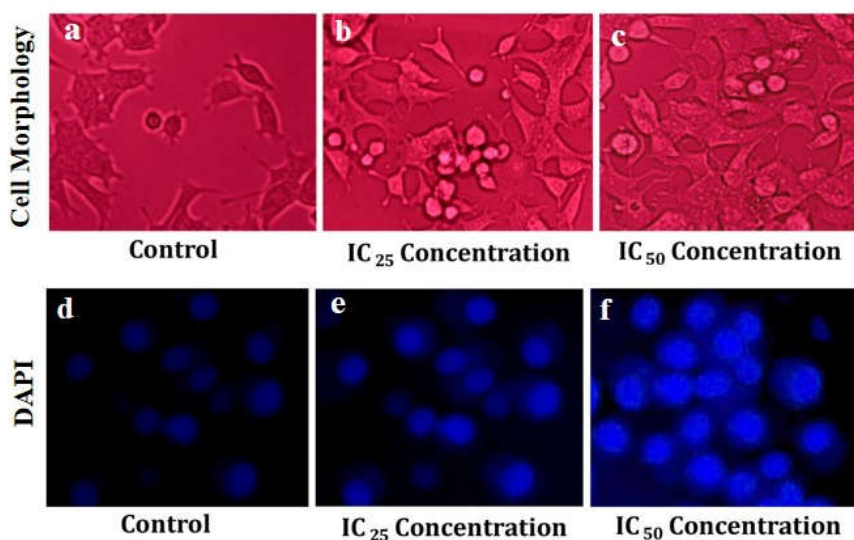


Fig. 2.13: Bright field inverted light microscopy images (a, b, c) and the DAPI nuclear staining (d, e, f) of control cells and 2.5a treated cells. The DAPI images exhibits condensed form of nuclear materials in apoptotic cells.

2.10 Conclusion:

In conclusion, we have developed a step economic and green strategy for the synthesis of a library of fluorescent chromene peptidomimetics with 2-in-1 properties such as fluorescent imaging and potential anticancer activity using a “Click with MCRs” concept. The fragments

(both chromene and peptide) were synthesized via multicomponent coupling reactions and were assembled using copper (I) catalyzed [3+2] azide-alkyne click chemistry. A total of 3 new alkynes, 10 new azides, and 24 new peptidomimetic fluorophores with anticancer activity were synthesized and discussed in this chapter. Fluorescence spectroscopic studies indicated that the efficiency of the new compounds, especially the Type 2 peptidomimetics are comparable with commercial Alexa Fluor® 405 and eFluor® 450, which are extensively used in flowcytometry. Similarly, the computation of drug property descriptors and the invitro cytotoxicity studies against human breast cancer cell lines MCF-7 suggests that, these molecules could modulate difficult target classes that have large, flat, and groove-shaped binding sites. This chapter has been published as a full length article in Molecular diversity (Springer) the copy of the paper is appended at the end of the thesis.

2.11 Structural characterization

2.11.1 Structure identification of 3-Amino-1-(2-(prop-2-yn-1-yloxy)phenyl)-1H-benzof[f]chromene-2-carbonitrile 2.1a

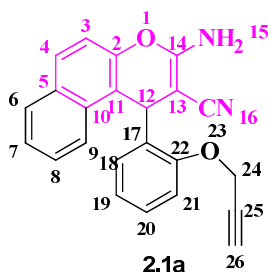


Fig. 2.14: structure of **2.1a**

The alkyne functionalized chromene **2.1a** is taken as a representative example for a general discussion on structure elucidation. The compound is numbered as shown in fig. 2.14. The FT-IR spectrum of the compound shows major absorptions at 3420, 3274, 3030, 2224, 2130, 1586, 1559, 1509 cm^{-1} . The band at 3420 cm^{-1} is due to the stretching vibration of free NH_2 group. The band at 2224 cm^{-1} due to the stretching vibration of C-N triple bond of nitrile group. The strong C-H stretching band of alkyl group is observed at 3274 and the weak band at 2130 represent the stretching vibration of C-C triple bond.

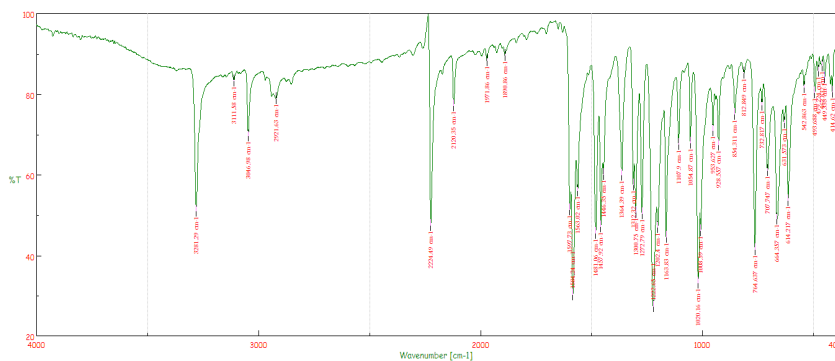


Fig. 2.15: FT-IR spectrum of compound **2.1a**

The initial information obtained from FT-IR spectrum was further confirmed by ^1H NMR analysis (Fig.2.16). The singlet observed at δ 8.75 in the ^1H NMR is attributed to $-\text{NH}_2$ proton at position 15. The singlet observed at δ 3.31 due to the CH proton at position 26. The singlet proton observed at δ 3.39 is attributed to $-\text{CH}_2$ proton at position 24. The singlet proton at δ 5.00 is due to the proton at C-12. The aromatic protons were observed as six set of signals such as 2 proton singlet at δ 7.13, a doublet at 7.20 with a J value of 7.5Hz, a doublet at 7.37 with a J value of 8Hz, multiplet between δ 7.67–7.77,

doublet at δ 7.80 with a J value of 8.5 Hz, a doublet at δ 8.00 with a J value of 8 Hz. The structure was further confirmed by ^{13}C NMR. The peak at δ 22.4 corresponds to the carbon at C-12 position. The peak observed at δ 78.2 and 79.2 corresponds to the carbons at position 25 and 26. The signal at δ 56.4 corresponds to the carbon at position 24. The signal at δ 59.2 corresponds to the carbon at position 13. The signal at δ 171.9 corresponds to the carbon at position 14. The aromatic carbons are observed at δ 112.9, 121.7-129.8, 130.5-133.9, 156.5, and 200.8. The peak observed at m/z 353.37 (M^+) in the mass spectrum (Figure 2.18) further confirms the structure of the compound.

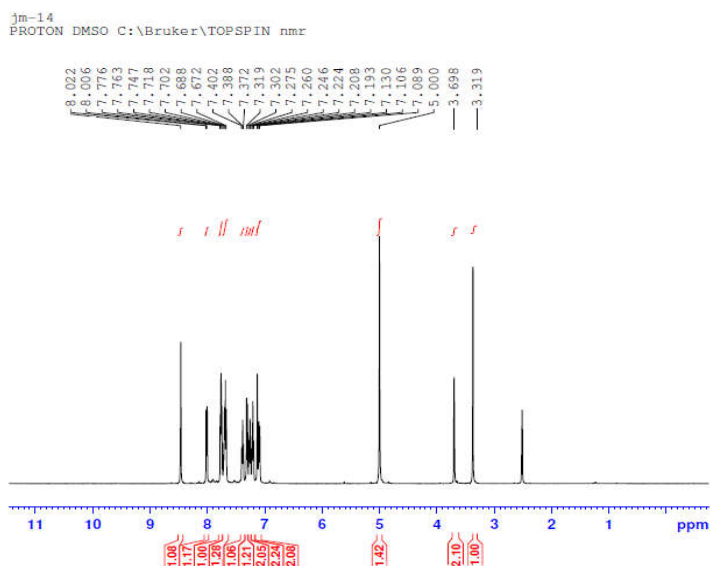


Fig. 2.16: ^1H -NMR spectrum of compound 2.1a

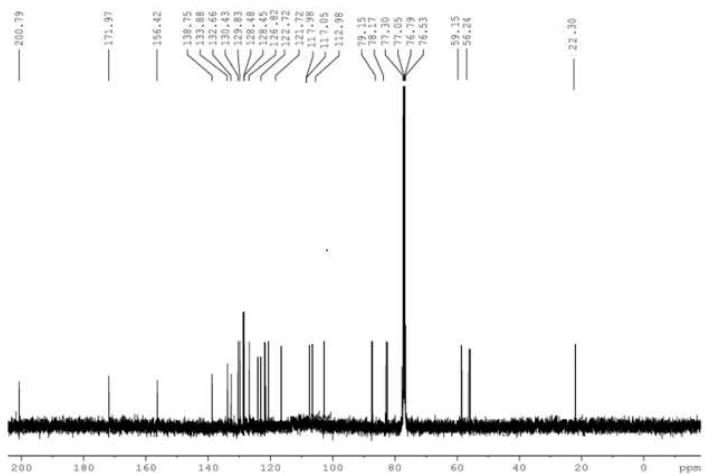


Fig. 2.17: ¹³C NMR spectrum of compound 2.1a

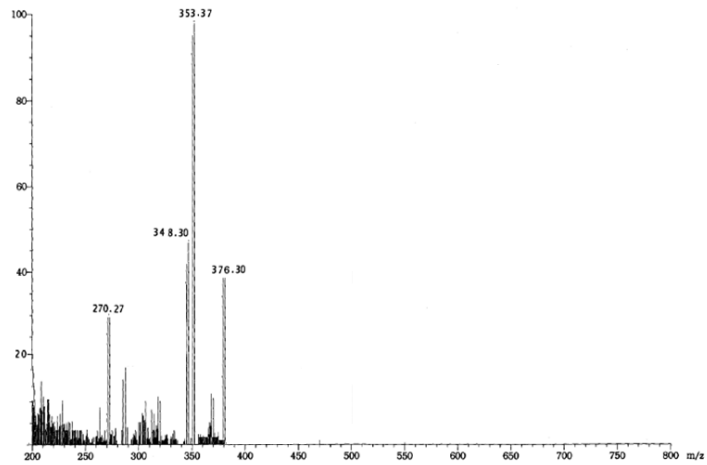


Fig. 2.18: EI-MS of compound 2.1a

2.11.2 Structure identification of 2-Azido-N-benzyl-N-(2-(tert-butylamino)-1-(2-chlorophenyl)-2-oxoethyl)acetamide 2.2a

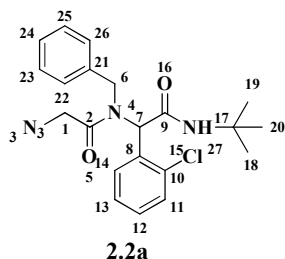


Fig.2.19: structure of 2.2a

The α -acyl amino acetamide **2.2a** was taken as the representative example for the structure elucidation. The compound is numbered as shown in fig. 2.19. The FT-IR spectrum of the compound showed major absorptions at 3304, 2101, 1685, 1649, 1552. The band observed at 3304 cm^{-1} is due to the NH stretching vibration of the acetamido group. The amide I band, i.e., band due to the C=O stretching vibration observed at 1685 cm^{-1} and the amide II band which arises from the interaction between the N-H bending and the C-N stretching of the C-N-H group is obtained at 1586 cm^{-1} . The absorption at 1649 cm^{-1} is due to the C=O stretching vibration of the ketone group.

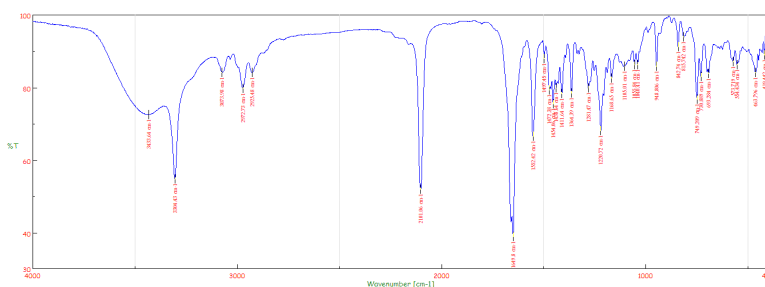


Fig. 2.20: FT-IR spectrum of compound 2.2a

The preliminary information obtained from FT-IR spectrum was further confirmed by ^1H NMR analysis. The 9 proton singlet observed at δ 1.15 corresponds to the three $-\text{CH}_3$ group present at position at 18, 19 and 20. The singlet at δ 1.62 is due to the $-\text{CH}_2$ group at the position 1. The singlet observed at δ 4.58 is attributed to $-\text{CH}_2$ protons at position 6. The singlet at δ 6.38 is attributed to $-\text{CH}$ proton at position 7. The aromatic protons were observed between δ 6.95-7.26. The NH proton singlet observed was observed at δ 7.53

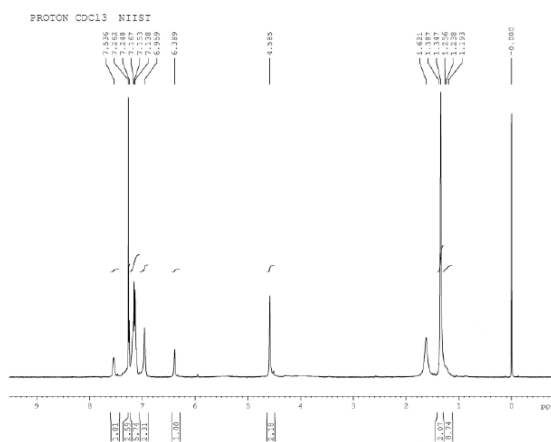


Fig. 2.21: ^1H -NMR spectrum of compound 2.2a

The structure was further confirmed by ^{13}C NMR analysis. The peaks observed at δ 30.6, 30.8, 31.1 are corresponds to the carbons at position 18, 19 and 20. The peak observed at δ 42.7 corresponds to the carbon at position 6. The peak observed at δ 48.3 corresponds to the carbon at position 17. The peak observed at δ 51.7 corresponds to the carbon at position 1. The peak at δ 52.2 corresponds to the carbon at position 7. The aromatic protons were observed at δ 126.8-129.7, and at 130.1-137.9. The peak observed at δ 167.0 corresponds to the carbon

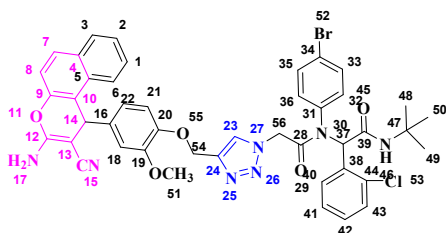


Fig. 2.24: structure of compound 2.3a

The chromene-triazole-carboxamide conjugate named as type one peptidomimetics obtained by the click ligation reaction of alkyne functionalized chromene and Ugi azide **2.3a** is taken as a representative example of this library for the structure elucidation. The compound is numbered as shown in fig.2.24. The FT-IR spectrum of the compound shows major absorptions at 3422, 3422, 3369, 2923, 2853, 2224, 1649, 1669, 1586, 1566 cm^{-1} . The band at 3369 cm^{-1} is due to the NH stretching vibration of the acetamido group. The amide I band, i.e., band due to the C=O stretching vibration occurs at 1669 cm^{-1} and the amide II band which arises from the interaction between the N-H bending and the C-N stretching of the C-N-H group is obtained at 1586 cm^{-1} . The absorption at 1649 cm^{-1} is due to the C=O stretching vibration of the ketone part. The band at 3422 cm^{-1} is due to the stretching vibration of free NH_2 group. The band at 2224 cm^{-1} due to the stretching vibration of C-N triple bond of nitrile group.

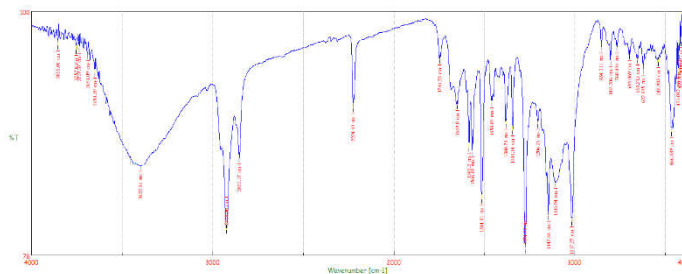


Fig. 2.25: the FT-IR spectrum of the compound **2.3a**

The initial information obtained from FT-IR spectrum was further confirmed by ^1H NMR studies. Fig. 2.26. The 9 proton singlet observed at δ 1.15 corresponds to the three $-\text{CH}_3$ group at the position at 48, 49 and 50. The singlet observed at δ 3.82 due to the three $-\text{OCH}_3$ proton at position 51. The singlet at δ 4.81 due to the CH_2 proton at position 56. The singlet proton observed at δ 4.91 attributed to $-\text{CH}$ proton at position 14. The singlet proton at δ 5.33 is due to the $-\text{CH}$ proton at C-12. The aromatic protons observed as four set of signals. 2 proton singlet at δ 5.89, a singlet at 6.31, the multiplet between δ 7.06–7.66, a singlet at δ 8.23. The singlet observed at δ 8.38 is attributed to $-\text{NH}_2$ proton at position 17. The structure was further confirmed by ^{13}C NMR. The peak at δ 24.8 corresponds to the carbon at C-14 position. The peak observed at 28.6, 28.7, and 28.8 corresponds to the carbon atom at positions 48, 49 and 50. The peak at δ 68.8 corresponds to the carbon at position 37. The peak observed at δ 75.2 corresponds to the carbon at position 54. The aromatic carbons are observed at δ 112.8-117.4, 121.2-129.6, 131.9-138.6, 148.6-151.8, 165.3, and 168.3. The signal at δ 177.3 corresponds to the carbon at position 12. The peak at m/z 862.17(M+1) in the mass spectrum (Fig. 2.28) further confirms the structure of the compound

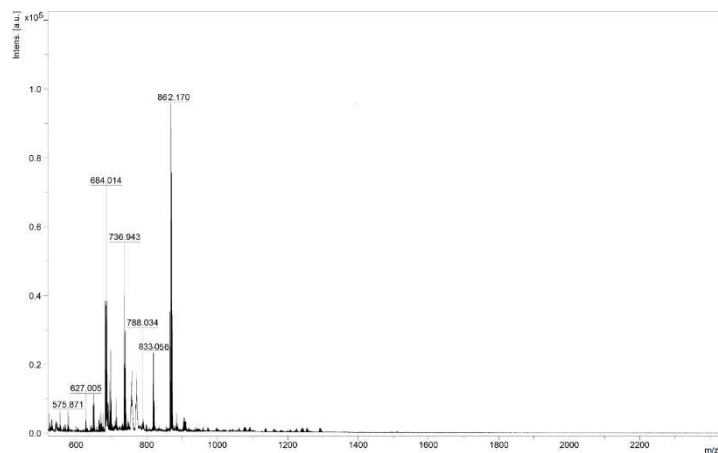


Fig. 2.28: the MALDI-Mass spectrum of the compound 2.3a

2.11.4 Structure identification of 3-Azido-N-(1-(2-chlorophenyl)-3-(4-chlorophenyl)-3-oxopropyl)propanamide

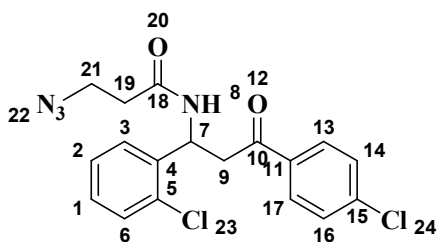


Fig.2.29: structure of compound 2.4a

The FT-IR spectrum of the compound showed major absorptions at 3294, 2923, 2852, 2112, 1683, 1646, 1588. The band at 3369 cm^{-1} is due to the NH stretching vibration of the acetamido group. The amide I band, i.e., the band due to the C=O stretching vibration of (C18) occurs at 1646 cm^{-1} and the amide II band which arises from the interaction between the N-H bending and the C-N stretching of the C-N-H group

is obtained at 1588cm^{-1} . The peak observed at 1686cm^{-1} is due to the $\text{C}=\text{O}$ stretching vibration of the ketone part at position 10.

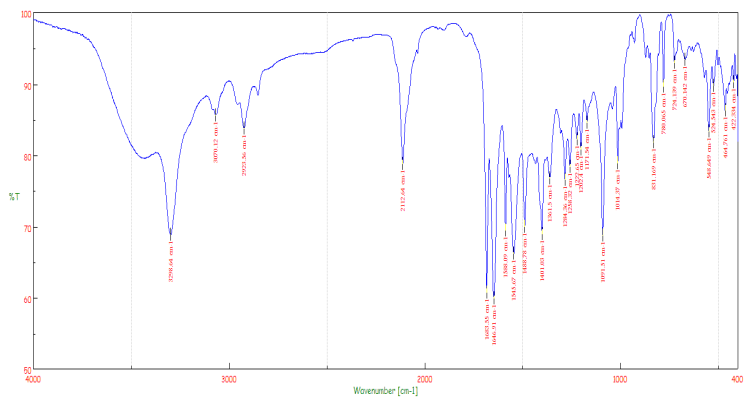


Fig. 2.30: the FT-IR spectrum of the compound 2.4a

The initial information obtained from FT-IR spectrum was further confirmed by ^1H NMR studies. The triplet at δ 1.73 due to the CH_2 proton at position 21. The triplet observed at δ 2.45 due to the CH_2 proton at position 19. The doublet of doublet observed at δ 2.67 and δ 3.38 is attributed to $-\text{CH}$ proton at position 9. The singlet at δ 5.46 due to the $-\text{CH}$ proton at position 7. The aromatic protons were observed between δ 6.89-7.43 (multiplet) and one proton doublet with $J=7$ Hz at 7.41-7.43.

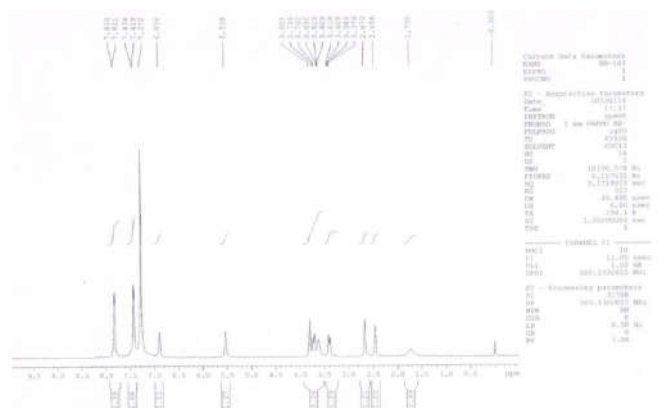


Fig. 2.31: the ^1H -NMR spectrum of the compound 2.4a

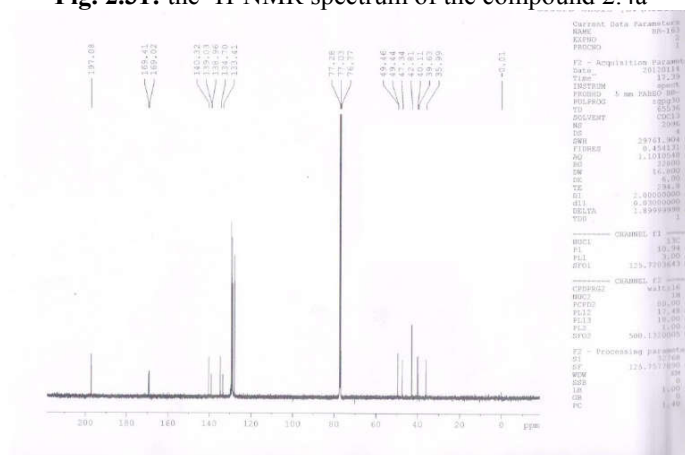


Fig. 2.32: The ^{13}C -NMR spectrum of the compound 2.4a

The structure was further confirmed by ^{13}C NMR. The peak observed at δ 35.6 corresponds to the carbon at C-19 position. The peak at δ 46.4 corresponds to the carbon at C-21 position. The peak observed at δ 48.2 corresponds to the carbon atom at positions 7. The peak at δ 77.3 corresponds to the carbon at position 9. The aromatic carbons are observed at δ 128.3-128.9, 130.3-137.6, and at 140.2-141.4. The signal at δ 197.5 corresponds to the carbon at position 10. The signal at δ 169.1 corresponds to the carbon at position 18. The structure was

further confirmed by Mass spectral analysis, EI-MS: m/z calculated for $C_{18}H_{16}Cl_2N_4O_2$: 391.25 and found: 391.0(M^+)

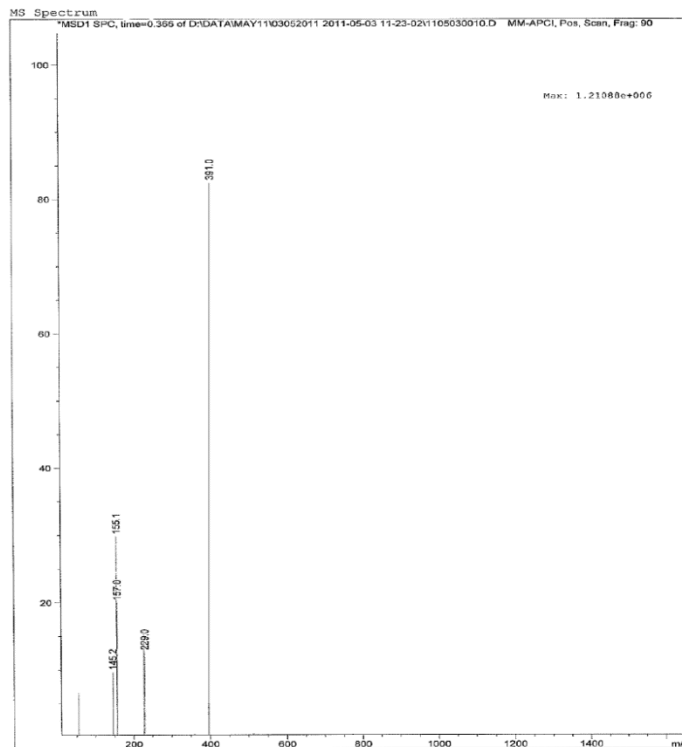


Fig.2.33: the Mass spectrum of the compound 2.4a

2.11.5: Structure identification of 3-(4-((4-(3-Amino-2-cyano-1H-benzo[f]chromen-1-yl)-2-methoxyphenoxy)methyl)-1H-1,2,3-triazol-1-yl)-N-(1-(4-bromophenyl)-3-(2-chlorophenyl)-3-oxopropyl)propanamide

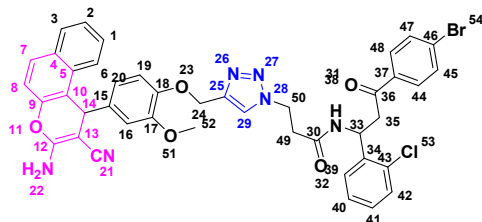


Fig. 2.34: structure of compound 2.5a

The chromene-triazole-ketoamide peptidomimetic **2.5a** was taken as a representative example for a discussion on structure elucidation. The compound is numbered as shown in fig.2.34. The FT-IR spectrum of the compound showed major absorptions at 3424, 3279, 2925, 2853, 2224, 1746, 1651, 1686, 1566 cm^{-1} . The band at 3369 cm^{-1} is due to the NH stretching vibration of the acetamido group. The amide I band, i.e., the band due to the C=O stretching vibration of (C-30) occurs at 1651 cm^{-1} and the amide II band which arises from the interaction between the N-H bending and the C-N stretching of the C-N-H group is obtained at 1566 cm^{-1} . The absorption at 1686 cm^{-1} is due to the C=O stretching vibration of the keto group at position 36. The band at 3424 cm^{-1} is due to the stretching vibration of free NH_2 group. The band at 2224 cm^{-1} due to the stretching vibration of C-N triple bond of nitrile group.

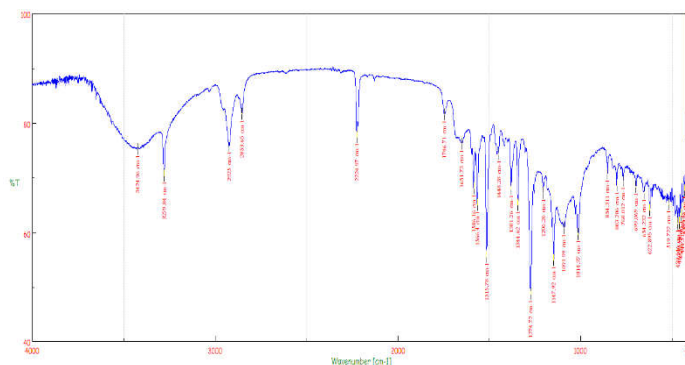


Fig.2.35: FT-IR spectrum of compound 2.5a

The initial information obtained from FT-IR spectrum was further confirmed by ^1H NMR analysis. The triplet at observed δ 2.66 is due to the CH_2 proton at position 49. The doublet of doublet observed at 3.23 is attributed to the CH proton at position 35. The singlet observed at δ 3.82 is due to the three $-\text{OCH}_3$ proton at position 52. The triplet at δ 4.06 is attributed to the CH_2 proton at position 50. The singlet observed at δ 4.98 is attributed to the proton at carbon 14. The singlet at δ 5.62 due to the CH_2 proton at position 24. The singlet at δ 5.46 due to the -CH proton at position 33. The aromatic protons were observed in the following regions. One proton singlets at δ 6.31, 6.63, δ 6.87 and a multiplet between δ 7.27–7.89. The triazole proton was observed at δ 7.57. The singlet observed at δ 8.23 is due to the NH proton at position 31. Finally, the singlet observed at δ 8.38 is attributed to $-\text{NH}_2$ protons at position 22.

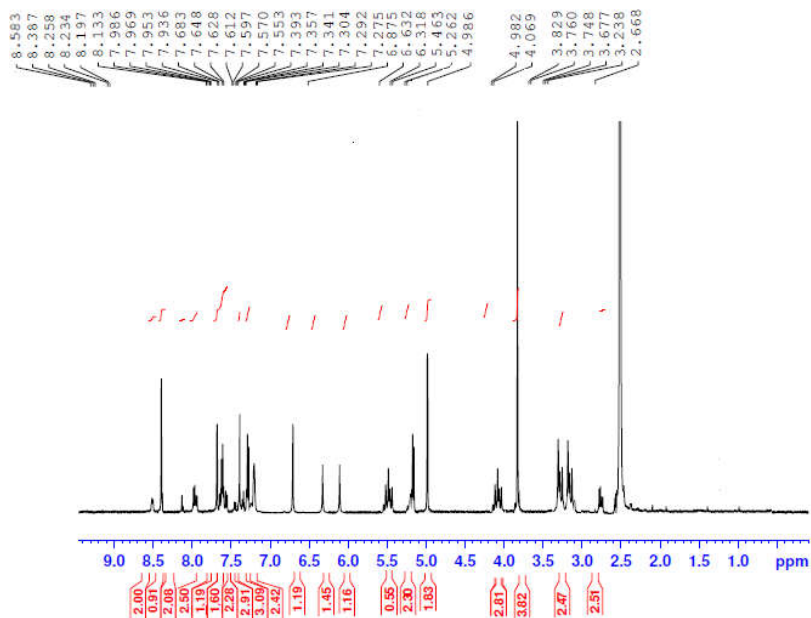


Fig. 2.36: $^1\text{H-NMR}$ spectrum of compound 2.5a

The structure was further confirmed by ^{13}C NMR. The peak observed at δ 28.1 corresponds to the carbon at C-14 position, the peak at δ 30.9 corresponds to the carbon at C-49 position, the peak observed at δ 45.5 corresponds to the carbon atom at positions 50 and the peak at δ 56.7 corresponds to the $-\text{OCH}_3$ carbon at position 52. The peak at δ 59.2 corresponds to the carbon at position 13 and the peak observed at δ 72.2 corresponds to the carbon at position 35. The peak at δ 73.5 corresponds to the carbon at position 24 and the peak observed at δ 117.3 corresponds to the carbon at position 21. The aromatic carbons were observed at δ 111.4-114.3, 121.9-129.0, 131.2-138.5, and 141.3-142.8. The signal at δ 150.0 corresponds to the carbon at position 9. The signal at δ 172.24 corresponds to the carbon at position 30. The

signal at δ 177.4 corresponds to the carbon at position 12. The signal at δ 206.8 corresponds to the carbon at position 36. Final confirmation of the structure of the compound was obtained from mass spectral analysis. MALDI: m/z calculated for $C_{42}H_{34}BrClN_6O_5$: 818.08, found: 819.040(M+1). (fig.2.38)

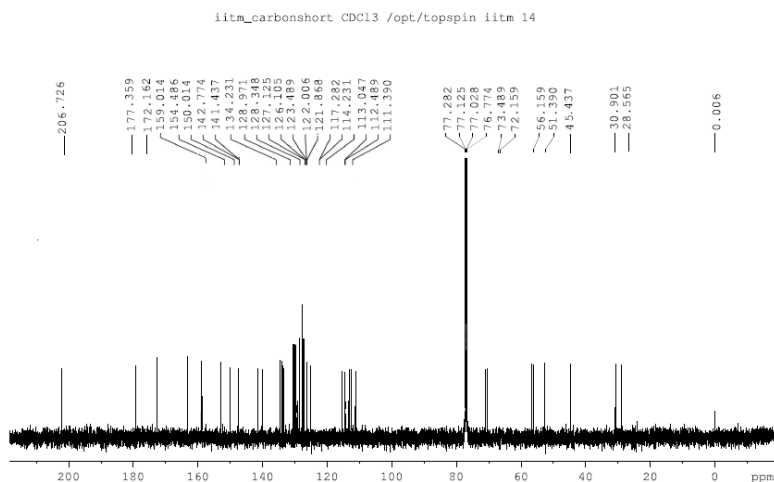


Fig. 2.37: ^{13}C -NMR spectrum of compound 2.5a

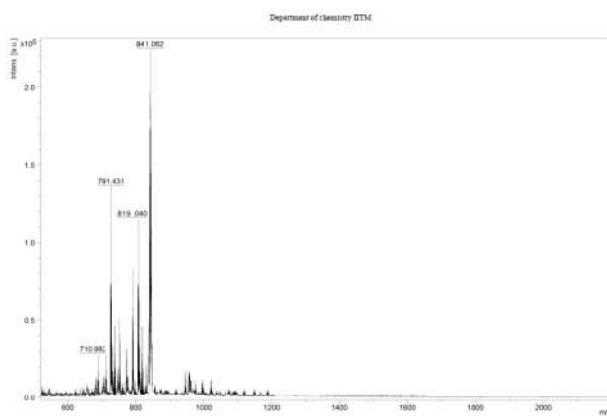


Fig. 2.38: Mass spectrum of compound 2.5a

2.12. Experimental Section

IR spectra were recorded on a JASCO-FT/IR-4100 Fourier transform infrared spectrometer by making KBr pellets of the samples. ^1H and ^{13}C NMR spectra were determined in DMSO using a Bruker amx 500 MHz spectrometer. The chemical shifts (δ) are given relative to tetramethylsilane (TMS) and the coupling constants (J) are reported in hertz (Hz). Electron spray ionization mass spectra were recorded with a Thermo scientific exactive mass spectrometer. HPLC analysis was done using aDionex Ultimate 3000 system. Fluorescence spectra were recorded with a Perkin Elmer LS 45 spectrometer. MALDI-TOF mass-spectra of the compounds were obtained from a Bruker Ultraflextreme using 2, 5-dihydroxybenzoic acid as a matrix and a ground steel target plate.

2.12.1. General experimental procedure for the synthesis of 3-Amino-1-(2-(prop-2-yn-1-yloxy)phenyl)-1H-benzo[*f*]chromene-2-

carbonitrile 2.1a: A mixture of propargylated aromatic aldehyde(160 mg, 1mmol),2-naphthol (144mg, 1 mmol), malononitrile (66mg, 1mmol) and sodium carbonate (0.106 mg, 0.01mmol) were mixed together by using a mortar and pestle. The resulted solid was heated in an oven at 80°C for 10 min. After cooling, the mixture was washed with hot water and the solid separated was filtered and dried. The solid was then recrystallized from hot ethanol to obtain pure **1a**: 300mg white solid M.P :110-112°C. ^1H NMR (DMSO,500MHz), δ_{H} (ppm): 3.319 (s,1H, CH), 3.398(s,2H), 5.00(s,1H), 7.089(d,2H, $J=8.5\text{Hz}$), 7.130(s,2H), 7.208 (d,2H, $J=7.5\text{Hz}$), 7.37(d,1H, $J=8\text{Hz}$), 7.672–7.776 (m, 3H), 7.809 (d,2H, $J=8.5\text{ Hz}$), 8.006(d,1H, $J=8\text{Hz}$), 8.022 (S, 1H,

$J=8\text{Hz}$). ^{13}C NMR (DMSO-(d₆), 125 MHz) δ_c (ppm): 22.4, 56.4, 59.2, 78.2, 79.2, 112.9, 117.1, 117.9, 121.7, 122.8, 126.9, 128.5, 128.5, 129.8, 130.5, 130.5, 132.7, 133.8, 133.9, 156.5, 171.9, 200.8. IR (KBr) ν max: 3274, 3030, 2921, 2851, 2224, 2130, 1747, 1601, 1586, 1559, 1509, 1454, 1428, 1375, 1318, 1261, 1237, 1186, 1125, 1009, 9680, 937, 835, 818, 720, 664, 632, 612, 534, 463, 446 cm^{-1} . m/z calculated for $\text{C}_{23}\text{H}_{16}\text{N}_2\text{O}_2$: 352.3847 and found: 353.37 (M⁺).

2.12.2. 3-Amino-1-(4-(prop-2-yn-1-yloxy)phenyl)-1H-benzo[*f*]chromene-2-carbonitrile 2.1b: 310mg, as white solid, M.P. 111-113^oC. ^1H NMR (DMSO, 500 MHz), δ_H (ppm): 3.13 (s, 1H, CH), 3.681 (s, 2H), 4.978 (s, 1H), 7.096 (s, 2H), 7.208 (d, 2H, $J=8\text{Hz}$), 7.37 (d, 1H, $J=8\text{Hz}$), 7.672–7.776 (m, 3H), 7.809 (d, 2H, $J=8.5\text{ Hz}$), 8.006 (d, 1H, $J=8\text{Hz}$), 8.022 (s, 1H, $J=8\text{Hz}$). ^{13}C NMR (DMSO-(d₆), 125 MHz) δ_c (ppm): 22.3, 56.3, 59.2, 78.2, 79.2, 112.9, 117.1, 117.9, 121.8, 122.8, 126.9, 128.5, 128.5, 129.8, 129.9, 130.4, 130.5, 132.6, 133.8, 133.8, 156.5, 171.9. IR (KBr) ν max: 3281, 3111, 3046, 2921, 2224, 2120, 1971, 1890, 1597, 1584, 1563, 1481, 1457, 1446, 1364, 1312, 1300, 1272, 1222, 1202, 1163, 1107, 1054, 1020, 1008, 953, 928, 854, 812, 764, 732, 707, 664, 6142, 631, 614, 542, 493, 479, 449, 414 cm^{-1} . m/z calculated for $\text{C}_{23}\text{H}_{16}\text{N}_2\text{O}_2$: 352.3847 and found: 353.37 (M⁺).

2.12.3. 3-Amino-1-(3-methoxy-4-(prop-2-yn-1-yloxy) phenyl)-1H-benzo[*f*]chromene-2-carbonitrile 2.1c: 330mg as yellow solid, M.P 111-113^oC. ^1H NMR (DMSO, 500MHz), δ_H (ppm): 3.339 (s, 1H), 3.675 (s, 1H), 3.827 (s, 3H), 4.981 (s, 1H), 7.089 (d, 2H, $J=8.5\text{Hz}$), 7.130 (s, 2H), 7.208 (d, 2H, $J=7.5\text{Hz}$), 7.37 (d, 1H, $J=8\text{Hz}$), 7.672-7.776

(m, 3H), 8.006 (d,1H,J=8Hz), 8.022 (d,1H,J=8Hz). ^{13}C NMR (DMSO- d_6),125MHz) δ_c (ppm):27.9, 54.3, 56.2, 59.3, 78.2, 79.2, 112.9, 117.1, 117.9, 121.8, 122.8, 122.8, 128.7, 128.8, 128.9, 129.8, 129.8, 130.9, 130.9, 132.7, 134.8, 139.8, 157.4, 172.9. IR (KBr) ν max : 3363, 3279, 3029, 2966, 2857, 2613, 2312, 2223, 2129, 1629, 1598, 1585, 1562, 1514, 1456, 1448, 1417, 1380, 1344, 1305, 1273, 1254, 1206, 1147, 1013, 958, 853,802, 767,741, 699, 653, 621, 611,552, 480,463,419 cm^{-1} . m/z calculated for $\text{C}_{24}\text{H}_{18}\text{N}_2\text{O}_3$:382.4106 and found : 382.32 (M+).

2.12.4. General experimental procedure for the synthesis of 2-{{N-Benzyl-(N-1-azidopropan-2-one)-N-tert-butyl-2-(2-chlorophenyl)}} acetamide 2.2a

acetamide 2.2a: An equimolar amount of 2-chlorobenzaldehyde (140 mg, 1 mmol), and benzyl amine (107 mg, 1 mmol), were taken in dichloromethane (8 ml), and stirred at room temperature for 20 min. to form the Schiff-base. To this, 1 equivalent of tertiary -butyl isocyanide (94 mg, 1 mmol) and chloroacetic acid (83 mg, 1 mmol) were added and stirring was continued at room temperature. The reaction was monitored by TLC and found to complete after 48h. The solvent was evaporated under vacuum and the residue was washed with petroleum ether (5 -15 ml) to afford the chloro derivative of the Ugi reaction product (carboxamide chloride). In a subsequent step, the carboxamide chloride (407 mg, 1 mmol), K_2CO_3 (414 mg, 3 mmol), and NaN_3 (65 mg, 1 mmol) were stirred at room temperature for 4 h in dimethyl formamide. After completion of the reaction, the reaction mixture was poured into ice cold water. The solid product obtained was filtered and dried under vacuum to afford 2-{{Nbenzyl-(N-1-azidopropan-2-one)-

N-tert-butyl-2-(2-chlorophenyl)]} acetamide **2.2a** 0.335 g (yield 81%) as white solid. M.P. 151-153°C. ¹H NMR (CDCl₃, 500 MHz) δ_H (ppm): 1.25 (s, 9H), 1.62 (s, 2H), 4.58 (s, 2H), 6.38 (s, 1H), 6.95–7.26 (m, 9H), 7.53 (s, 1H). ¹³C NMR (DMSO-(d₆), 125 MHz) δ_C (ppm): 31.1, 42.7, 48.3, 51.7, 52.2, 126.8, 127.2, 128.4, 129.6, 129.7, 130.1, 132.5, 134.7, 137.7, 137.9, 167.0, 167.2. IR (KBr) ν max: 3304, 3073, 2972, 2925, 2100, 1659, 1648, 1552, 1497, 1472, 1454, 1438, 1411, 1365, 1282, 1220, 1168, 1055, 1040, 994, 842, 816, 748, 728, 693, 574, 555 cm⁻¹. m/z calculated for C₂₁ H₂₄ Cl N₅O₂: 413.8996 and found EI-MS: 414.4 (M⁺).

2.12.5. General experimental procedure for the Synthesis of 2-(4-((4-(3-Amino-2-cyano-1H-benzof[f]chromen-1-yl)-2-methoxyphenoxy)methyl)-1H-1,2,3-triazol-1-yl)-N-(4-bromophenyl)-N-(2-(tert-butylamino)-1-(2-chlorophenyl)-2-oxoethyl) acetamide 2.3a: The chromene **2.1c** (353mg, 1 mmol) and the carboxamide azide **2b** (379g, 1 mmol) were dissolved in minimum amount of DMSO. To this, 2 ml of *t*-BuOH, 1 ml of water, CuSO₄ 5H₂O (11 mg), and sodium ascorbate (50 mg) were added and stirred at room temperature for 12 h. After 12 h, the mixture was poured in to cold water. The precipitated solid was collected and washed with water and dried. The dried product was washed with diethyl ether (3.5 ml) to afford **3a**: ¹H NMR (DMSO, 500MHz) δ_H (ppm): 1.154(s,9H), 3.825(s, 3H), 4.814(s,2H), 4.917(s,2H), 5.337(s,3H), 5.529(s, 2H), 5.892(s,2H), 6.318(s,1H), 7.069-7.668(m, 16H), 8.234(s,2H), 8.350(s, 1H), 8.388(s,2H). ¹³C NMR (DMSO-(d₆), 125 MHz) δ_C (ppm): 24.8, 28.6, 28.7, 28.8, 52.8, 57.1, 59.6, 68.8, 75.2, 112.8, 112.9, 115.8, 115.9, 117.4, 121.2, 121.2,

122.2, 122.3, 122.4, 122.9, 124.7, 124.8, 126.2, 126.4, 127.4, 128.1, 128.2, 128.8, 128.9, 129.4, 129.6, 131.9, 132.2, 138.3, 138.3, 138.5, 138.6, 148.6, 148.8, 150.3, 151.8, 165.3, 168.3, 177.3. IR (KBr) ν max: 3369, 2924, 2853, 2225, 1669, 1586, 1567, 1508, 1455, 1426, 1365, 1337, 1274, 1144, 1020, 851, 808, 755, 730, 697, 626, 538, 466, 451, 420 cm^{-1} . m/z calculated for $\text{C}_{44}\text{H}_{39}\text{BrClN}_7\text{O}_5$: 861.1528 and found MALDI: 862.17(M+1).

2.12.6. 2-(4-((4-(3-Amino-2-cyano-1H-benzof[f]chromen-1-yl)-2-methoxyphenoxy) methyl)-1H-1, 2, 3-triazol-1-yl)-N-benzyl-N-(2-(tert-butylamino)-1-(2-chlorophenyl)-2-oxoethyl)acetamide 3b:

Yellow Solid, 309 mg, 76%, M.P: 163-164 $^{\circ}$ C. ^1H NMR (DMSO, 500MHz) δ_{H} (ppm): 1.256 (s, 9H), 1.621 (s, 2H), 3.825 (s, 3H), 4.286 (s, 1H), 4.918 (s, 2H), 4.952 (s, 1H), 5.318 (s, 1H), 6.273 (s, 1H), 6.965 (s, 1H), 7.128-7.630 (m, 18H), 8.058 (s, 1H), 8.197 (s, 1H), 8.387 (s, 1H). ^{13}C NMR (DMSO-(d₆), 125 MHz) δ_{C} (ppm): 28.2, 29.7, 29.8, 29.9, 49.1, 56.1, 56.2, 57.2, 62.9, 64.9, 72.2, 111.2, 113.3, 113.5, 114.4, 121, 122.2, 122.3, 122.4, 122.9, 124.7, 124.8, 125.3, 126.2, 126.3, 127.3, 128.2, 128.2, 128.8, 128.9, 129.1, 131.8, 131.9, 135.4, 138.3, 138.4, 138.5, 142.2, 149.9, 152.2, 159.2, 165.2, 167.6, 177.2. IR (KBr) ν max: 3322, 2923, 2853, 2224, 1746, 1677, 1655, 1567, 1513, 1486, 1458, 1425, 1377, 1343, 1147, 107, 1017, 853, 723, 591, 522, 496, 467, 410 cm^{-1} . m/z calculated for $\text{C}_{45}\text{H}_{42}\text{ClN}_7\text{O}_5$: 819.272 and found MALDI: 819.31(M+1).

2.12.7. **2-(4-((4-(3-Amino-2-cyano-1H-benzof[f]chromen-1-yl)phenoxy)methyl)-1H-1,2,3-triazol-1-yl)-N-(4-bromophenyl)-N-(2-(tert-butylamino)-1-(2-chlorophenyl)-2-oxoethyl)acetamide** **3e:**
Yellow Solid, 301 mg, 73%, M.P: 161-163⁰C. ¹H NMR (DMSO, 500 MHz) δ_{H} (ppm): 1.129 (s,3H), 4.819 (s,2H), 4.920 (s,2H), 5.368 (s,3H), 5.320 (s,1H), 5.898 (s, 2H), 5.892 (s,2H), 6.334 (s,1H), 7.099-7.688 (m,12H), 8.032 (s,1H), 8.364 (s, 1H), 8.378 (s,2H). ¹³C NMR (DMSO-(d6), 125 MHz) δ_{C} (ppm):27.2, 28.7, 29.8, 30.9, 56.2, 57.3, 62.9, 64.9, 72.2, 111.4,113.2,113.5, 114.4, 117.2, 118.3, 121.2,122.2, 122.3, 122.3, 123.4, 125.4, 127.5, 128.1, 128.2 , 128.4, 128.4, 128.9,129.0 , 129.2, 129.5 ,131.8, 135.4, 135.5, 138.3,138.4,138.5, 142.2, 149.9, 152.2, 159.3, 165.2, 167.6, 177.2. IR (KBr) ν max: 3422, 2923, 3853, 2224, 1747, 1671, 1601, 1586, 1559, 1509, 1460, 1377, 1262, 1184, 1017, 835, 720, 664, 613, 536, 470, 455, 428 cm^{-1} . m/z calculated for C₄₃H₃₇BrClN₇O₄:831.1323 and found MALDI: 832.140(M+1).

2.12.8. **2-(4-((4-(3-Amino-2-cyano-1H-benzof[f]chromen-1-yl)phenoxy)methyl)-1H-1,2,3-triazol-1-yl)-N-benzyl-N-(2-(tert-butylamino)-1-(2-chlorophenyl)-2-oxoethyl)acetamide** **3f:** Yellow Solid, 313mg, 76%, M.P: 162-164⁰C ¹H NMR (DMSO, 500 MHz) δ_{H} (ppm): 1.193 (s,9H), 4.468 (s,2H), 4.919 (s,2H), 4.980 (s,1H), 5.136 (s,2H), 7.099-7.630 (m,18H), 8.234 (s,2H), 8.285 (s,1H), 8.364 (s,2H). ¹³C-NMR(DMSO-(d6),125MHz) δ_{C} (ppm): 28.7, 28.7, 29.8, 30.9, 56.1, 57.3, 62.9, 64.9, 72.2, 111.2, 113.3, 113.4, 114.5, 117.2, 118.3, 121.0, 121.1, 122.2, 122.3, 122.4, 123.4, 125.4, 127.5, 128.8, 128.0 , 128.4, 128.4, 128.8, 129.0 , 129.1, 129.5 ,131.8, 135.4, 135.5

,138.3,138.4,138.432, 142.2, 149.9, 152.2, 159.2, 165.2, 167.9, 177.2.
IR (KBr) ν max: 3411, 2923, 2853, 2224, 1746, 1649, 1601, 1587,
1559, 1509, 1465, 1429, 1401, 1376, 1318, 1262, 1237, 1186, 1017,
937, 835, 755, 721, 604, 632, 612, 534, 464, 420 cm^{-1} . m/z calculated
for $\text{C}_{44}\text{H}_{40}\text{ClN}_7\text{O}_4$:766.2627 and found MALDI: 767.853(M+1).

**2.12.9. 2-(4-((2-(3-Amino-2-cyano-1H-benzof[f]chromen-1-yl)
phenoxy)methyl)-1H-1,2,3-triazol-1-yl)-N-(4-bromophenyl)-N-(2-
(tert-butylamino)-1-(2-chlorophenyl)-2-oxoethyl)acetamide 3i:**

Yellow Solid, 309 mg, 75%, M.P: 163-164 $^{\circ}\text{C}$. ^1H -NMR (DMSO, 500
MHz) δ_{H} (ppm): 1.272(s,9H), 4.268(s,2H), 4.986(s,2H), 5.262(s,2H),
5.896(s, 2H), 5.892(s,2H), 6.318(s,1H), 7.275-7.986(m, 16H),
8.136(s,2H),8.468(s, 1H), 8.501(s,2H). ^{13}C NMR(DMSO-
(d6),125MHz) δ_{C} (ppm): 27.8, 28.3, 28.3, 28.3, 56.2, 59.6, 60.7, 67.5,
72.2, 79.6, 112.9, 112.9, 113.2, 114.3, 115.9, 116.0, 117.4, 122.4,
122.9, 124.7, 124.8, 126.3, 126.4, 127.4, 128.3, 128.4, 128.8, 128.9,
129.6, 129.7, 131.9, 132.2, 138.3, 138.3, 138.5, 138.6, 148.7, 148.8,
150.3, 151.8, 165.3, 168.3, 177.3. IR (KBr) ν max: 3369, 2924, 2853,
225, 1669, 1586, 1567, 1508, 1455, 1426, 1365, 1274, 1145, 1020,
851, 808, 755, 730, 697, 626, 538, 466, 457, 420 cm^{-1} . m/z calculated
for $\text{C}_{43}\text{H}_{37}\text{BrClN}_7\text{O}_4$:831.1323 and found MALDI: 832.025(M+1).

**2.12.10. 2-(4-((2-(3-Amino-2-cyano-1H-benzof[f]chromen-1-
yl)phenoxy)methyl)-1H-1,2,3-triazol-1-yl)-N-benzyl-N-(2-(tert-
butylamino)-1-(2-chlorophenyl)-2-oxoethyl)acetamide 3j:**

Yellow Solid, 297 mg, 72%, M.P: 160-162 $^{\circ}\text{C}$. ^1H NMR (DMSO, 500 MHz)
 δ_{H} (ppm):1.331 (s,9H), 4.013 (s,2H), 4.560 (s,2H), 4.982 (s,1H), 5.272
(s,2H), 5.683(s, 1H), 7.298-7.989 (m, 18H), 8.386 (s,1H), 8.569

(s,1H), 8.584 (s,2H). ^{13}C -NMR(DMSO-(d₆),125MHz) δ_{C} (ppm): 29.0, 29.8, 30.9, 48.7, 56.4, 57.3, 62.9, 64.9, 72.1, 111.2, 113.3, 113.6, 114.4, 121.2, 121.2, 122.2, 122.4, 122.4, 122.9, 124.8, 124.8, 125.4, 126.4, 126.5, 127.4, 128.1, 128.3, 128.3, 128.8, 128.9, 129.2, 131.7, 131.8, 135.4, 138.3, 138.4, 138.5, 142.2, 149.9, 152.2, 159.1, 165.2, 167.6, 177.2. IR (KBr) ν max: 3410, 3304, 2923, 2853, 2227, 1714, 1684, 1657, 1598, 1552, 1486, 1456, 1392, 1254, 1226, 1109, 1016, 806, 754, 670, 615, 559, 468, 429, 418 cm^{-1} . m/z calculated for $\text{C}_{44}\text{H}_{40}\text{ClN}_7\text{O}_4$:766.267 and found MALDI: 767.247(M+1).

2.12.11. General procedure for the synthesis of 3-Aromo-N-[1-(2-chlorophenyl)-3-(4-chlorophenyl)-3-oxopropyl]propanamide 2.4a: A mixture of 4-chloroacetophenone (140 mg, 1 mmol), 2-chlorobenzaldehyde (154 mg, 1 mmol), and 3-bromopropionitrile (133 mg, 1 mmol) in acetonitrile (8 ml) were stirred in the presence of 5 mol % CuSO_4 at room temperature for 8 h. After completion of the reaction as indicated by TLC, the reaction mixture was poured into ice cold water and extracted with CH_2Cl_2 (15 ml). Evaporation of the solvent followed by purification on silica gel (100–200 mesh), ethyl acetate/hexane (3:1) afford 3-bromo-N-[1-(2-chlorophenyl)-3-(4-chlorophenyl)-3-oxopropyl] propanamide. The resulted bromide (426 mg, 1 mmol), K_2CO_3 (414 mg, 3 mmol), and NaN_3 (65 mg, 1 mmol) were dissolved in dimethylformamide and stirred for 6–8 h. After completion, the reaction mixture was poured into ice cold water and the precipitate was filtered and dried under vacuum to afford the azide **2.4a**: 0.332 g (86%) as white solid ^1H NMR (CDCl_3 , 500 MHz) δ_{H} (ppm): 1.73 (t, 2H), 2.45 (t, 2H), 2.67 (dd, 1H), 3.38 (dd, 1H), 5.53 (m,

1H), 6.89– 7.43 (m,8H,), 7.83 (d, J = 7.5 Hz, 1H). ¹³C NMR (CDCl₃, 125 MHz) δ_C (ppm): 35.6, 46.4, 48.2, 77.3, 128.3, 128.4, 128.9, 129.0, 129.6, 129.9, 130.3, 132.4, 134.7, 137.6, 140.2, 141.1, 169.1, 197.5. IR (KBr) ν_{max}: 3286, 3038, 2921, 2852, 2088, 1685, 1647, 1590, 1550, 1475, 1442, 1402, 1356, 1285, 1231, 1260, 1177, 1148, 1094, 1065, 1029, 997, 936, 815, 754 cm⁻¹. EI-MS: 391.0 (M⁺).

2.12.12. 3-Azido-N-(3-(4-bromophenyl)-1-(4-chlorophenyl)-3-oxopropyl) propanamide 2.4e: 0.455mg (yield 99%) M.p: 134-137^oC. as white solid¹H NMR (CDCl₃, 500 MHz) δ_H (ppm):1.61(t, 2H), 2.46-2.48(t, 2H), 2.67-2.69(t, 2H), 3.37-3.42(dd, 1H), 5.52-5.57(m, 1H), 6.83-7.77(m, 9H). ¹³C NMR (CDCl₃, 125 MHz) δ_C (ppm):36.0, 39.6, 40.1, 42.7, 47.3, 49.4, 77.0, 127.8, 128.8, 128.9, 129.1, 132.1, 135.1, 169.8, 197.3. IR (KBr) ν max: 3300, 2922, 2852, 2113, 1684, 1649, 1583, 1548, 1488, 1398, 1363, 1285, 1258, 1219, 1200, 1088, 1071, 1015, 872, 832, 812, 779, 723, 712, 672, 547, 460 cm⁻¹. m/z calculated for C₁₈H₁₆BrClN₄O₂: 435.7022, found EI-MS: 435.1 (M⁺).

2.12.13. 3-(4-((4-(3-Amino-2-cyano-1H-benzof[f]chromen-1-yl)-2-methoxyphenoxy)methyl)-1H-1,2,3-triazol-1-yl)-N-(1-(4-bromophenyl)-3-(2-chlorophenyl)-3-oxopropyl)propanamide 2.5a: Yellow Solid, 336 mg, 80%, M.P: 172-174^oC ¹H-NMR (DMSO,500MHz)δ_H(ppm): 2.668 (t,2H), 3.238 (dd,2H), 3.829 (s,3H), 4.069 (t,2H), 4.986 (s,1H), 5.262 (s,2H), 5.463 (m,1H), 6.318 (s,1H), 6.632 (s,1H), 6.875 (,1H), 7.275-7.896 (m,13H), 8.197 (s,2H), 8.234 (s,1H), 8.387 (s,2H). ¹³C-NMR (CDCl₃, 125 MHz) δ_C (ppm): 28.6, 30.9, 45.5, 51.4, 56.2, 72.2, 73.5, 111.4, 112.5, 113.0, 114.3, 117.3,

121.9, 121.6, 122.0, 123.5, 126.1, 123.2, 126.8, 126.9, 127.2, 127.3, 128.4, 128.5, 128.7, 128.9, 129.0, 131.2, 131.5, 131.5, 133.3, 133.6, 134.3, 138.5, 141.3, 142.8, 150.0, 154.5, 159.1, 172.2, 177.4, 206.8. IR (KBr) ν max: 3274, 3083, 3031, 2923, 2852, 2224, 1745, 1680, 1601, 1587, 1559, 1509, 1454, 1429, 1397, 1375, 1318, 1262, 1238, 1186, 1158, 1126, 1071, 1009, 969, 937, 835, 819, 773, 721, 664, 632, 613, 535, 487, 465, 437cm^{-1} . m/z calculated for $\text{C}_{42}\text{H}_{34}\text{BrClN}_6\text{O}_5$: 818.08, found MALDI: 819.04 (M+1).

2.12.14. *3-(4-((4-(3-Amino-2-cyano-1H-benzof[f]chromen-1-yl)-2-methoxyphenoxy)methyl)-1H-1,2,3-triazol-1-yl)-N-(1,3-bis(4-chlorophenyl)-3-oxopropyl)propanamide 2.5b*: Yellow Solid, 306 mg, 73%, M.P: 174-175^oC ¹H-NMR(DMSO, 500MHz) δ_{H} (ppm): 2.668 (t,2H),3.238 (dd,2H),3.829 (s,3H), 4.069 (t,2H) ,4.986 (s,1H), 5.262 (s,2H), 5.463 (m,1H), 6.318 (s,1H), 6.632(s,1H), 6.875(,1H), 7.275-7.896 (m,13H), 8.197 (s,2H), 8.258 (s,1H), 8.583 (s,2H). ¹³C NMR (CDCl₃, 125 MHz) δ_{C} (ppm): 28.6, 30.9, 45.5, 51.4, 56.6, 72.9, 73.5, 111.4, 112.5, 113.1, 114.3, 117.3, 121.9, 121.6, 122.1, 123.2, 123.5, 126.2, 126.8, 126.9,127.2, 127.3, 128.4, 128.5, 128.7, 128.9, 129.1, 131.1, 131.5, 131.5, 133.3, 134.4, 133.6, 138.5, 141.5, 142.8, 150.9, 154.5, 159.1, 172.2, 177.4, 206.2s. IR (KBr) ν max: 3424, 3279, 2925, 2853, 2224, 1746, 1651, 1586, 1566, 1515, 1444, 1381, 1274, 1206, 1147, 1091, 1014, 854, 803, 768, 699, 654, 322, 519 cm^{-1} . m/z calculated for $\text{C}_{42}\text{H}_{34}\text{Cl}_2\text{N}_6\text{O}_5$: 773.5882, found MALDI : 774.054(M+1).

2.12.15. **3-(4-((4-(3-Amino-2-cyano-1H-benzof[f]chromen-1-yl)phenoxy)methyl)-1H-1,2,3-triazol-1-yl)-N-(1,3-bis(4-bromophenyl)-3-oxopropyl)propanamide 2.5e:** Yellow Solid, 301 mg, 73%, M.P: 173-175^oC ¹H-NMR(DMSO, 500MHz) δ_{H} (ppm): 2.514 (t,2H), 3.300 (dd,2H), 4.243 (t,2H), 4.827 (s,1H), 5.287 (s,2H), 5.463 (m,1H), 6.486 (s,1H), 6.675 (s,1H), 6.983 (s,1H), 7.275-7.896 (m,14H), 8.489 (s,2H), 8.514 (s,1H), 8.594 (s,2H). ¹³C-NMR (CDCl₃, 125 MHz) δ_{C} (ppm): 27.6, 31.9, 45.5, 51.9, 56.6, 72.2, 111.4, 112.5, 113.1, 114.4, 117.3, 121.9, 121.6, 122.1, 123.2, 123.5, 126.2, 126.8, 126.9, 127.2, 127.3, 128.4, 128.5, 128.7, 128.9, 129.1, 131.1, 131.5, 131.5, 133.3, 134.3, 133.6, 138.5, 142.4, 142.5, 150.1, 154.2, 159.1, 173.2, 177.2, 206.2. IR (KBr) ν max: 3363, 2936, 2853, 2227, 1745, 1670, 1598, 1543, 1456, 1364, 1310, 1224, 1167, 1110, 1018, 849, 808, 754, 697, 615, 467, 417 cm⁻¹. m/z calculated for C₄₁H₃₂Br₂N₆O₄ : 832.5157, found MALDI : 833.520(M+1).

2.12.16. **3-(4-((4-(3-Amino-2-cyano-1H-benzof[f]chromen-1-yl)phenoxy)methyl)-1H-1,2,3-triazol-1-yl)-N-(1,3-bis(4-chlorophenyl)-3-oxopropyl)propanamide 2.5f:** Yellow Solid, 306 mg, 74%, M.P: 172-174^oC. ¹H-NMR(DMSO, 500MHz) δ_{H} (ppm): 2.252 (t,2H), 3.300 (dd,2H), 4.318 (t,2H), 4.965 (s,1H), 5.273 (s,2H), 5.455 (m,1H) 6.466 (s,1H), 6.725 (s,1H), 6.915(s,1H), 7.275-7.896 (m,14H), 8.489 (s,2H), 8.350 (s,1H), 8.588 (s,2H). ¹³C-NMR (CDCl₃, 125 MHz) δ_{C} (ppm): 28.6, 31.9, 45.5, 51.4, 56.6, 72.2, 73.5, 111.4, 112.5, 113.1, 114.3, 117.3, 121.9, 122.1, 123.2, 123.5, 126.2, 126.8, 126.9, 127.2, 127.3, 128.5, 128.5, 128.7, 128.9, 129.1, 131.1, 131.5, 131.5, 133.3, 134.3, 133.6, 138.5, 141.5, 142.8, 150.1, 154.5, 159.1, 172.2, 177.4,

199.4 IR (KBr) ν max:3429, 2923, 2855, 2225, 1674, 1647, 1587, 1566, 1510, 1463, 1427, 1345, 1296, 1229, 1200, 1176, 1091, 1030, 997, 819, 755, 604, 622, 527, 422 cm^{-1} . m/z calculated for $\text{C}_{41}\text{H}_{32}\text{Cl}_2\text{N}_6\text{O}_4$: 743.6353 and found MALDI: 744.234(M+1).

2.12.17. *3-(4-((2-(3-Amino-2-cyano-1H-benzof[f]chromen-1-yl)phenoxy)methyl)-1H-1,2,3-triazol-1-yl)-N-(3-(2-chlorophenyl)-1-(4-chlorophenyl)-3-oxopropyl)propanamide 2.5i*: Yellow Solid, 296 mg, 70%, M.P: 173-174 $^{\circ}\text{C}$. $^1\text{H-NMR}$ (DMSO,500MHz) δ_{H} (ppm): 2.514 (t,2H),3.339 (dd,2H), 4.825 (t,2H),4.917 (s,1H), 5.303(s,2H), 5.337 (m,1H) 5.892 (s,1H), 6.318 (s,1H), 6.875 (s,1H), 7.069-7.668 (m,12H), 8.086 (s,2H), 8.234 (s,2H), 8.497 (s,1H), 8.583 (s,2H). $^{13}\text{C-NMR}$ (CDCl_3 , 125 MHz) δ_{C} (ppm):29.8, 30.9, 49.1, 56.1, 56.1, 57.3, 62.9, 64.9, 72.1, 111.1, 113.3, 113.6, 114.4, 121.2, 122.2, 122.4, 122.9, 124.8, 125.4, 126.4, 126.4, 127.4, 128.1, 128.3, 128.9, 128.9, 129.2, 131.78, 131.8, 135.4, 138.3, 138.3, 138.5, 142.2, 149.9, 152.2, 159.0, 165.2, 167.6, 177.1, 200.3. IR (KBr) ν max:3405, 3280, 3030, 2922, 2851, 2312, 2221, 1674, 1639, 1586, 1566, 1515, 1490, 1456, 1419, 1381, 1344, 1305, 1276, 1254, 1206, 1178, 1158, 1147, 1091, 1029, 1016, 854, 819, 803, 767, 698, 655, 622, 522,464, 424 cm^{-1} .m/z calculated for $\text{C}_{41}\text{H}_{32}\text{Cl}_2\text{N}_6\text{O}_4$:743.6353,found MALDI : 744.234(M+1).

2.12.18. *3-(4-((2-(3-Amino-2-cyano-1H-benzof[f]chromen-1-yl)phenoxy)methyl)-1H-1,2,3-triazol-1-yl)-N-(1-(4-chlorophenyl)-3-(2-fluorophenyl)-3-oxopropyl)propanamide 2.5j*: Yellow Solid, 316 mg, 76%, M.P: 161-163 $^{\circ}\text{C}$. $^1\text{H-NMR}$ (DMSO, 500MHz) δ_{H} (ppm):

2.565 (t,2H),3.994 (dd,2H), 4.318 (t,2H),4.965 (s,1H), 5.273 (s,2H), 5.337 (m,1H) 5.892 (s,1H), 6.318 (s,1H)6.875(s,1H), 7.069-7.668 (m,12H), 8.086 (s,2H), 8.234 (s,2H), 8.497 (s,1H), 8.565 (s,2H). ¹³C-NMR (CDCl₃, 125 MHz) δ_C (ppm):24.8, 28.6, 52.8, 57.1, 56.2, 57.1, 59.6, 68.8, 75.2, 112.9, 112.9, 115.9, 117.4, 121.5, 122.2, 122.4, 122.9, 124.8, 126.4, 126.4, 127.4, 128.3, 128.3, 128.9, 128.9, 129.6, 129.6, 131.9, 132.2, 138.3, 138.3, 138.5, 138.5, 148.8, 148.8, 154.5, 159.5, 165.6, 168.2,2 .281,206.8 . IR (KBr) ν max: 3083, 3031, 2923, 2852, 2224, 1745, 1680, 1601, 1587, 1559, 1509, 1454, 1429, 1397, 1375, 1318, 1262, 1238, 1186, 1158, 1126, 1071, 1009, 969, 937, 835, 819, 773, 721, 664, 632, 613, 535, 487, 465, 437cm⁻¹. m/z calculated for C₄₁H₃₂ClFN₆O₄ : 727.1807,found MALDI: 728.173(M+1).

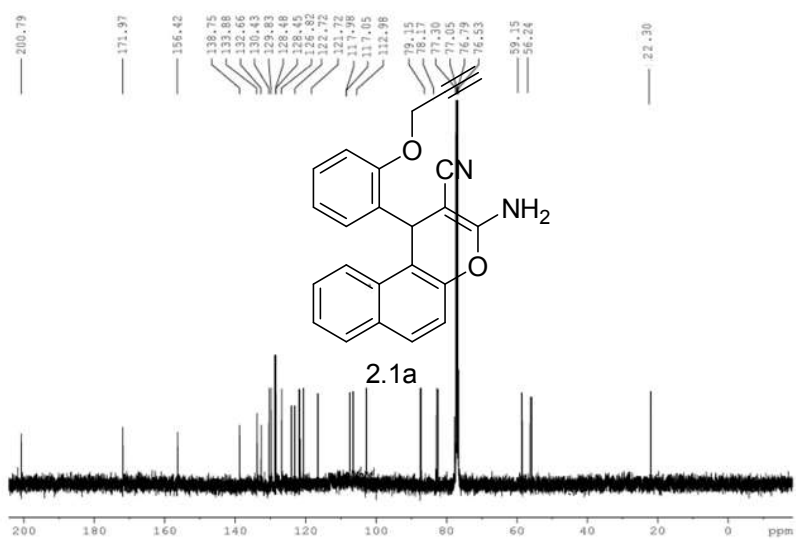
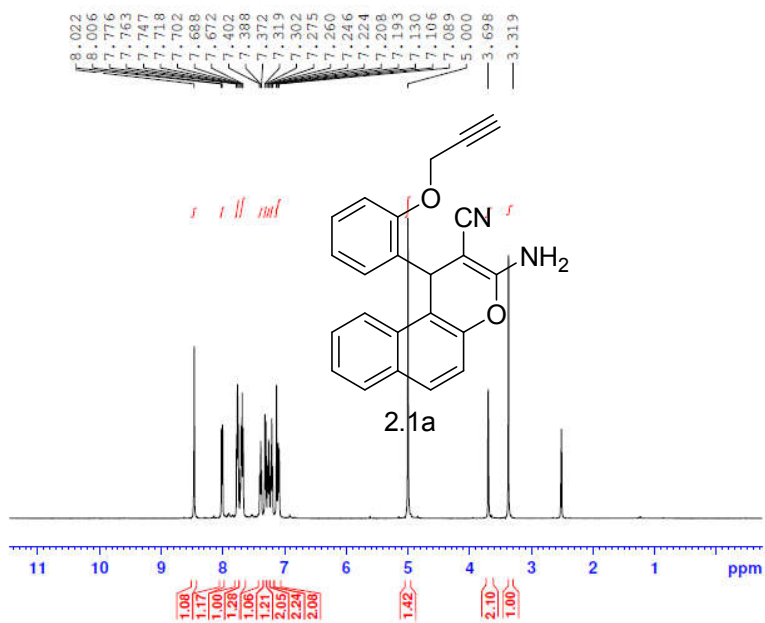
References

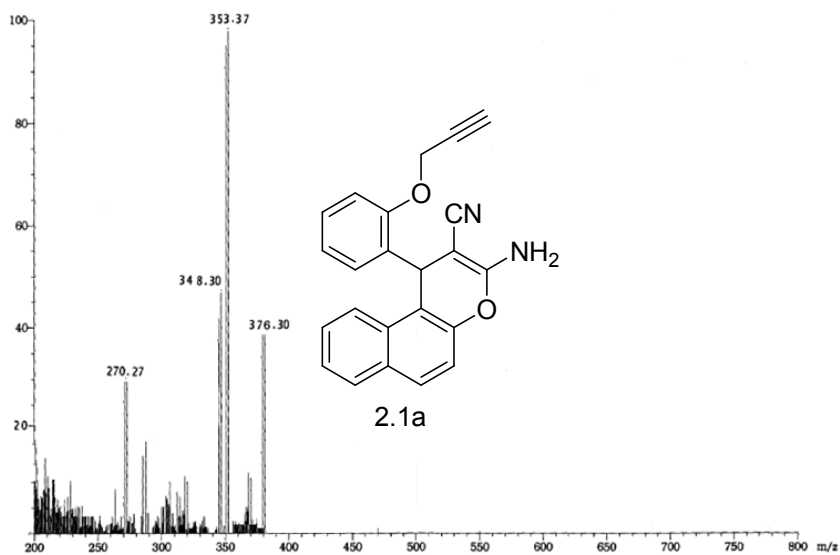
1. Stockwell, B.R. *Nature*, **2004**, 432, 846-854.
2. Schreiber, S. L.; Burke, M.D. *Angew. Chem. Int. Ed.* **2004**, 43, 46-58.
3. (a) Feuer, G. *Progress in Medicinal Chemistry*; Ellis, G. P., West, G. P., Eds.; North-Holland Publishing Company: New York, **1974**; 10, 85-158. (b) Dean, F. M. *Naturally Occurring Oxygen Ring Compounds*; Butterworth-Heinemann: London, **1963**, 176-220. (c) Goel, A.; Ram, V. J. *Tetrahedron*, **2009**, 65, 7865-7913.
4. (a) Halland, N.; Hansen, T.; Jørgensen, K. A. *Angew. Chem., Int. Ed.* **2003**, 42, 4955-4957. (b) Kim, H.; Yin, C.; Preston, P. *J. Org. Lett.* **2006**, 8, 5239- 5242. (c) Xie, J. W.; Yue, L.; Chen, W.; Du, W.; Zhu, J.; Deng, J. G.; Chen, Y. C. *Org. Lett.* **2007**, 9, 413-415. (d) Xu, D.-Q.; Wang, Y.-F.; Zhang, W.; Luo, S.-P.; Zhong, A.-G.; Xia, A.-B.; Xu, Z.-Y. *Chem. Eur. J.* **2010**, 16, 4177-4180. (e) Elinson, M. N.; Dorofeev, A. S.; Miloserdov, F. M.; Ilovaisky, A. I.; Feducovich, S. K.; Belyakov, P. A.; Nikishin, G. I. *Adv. Synth. Catal.* **2008**, 350, 591-601.
5. Panda, D.; Singh, J.P.; Wilson, L. *J. Biol. Chem.* **1997**, 272, 7681-7687. (b) Wood, D.L.; Panda, D.; Wiernicki, T.R.; Wilson, L.; Jordan, M.A.; Singh, J.P. *Mol. Pharmacol.* **1997**, 52, 437-444. (c) Wiener, C.; Schroeder, C.H.; West, B.D.; Link, K.P. *J. Org. Chem.* **1962**, 27, 3086-3088.
6. Patil, S.; Patil, R.; Pfeffer, L.; Miller, D. *Future Med. Chem.* **2013**, 5, 1647-1660.
7. (a) Kemnitzer, W.; Kasibhatla, S.; Jiang, S.; Zhang, H.; Zhao, J.; Jia, S.; Xu, L.; Grundy, C.C.; Denis, R.; Barriault, N. *Bioorg. Med. Chem. Lett.* **2005**, 15, 4745-4751. (b) Wang, J.-L.; Liu, D.; Zhang, Z. J.; Shan, S.; Han, X.; Srinivasula, S.M.; Croce, C.M.; Alnemri, E.S.; Huang, Z. *Proc. Natl. Acad. Sci. USA.* **2000**, 97, 7124-7129. (c) Doshi, J.M.; Tian, D.; Xing, C. *J. Med. Chem.* **2006**, 49, 7731-7739. (d) Panda, D.; Singh, J.P.; Wilson, L. *J. Biol. Chem.* **1997**, 272, 7681-7687.
8. Hed, J. *FEMS Microbiol Lett.* **1977**, 1, 357-361.
9. Wang, F.; Tan, W.B.; Zhang, Y.; Fan, X.; Wang, M. *Nanotechnology.* **2006**, 17, 933-939.
10. (a) Voloshina, P.N.; Haugland, R.P.; Stewart, B.J. et al. *J. Histochem. Cytochem.* **1999**, 47, 1179-88. (b) Graham, T. D.;

- Joshua, C. V.; Kok Hao, C.; Mark, B.; Xiaowei, Z. *Nature Methods*, **2011**, 8, 1027-1040. (c) Jianjun, Q.; Myung-Shin, H.; Yu-Cheng, C.; Ching-Hsuan, T. *Bioconjug. Chem.* **2011**, 22, 1758–1762
11. Laskar, S.; Brahmachari, G. *Org. Biomol. Chem.* **2014**, 2, 1-50.
 12. Rupnar B.D.; Rokade P. B.; Gaikwad P. D.; Pangrikar P.P.; *IJCBS*, **2014**, 2, 1, 2320–4087.
 13. Naimi-Jamal, N.R.; Mashkouri, S.; Ali Sharifi. *Mol Divers*, **2010**, 14, 473-477.
 14. (a) Ugi, I.; Lohberger, S.; Karl, R. *J. Org. Biomol. Chem.* **2006**, 1, 01-50. (b) Trost, B. M., Fleming, I., Heathcock, H., Eds.; *Pergamon: New York*, **1991**; 2, 1083–1109. (b) Ugi, I. *Angew. Chem., Int. Ed.* **1982**, 21, 810–819; (c) Keating, T. A.; Armstrong, R. W. *J. Org. Chem.* **1998**, 63, 867–871.
 15. (a) Kolb, H. C.; Finn, M. G.; Sharpless, K. B. *Angew. Chem., Int. Ed.* **2001**, 40, 2004-2021. (b) Sreeman K. M., Finn, M. G. *Chem. Soc. Rev.* **2010**, 39, 1252–1261; (c) Droumaguet, C. L.; Wang, C.; Wang, Q. *Chem. Soc. Rev.* **2010**, 39, 1233–1239. (d) El-Sagheer, A. H.; Brown, T. *Chem. Soc. Rev.* **2010**, 39, 1388–1405; (e) Manzenrieder, F., Luxenhofer, R.; Retzlaff, M.; Jordan, R.; Finn, M. G. *Angew. Chem. Int. Ed.* **2011**, 50, 2601 –2605. (f) Suzuki, T.; Ota, Y.; Kasuya Y.; Mutsuga, M.; Kawamura, Y.; Tsumoto, H.; Nakagawa, H.; Finn, M.G.; Miyata, N. *Angew. Chem. Int. Ed.* **2010**, 49, 6817 –6820 (g) Hong, V.; Presolski, S. I.; Ma, C.; Finn, M.G. *Angew. Chem. Int. Ed.* **2009**, 48, 9879-9883; (h) Ganesh, V.; Sudhir, S.; Kundu, T.; Chandrasekharan, S. *Chem. Asian J.* **2011**, 6, 2670–2694; (h) Prakasan, T.; Dariusz, M.; Krzysztof, J. *Chem. Rev.* **2013**, 113, 4905-4979; (i) Liang, X, L.; Yongjun, L.; Yuliang, L. *Asian J. Org. Chem.* **2014**, 3, 582-602. (j) Schulz, D.; Rentmeister, A. *ChemBioChem*, **2014**, 15, 2342-2347. (k) Ragoussi, M.-E.; Torres, T. *Chem. Asian J.* **2014**, 9, 2676-2707.
 16. MOLINSPIRATION software or free molecular property calculation service. URL: <http://www.molinspiration.com/>
 17. Lipinski, C.A.; Lombardo, F.; Dominy, B.W.; Feeney, P.J. *Adv Drug Deliv Rev.* **2001**, 46, 3–26.
 18. Doak, B.C.; Zheng, J.; Dobritsch, D.; Kihlberg, J. *J. Med. Chem.* **2016**, 59:2312–2327.

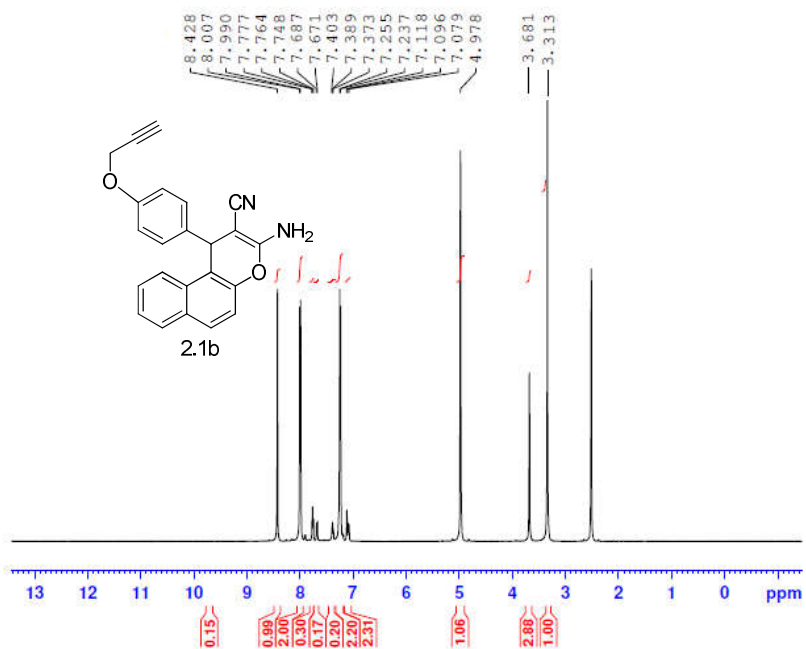
19. (a) Bahulayan, D.; Das, S.K.; Iqbal, J. *J. Org. Chem.* **2003**, *68*, 5733-5738. (b) Shinu V, Sheeja B, Purushothaman E, Bahulayan D. *Tetrahedron Lett.* **2009**, *50*, 4838-4843. (c) Pandey, G.; Singh, R.P.; Garg, A.; Singh, V.K. *Tetrahedron Lett.* **2005**, *46*, 2137-2140. (d) Arend, M.; Westermann, B.; Risch, N.; *Angew. Chem. Int. Ed.* **1998**, *37*, 1044 - 1070. (e) Chowdari, N.S.; Suri, J.T.; Barbas, C.F. *Org. Lett.*, **2004**, *6*, 15, 2507-2510.

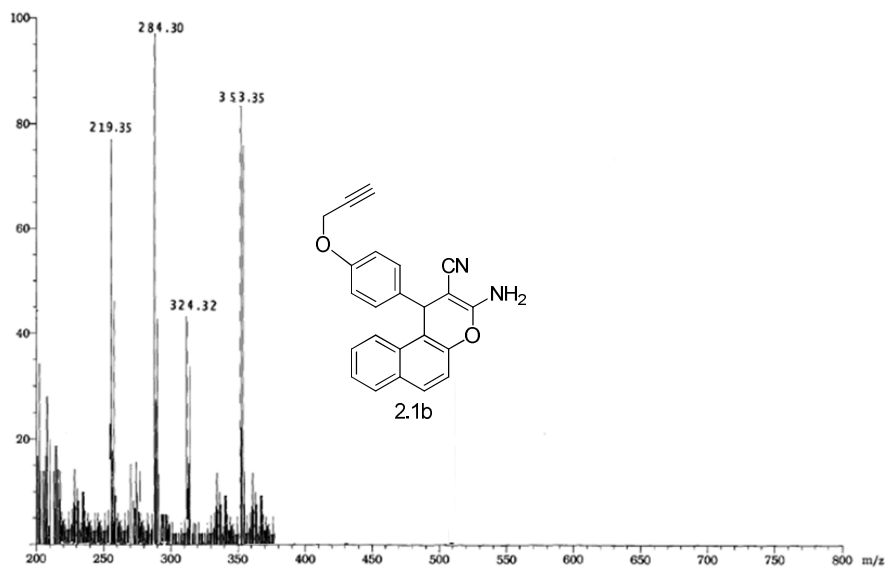
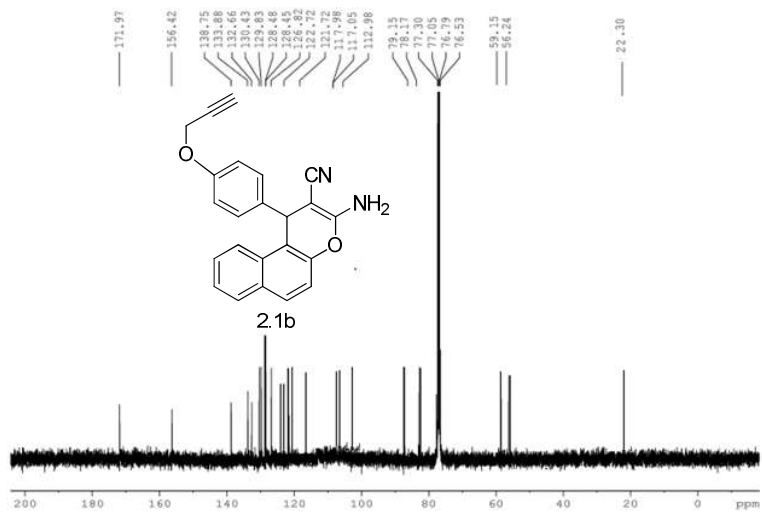
jm-14
PROTON DMSO C:\Bruker\TOPSPIN nmr



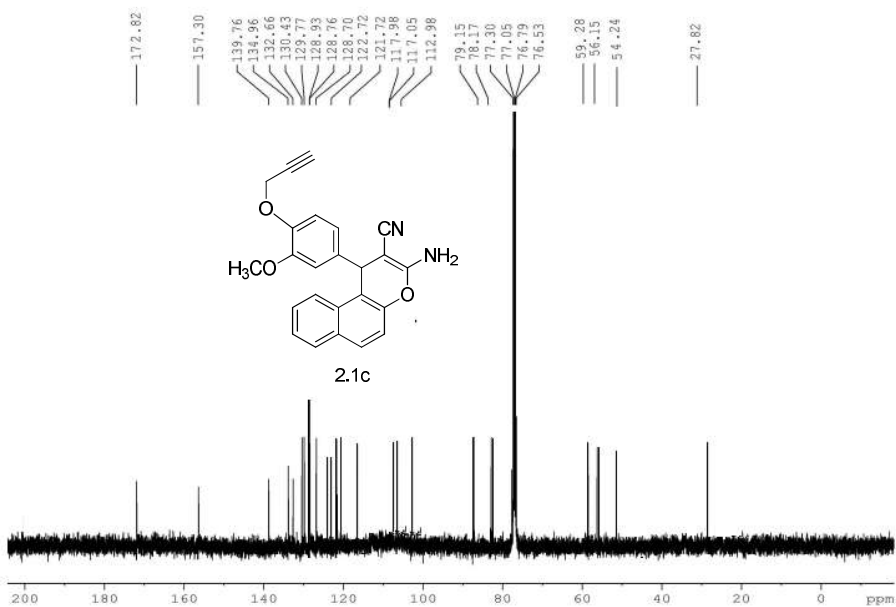
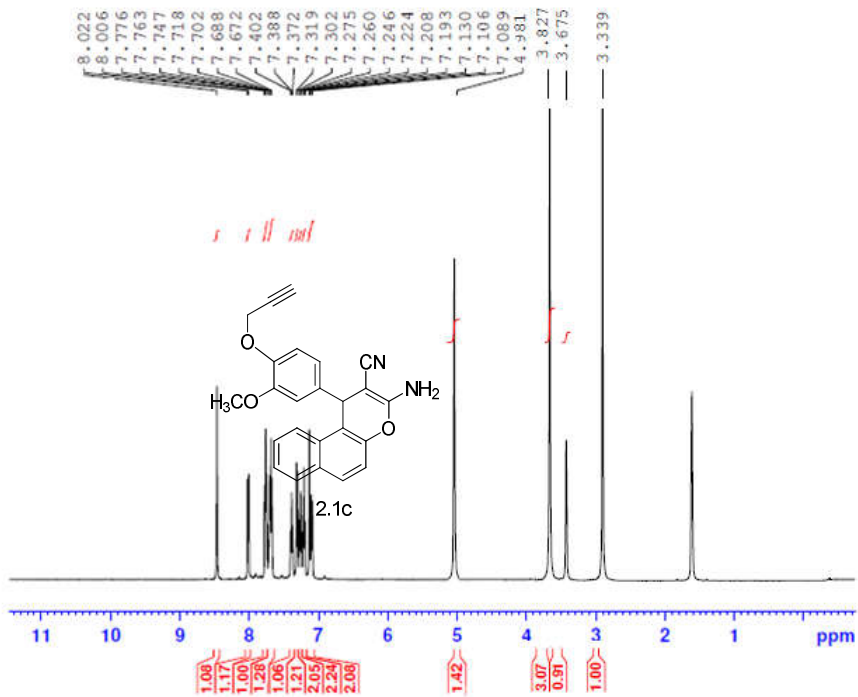


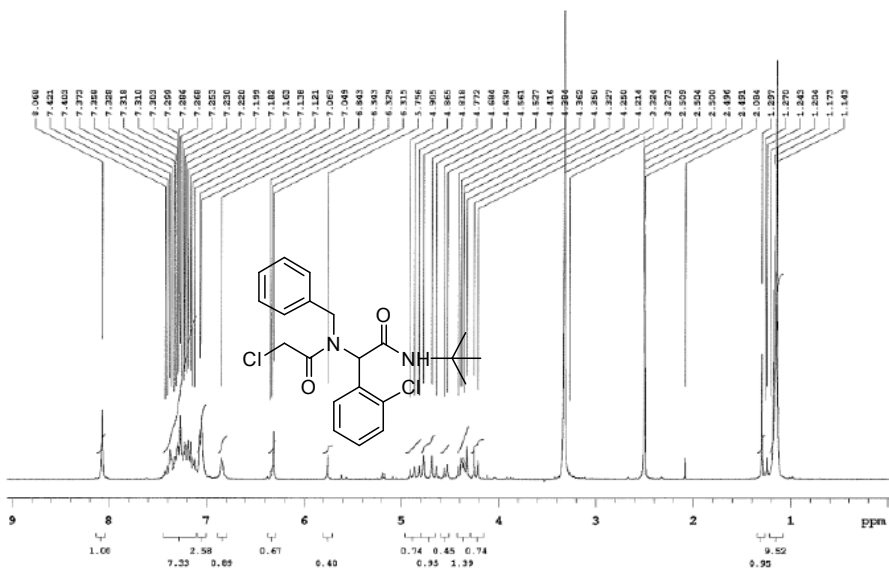
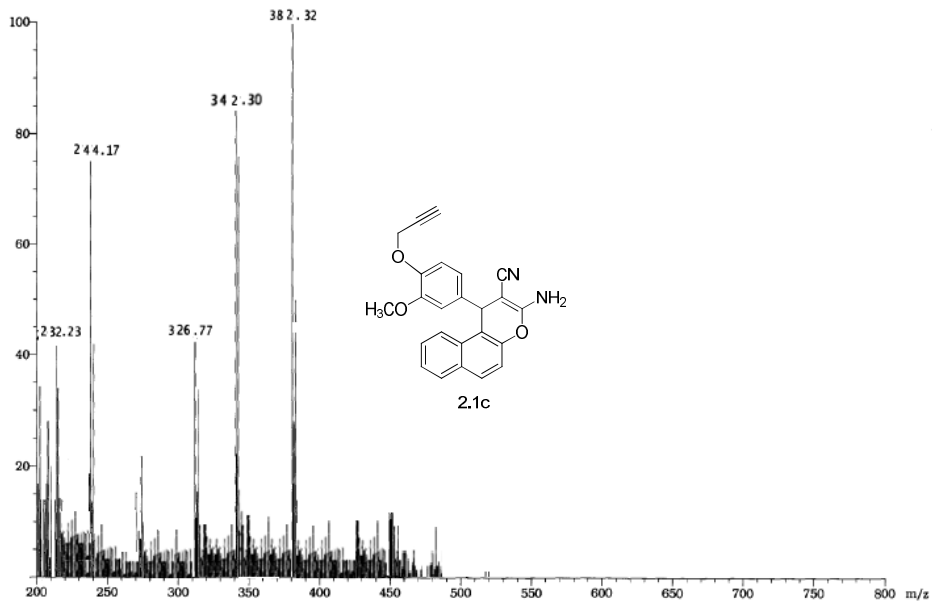
jm-26
 PROTON DMSO C:\Bruker\TOPSPIN nmr



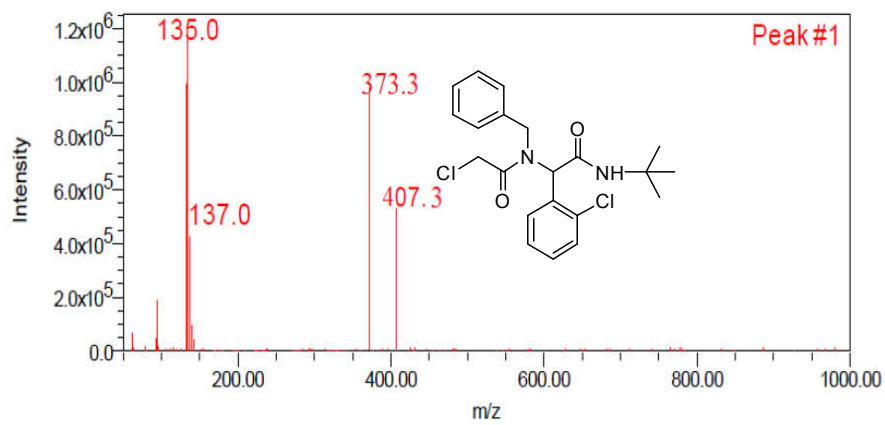
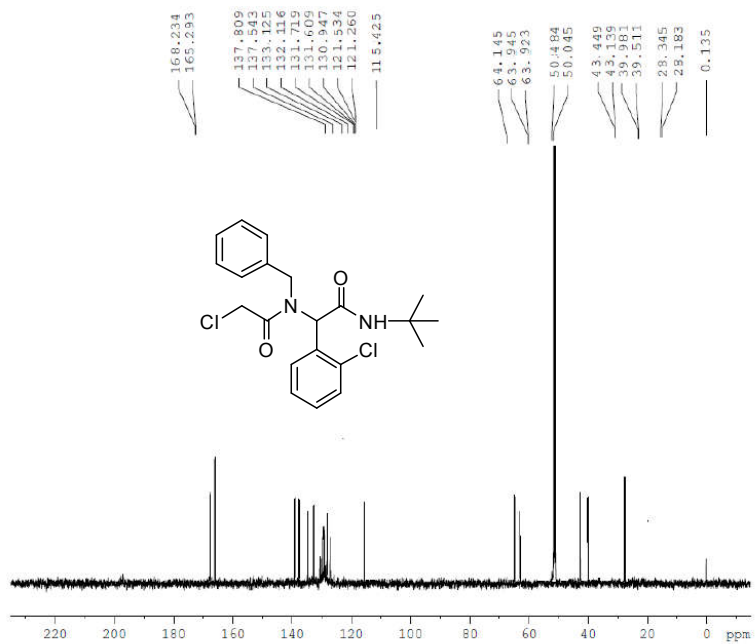


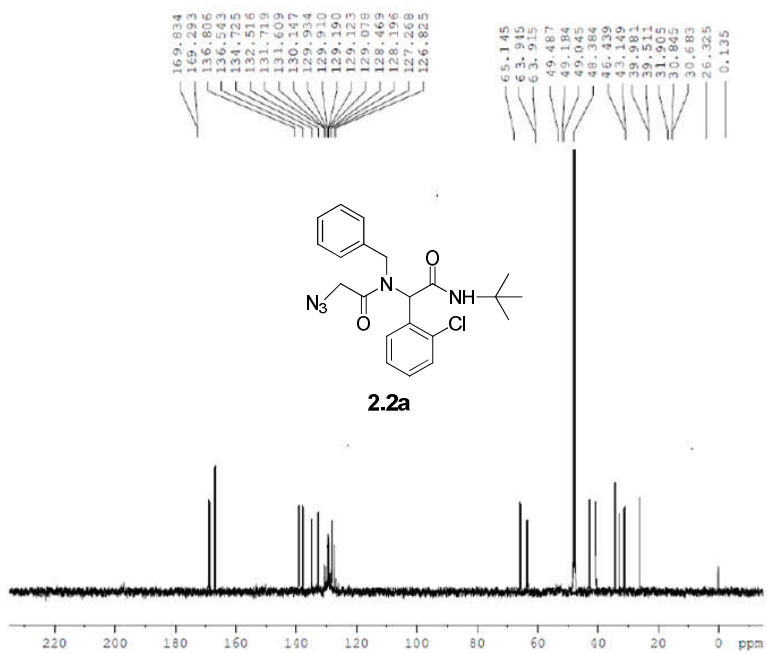
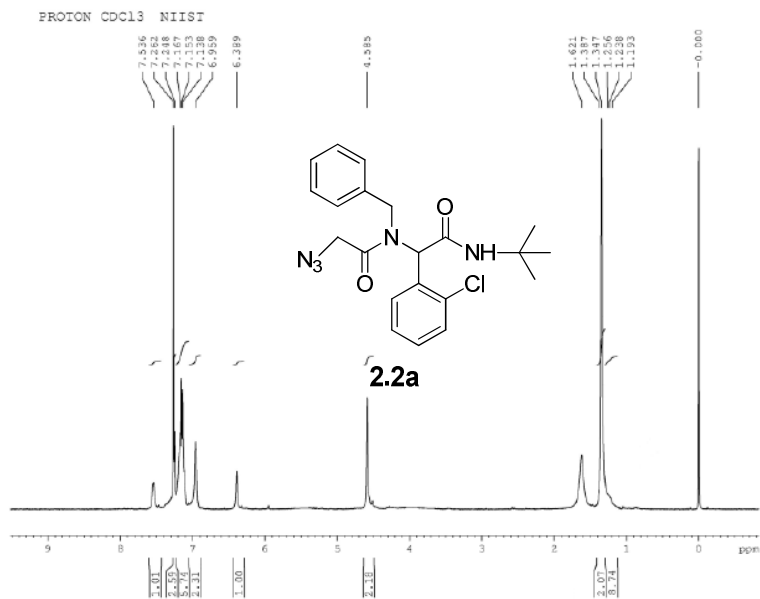
jm-27
PROTON DMSO C:\Bruker\TOPSPIN nmr

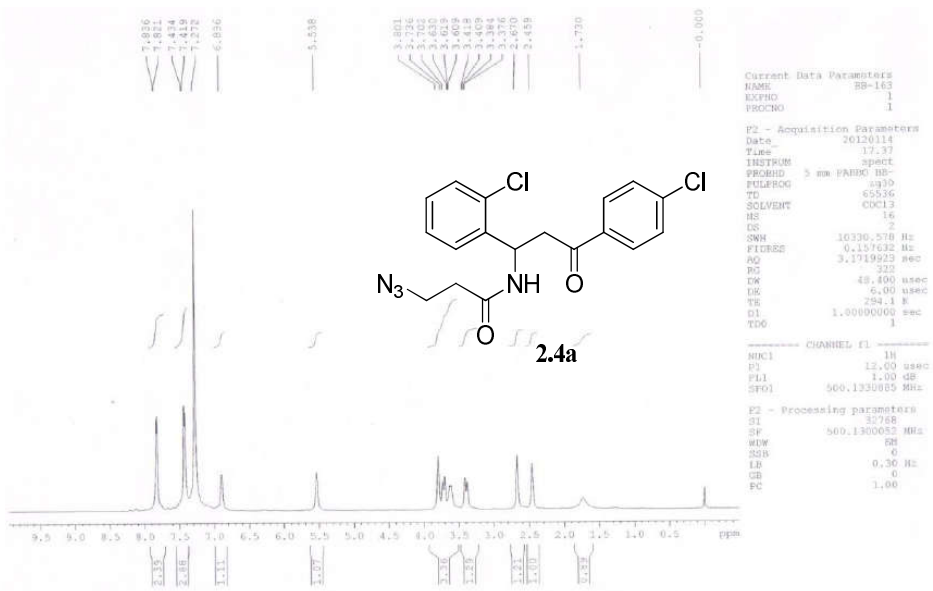
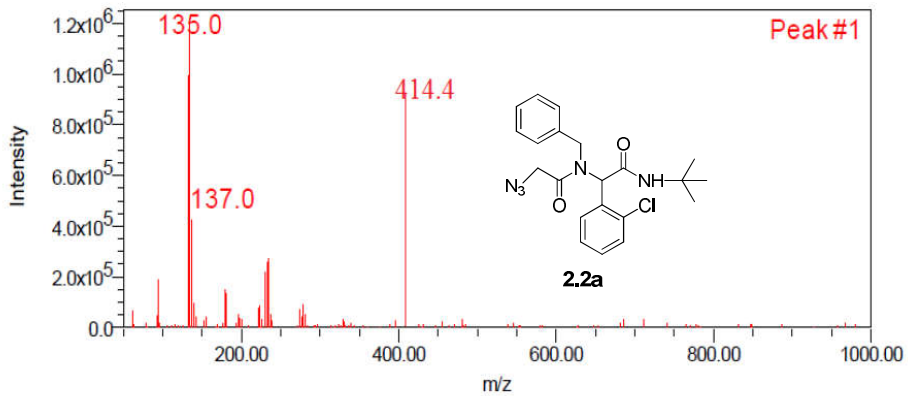


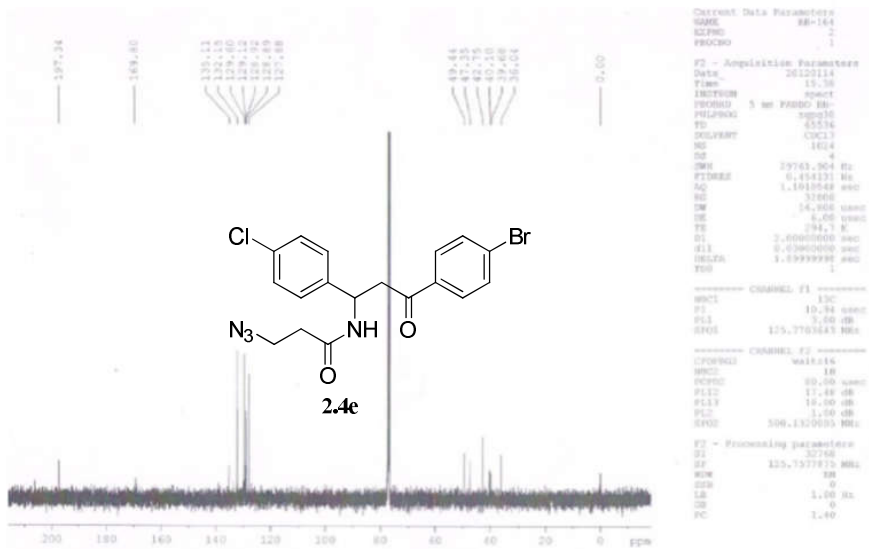
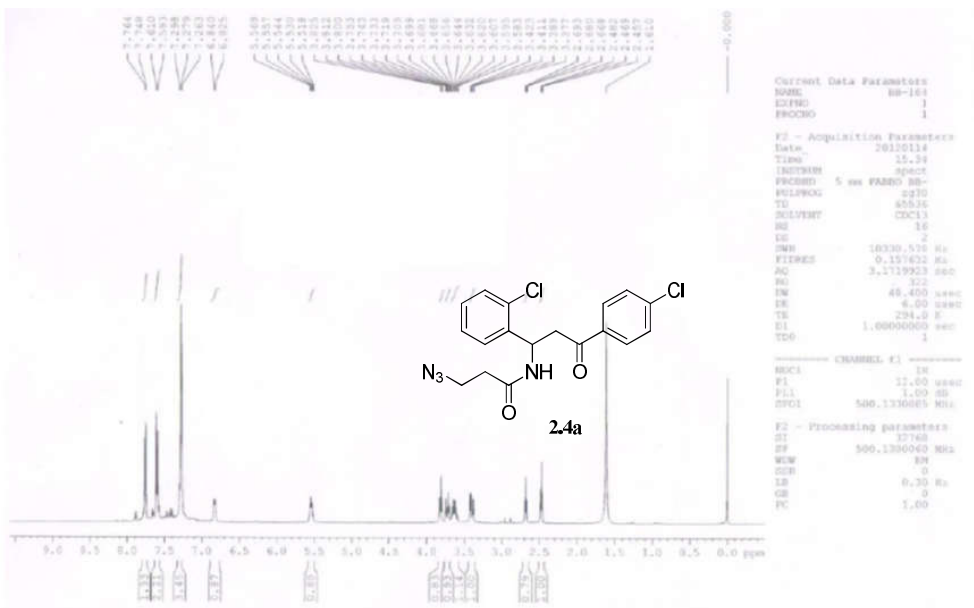


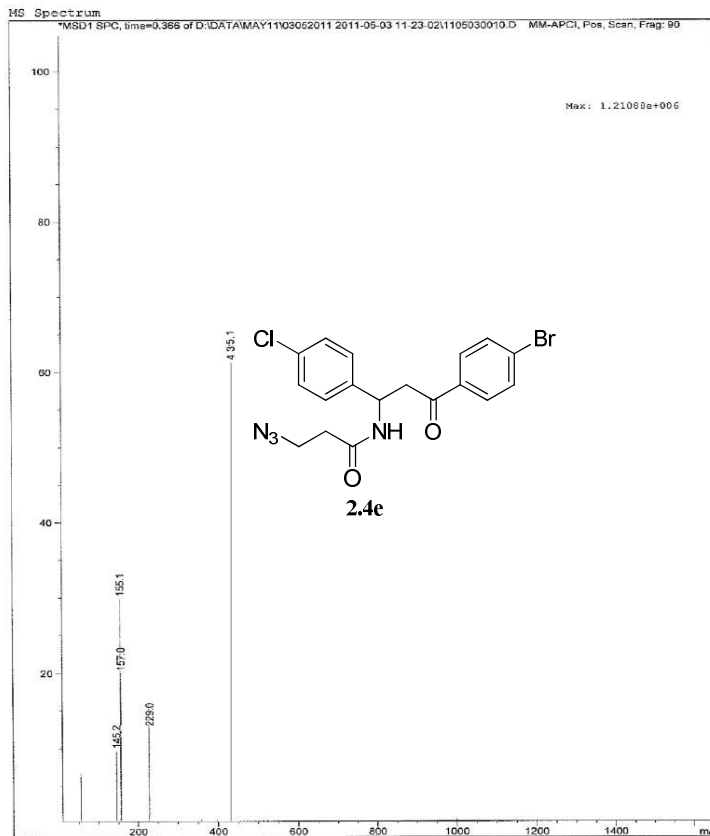
PULSE SEQUENCE Relax. delay 1.000 sec Pulse 45.0 degrees Acq. time 2.049 sec Width 6410.3 Hz 32 repetitions	CRMSRVE XL 399.2891663	DATA PROCESSING Resol. enhancement -0.0 Hz FT size 65536 Total time 1 minutes	Solvent: dmsc Temp. 25.0 C / 290.1 K Sample #5, Operator: walkup File: 0349-0_61 VNMR-490 "400MHz"	SAMPLE: 0349-BB Sample: 0349-B Sample ID: s_0349-0_01 File: /home/walkup/vnmrpy/data/0349-0_01.f1 Data filename: s0349
File: /home/walkup/vnmrpy/data/0349-0_01.f1d				



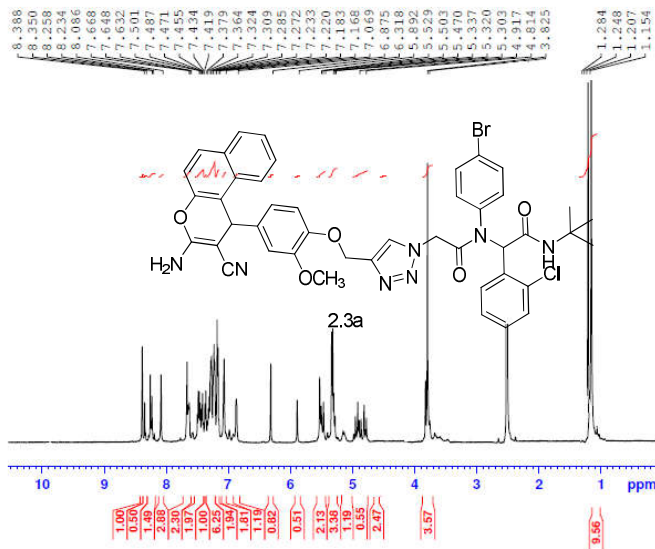








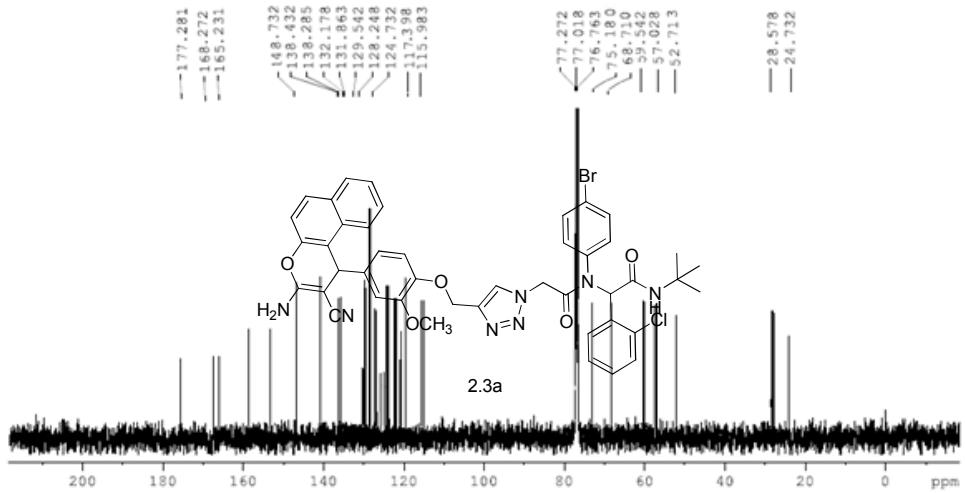
jm-73
 PROTON DMSO C:\Bruker\TOPSPIN nmr

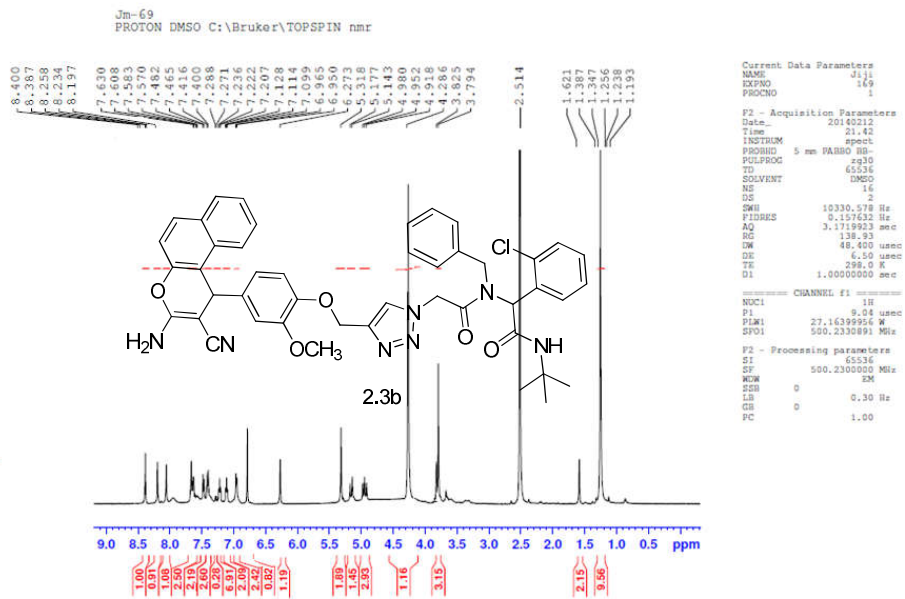
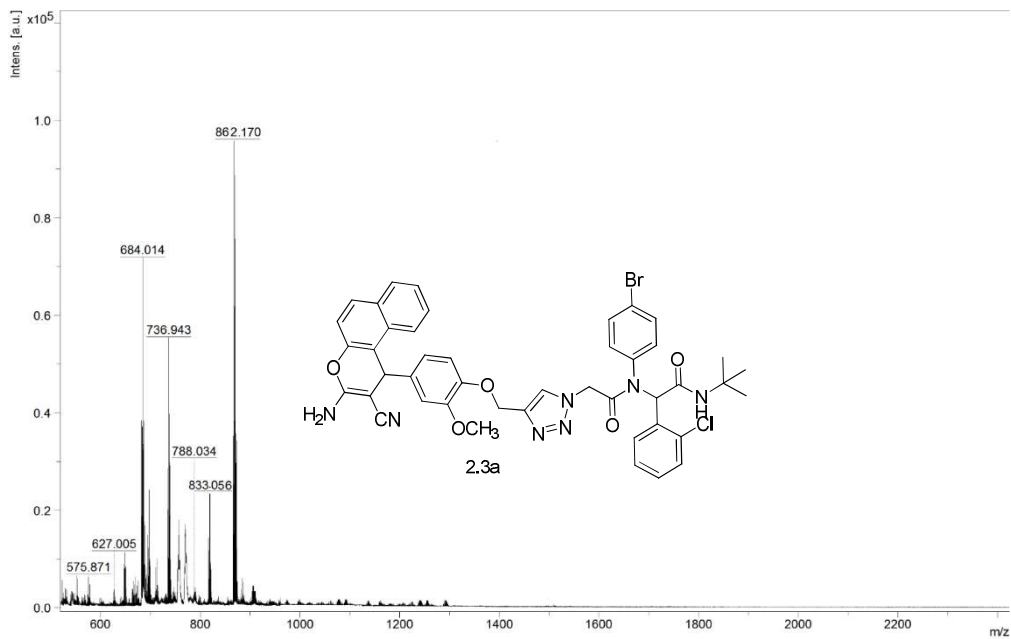


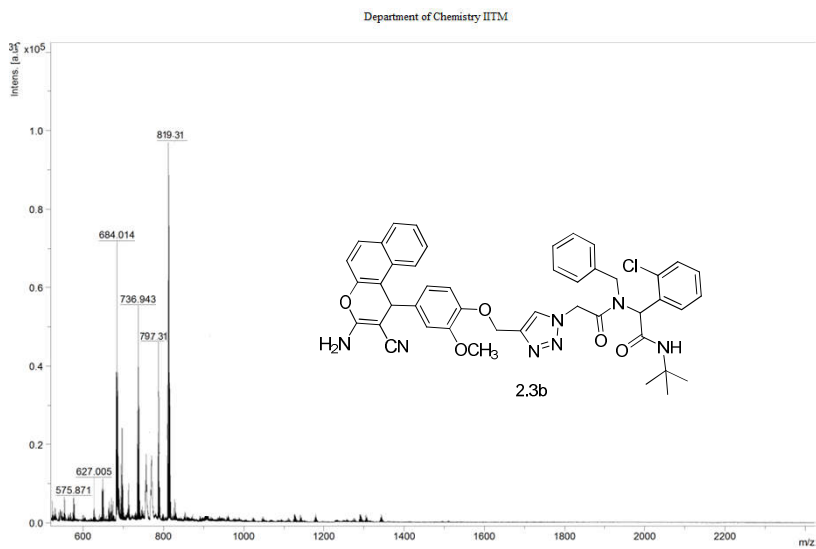
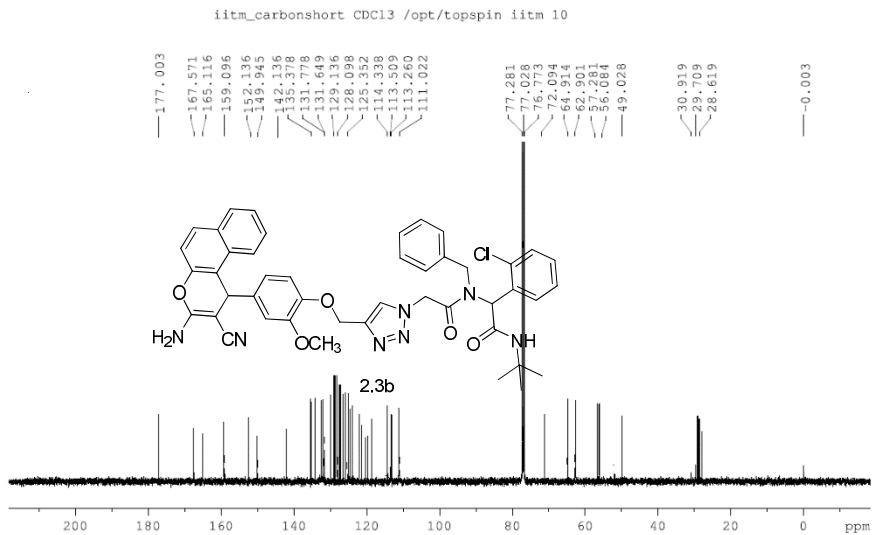
Current Data Parameters
 NAME: jm73
 EXPNO: 168
 PROCNO: 1

F2 - Acquisition Parameters
 Date_: 20140212
 Time: 21.38
 INSTRUM: spect
 PROBRD: 5 mm F4BBO BB-
 PULPROG: zgpg30
 TD: 65536
 SOLVENT: DMSO
 NS: 16
 DS: 2
 SWH: 10330.578 Hz
 FIDRES: 0.157632 Hz
 AQ: 3.1719923 sec
 RG: 138.93
 DW: 48.400 usec
 DE: 6.50 usec
 TE: 298.0 K
 D1: 1.0000000 sec

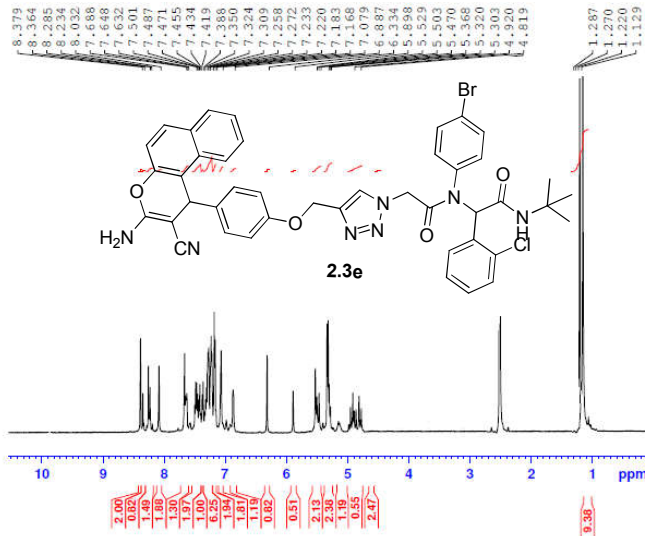
==== CHANNEL f1 =====
 NUC1: 1H
 P1: 9.04 usec
 PCW1: 27.1639956 W
 SFO1: 500.2330891 MHz
 F2 - Processing parameters
 SI: 65536
 SF: 500.2330891 MHz
 WCN: ...
 SSB: ...
 LB: 0.30 Hz
 GB: 0
 PC: 1.00







PROTON DMSO C:\Bruker\TOPSPIN nmr



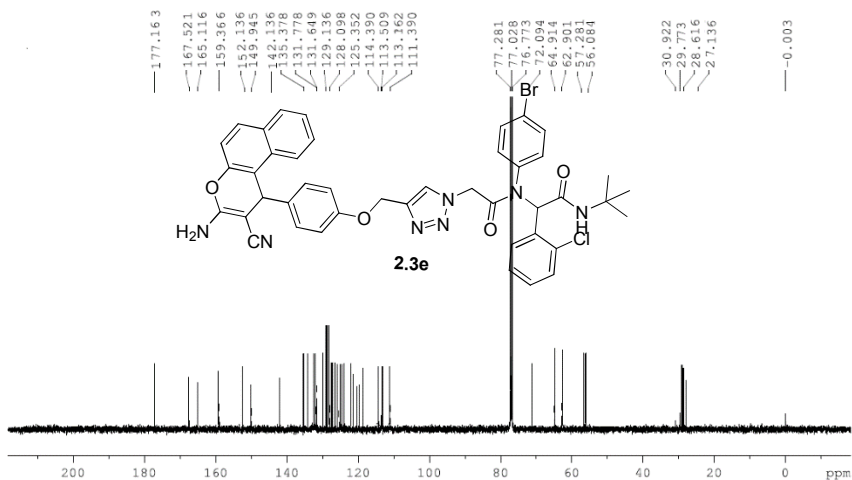
Current Data Parameters
 NAME: 2.3e
 EXPNO: 168
 PROCNO: 1

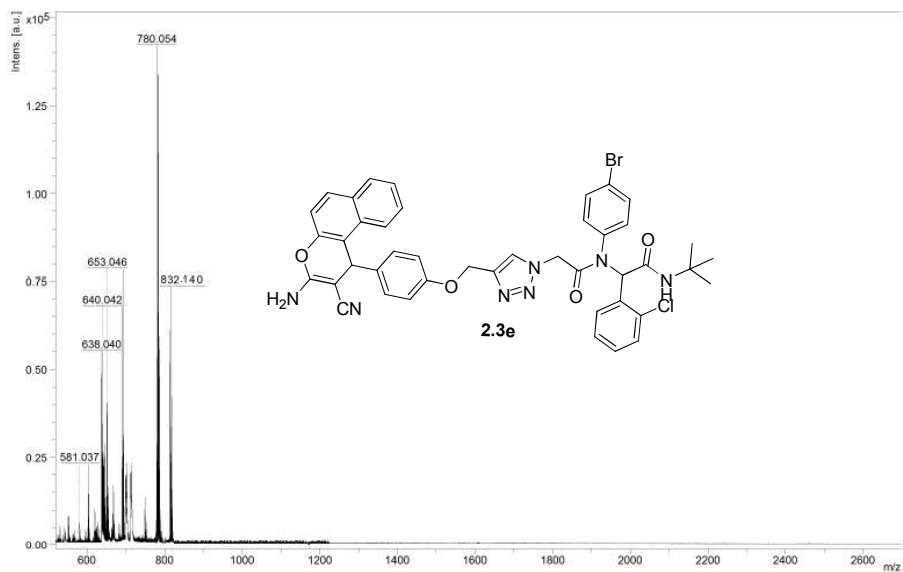
F2 - Acquisition Parameters
 Date_: 20140212
 Time: 21.38
 INSTRUM: spect
 PROBNM: 5 mm PABBO BH-
 PULPROG: zg30
 TD: 65536
 SOLVENT: DMSO
 NS: 16
 DS: 2
 SWH: 10330.578 Hz
 FIDRES: 0.157632 Hz
 AQ: 3.1719223 sec
 RG: 138.93
 LW: 48.400 usec
 DE: 6.50 usec
 TE: 298.0 K
 DI: 1.00000000 sec

===== CHANNEL f1 =====
 NUC1: 1H
 P1: 9.04 usec
 PLM1: 27.1639956 W
 SFO1: 500.2330891 MHz

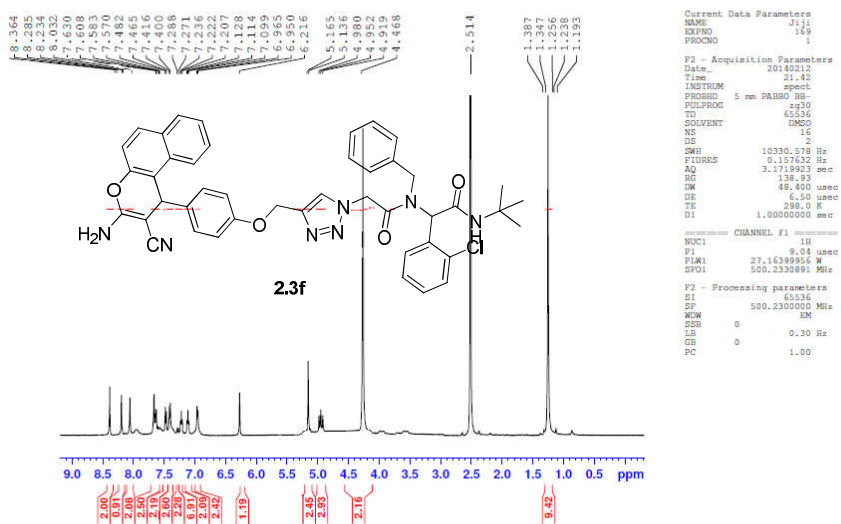
F2 - Processing parameters
 SI: 65536
 SF: 500.2330891 MHz
 WDW: -
 SSB: 0
 LB: 0.30 Hz
 GB: 0
 PC: 1.00

iitm_carbonshort CDC13 /opt/topspin iitm 10

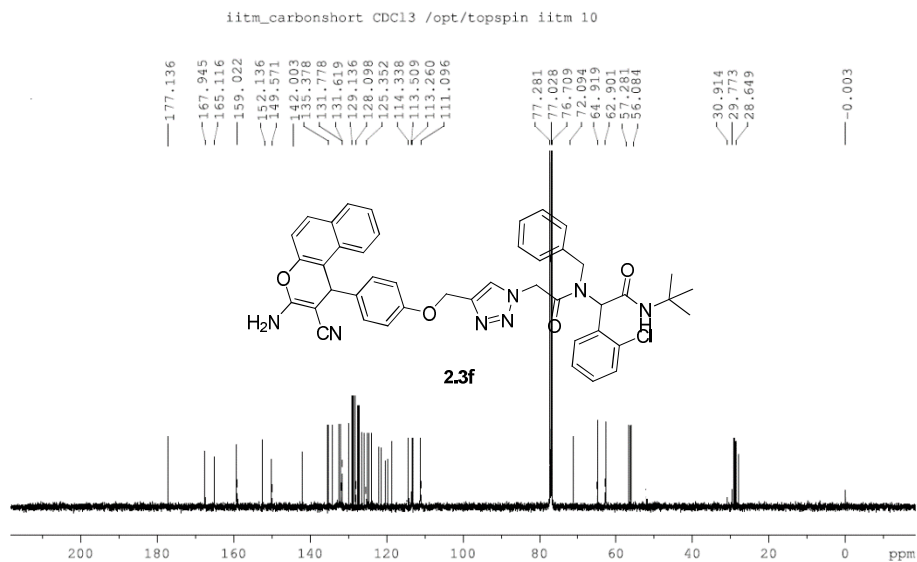




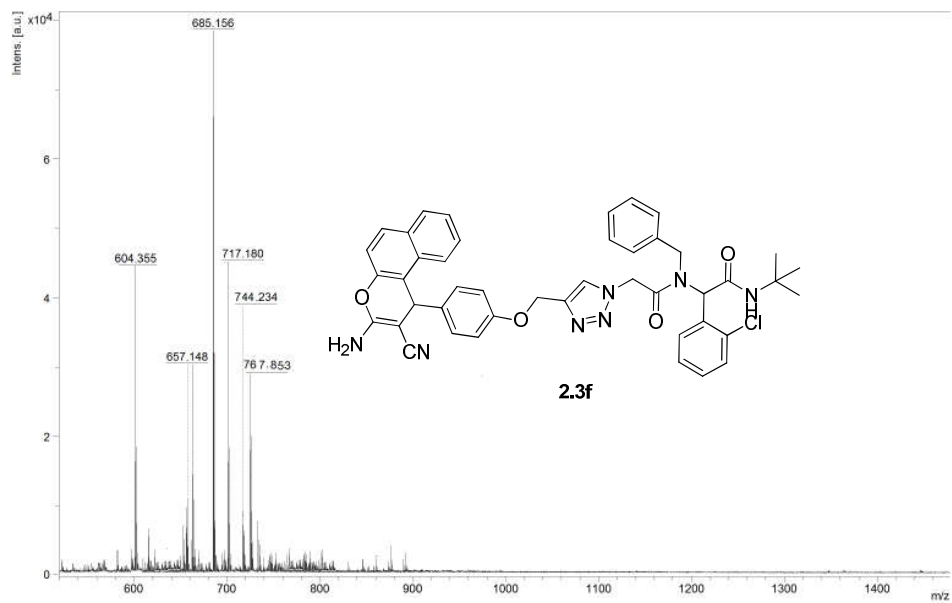
PROTON DMSO C:\Bruker\TOPSPIN nmr

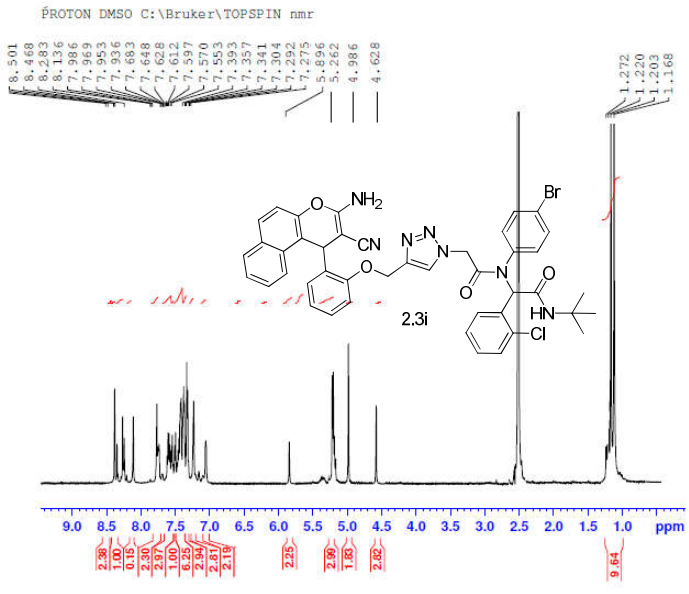


Current Data Parameters
 Name: 2.3f
 EXPNO: 169
 PROCNO: 1
 F2 - Acquisition Parameters
 Date_: 20140212
 Time: 21.42
 INSTRUM: spect
 PROBHD: 5 mm PABBO BB-
 PULPROG: zg30
 TD: 65536
 SOLVENT: DMSO
 NS: 16
 DS: 2
 SWH: 10330.578 Hz
 FIDRES: 0.151632 Hz
 AQ: 3.1115921 sec
 RG: 138.93
 RW: 48.400 usec
 DE: 6.50 usec
 TE: 298.0 K
 D1: 1.00000000 sec
 CHANNEL f1
 NUC1: 1H
 P1: 9.04 usec
 PLM1: 27.16399956 W
 SFO1: 500.2330991 MHz
 F3 - Processing parameters
 SI: 65536
 SF: 500.2300000 MHz
 NCV: 5M
 SSB: 0
 LB: 0.30 Hz
 GB: 0
 PC: 1.00



Department of chemistry IITM.



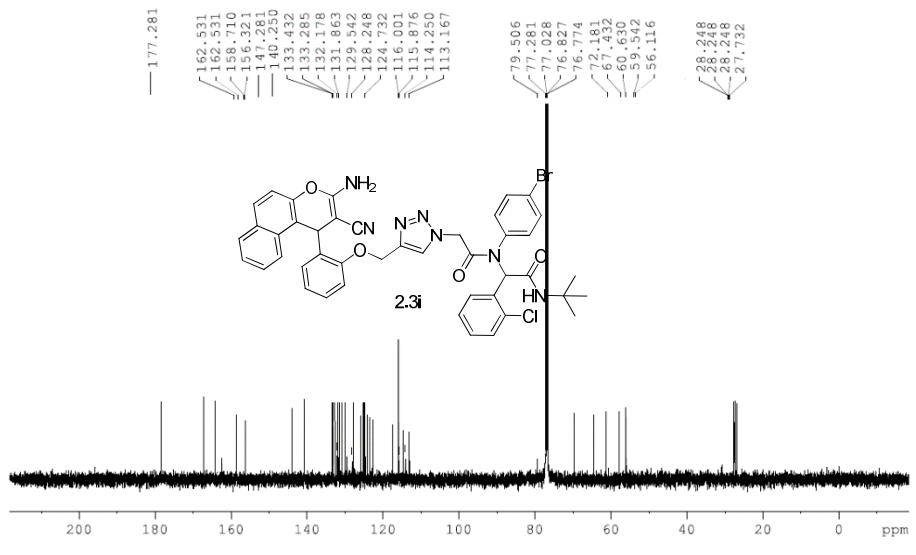


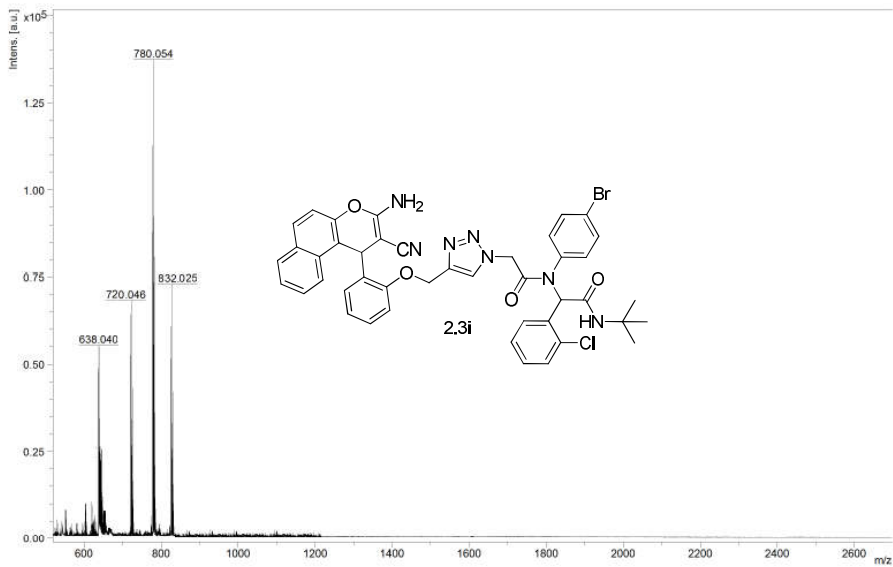
Current Data Parameters
 NAME: J111
 EXPNO: 166
 PROCNO: 1

F2 - Acquisition Parameters
 Date_: 20140212
 Time: 21:30
 INSTRUM: spect
 PROBR: 5 mm F4BBO BH-
 PULPROG: zg30
 TD: 65536
 SOLVENT: DMSO
 NS: 16
 DS: 2
 SWH: 10330.578 Hz
 FIDRES: 0.157632 Hz
 AQ: 3.1719923 sec
 RG: 171.32
 DW: 48.400 usec
 DE: 6.50 usec
 TE: 298.0 K
 D1: 1.0000000 sec

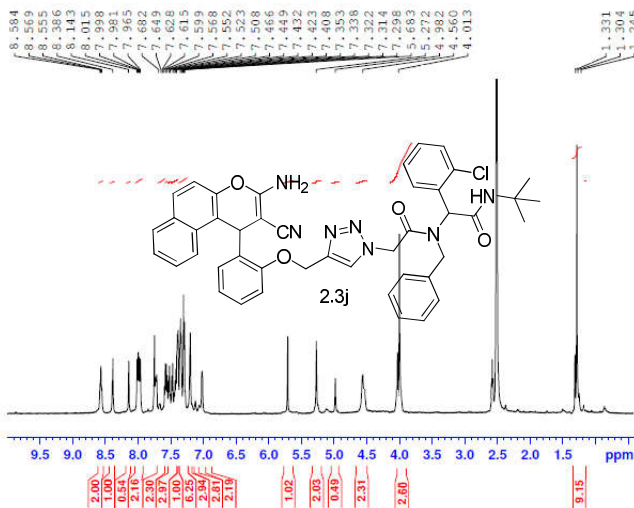
==== CHANNEL f1 =====
 NUC1: 1H
 P1: 9.04 usec
 P1M1: 27.639996 W
 SFO1: 500.2330891 MHz

F2 - Processing parameters
 SI: 65536
 SF: 500.2330000 MHz
 WUW: DM
 SSB: 0
 LB: 0.30 Hz
 GB: 0
 PC: 1.00





PROTON DMSO C:\Bruker\TOPSPIN nmr

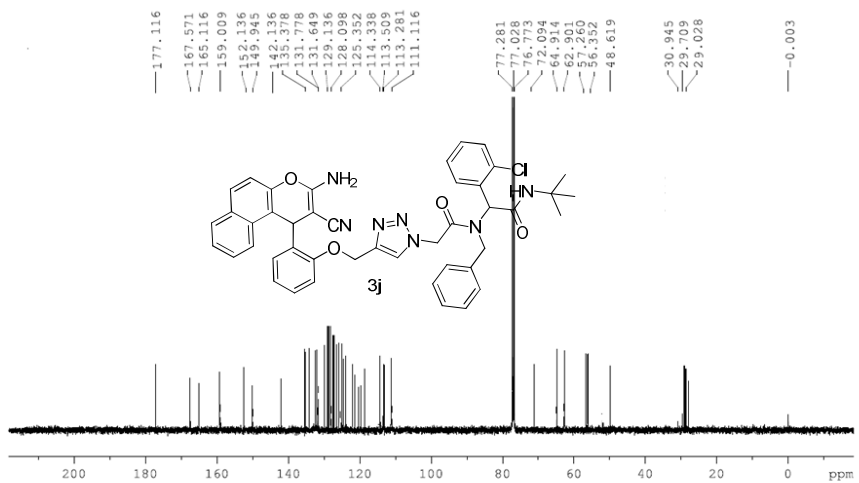


Current Data Parameters
 NAME: Jiji
 EXPNO: 170
 PROCNO: 1

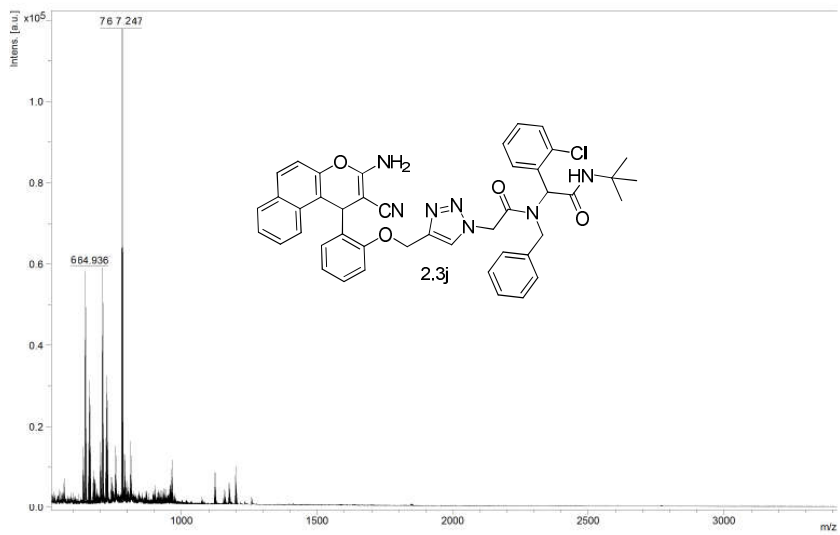
F2 - Acquisition Parameters
 Date_: 20140212
 Time: 21.46
 INSTRUM: spect
 PROBHD: 5 mm PABBO BB-
 PULPROG: zgpg30
 TD: 65536
 SOLVENT: DMSO
 NS: 16
 DS: 2
 SWH: 10330.578 Hz
 FIDRES: 0.157632 Hz
 AQ: 3.1719523 sec
 RG: 153.65
 DW: 48.400 usec
 DE: 6.50 usec
 TE: 298.0 K
 D1: 1.00000000 sec

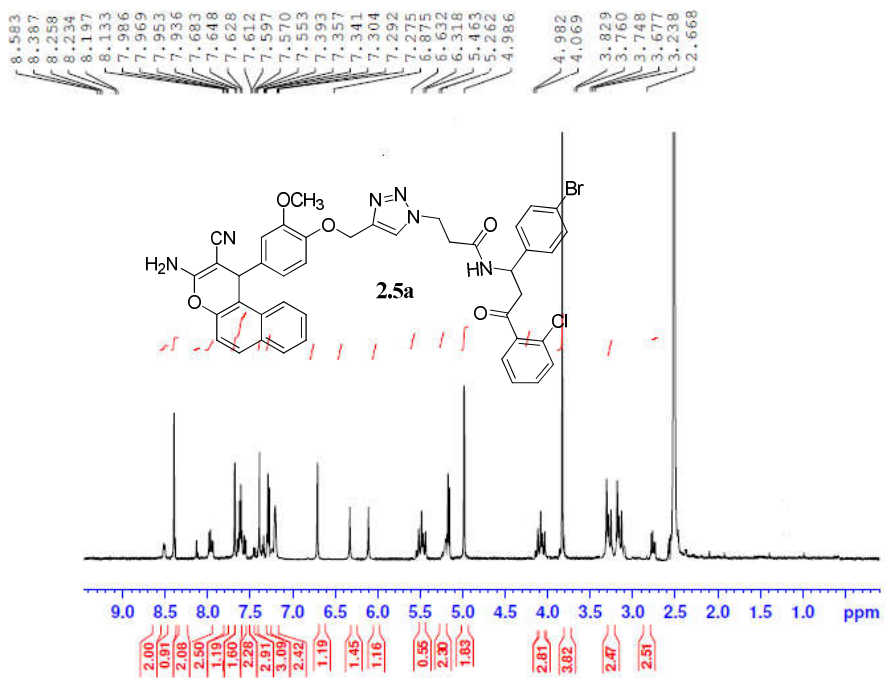
==== CHANNEL f1 =====
 NUC1: 1H
 P1: 9.04 usec
 PLM1: 27.1639986 W
 SFO1: 500.2300001 MHz

F2 - Processing parameters
 SI: 65536
 SF: 500.2300000 MHz
 WDW: EM
 SSB: 0
 LB: 0.30 Hz
 GB: 0
 PC: 1.00

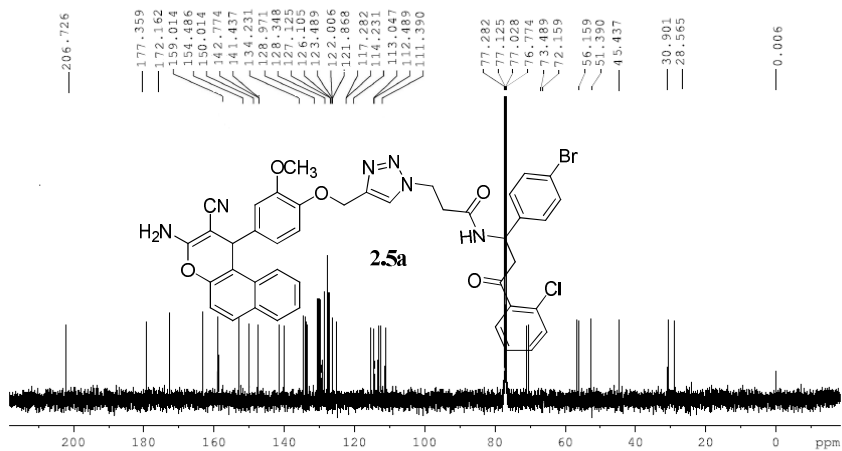


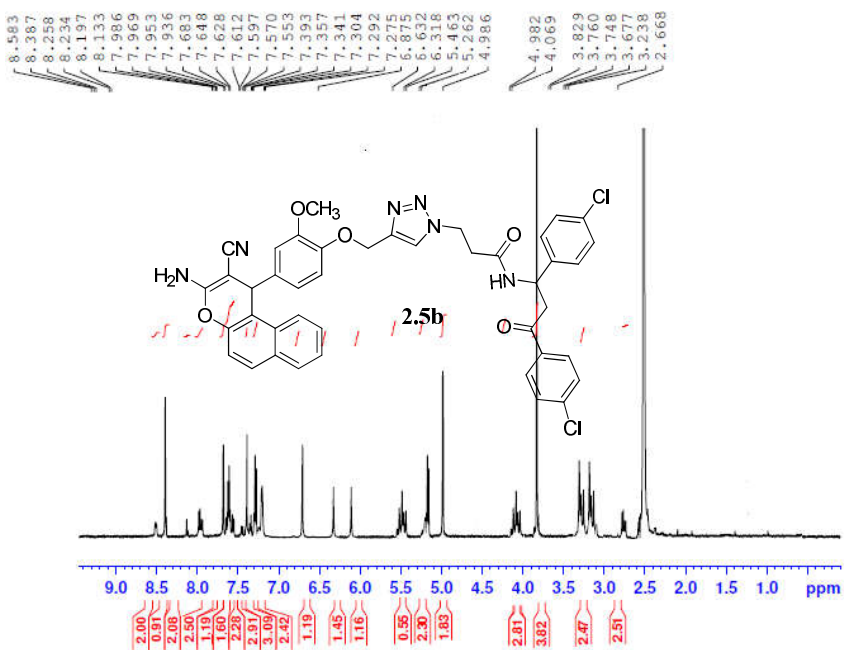
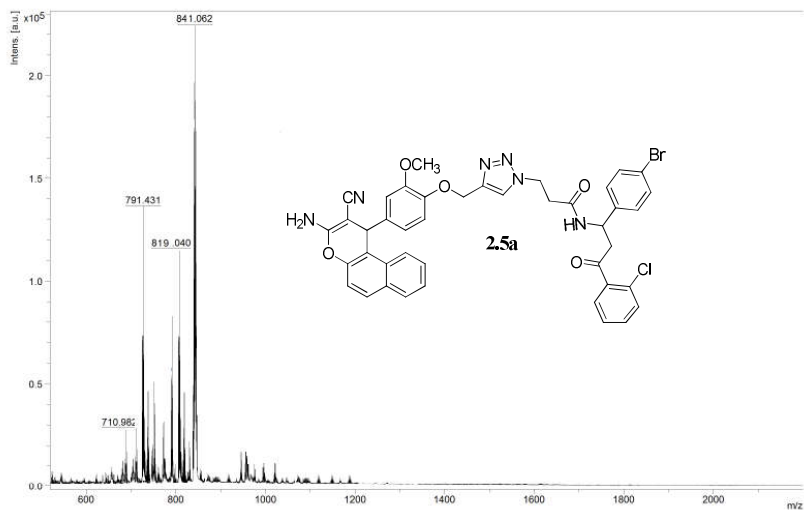
Department of chemistry IITM

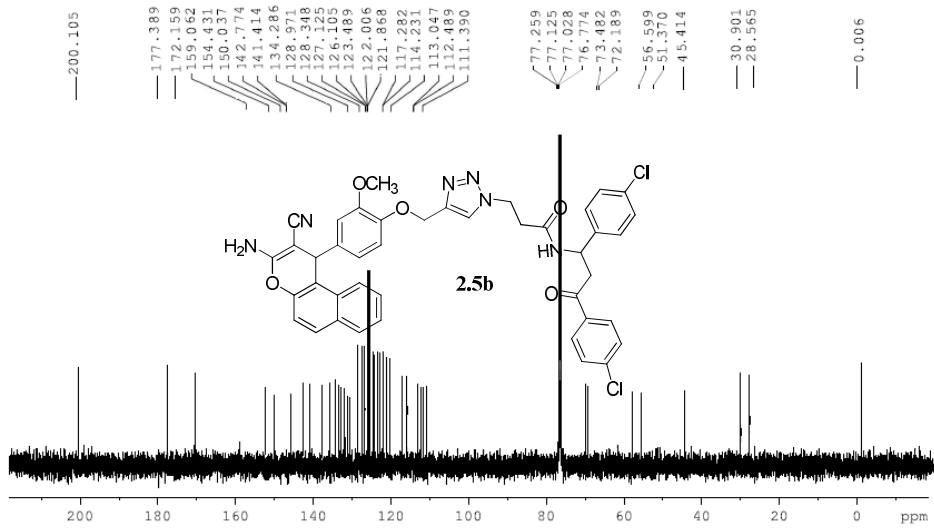




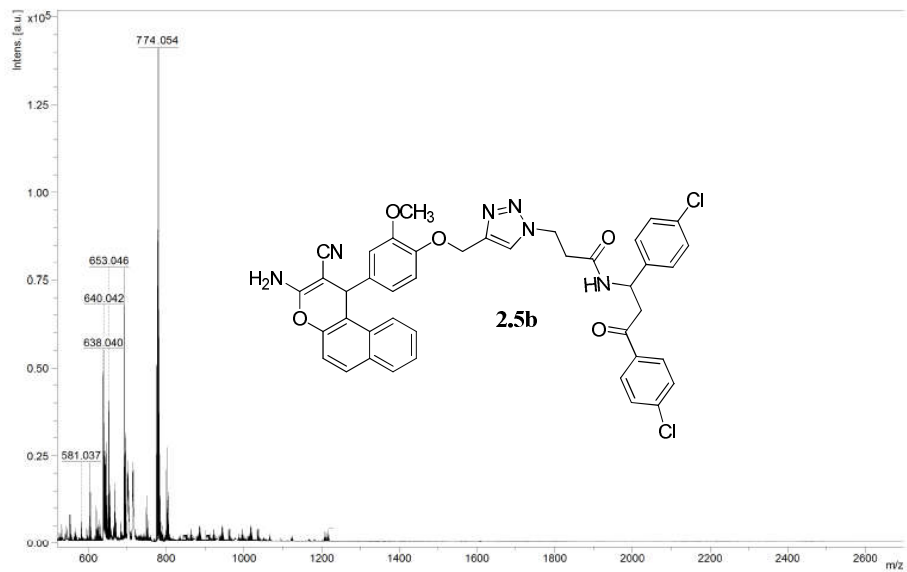
iitm_carbonshort CDCl3 /opt/topspin iitm 14

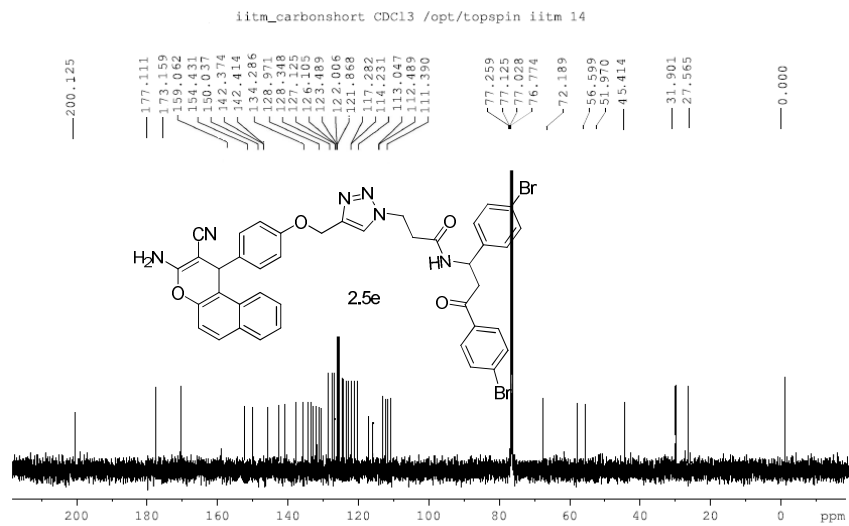
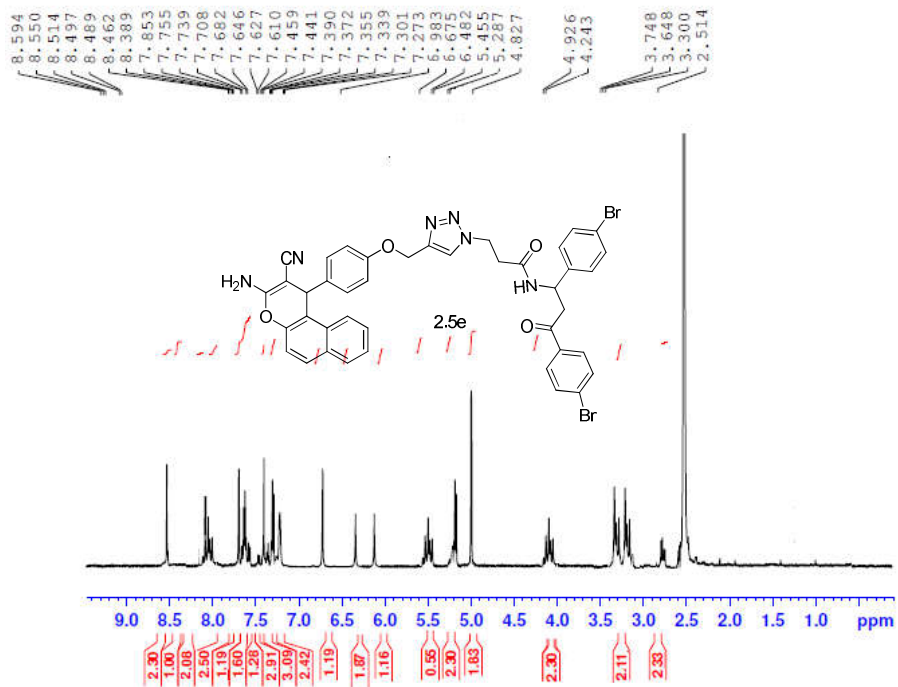


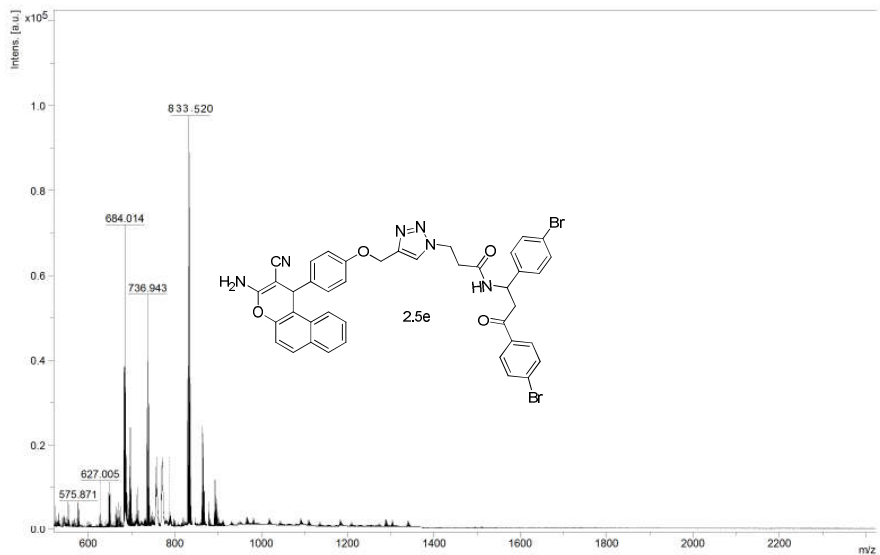




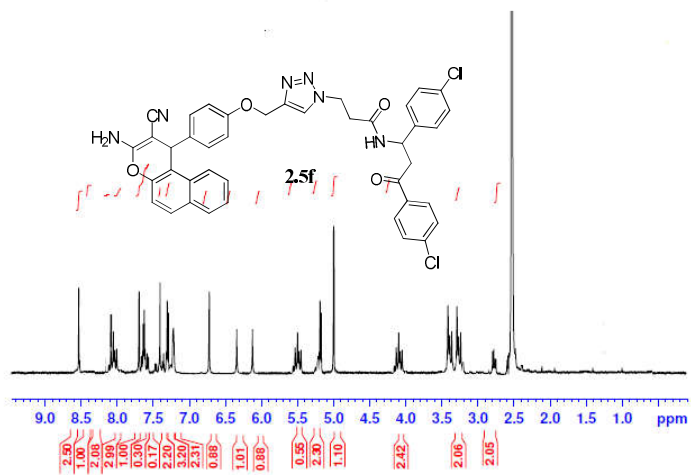
Department of chemistry IITM

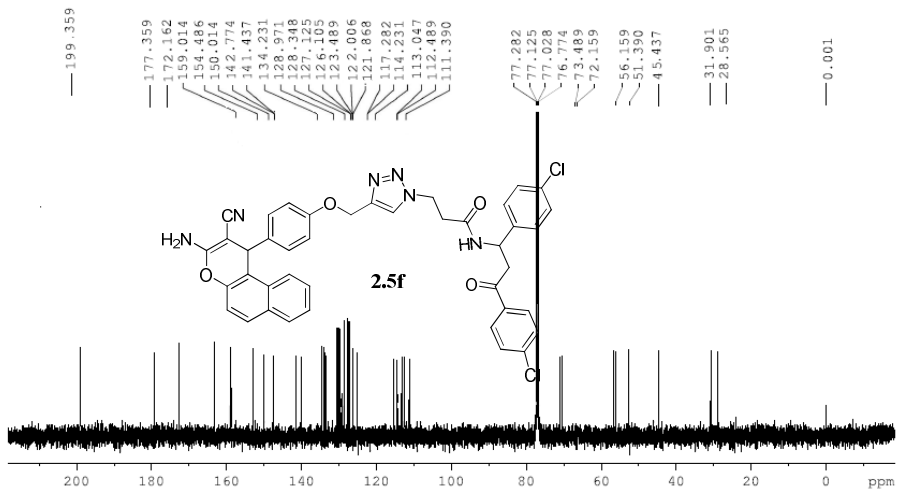




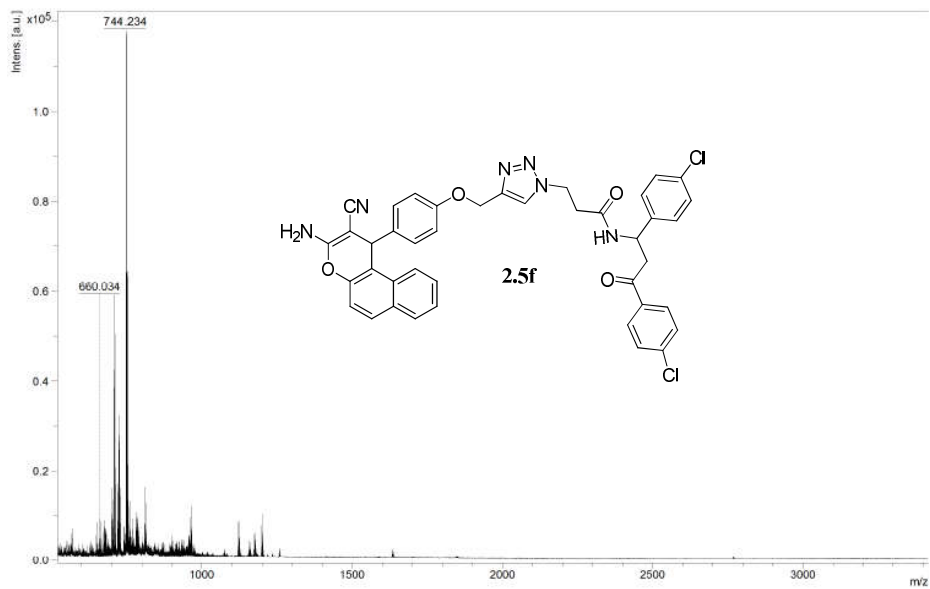


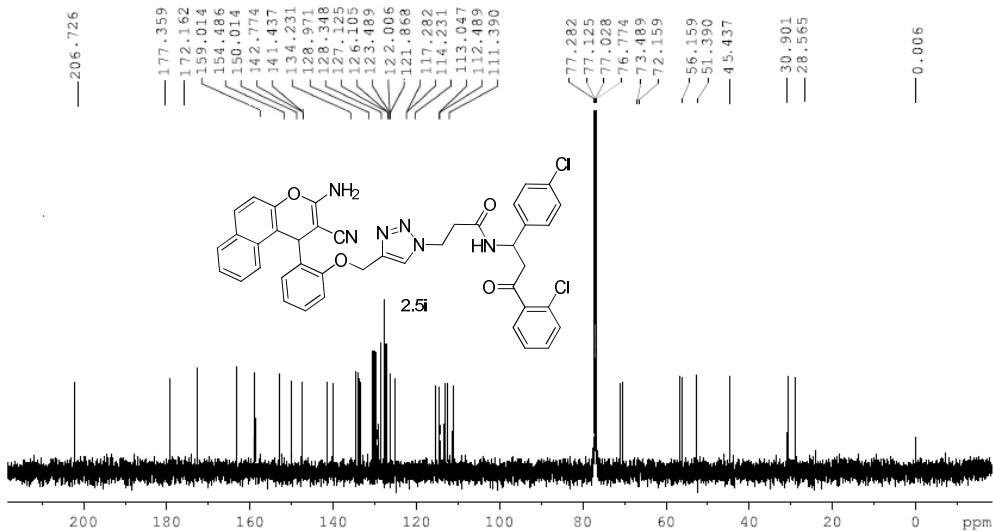
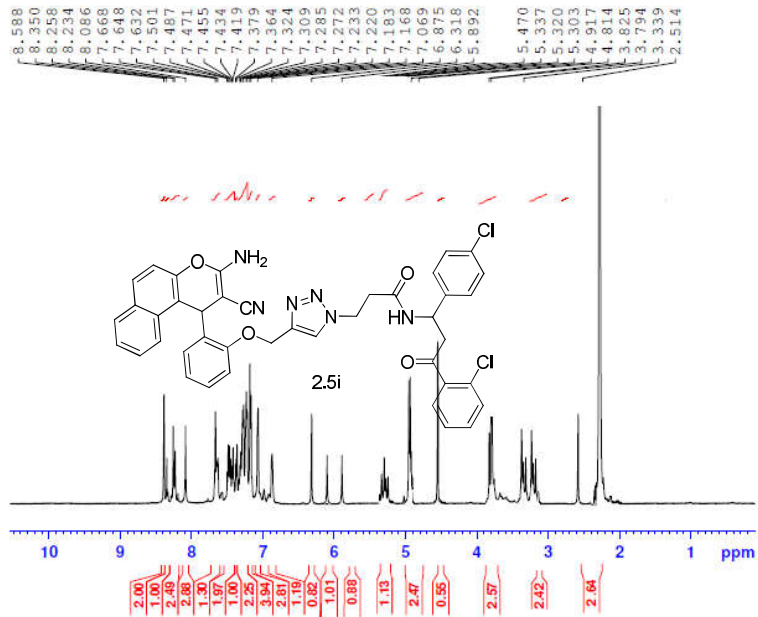
8.1583
8.5710
8.5114
8.4937
8.4859
8.022
7.776
7.763
7.747
7.718
7.702
7.688
7.672
7.402
7.388
7.372
7.319
7.302
7.275
7.260
7.246
7.224
6.728
6.466
5.455
5.273
4.965
4.318
4.318
3.794
3.648
3.300
2.252

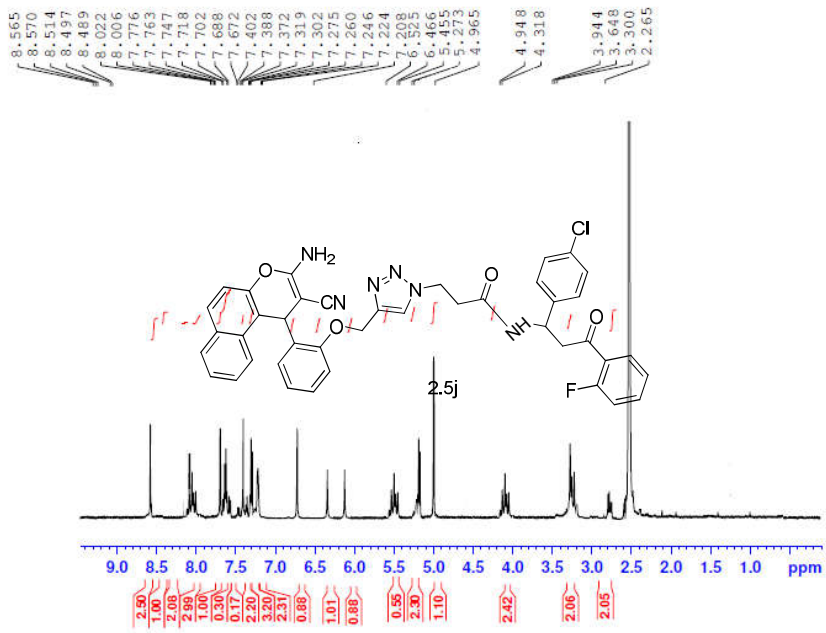
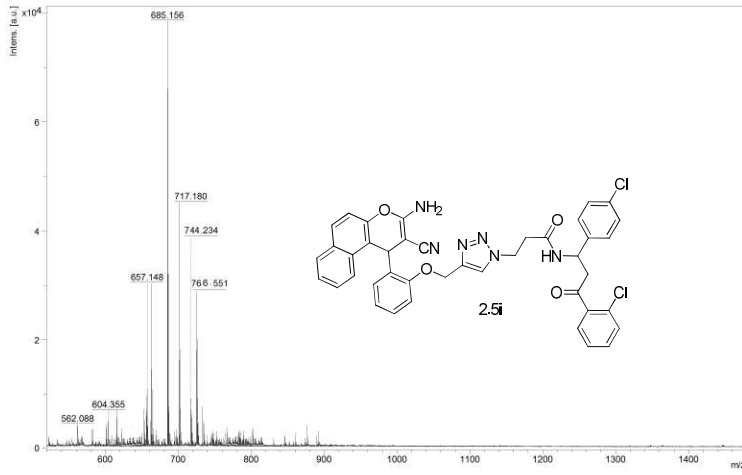


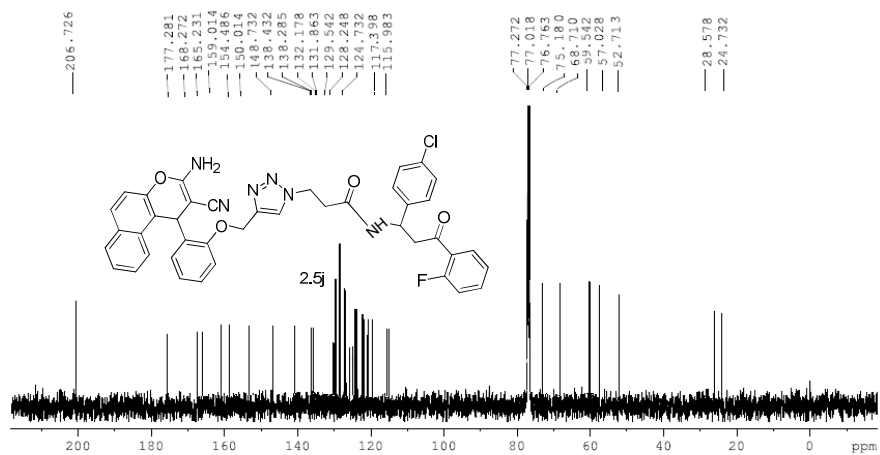


Department of chemistry IITM

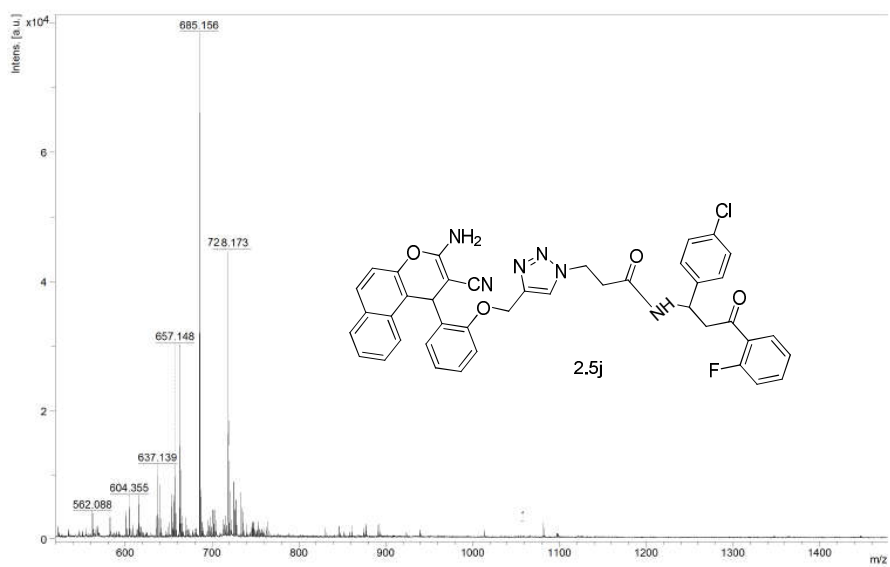








Department of chemistry IITM

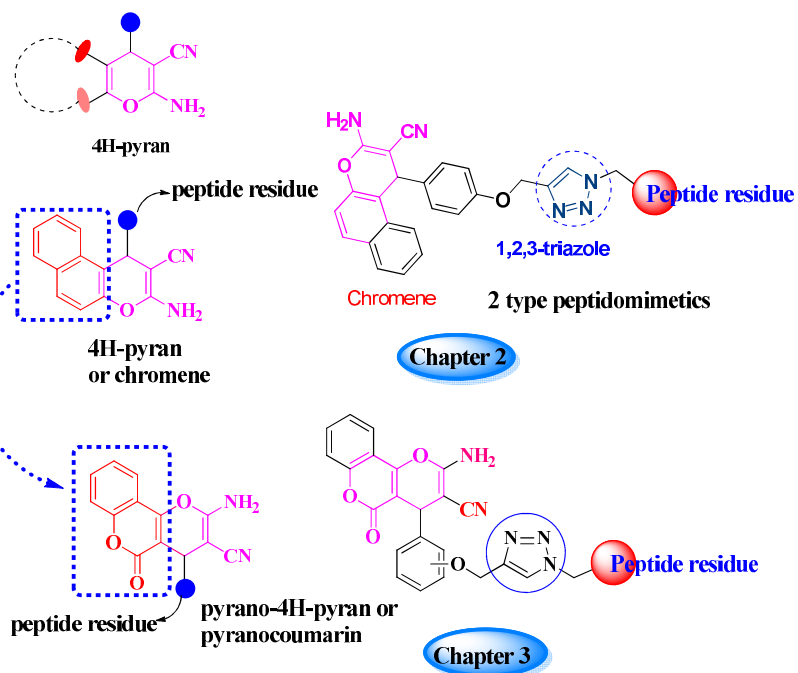


Chapter 3
**Design, synthesis and anticancer activity of
Pyranocoumarin peptidomimetic
fluorophores**

3.1 Introduction	134
3.2 Result and discussion	136
3.3 Photophysical properties	142
3.4: Biological property evaluation	145
3.5. Structural characterization	150
3.6. Experimental section	159
References	170
Supplementary data	172

3.1 Introduction

In chapter 2 we have discussed the synthesis of two types of triazole linked blue emitting chromene peptidomimetic fluorophores with in vitro cytotoxicity against MCF-7 cell lines. For the synthesis of these molecules we have used privileged 2-Amino-3-cyano-4H-Chromene derivatives as core scaffolds. Similar to 4H-pyrans, pyran annulated 4H-pyrans or pyranocoumarin is also a privileged structural motif widely distributed in various natural products with diverse biological activities¹ and are found in many medicinal plants that are traditionally being used for the treatment of hypertension, anemia, pulmonary arteries, malaria, various bacterial and fungal diseases etc.² Similarly several synthetic pyran/pyranocoumarin derivatives have been reported as potential therapeutic agents for a verity of cancers including human breast cancer.³ The other biological activities of these scaffolds include anti-microbial, anti-HIV, antioxidant, anti-allergic,⁴ anti-dyslipidemic, anti-hyperglycemic,⁵ xanthine oxidase inhibitory,⁶ butyryl cholinesterase inhibitory, acetylcholinesterase inhibitory,⁷ and Src kinase inhibitory activities.⁸



Scheme 3.1: General scheme for the synthesis of pyranochromene peptidomimetics

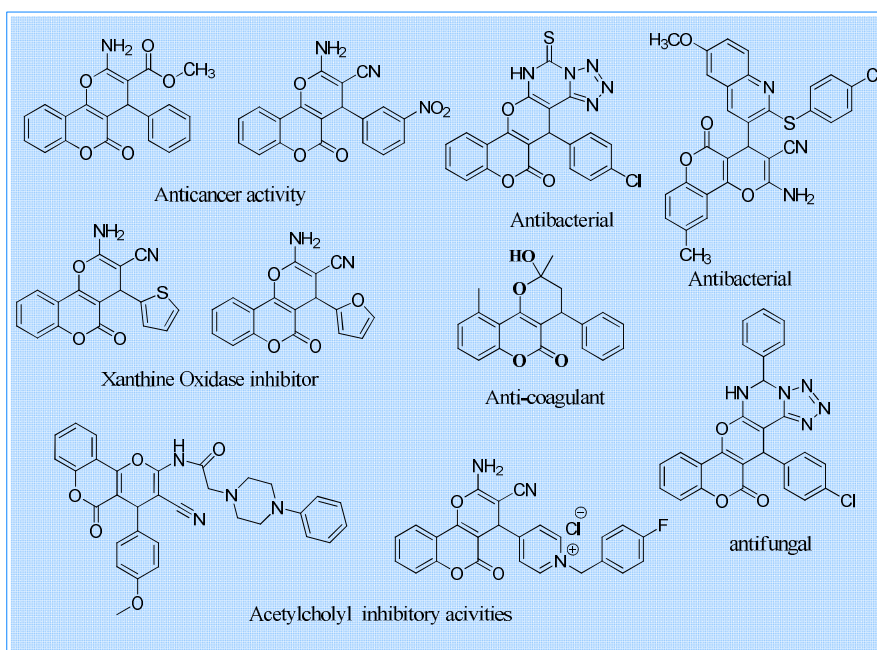
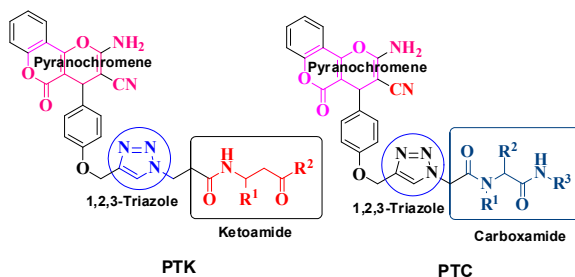


Fig. 3.1: selected examples of pyrano coumarins with potential biological activity.⁹

As described in the previous chapter, coumarin derivatives are also known for their use as fluorescent probes for bio-imaging. Dyes such as Alexa Fluors® and DyLight Fluors® are examples of such commercially available coumarin probes.¹⁰ However, the toxicity of coumarin, the absence of selectivity and the persistence of the probe in the inner cellular atmosphere after the imaging are the major limiting factors restricting the wide spread use of coumarin probes in imaging/therapy. A recent development in this field is the development of selective affinity based probes with anticancer or other biological activity without the need of wash-out process.¹¹ A careful literature survey revealed that pyranocoumarin scaffolds linked with both 1,2,3-triazole and a peptide residue such as carboxamide or acetamides are not yet explored for developing such bifunctional therapeutic agents. In continuation of the work discussed in the previous chapter, we decided to synthesis a series of pyranocoumarin peptidomimetics functionalized with carboxamide (PTC) or acetamides (PTK) residues spaced with a linker 1,2,3-triazole as shown in scheme 3.2 for exploring their bioimaging and cytotoxicity properties.

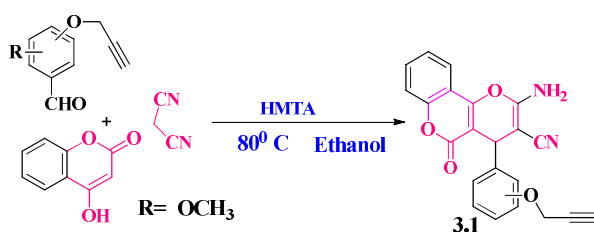
3.2 Result and discussion



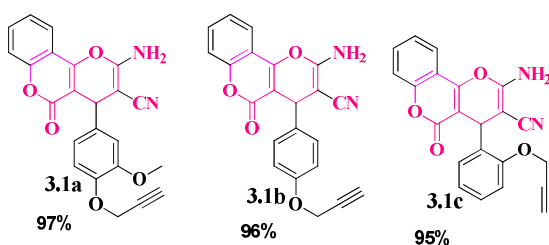
Scheme 3.2: General structures of the two series of pyranocoumarin peptidomimetics

3.2.1 Synthetic strategy pyranocoumarin peptidomimetics

The alkyne functionalized pyranocoumarin **3.1** was prepared by following a three component reaction as shown in scheme 3.3. The reaction between 4-hydroxy coumarin, propargylated benzaldehyde and malononitrile under ethanol medium using hexamethylenetetramine (HMTA) as catalyst¹² afforded the alkyne **1** in near quantitative yield as precipitate and was purified by water wash and were systematically characterized using ¹H NMR, MS and IR spectroscopy.



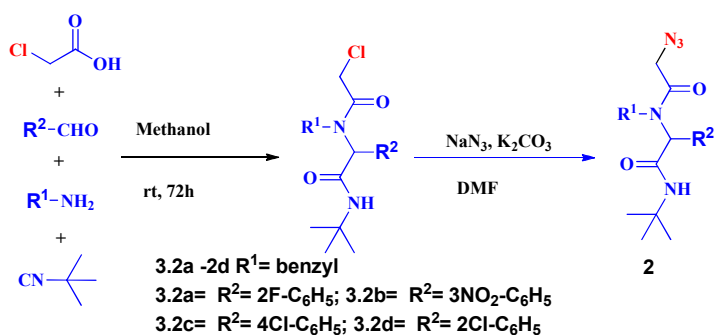
Scheme 3.3: Synthetic strategy of alkyne functionalized pyranochromenes



Scheme 3.4: synthesized alkyne functionalized pyranochromene derivatives.

We then moved on to the synthesis of azides **3.2** and **3.4** in which the former one is a carboxamide derivative and the later one is an

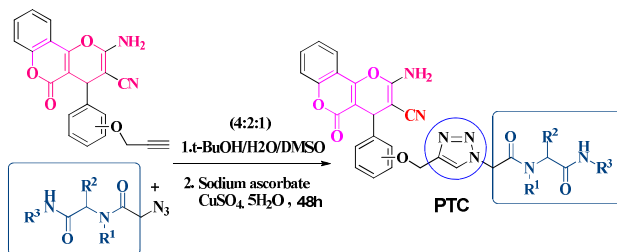
acetamide derivative. Carboxamide azides **3.2a-d** were synthesized by following an Ugi four component reaction¹³ (Ugi-4CR) as shown in scheme 3.5. The Ugi-4CR between a suitably substituted aldehyde, an amine, *t*-butyl isocyanide and chloroacetic acid afforded the chloro derivative of the carboxamide. The chloro derivatives on subsequent treatment with sodium azide afforded the small peptide like carboxamide azides **3.2a-d** in 85-94% isolated yield.



Scheme 3.5: Ugi-4CR to Ugi-type α -amino acyl amide azides

The pyrano chromene alkynes were then ligated to Ugi-azides via Cu (I) catalyzed click cycloaddition reaction under Sharpless condition using the catalytic system comprising of CuSO₄·5H₂O/Sodium ascorbate in tertiary-butanol/water/DMSO.¹⁴ In a typical reaction, the scaffolds **1a** and **2a** were mixed with 0.2 equivalent of CuSO₄ and 0.4 equivalent of sodium ascorbate in a mixed solvent system containing *t*-butanol, water and DMSO in 4:2:1 ratio at room temperature for 12 hours as shown in scheme 3.6. After that the reaction mixture was diluted with cold water to afford the click product **3.3a** in solid form with 85% yield. The scaffolds generated via click ligation reaction are designated as type 1 peptidomimetics and are listed in table 1.

Following the same protocol, we have successfully synthesized 6 new peptidomimetics **3.3a-f** with 80-85% yield.

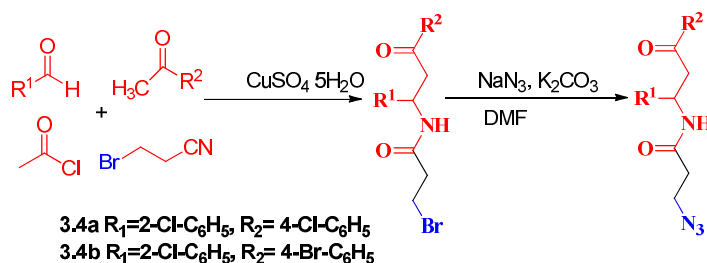


Scheme 3.6: Synthesis of PTC peptidomimetics through click chemistry

Table 3.1: Structure, isolated yield and photophysical data of pyranocoumarin carboxamide (PTC) peptidomimetics 2.3a-f.

Entry	Peptidomimetic	% yield	Abs _{max} (nm)	Em _{max} (nm)	Stokes shift (nm)
3.3a		85%	262	436	174
3.3b		84%	265	432	174
3.3c		81%	259	430	171
3.3d		83%	264	435	171
3.3e		81%	258	432	174
3.3f		82%	258	434	176

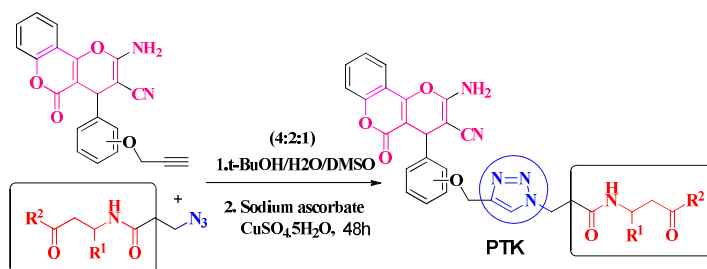
After the click ligation reaction of pyrano chromenes with carboxamide azides the studies were extended to the synthesis of pyranocoumarin ketoamide peptidomimetics (PTK) by using another set of azides synthesized via an alternative Mannich type reaction as shown in scheme 7.¹³ In this reaction a bromo propionitrile react with an enolizable (usually a ketone) and a non enolizable (an aldehyde) oxo compounds in presence of acid chloride and $\text{CuSO}_4 \cdot 5\text{H}_2\text{O}$ as catalyst resulted in the formation of a bromo derivative of β -keto amides. These bromo derivatives were then converted to corresponding azides by treating them with sodium azide in presence of potassium carbonate in DMF at room temperature as shown in scheme 3.7. Two azide derivatives **3.4a** and **3.4b** were prepared and were used for the click ligation reaction with pyrano chromenes as shown in scheme 8. Six new peptidomimetics **3.5a-3.5f** were synthesized as listed in table 3.1.



Scheme 3.7: Alternative Mannich 4CR for β -keto amide azides

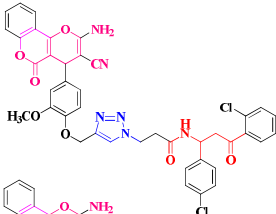
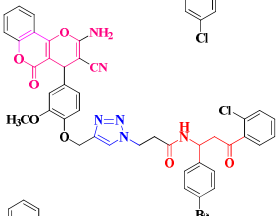
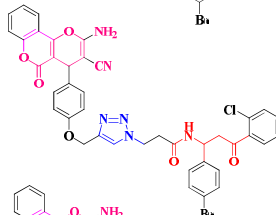
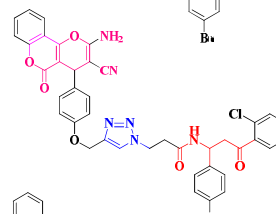
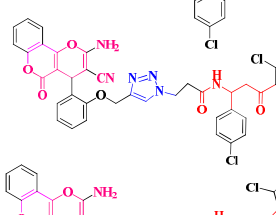
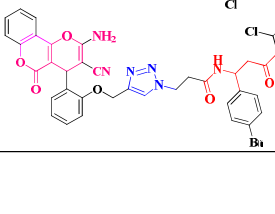
The click reactions of alkynes **3.1a** were then continued with acetamide azides **3.4** under the same conditions to obtain the pyranocoumarin acetamide peptidomimetics **3.5a-f** listed in table 3.2.

The acetamide peptidomimetics were also obtained in >80% yield from the aqueous workup of the reaction mixture and their structures were also confirmed from HRMS analysis. As shown in tables 3.1 and 3.2, the click reactions to form both carboxamide and acetamide peptidomimetics were free from any electronic effects imparted by the substituents present in the starting alkyne and azide scaffolds and were completed within 12 h with the excellent conversion of the starting materials to the desired product without the aid of any accelerating ligands



Scheme 3. 8: Synthesis of PTK peptidomimetics through click chemistry

Table 3.2: Structure, isolated yield and photophysical data of pyranocoumarin carboxamide (PTC) peptidomimetics 2.3a-f.

Entry	Peptidomimetic	% yield	Abs _{max} (nm)	Em _{max} (nm)	Stokes shift (nm)
3.5a		80%	265	431	166
3.5b		82%	265	435	166
3.5c		80%	266	435	165
3.5d		83%	266	436	165
3.5e		85%	265	430	165
3.5f		81%	266	432	166

3.3 Photophysical properties

To study the photo physical properties, the absorption and emission spectra of all the compounds **3.3a-f** and **3.5a-f** were recorded in

DMSO at pH range 0-10. The normalized absorption and emission of representative compounds **3.3a** and **3.5b** are shown in figures 3.2 and 3.3. Both compounds showed emission in the blue region with large Stokes shift values. The compound **3.3a** showed an absorption maxima centered at 262 nm and emission maxima centered at 436 nm with a high Stokes shift value of 174 nm. Similarly the compound **3.5b** showed an absorption maxima centered at 258 nm and an emission maxima centered at 434 nm with Stokes shift value of 180 nm. These values are higher than the 2-amino-4H-chromene peptidomimetics discussed in chapter 2.

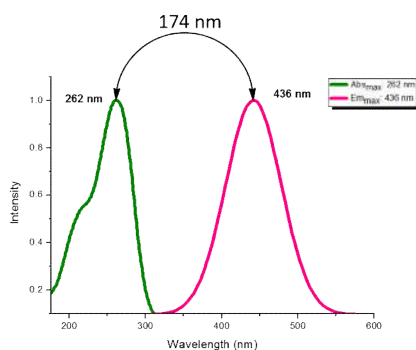


Fig. 3.2: The normalized absorption and emission spectra of the compound 3.3a

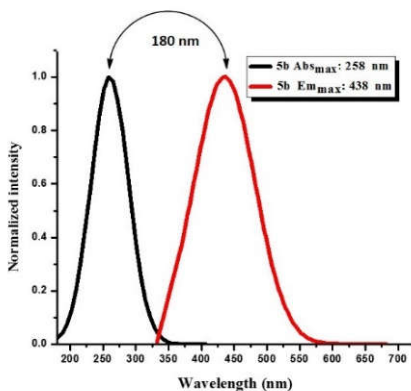


Fig. 3.3: The normalized absorption and emission spectra of the compound 3.5a

To explain the observed fluorescence properties, we have carried computational calculations to obtain the bandgap of the molecules. The bandgap of selected molecules **3.4a** and **3.5a** were calculated from DFT modelling using B3LYP/6-31G method basis set (Gaussian 09). **3.3a** showed a wide band gap of 2.726 eV and **3.5a** showed a relatively high band gap of 2.285 eV. The wide band gap obtained for these molecules clearly explains the blue emission properties of the molecules. The large Stokes shifted emission observed are also promising since probes with large Stokes shifted emission are free from background signal overlapping and such molecules are better candidates for the development of selective affinity-based fluorescent probes for drug-target binding imaging at the cellular level if they possess fluorescence property coupled with anticancer activity. The energy minimized structure of compound **3.3a** and **3.5a** are shown in figures 3.6 and 3.6 respectively.

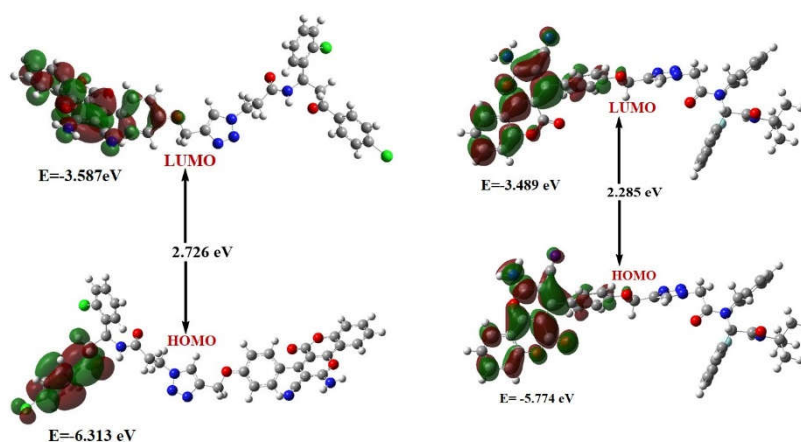


Fig. 3.4: The Frontier molecular energy level and band gap of 3.3a and 3.5a.

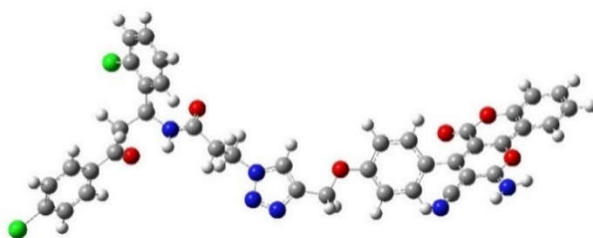


Fig.3.5: The energy minimized structure of **3.3a**

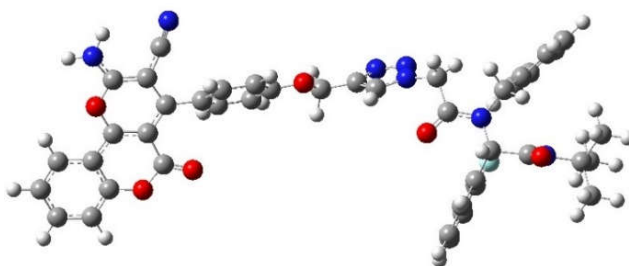


Fig.3.6: The energy minimized structure of **3.3a**

3.4: Biological property evaluation

3.4.1: Evaluation of drug-likeness

As done in the previous cases, here also we have calculated the drug property descriptors of all the molecules using the online service, www.molinspiration.com and were tabulated in table 3.3

Table 3.3: drug property descriptors of the click products 3.3a-3.3f and 3.5a-3.5f

Entry	Number of violations	Number of atoms	Log p <5	Molecular weight <500	Number of ON <10	Number of OH NH <5	Number of rotatable of bonds
3.3a	2	56	4.90	791.65	13	3	13
3.3b	3	56	5.03	836.10	13	3	13
3.3c	3	56	5.44	806.07	12	3	12
3.3d	3	54	5.31	761.62	12	3	12
3.3e	3	54	5.26	761.62	12	3	12
3.3f	3	54	5.39	806.07	12	3	12
3.5a	2	59	4.86	797.84	14	3	13
3.5b	2	61	4.67	824.85	17	3	14
3.5c	3	59	5.42	814.30	14	3	13
3.5d	3	57	5.68	784.27	13	3	12
3.5e	3	57	5.63	784.27	13	3	12
3.5f	3	59	5.04	794.83	16	3	12

As shown in table 3.3, the click products **3.3a-f** and **3.5a-f** are deviating from the rule of five with log P values in between 4.67- 5.68 and molecular weights in between 700-850 qualifying to be considered as beyond rule of 5 (bRo5) molecules for modulating difficult and emerging target classes.²⁴

3.4.2 The in vitro anti-cancer study against MCF-7 Cell lines

3.4.2 (A) Cell culture and maintenance

A representative compound **3.3a** and **3.5a** were used for the cytotoxicity evaluation to study the potential of these molecules as anticancer agents. Human breast cancer MCF-7 cells were maintained

in RPMI medium 1640 supplemented with 10% fetal bovine serum as well as 100 µg/mL streptomycin, 100 U/mL penicillin, 2 mM L-glutamine and Earle's BSS adjusted to contain 1.5 g/l Na bicarbonate, 0.1 mM nonessential amino acids, and 1.0 mM of Na pyruate in a humidified atmosphere containing 5% CO₂ at 37⁰C.

3.4.2. (B): In vitro cytotoxicity of synthesized 3.3a and 3.5a

Cell viability was determined by MTT assay. MCF-7 cells were seeded in 96-well plates at a concentration of 1.0x10⁴ cells/well and incubated overnight at 37⁰C in a 5% CO₂ humidified environment. Then the cells were treated with different concentrations of the sample **3.3a** and **3.5a** separately, like 10, 20, 30, 40, 50, 60, 70, 80, 90, and 100µM/mL (dissolved with RPMI medium 1640), respectively. Controls were cultivated under the same conditions without addition of sample **3.3a** and **3.5a**. The treated cells were incubated for 48 h for MTT assay. The stock concentration (5 mg/mL) of MTT-(3-(4,5-Dimethylthiazol-2-yl)-2,5-diphenyltetrazolium bromide, a yellow tetrazole) was prepared and 100 µL of MTT was added in each wells and incubated for 4 h. Purple color formazan crystals were observed and these crystals were dissolved with 100 µL of dimethyl sulphoxide (DMSO), and read at 620 nm in a multi well ELISA plate reader (Thermo, Multiskan). The molecules showed excellent cytotoxicity against MCF-7 cell lines with an IC₅₀: 50µM as shown in figures 3.7 and 3.8.

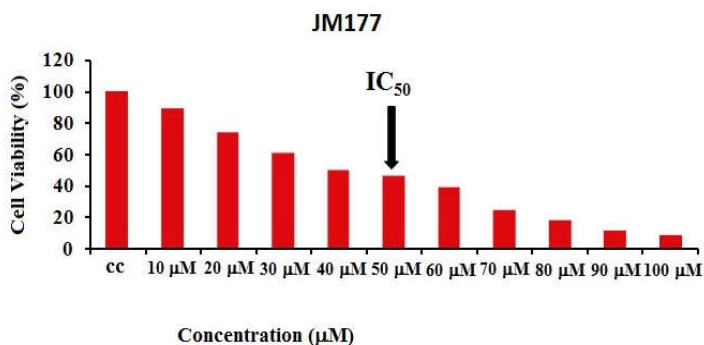


Fig. 3.7: MTT assay results confirming the in vitro cytotoxicity effect of **3.3a** against the MCF-7 cells. The detected IC₅₀ concentration was 50µM.

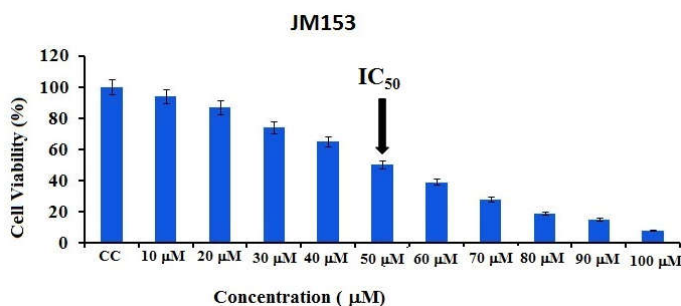


Fig. 3.8: MTT assay results confirming the in vitro cytotoxicity effect of **3.5a** against the MCF-7 cells. The detected IC₅₀ concentration was 50µM.

3.4.2 (C): In vitro imaging studies: *DAPI (4, 6-diamidino-2-phenylindole, dihydrochloride) staining*

MCF-7 cells were treated with **3.3a** and **3.5a** at its IC₅₀ concentration (50µM/mL) for 48 h, and then fixed with methanol: acetic acid (3:1, v/v) prior to washing with PBS. The washed cells were then stained with 1mg/mL DAPI (4,6-Diamidino-2-phenylindole, dihydrochloride) for 20 min in the dark atmosphere. Stained images were recorded with fluorescent microscope with appropriate excitation filter. The bright field and fluorescence microscopic images

are shown in figures. **3.8 and 3.9**. The strong bluish fluorescence and cellular uptake observed in the imaging studies with **3.3a and 3.5a** reveals that these molecules have potency to selectively locate malignant cell lines such as MCF-7.

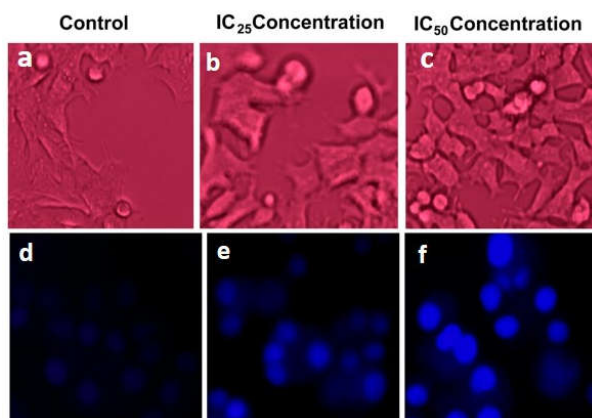


Fig. 3.9: Bright field inverted light microscopy images (a) (cc), (b) (IC 25) and (c) (IC 50) and fluorescence microscopy images (d) (CC), (e) (ICC 25) and (f) (IC50) of **3.3a** treated MCF-7 cells.

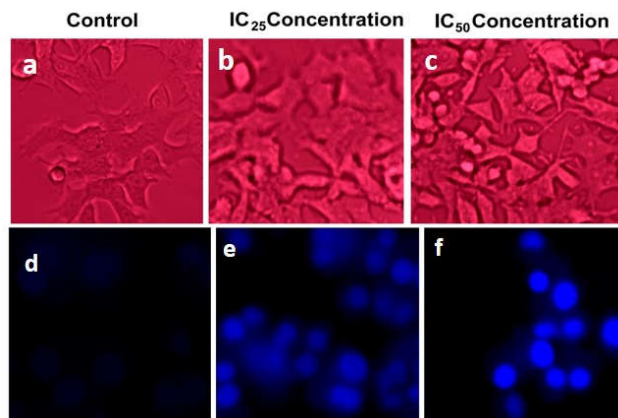


Fig. 3.10: Bright field inverted light microscopy images (a) (cc), (b) (IC 25) and (c) (IC 50) and fluorescence microscopy images (d) (CC), (e) (ICC 25) and (f) (IC50) of **3.5a** treated MCF-7 cells.

In summary in this chapter also we have demonstrated a click chemistry strategy for the synthesis of a series of bifunctional pyranocoumarin peptidomimetics with inhibitory property towards human breast cancer cell lines MCF-7 and at the same time having excellent intracellular imaging properties. The chemistry demonstrated for the synthesis is close to green in terms of fewer number of synthetic steps, operational ease and reaction conditions. The biological and photophysical properties of the molecules are promising for the development of intracellular imaging agents or potential anticancer agents based on these new molecules.

3.5. Structural characterization

3.5.1. Structure identification of 2-Amino-4-(4-(ethynyloxy)-3-methoxyphenyl)-5-oxo-4, 5-dihydropyrano [3,2-c]chromene-3-carbonitrile **3.1a**

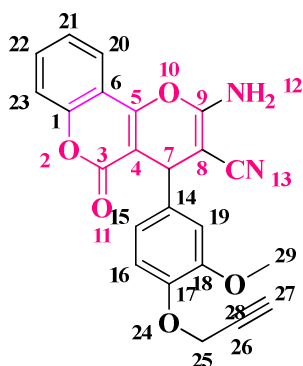


Fig.3.11: structure of compound 3.1a

4-hydroxy coumarin **3.1a** is taken as a representative example for the structure elucidation. The compound is numbered as shown in figure 3.11. The FT-IR spectrum of the compound showed major absorptions at 3394, 3275, 3200, 2924, 2224, 2191, 1709, 1671, 1559 and 1508

cm⁻¹. The band at 3394 cm⁻¹ is due to the stretching vibration of free NH₂ group. The band at 2224 cm⁻¹ due to the stretching vibration of C-N triple bond of nitrile group. The strong C-H stretching band of alkyl group is observed at 3200 and the weak band at 2130 represent the stretching vibration of C-C triple bond. The C=O stretching vibration is found at 1709 cm⁻¹ and the C=C vibration is observed at 1559 cm⁻¹

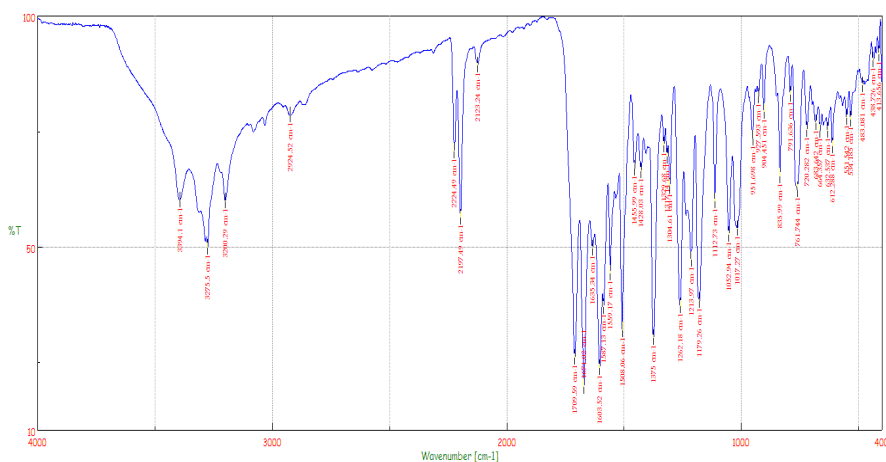


Fig. 3.12: FT-IR spectrum of the compound 3.1a

The initial information obtained from FT-IR spectrum was further confirmed by ¹H NMR studies. The one proton singlet observed at δ 3.49 corresponds to the proton at position 27. i.e., the proton at C-C triple bond. The singlet observed at δ 3.87 corresponds to the three –OCH₃ proton at position 29. The one proton singlet at δ 4.42 is due to the CH proton at position 7. The singlet proton observed at δ 4.95 attributed to –CH₂ proton at position 25. The aromatic protons are observed as seven distinct peaks such as a doublet at δ 6.75 with a J=8.0 Hz, a one proton doublet at δ 6.88 with a J=8.0 Hz, a one proton singlet at δ 6.97, a one proton doublet at 7.25 with J=8.8 Hz, a one

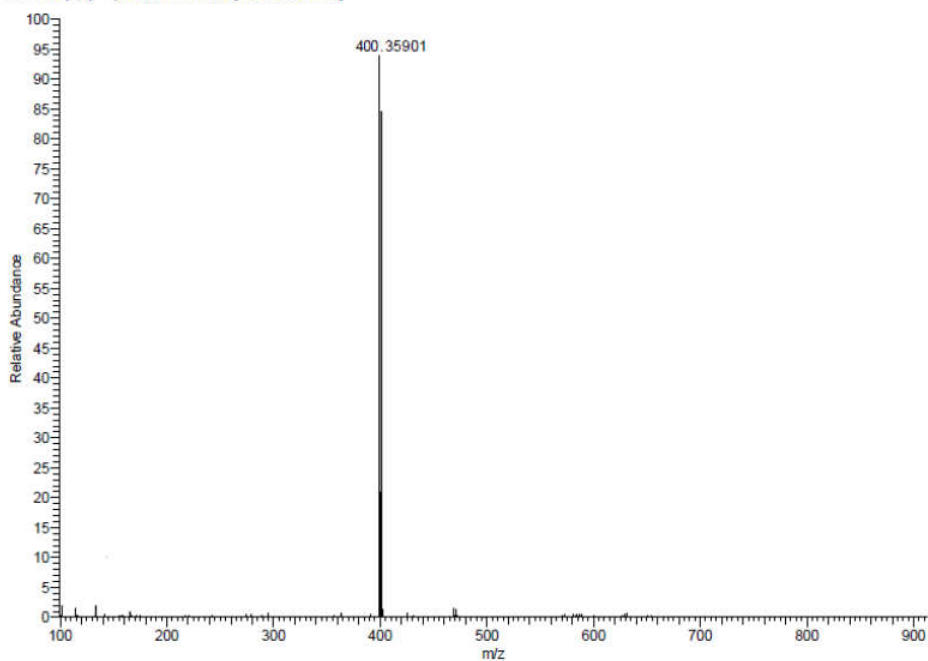


Fig. 3.14: Mass spectra of 3.1a

2.5 Structure of the Click peptidomimetic 3.3a

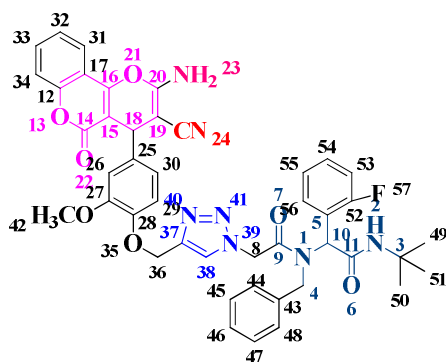


Fig. 3.15: structure of compound 3.3a

The compound is numbered as shown in figure 3.15. The FT-IR spectrum of the compound showed major absorptions at 3422, 3376, 2923, 2227, 1747, 1675, 1598 and 1486 cm^{-1} . The band at 3376 cm^{-1} is due to the NH stretching vibration of the acetamido group. The amide I band, i.e., band due to the C=O stretching vibration occurs at 1675 cm^{-1} and the amide II band which arises from the interaction between the N-H bending and the C-N stretching of the C-N-H group is obtained at 1598 cm^{-1} . The absorption at 1747 cm^{-1} is due to the C=O stretching vibration of the ketone part. The band at 3422 cm^{-1} is due to the stretching vibration of free NH_2 group. The band at 2224 cm^{-1} due to the stretching vibration of C-N triple bond of nitrile group

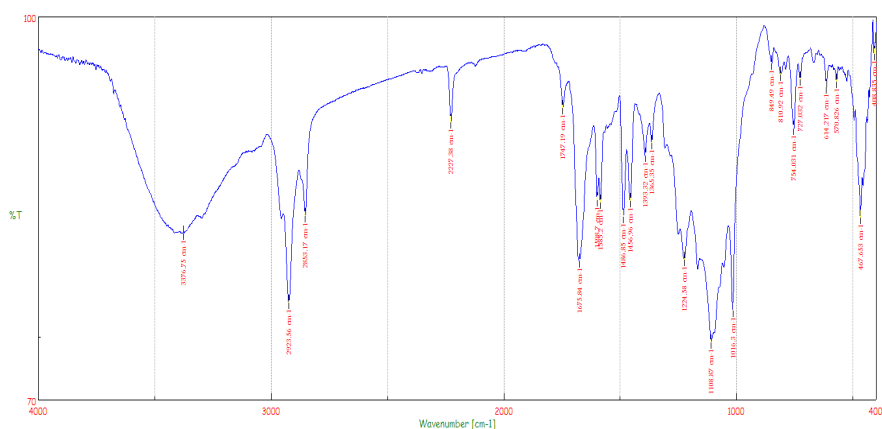


Fig. 3.16: FT-IR spectrum of 3.3a

The initial information obtained from FT-IR spectrum was further confirmed by ^1H NMR studies. In the ^1H NMR spectrum showed in figure 3.16, the 9 proton singlet observed at δ 1.71 corresponds to the three $-\text{CH}_3$ group at the position at 49, 50 and 51. The singlet observed at δ 3.83 is attributed to the three $-\text{OCH}_3$ protons at position 42. The

singlet at δ 4.92 due to the CH proton at position 18. The singlet proton observed at δ 4.95 is attributed to $-\text{CH}_2$ proton at position 4. The singlet proton observed at δ 4.96 is attributed to $-\text{CH}_2$ proton at position 8. The singlet proton at δ 5.30 is due to the $-\text{CH}_2$ proton at C-36. The singlet proton observed at δ 5.90 is attributed to $-\text{CH}$ proton at position 10. The aromatic protons were observed as four set of signals such as a 3 proton multiplet at δ 6.82- δ 6.90 and a four proton multiplet between δ 7.21-7.45. The triazole proton is observed at δ 7.51. The one proton singlet observed at δ 8.25 is attributed to $-\text{NH}$ proton at position 2. The two proton singlet observed at δ 8.30 is attributed to $-\text{NH}_2$ proton at position 23. The structure was further confirmed by mass spectral studies. m/z calculated for $\text{C}_{41}\text{H}_{42}\text{ClN}_7\text{O}_7$: 779.28 and HR-MS found to be 780.2941(M+1).

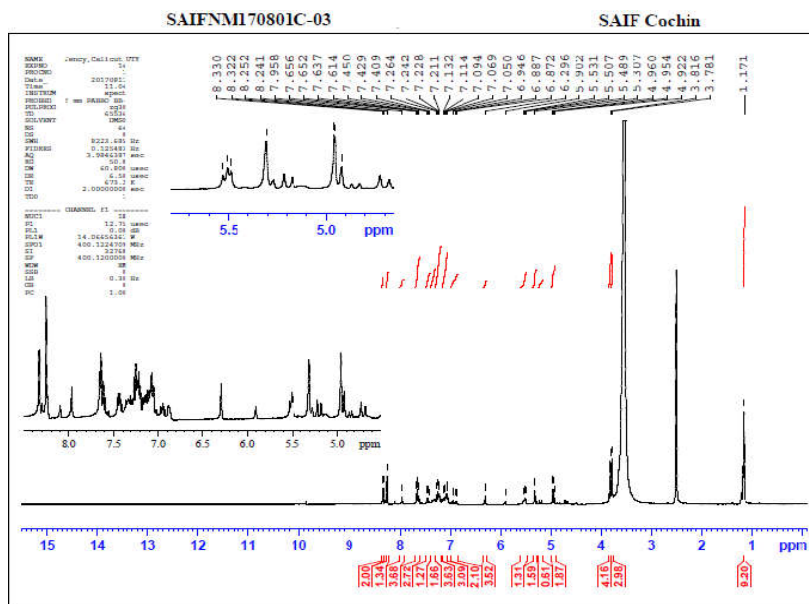


Fig. 3.17: ^1H -NMR spectra of 3.3a

Single Mass Analysis

Tolerance = 20.0 PPM / DBE: min = -1.5, max = 50.0
 Element prediction: Off
 Number of isotope peaks used for i-FIT = 3

Monoisotopic Mass, Even Electron Ions
 4 formula(e) evaluated with 1 results within limits (up to 50 closest results for each mass)
 Elements Used:
 C: 41-41 H: 35-43 N: 5-9 O: 5-9 Cl: 1-1
 C41H42ClN7O7
 C208 2 (0.064)

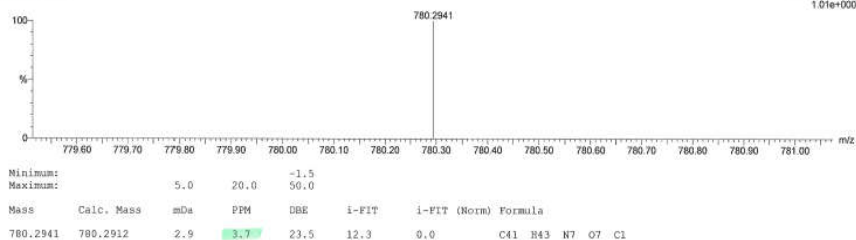


Fig.3. 18: Mass spectrum of 3.3a

Structure of the Click peptidomimetic 3.5d

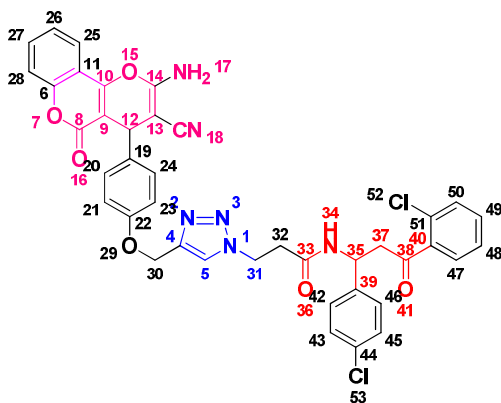


Fig. 3.19: structure of compound 3.5d

The compound is numbered as shown in 3.19. The FT-IR spectrum of the compound shows major absorptions at 3334, 3279, 2923, 2224, 1745, 1650, 1586, 1514 and 1449 cm^{-1} . The band at 3334 cm^{-1} is due to the NH stretching vibration of the acetamido group. The amide I band, i.e., the band due to the C=O stretching vibration of (C-30)

occurs at 1650cm^{-1} and the amide II band which arises from the interaction between the N-H bending and the C-N stretching of the C-N-H group was observed at 1514cm^{-1} . The absorption observed at 1745cm^{-1} is due to the C=O stretching vibration of the keto group at position 20. The band observed at 3424cm^{-1} is due to the stretching vibration of free NH_2 group. Similarly, the band observed at 2224cm^{-1} is attributed to the stretching vibration of C-N triple bond of the nitrile group.

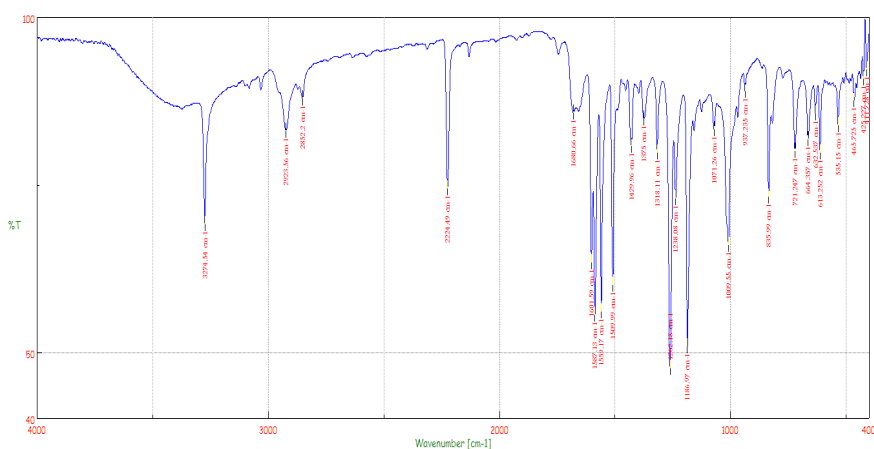


Fig. 3.20: FT-IR spectrum of **3.5a**

The initial information obtained from FT-IR spectrum was further confirmed by ^1H NMR studies. In figure 3.20, the triplet observed at δ 2.32 is due to the CH_2 proton at position 32. The doublet of doublet observed at δ 2.44-3.81 is attributed to -CH proton at position 37. The singlet proton at δ 4.95 is attributed to the CH proton at position 12. The singlet proton δ 4.96 is attributed to the proton at carbon 35. The singlet at δ 5.32 is due to the CH_2 proton at position 31. The singlet at δ 5.42 is due to the -CH_2 proton at position 30. The aromatic protons

were observed in following regions as a four proton multiplet at δ 6.09 and a five proton multiplet between δ 7.26–7.49. The triazole proton was observed at δ 7.50. A singlet at δ 8.21 is due to the NH proton at position 34. The singlet observed at δ 8.33 is attributed to $-\text{NH}_2$ proton at position 17. Structure was further confirmed from the mass spectra of the compound. In the mass spectra m/z calculated for $\text{C}_{40}\text{H}_{32}\text{Cl}_2\text{N}_6\text{O}_6$: 763.18 and found HR-MS: 763.1899 (M^+) further confirmed the structure of the compound.

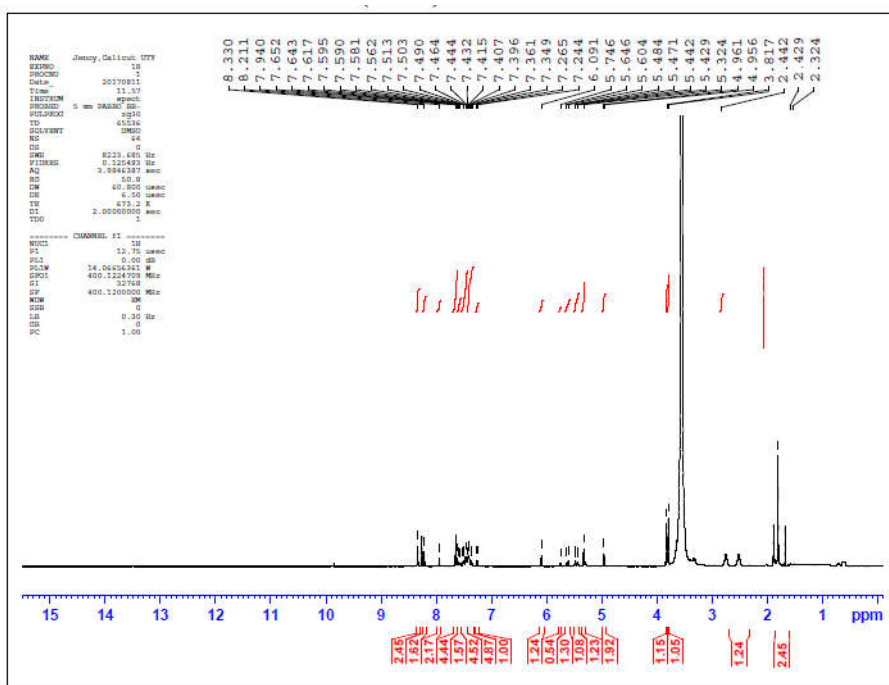


Fig. 3.21: ^1H -NMR spectrum of **3.5a**

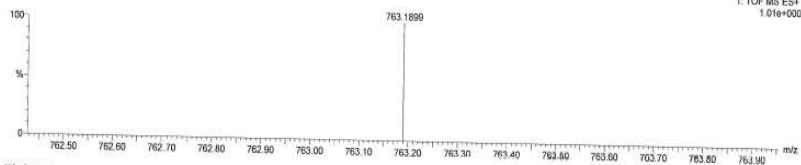
Elemental Composition Report

Page 1

Single Mass Analysis

Tolerance = 20.0 PPM / DBE: min = -1.5, max = 50.0
Element prediction: Off
Number of isotope peaks used for i-FIT = 3

Monoisotopic Mass, Even Electron Ions
33 formula(e) evaluated with 1 results within limits (up to 50 closest results for each mass)
Elements Used:
C: 20-40 H: 15-33 N: 2-7 O: 2-6 Cl: 1-2
C₄₀H₃₃N₆O₆Cl₂
618.064 (1.398)



Minimum:									
Maximum:									
Mass	Calc. Mass	mDa	PPM	DBE	i-FIT	i-FIT (Norm)	Formula		
763.1899	763.1839	6.0	7.9	26.5	12.7	0.0	C ₄₀ H ₃₃ N ₆ O ₆ Cl ₂		

Fig. 3.22: Mass spectrum of compound 3.5a

3.6. Experimental section

3.6.1 General.

IR spectra were recorded on a JASCO-FT/IR-4100 Fourier transform infrared spectrometer and measured as KBr pellets. ¹H and ¹³C NMR spectra were determined in DMSO with a Bruker amx 500 MHz spectrometer. The chemical shifts (δ) are given relative to tetramethylsilane (TMS) and the coupling constants (J) are reported in hertz (Hz). Electron spray ionization mass spectra were recorded with a Thermo scientific exactive mass spectrometer.

3.6.2. 2-Amino-4-(3-methoxy-4-(prop-2-yn-1-yloxy)phenyl)-5-oxo-4,5-dihydropyranof[3,2-c]chromene-3-carbonitrile 3.1a:

A mixture of propargylated aromatic aldehyde (190 mg, 1m mol), 4-hydroxy coumarin (162mg, 1 m mol), malononitrile (66mg, 1m mol) and hexamethylenetetramine (0.140 mg, 0.01m mol) were dissolved in minimum amount of ethanol. The reaction mixture is refluxed in a round bottom flask for one hour. After cooling, the precipitated solid was filtered. The solid product was washed with hot water filtered and dried. Recrystallized from hot ethanol to obtain pure product 308 mg, as white solid, M. p 120-123°C. ¹H NMR (DMSO, 500MHz), δH (ppm): 3.49(s,1H), 3.87 (s,3H), 4.42 (s, 1H), 4.95 (s,2H), 6.75 (d,1H, J=8.0), 6.88 (d,1H,J=8.0), 6.97(s,1H), 7.25 (d,1H,J=8.8), 7.47 (t,1H), 7.60 (t,1H), 7.72(d,1H), 8.56(s,2H). IR (KBr) ν_{max}: 3394, 3275, 3200, 2924, 2224, 2191, 1709, 1671, 1559, 1508 cm⁻¹. HRMS M⁺, found 400.3590 C₂₁H₁₂N₂O₄ requires: 400.3590.

3.6.3. 2-Amino-4-(4-(ethynyloxy)phenyl)-5-oxo-4,5 dihydropyrano [3,2-c]chromene-3-carbonitrile 3.1b:

320 mg, as white solid, M.p. 123-125°C. ¹H NMR (DMSO, 500MHz), δH (ppm) 3.83(s, 1H), 4.66(s, 1H), 4.84 (s, 2H), 6.91 (s, 1H), 6.92-7.86 (m, 7H), 8.82(s, 2H). IR (KBr) ν max: 3386, 3281, 2922, 2224, 2121, 1703, 1674, 1597, 1482⁻¹. HRMS M⁺, found 370.3352 C₂₂H₁₄N₂O₄ requires: 370.3354.

3.6.4. 2- Amino- 4- (2- (ethynyloxy) phenyl) - 5-oxo- 4,5-dihydropyrano [3,2-c] chromene-3-carbonitrile 3.1c:

318 mg, as white solid, M.P. 120-122°C. ¹H-NMR (DMSO, 500MHz), δH (ppm) 3.86 (s, 1H), 4.66 (s, 1H), 4.79(s 2H), 6.91(s, 1H), 6.92-7.86 (m, 7H), 8.30(s, 2H). IR (KBr) ν max: 3433, 3291, 2926, 2224, 2121, 1710, 1671, 1564, 1454⁻¹. HRMS M+, found 370.3351. C₂₁H₁₂N₂O₄ requires: 370.3354.

3.6.5. 2- 2-{{N-Benzyl-(N-1-azidopropan-2-one)-N-tert-butyl-2-(2-chlorophenyl)}} acetamide 3.2a:

An equimolar amount of 2-chlorobenzaldehyde (124 mg, 1 mmol), and benzyl amine (107 mg, 1 mmol), were taken in dichloromethane (8 ml), and stirred at room temperature for 20 min to form the Schiff-base. To this, 1 equivalent of tertiary -butyl isocyanide (94 mg, 1 mmol) and chloroacetic acid (83 mg, 1 mmol) were added and stirring was continued at room temperature. The reaction was monitored by TLC and found to complete after 72 h. The solvent was evaporated under vacuum and the residue was washed with petroleum ether (5 -15 ml) to afford the chloro derivative of the carboxamide. In a subsequent step, the chloride (407 mg, 1 mmol), K₂CO₃ (414 mg, 3 mmol), and NaN₃ (65 mg, 1 mmol) were stirred at room temperature for 4 h in dimethyl formamide. After completion of the reaction, the mixture was poured into ice cold water. The solid product obtained was filtered and dried under vacuum to afford 2-{{Nbenzyl-(N-1-azidopropan-2-one)-N-tert-butyl-2-(2-chlorophenyl)}} acetamide 2a:2-azido-N-benzyl-N-(2-tert-butylamino)-1-(2-fluorophenyl)-2-oxo ethyl acetamide **3.2a**:

White solid; 0.337g, M.P. 122-123⁰C. IR (KBr) ν max : 3351, 2102, 1685, 1647, 1547, 1490, 1454, 1225, 759 cm⁻¹; ¹H NMR (CDCl₃, 500 MHz) δ H (ppm): 8.750 (1H, s); 7.573-6.791 (10H, m); 5.803 (1H, s); 4.946 (2H, s); 2.171 (2H, s); 1.253 (9H, s); ¹³C NMR (DMSO(d₆), 125 MHz) (ppm): 169.0, 168.0, 161.0, 136.0, 131.0, 128.0, 127.0, 127.5, 127.2, 124.0, 122.0, 116.0, 65.0, 55.0, 50.0, 48.0, 29.0.

3.6.6. 2-Azido-N-benzyl-N-(2-tert-butylamino)-1-(2-nitrophenyl)-2-oxo ethyl acetamide 3.2b:

White solid, 320mg, M.P. 122-123⁰C IR (KBr) ν max: 3321, 2965, 2109, 1682, 1637, 1557, 1526, 1495, 1451, 1419, 1345, 1253, 1222, 940, 860, 790, 736, 698, 621, 592, 508 cm⁻¹.

3.6.7. 2-Azido-N-benzyl-N-(2-tert-butylamino)-1-(2-chlorophenyl)-2-oxo ethyl acetamide 3.2c:

White solid; 0.368 g, M.P. 124-125⁰C. IR (KBr) ν max : 3294, 2102, 1660, 1650, 1560, 1491, 1455, 1409, 1364, 1223, 1092, 949, 818, 724, 694 cm⁻¹. ¹H-NMR (CDCl₃, 500 MHz) δ H (ppm): 7.974 (1H, s); 7.261-6.91 (9H, m); 6.208 (1H, s); 4.884 (2H, s); 2.427 (2H, s); 1.208 (9H, s); ¹³C-NMR (DMSO-(d₆), 125 MHz) δ C (ppm): 169.92, 168.84, 136.76, 132.42, 131.03, 130.18, 128.57, 128.03, 127.26, 126.75, 70.18, 56.76, 51.82, 48.57, 28.57.

3.6.8. 2-{{N-Benzyl-(N-1-azidopropan-2-one)-N-tert-butyl-2-(2-chlorophenyl)}} acetamide 3.2d.

White solid, 0.335g, M.P. 120-122⁰C. ¹H-NMR (CDCl₃, 500 MHz) H (ppm): 1.25 (s, 9H), 1.62 (s, 2H), 4.58 (s, 2H), 6.38 (s, 1H), 6.95-7.26

(m, 9H), 7.53 (s, 1H). ^{13}C -NMR (DMSO-(d₆), 125 MHz) δC (ppm): 31.1, 42.7, 48.3, 51.7, 52.2, 126.8, 127.2, 128.4, 129.6, 129.7, 130.1, 132.5, 134.7, 137.7, 137.9, 167.0, 167.2. IR (KBr) ν max: 3304, 3073, 2972, 2925, 2100, 1659, 1648, 1552, 1497, 1472, 1454, 1438, 1411, 1365, 1282, 1220, 1168, 1055, 1040, 994, 842, 816, 748, 728, 693, 574, 555 cm^{-1} . EI-MS: 414.4 (M⁺).

3.6.9. Procedure for the synthesis of 3-Bromo-N-[1-(2-chlorophenyl)-3-(4-chlorophenyl)-3-oxopropyl]propanamide 3.3a:

A mixture of 4-chloroacetophenone (140 mg, 1 mmol), 2-chlorobenzaldehyde (154 mg, 1 mmol), and 3-bromopropionitrile (133 mg, 1 mmol) in acetonitrile (8 ml) were stirred in the presence of 5 mol % CuSO_4 at room temperature for 8 h. After completion of the reaction as indicated by TLC, the reaction mixture was poured into ice cold water and extracted with CH_2Cl_2 (15 mL). Evaporation of the solvent followed by purification on silica gel (100–200 mesh), ethyl acetate/hexane (3:1) afford 3-bromo-N-[1-(2-chlorophenyl)-3-(4-chlorophenyl)-3-oxopropyl] propanamide. The resulted bromide (426 mg, 1 mmol), K_2CO_3 (414 mg, 3 mmol), NaN_3 (65 mg, 1 mmol) were dissolved in dimethylformamide and stirred for 6–8 h. After completion, the reaction mixture was poured into ice cold water and the precipitate was filtered, dried under vacuum to afford the azide 3a: 0.332 g (yield 86%) as white solid. ^1H NMR (CDCl_3 , 500 MHz) δH (ppm): 1.73 (t, 2H), 2.45 (t, 2H), 2.67 (dd, 1H), 3.38 (dd, 1H), 5.53 (m, 1H), 6.89– 7.43 (m, 8H), 7.83 (d, $J = 7.5$ Hz, 1H). ^{13}C NMR (CDCl_3 , 125 MHz) δC (ppm): 35.6, 46.4, 48.2, 77.3, 128.3, 128.4, 128.9, 129.0, 129.6, 129.9, 130.3, 132.4, 134.7, 137.6, 140.2, 141.1, 169.1, 197.5. IR

(KBr) ν_{max} : 3286, 3038, 2921, 2852, 2088, 1685, 1647, 1590, 1550, 1475, 1442, 1402, 1356, 1285, 1231, 1260, 1177, 1148, 1094, 1065, 1029, 997, 936, 815, 754 cm^{-1} . EI-MS: 391.0 (M⁺).

3.6.10. 3-Azido-N-(3-(4-bromophenyl)-1-(4-chlorophenyl)-3-oxopropyl) propanamide 3.3b:

White solid, 0.455g, M.P: 134-137°C. ¹H-NMR (CDCl₃, 500 MHz) δ H (ppm):1.61 (t, 2H), 2.46-2.48(t, 2H), 2.67-2.69(t, 2H), 3.37-3.42 (dd, 1H), 5.52-5.57(m, 1H), 6.83-7.77(m, 9H). ¹³C NMR (CDCl₃, 125 MHz) δ C (ppm):36.0, 39.6, 40.1, 42.7, 47.3, 49.4, 77.0, 127.8, 128.8, 128.9, 129.1, 132.1, 135.1, 169.8, 197.3. IR (KBr), ν_{max} : 3300, 2922, 2852, 2113, 1684, 1649, 1583, 1548, 1488 cm^{-1} . EI-MS: found, 435.1 (M⁺). Requires, 435.7022.

3.6.11. General experimental procedure for the synthesis of pyranocoumarin peptidomimetics 3.4a.

3.1a (353mg, 1 m mol) and **3.2a** (377g, 1 m mol) were dissolved in minimum amount of DMSO. To this, 2 ml of *t*-BuOH, 1 mL of water, CuSO₄ 5H₂O (11 mg), and sodium ascorbate (50 mg) were added and stirred at room temperature for 12 h. After 12 h, the mixture was poured in to cold water. The precipitated solid was collected and washed with water and dried. The dried product was washed with diethyl ether (3.5 mL) to afford **3.4a**: ¹H NMR (DMSO, 500 MHz) δ H (ppm): 1.71 (s,9H), 3.83 (s,3H), 4.92 (s,1H),4.95 (s,2H),4.96 (s,2H), 5.30 (s,2H), 5.90 (s,1H), 6.82-6.90 (m,3H), 7.05-7.13 (m,5H),7.21-7.45 (m,5H),7.16 (s,1H, triazole), 7.61-7.95 (m,4H), 8.25 (s,1H), 8.30

(s,2H). IR (KBr) ν max: 3376, 2923, 2227, 1747, 1675, 1598, 1486 cm^{-1} . HR MS found 780.2941(M+1). $\text{C}_{41}\text{H}_{42}\text{C}_1\text{N}_7\text{O}_7$ requires 779.28.

3.6.12. *2-(4-((4-(2-Amino-3-cyano-5-oxo-4,5-dihydropyranof[3,2-c]chromen-4-yl)-2-methoxyphenoxy)methyl)-1H-1,2,3-triazol-1-yl)-N-benzyl-N-(2-(tert-butylamino)-1-(3-nitrophenyl)-2-*

oxoethyl)acetamide 3.4b: White solid, 0.435g, M.P: 134-137 $^{\circ}$ C. ^1H -NMR (DMSO, 500 MHz), δH (ppm): 1.24 (s,9H), 3.79(s,3H), 4.85(s,1H), 4.95(s,2H), 4.96 (s,2H), 5.32(s,2H), 5.74(s,1H), 6.90(s,2H), 7.36-7.49(m,6H), 7.50 (s, 1H ,triazole), 7.58-7.94 (m, 6H), 8.21 (s,1H), 8.33(s, 2H). IR (KBr) ν max: 3405, 2922, 2224, 1745, 1670, 1598, 1456 cm^{-1} . HR- MS: found 825.2941 (M+1). Requires 824.29.

3.6.13. *2-(4-((4-(2-Amino-3-cyano-5-oxo-4,5-dihydropyranof[3,2-c]chromen-4-yl)phenoxy)methyl)-1H-1,2,3-triazol-1-yl)-N-benzyl-N-(2-(tert-butylamino)-1-(4-chlorophenyl)-2-oxoethyl)acetamide 3.4c:*

White solid, 0.455g, M.P: 134-137 $^{\circ}$ C. ^1H -NMR (DMSO, 500 MHz) H (ppm): 1.18(s,1H), 4.11(s,1H), 4.48(s,2H), 4.77(s,2H), 5.71(s, 2H), 6.11 (s, 2H), 6.96 (s,2H), 7.18-.48 (m,8H), 7.50 (s,1H, triazole), 7.59-7.98 (m, 9H), 8.25 (s,1H), 8.58 (s,2H). IR (KBr) ν max: 3363, 2922, 2227, 1745, 1670, 1598, 1456. HR-MS, found: 784.2651(M+1). Requires: 783.26.

3.6.14. *2-(4-((4-(2-Amino-3-cyano-5-oxo-4,5-dihydropyranof[3,2-c]chromen-4-yl)phenoxy)methyl)-1H-1,2,3-triazol-1-yl)-N-benzyl-N-(2-(tert-butylamino)-1-(2-chlorophenyl)-2-oxoethyl)acetamide 3.4d:*

White solid, 0.425g M.P: 132-134 $^{\circ}$ C. ^1H NMR (DMSO, 500 MHz) δH

(ppm):1.48 (s,9H), 4.424 (s,1H), 4.72 (s,2H), 4.95 (s,2H), 5.12 (s,1H), 6.75 (s,2H), 6.9 (s,2H), 7.23-7.49 (m,7H), 7.58 (s,1H), 7.58-7.93 (m,8H), 8.24 (s,1H), 8.31 (s,2H). IR (KBr) ν max: 3424, 2925, 2224, 1746, 1651, 1586, 1448 cm^{-1} . HR-MS: found 784.2606(M+1). Requires: 783.26.

3.6.15. *2-(4-((4-(2-Amino-3-cyano-5-oxo-4,5-dihydropyrano[3,2-c]chromen-4-yl)-2-methoxyphenoxy)methyl)-1H-1,2,3-triazol-1-yl)-N-benzyl-N-(2-(tert-butylamino)-1-(4-chlorophenyl)-2-oxoethyl)acetamide 3.4e*: White solid,0.402mg M.P: 130-132⁰C. ¹H-NMR (DMSO, 500 MHz) δ H (ppm):1.17 (s,1H), 3.98 (s,3H), 4.06 (s,1H), 4.52 (s,2H), 4.78 (s,2H), 5.62 (s,2H), 6.98 (s,2H), 7.23-7.49 (m,8H), 7.50 (s,1H, triazole), 7.60-7.98 (m,9H), 8.54 (s,1H), 8.58 (s,2H). IR (KBr) ν max: 3429, 2923, 2225, 1764, 1647, 1587, 1462. HR-MS, found: 814.2738 (M+1). Requires: 813.27.

3.6.16. *2-(4-((4-(2-Amino-3-cyano-5-oxo-4,5-dihydropyrano[3,2-c]chromen-4-yl)phenoxy) methyl)-1H-1,2,3-triazol-1-yl)-N-benzyl-N-(2-(tert-butylamino)-1-(3-nitrophenyl)-2-oxoethyl)acetamide 3.4f*: White solid,0.432mg, M.P: 133-134⁰C. ¹H-NMR (DMSO, 500 MHz) δ H (ppm): 1.20 (s,9H), 4.04 (s,1H), 4.52 (s,2H), 4.82(s,2H), 5.71(s,2H), 6.18 (s,2H), 6.97 (s,2H), 7.15-7.48 (m,9H), 7.51 (s,1H), 7.53-7.98 (m,5H), 8.05(s,1H), 8.58(s,2H). IR (KBr) ν max: 3412, 2924, 2225, 1746, 1676, 1560, 1409 cm^{-1} . HR MS, found: 795.2932 (M+1). Requires: 794.28.

3.6.17. *3-(4-((4-(2-Amino-3-cyano-5-oxo-4,5-dihydropyrano[3,2-c]chromen-4-yl)-2-methoxyphenoxy) methyl)-1H-1,2,3-triazol-1-yl)-*

N-(3-(2-chlorophenyl)-1-(4-chlorophenyl)-3-oxopropyl)propanamide **3.5a**: White solid, 0.402 mg, M.P: 137-138°C. ¹H-NMR (DMSO, 500 MHz) δH (ppm): 2.5 (s, 2H), 2.79-3.22 (dd, 2H), 3.82 (s, 3H), 4.28 (s, 1H), 4.98 (s, 1H), 5.14 (s, 2H), 5.31 (s, 1H), 6.27 (m, 3H), 7.69-7.48 (m, 9H), 7.57 (s, 1H, triazole), 7.58-7.95 (m, 4H), 8.19 (s, 1H), 8.38 (s, 2H). IR (KBr) ν_{max}: 3424, 3279, 2925, 2224, 1746, 1651, 1515, 1448 cm⁻¹.

3.6.18. *3-(4-((4-(2-Amino-3-cyano-5-oxo-4,5-dihydropyrano[3,2-c]chromen-4-yl)-2-methoxyphenoxy)methyl)-1H-1,2,3-triazol-1-yl)-N-(1-(4-bromophenyl)-3-(2-chlorophenyl)-3-oxopropyl)propanamide* **3.5b**: White solid, 0.425 mg, M.P: 134-137°C. ¹H-NMR (DMSO, 500 MHz), δH (ppm): 2.56 (s, 2H), 2.94-3.33 (dd, 2H), 3.79 (s, 3H), 4.81 (s, 1H), 4.91 (s, 1H), 5.30 (s, 1H), 5.52 (s, 1H), 6.31-6.87 (m, 3H), 7.22-7.48 (m, 5H), 7.50 (s, 1H, triazole), 7.63-7.66 (m, 8H), 8.23 (s, 1H), 8.38 (s, 2H). IR (KBr), δ_{max}: 3429, 3279, 2923, 1725, 1674, 1647, 1587, 1465 cm⁻¹.

3.6.19. *3-(4-((4-(2-Amino-3-cyano-5-oxo-4,5-dihydropyrano[3,2-c]chromen-4-yl)phenoxy)methyl)-1H-1,2,3-triazol-1-yl)-N-(1-(4-bromophenyl)-3-(2-chlorophenyl)-3-oxopropyl)propanamide* **3.5c**: White solid, 0.428 mg, M.P: 130-131°C. ¹H-NMR (DMSO, 500 MHz), δH (ppm): 2.78 (s, 2H), 2.81-3.81 (dd, 2H), 4.95 (s, 1H), 4.96 (s, 1H), 5.62 (s, 1H), 5.67 (s, 2H), 6.21-6.71 (m, 3H), 7.23-7.42 (m, 10H), 7.58 (s, 1H, triazole), 7.60-7.87 (m, 10H), 8.30 (s, 1H), 8.54 (s, 2H). IR (KBr) δ_{max}: 3363, 2923, 2227, 1745, 1670, 1543, 1456 cm⁻¹.

3.6.20. **3-(4-((4-(2-Amino-3-cyano-5-oxo-4,5-dihydropyranof[3,2-c]chromen-4-yl)phenoxy)methyl)-1H-1,2,3-triazol-1-yl)-N-(3-(2-chlorophenyl)-1-(4-chlorophenyl)-3-oxopropyl)propanamide** **3.5d:**
White solid, 0.405mg, M.P: 130-132^oC. ¹H-NMR (DMSO, 500 MHz),
δH (ppm): 2.329s, 1H), 2.44-3.81(dd, 2H), 4.95 (s, 1H), 4.96(s, 1H),
5.32(s, H), 5.42 (s, 1H), 6.09(m, 4H), 7.26-7.49(m, 5H), 7.50(s,
1H, triazole), 7.51-7.65 (m, 6H), 8.21 (s, 1H), 8.33(s, 2H). IR (KBr),
ν_{max}: 3334, 3279, 2923, 2224, 1745, 1650, 1586, 1514, 1449 cm⁻¹.
HR-MS: Found, 763.1899 (M⁺). Required, 763.18.

3.6.21. **3-(4-((2-(2-Amino-3-cyano-5-oxo-4,5-dihydropyranof[3,2-c]chromen-4-yl)phenoxy)methyl)-1H-1,2,3-triazol-1-yl)-N-(3-(2-chlorophenyl)-1-(4-chlorophenyl)-3-oxopropyl)propanamide** **3.5e :**
White solid, 0.425mg, M.P: 134-137^oC. ¹H-NMR (DMSO, 500 MHz)
, δH (ppm): 2.57(s, 2H), 2.98-3.67(dd, 2H), 4.96 (s, 1H), 4.98 (s, 1H),
5.26 (s, 1H), 5.96 (s, 1H), 6.82-7.0 (m, 3H), 7.27-7.39 (m, 6H), 7.55
(s, 1H, triazole), 7.57-7.98 (m, 8H), 8.13(s, 1H), 8.46 (s, 2H). IR (KBr),
ν_{max}: 3476, 2923, 2224, 1745, 1650, 1586, 1514, 1449 cm⁻¹.

3.6.22. **3-(4-((2-(2-Amino-3-cyano-5-oxo-4,5-dihydropyranof[3,2-c]chromen-4-yl)phenoxy)methyl)-1H-1,2,3-triazol-1-yl)-N-(1-(4-bromophenyl)-3-(2-chlorophenyl)-3-oxopropyl)propanamide** **3.5f:**
White solid, 0.400mg, M.P: 134-135^oC. ¹H NMR (DMSO, 500 MHz),
δH (ppm): 2.21(s, 2H), 2.52-3.67(dd, 2H), 4.14(s, 1H), 4.98(s, 1H),
5.16(s, 1H), 5.72(s, 1H), 6.82-7.0(m, 3H), 7.27-7.39(m, 6H),
7.55(s, 1H, triazole), 7.61-7.90(m, 8H), 8.33(s, 1H), 8.39(s, 2H). IR (KBr),
ν_{max}: 3412, 3275, 2924, 2225, 1746, 1676, 1587, 1560, 1487 cm⁻¹.

3.6.23. General procedure for the cytotoxicity evaluation:

The MCF-7 cells in the log phase were seeded in a 96-well plates at a concentration of 1.0×10^4 cells/well and incubated overnight at 37 °C in 5% CO₂ humidified environment. The cells were then treated with different concentrations of the **4a** (dissolved with RPMI medium 1640). Controls were also cultivated under same conditions without **4a**. The treated cells were incubated for 48 h. Subsequently a stock concentration (5 mg/mL) of MTT-(3-(4,5-Dimethylthiazol-2-yl)-2,5-diphenyltetrazolium bromide) was prepared and 100 µL of MTT was added in each **3a** treated wells and incubated for 4h. Purple colour formazan crystals were observed and these crystals were dissolved in 100 µL of dimethyl sulphoxide (DMSO), and read at 620 nm in a multi well ELISA plate reader (Thermo, Multiskan). The dose dependent cytotoxicity was observed in **3a** treated MCF-7 cells with IC₅₀ 50 µM.

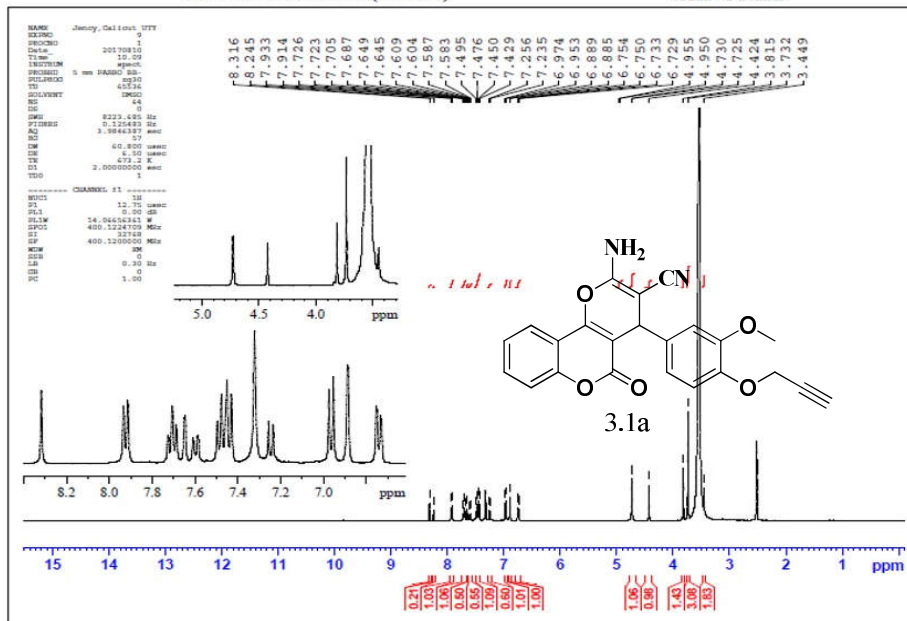
References

1. Feuer, G.; Ellis, G. P., West, G. P., *Progress in Medicinal Chemistry* Eds.; North-Holland Publishing Company: New York, **1974**, 10, 85–158.(b) Dean, F. M. *Naturally Occurring Oxygen Ring Compounds*; Butterworth-Heinemann: London, **1963**, 176–220. (c) Goel, A.; Ram, V. J. *Tetrahedron* **2009**, 65, 7865–7913.
2. (a) Jyoti, D., Ramit, S.; Manvendra, K.; Vikas, J. *Eur. J. Med. Chem.* **2016**, 119, 141-168. (b) Fernanda G. M. et al. *Nat. Prod. Rep.*, **2015**, 32, 1472–1507. (c) Calcio Gaudino, E.; Tagliapietra, S.; Martina, K.; Palmisano, G.; Cravotto, G. *RSC Adv.* **2016**, 6, 46394–46405. (d) Dinesh K. et al. *RSC Adv.*, **2017**, 7, 36977–36999.
3. Hansch, C.; Sammes, P. G.; Taylor, J. B., *Comprehensive Medicinal Chemistry* Eds. Pergamon: New York, **1990**. Vol. 6.
4. (a) Cardellina, J. H.; Bokesch, H. R.; McKee, T. C.; Boyd, M. R. *Bioorg. Med. Chem. Lett.* **1995**, 5, 1011-1018.(b) McKee, T.; Fuller, R. W.; Covington, C. D.; Cardellina, J. H., II; Gulakowski, R. J.; Krepps, B. L.; McMahan, J. B.; Boyd, M. R. *J. Nat. Prod.* **1996**, 59, 754-758.(c) Galinis, D. L.; Fuller, R. W.; McKee, T. C.; Cardellina, J. H., II; Gulakowski, R. J.; McMahan, J. B.; Boyd, M. R. *J. Med. Chem.* **1996**, 39, 4507-4510.
5. Kumar, A.; Maurya, R. A.; Sharma, S.; Ahmad, A.; Singh, A. B.; Bhatia, G.; Srivastava, A. K. *Bioorg. Med. Chem. Lett.* **2009**, 19, 6447-6451.
6. Kaur, R.; Naaz, F., Bedi, P. M. S.; Sharma, S.; Nepali, K.; Mehndiratta, S.; Gupta, M. K. *Med. Chem. Res.* **2015**, 24, 3334–3349.
7. Khoobi, M.; Alipour, M.; Sakhteman, A. H.; Moradi, A.; Ghandi, M.; Emami, S.; Nadri, H.; Foroumadi, A.; Shafiee, A. *Eur. J. Med. Chem.* **2013**, 68, 260–269.
8. Rafinejad, A.; Fallah-Tafti, A.; Tiwari, R.; Shirazi, A. N.; Mandal, D.; Parang, K.; Foroumadi, A.; Akbarzadeh, T.; Shafiee, A.; Daru, J. *Pharm. Sci.* **2012**, 20, 2-7.
9. Jyoti, T.; Saquib, M.; Singh, S.; Tufail, F.; Singh, M.; Jaya, S.; Jagdamba, S. *Green Chem.* **2016**, 18, 3221-3231.

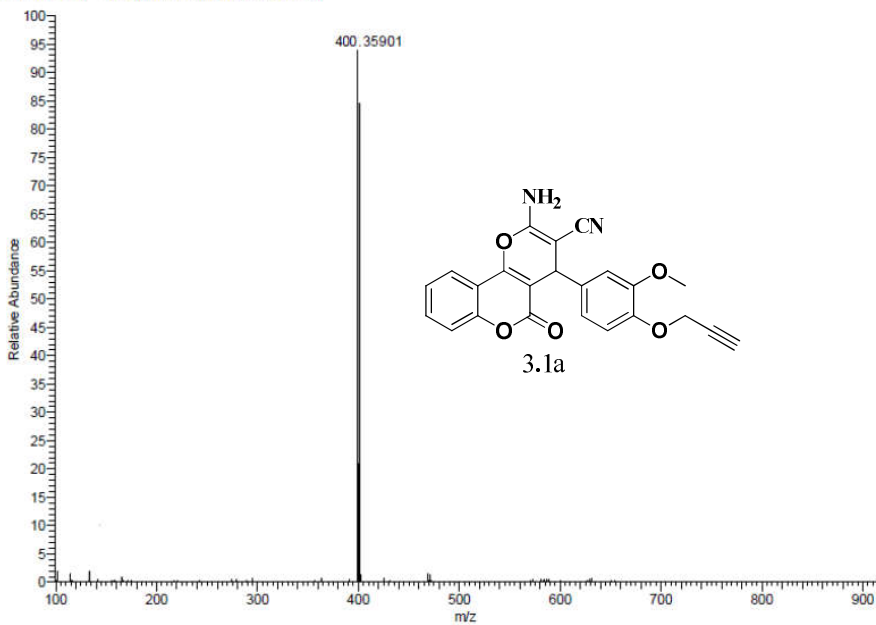
10. Panchuk-V, N.; Haugland, R.P.; Bishop-Stewart, J.; Bhalgat, M.K.; Millard, P.J.; Mao, F.; Leung, W. Y.; Haugland, R. P. *Histochem Cytochem*, **1999**, 47:1179–1188.
11. Sato, S.; Murata, A.; Shirakawa, T.; Uesug, M. *Chem. Biol.* **2010**, 17, 6, 616-623.
12. H.J. Wang, J. Lu, Z.H. Zhang, Wang, H.J.; Lu, J.; Zhang, Z.H.E.N. *Monatsh. Chem.* **2010**, 141, 1107-1112
13. (a) Dömling, A.; Ugi, I. *Angew. Chem. Int. Ed.* **2000**, 39, 3168–3210; (b) Dömling, A. *Chem. Rev.* 2006, 106, 17–89; (c) Dömling, A.; Wang, W.; Wang, K. *Chem. Rev.* **2012**, 112, 3083–3135.
14. (a) Kolb, H. C.; Finn, M. G.; Sharpless, K. B. *Angew. Chem. Int. Ed.* **2001**, 40, 2004-2021. (b) Sreeman, K.M.; Finn, M. G. *Chem. Soc. Rev.* **2010**, 39, 1252-1261; (c) Ganesh, V.; Sudhir, S.; Kundu, T.; Chandrasekharan, S. *Chem. Asian. J.* **2011**, 6, 2670-2694. (d) Ladomenou, K.; Nikolaou, V.; Charalambidis, G.; Coutsolelos, A. G. *Coord. Chem. Rev.* **2016**, 306, 1-42. (e) Xi Chen. *Chem. Rev.* **2016**, 116, 3086–3240.
15. a) Bahulayan, D.; Das, S.K.; Iqbal, J. *J. Org. chem.* 2003, 68, 5733-5738 (b) Pandey, G.; Singh, R.P.; Garg, A.; Singh, V.K. *Tetrahedron Lett.* **2005**, 46, 2137-2140. (d) Arend, M.; Westermann, B.; Risch, N.; *Angew. Chem. Int. Ed.* **1998**, 37, 1044 – 1070. (e) Chowdari, N.S.; Suri, J.T.; Barbas, C.F. *Org. Lett.*, **2004**, 6, 15, 2507–2510,
16. Doak, B.C.; Zheng, J.; Dobritsch, D.; Kihlberg, J. *J. Med. Chem.* **2016**, 59:2312–2327.

SAIFNMI70801C-08(JM 130)

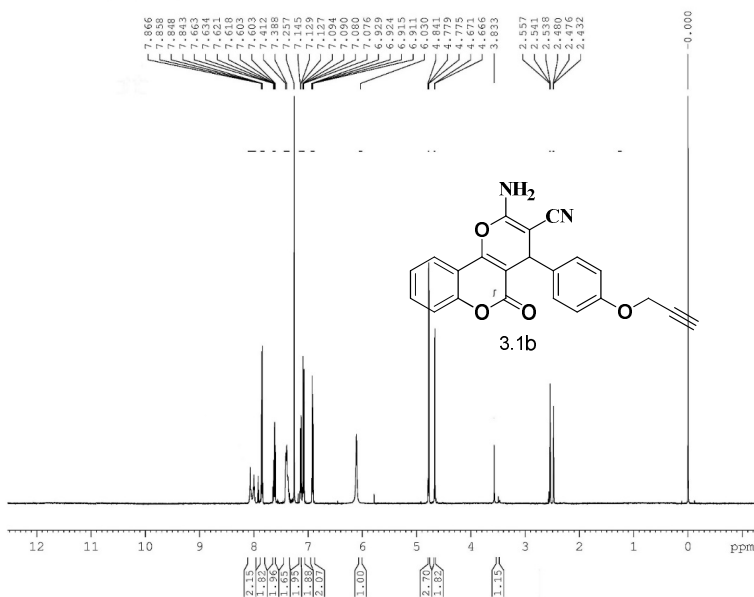
SAIF Cochlin



JM #11 RT: 0.86 AV: 1 SB: 304 0.02-0.71, 1.06-4.93 NL: 7.71E5
 T: FTMS(1,1) + p ESI Full lock ms [100.00-2000.00]



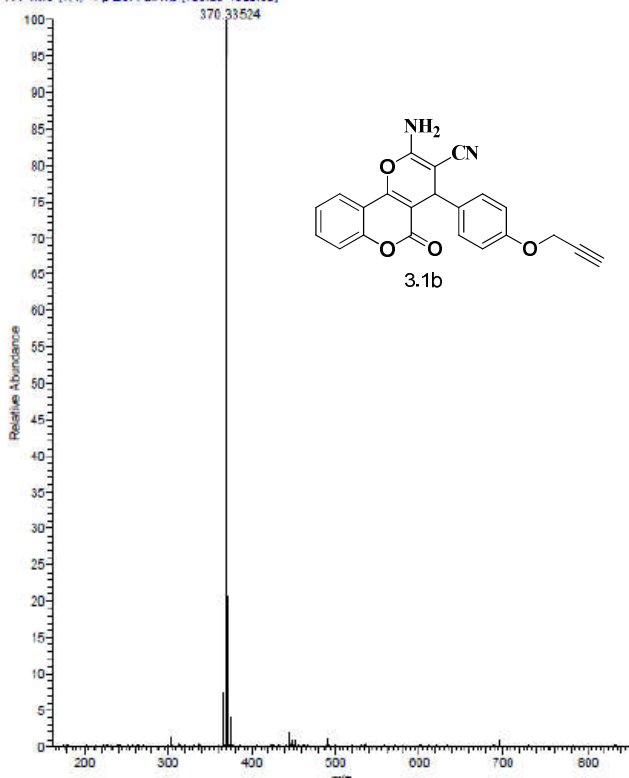
JM126
 PROTON CDCl3 (D:\Shimi) NIIST 37

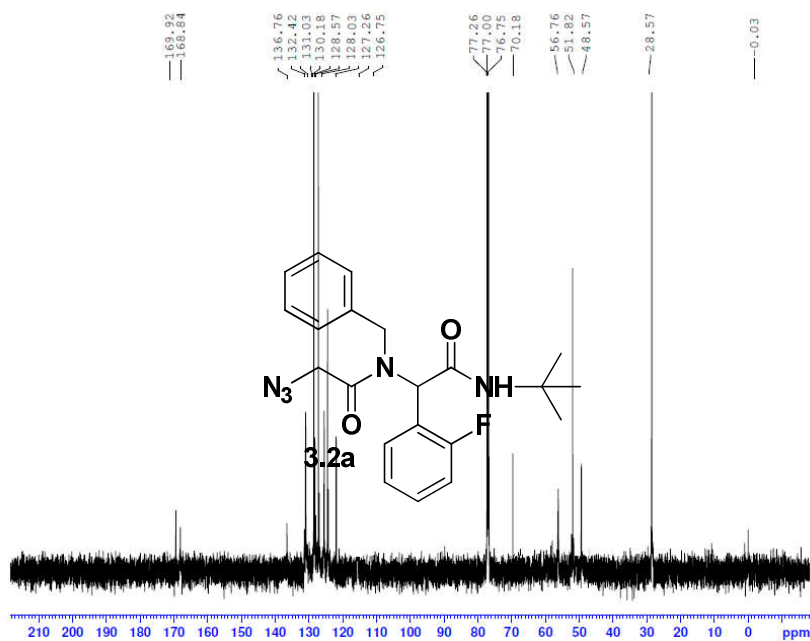
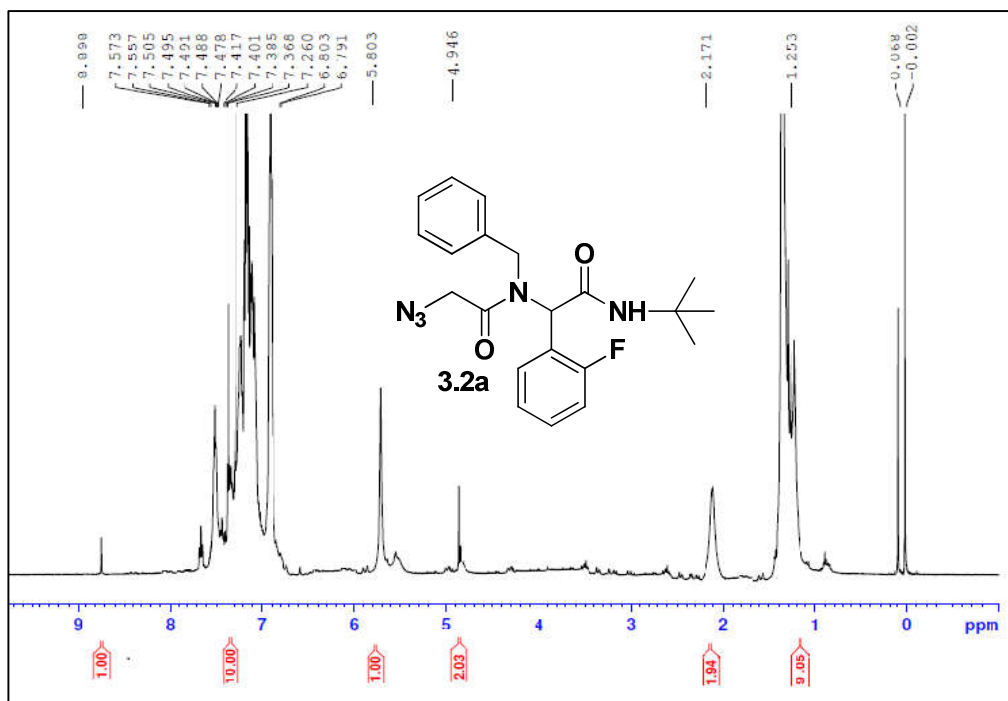


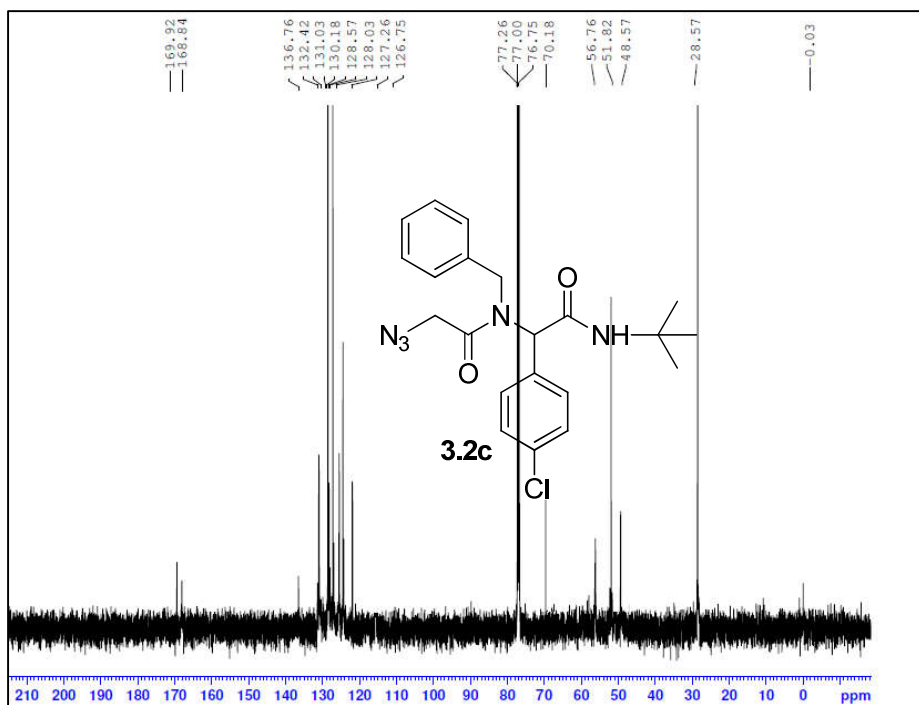
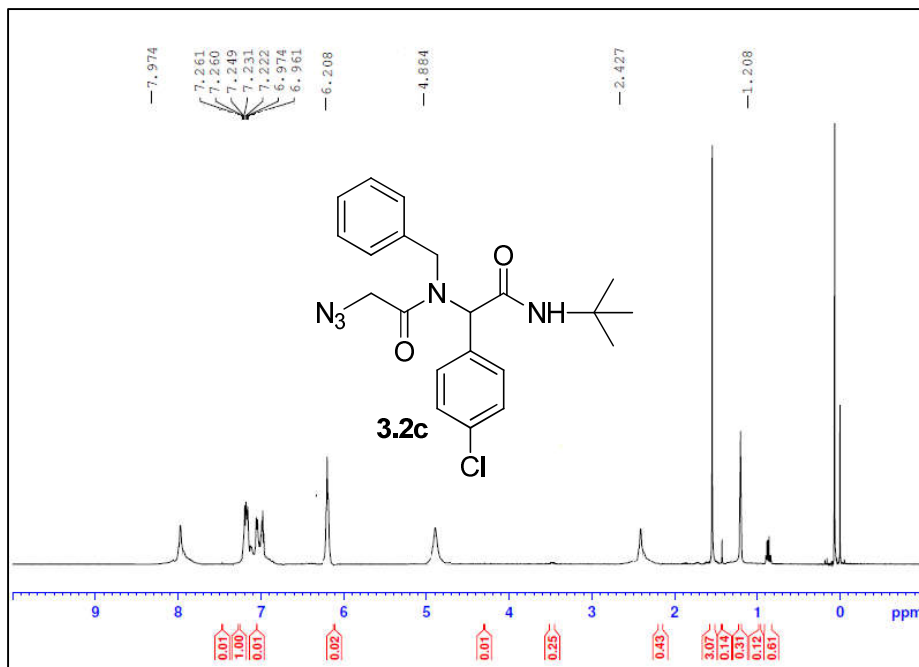
Current Data Parameters
 NAME JM126
 EXPNO 1
 PROCNO 1
 F2 - Acquisition Parameter
 Date_ 20150611
 Time 15:40
 INSTRUM spect
 PROBRG 5 mm PNP 1H/
 PULPROG zg30
 TD 65536
 ID
 SOLVENT CDCl3
 NS 15
 DS 2
 SWH 10330.578 Hz
 FIDRES 0.157632 Hz
 AQ 3.171923 sec
 RG 724
 DW 48.400 us
 DE 6.00 us
 TE 306.7 K
 D1 1.0000000 sec
 TDO 1
 ===== CHANNEL f1 =====
 NUCL 1H
 P1 14.00 us
 PL1 0.00 dB
 SFO1 500.130885 MHz
 F2 - Processing parameters
 SI 32768
 SF 500.1300100 MHz
 WDW HM
 SSB 0
 LB 0.30 Hz
 GB 0
 PC 1.00

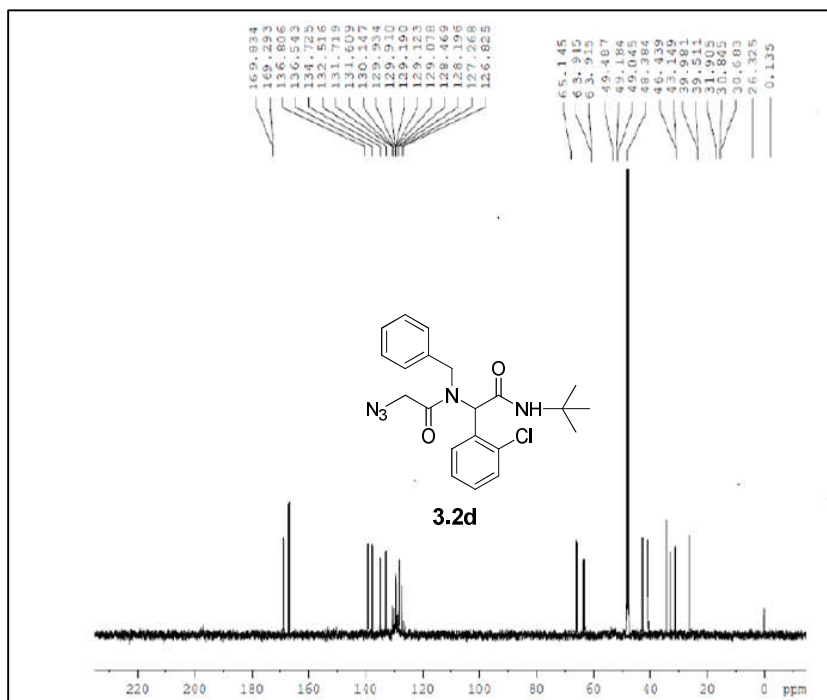
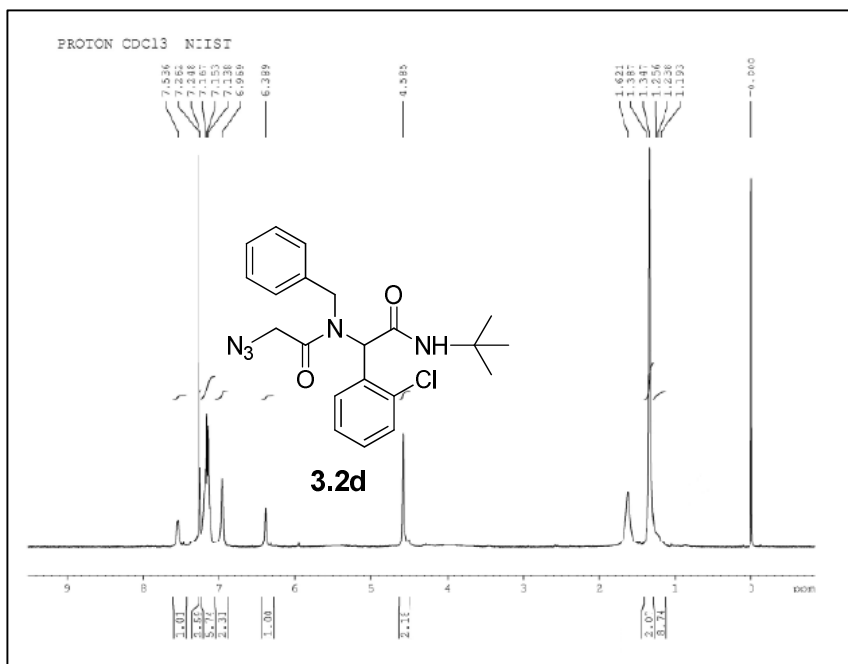
C:\xcalibur\data\JULY2014

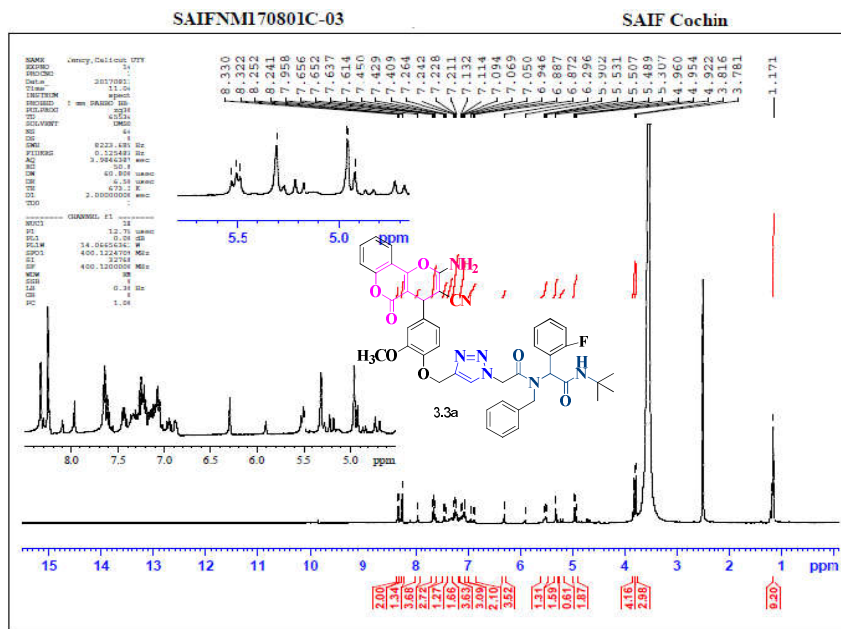
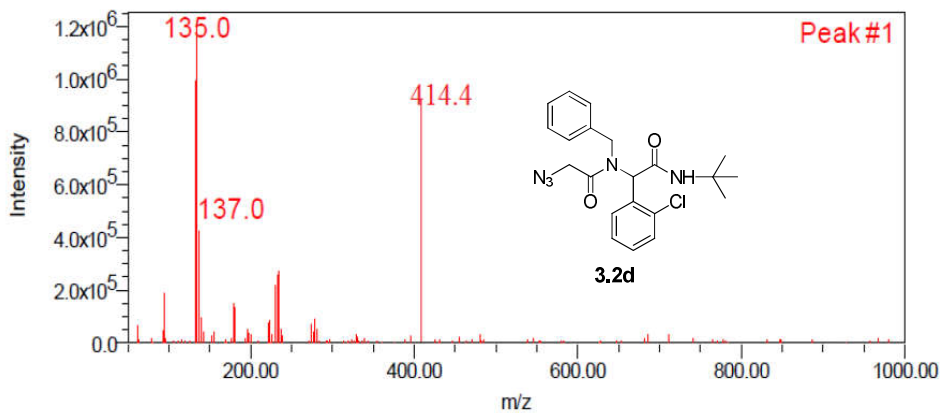
JM #10 RT: 1.03 AU: 1 NL: 4.55E3
 T: FTMS (f.1) - p ESI Full ms [100.00-1500.00]











Elemental Composition Report

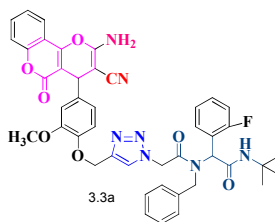
Single Mass Analysis

Tolerance = 20.0 PPM / DBE: min = -1.5, max = 50.0
 Element prediction: Off
 Number of isotope peaks used for i-FIT = 3

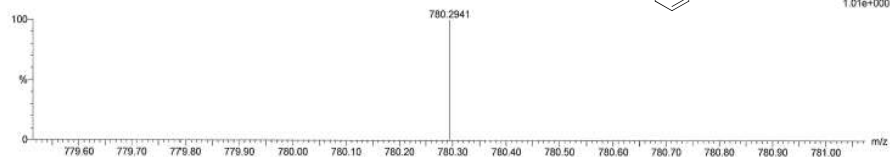
Monoisotopic Mass, Even Electron Ions
 4 formula(e) evaluated with 1 results within limits (up to 50 closest results for each mass)
 Elements Used:

C: 41-41 H: 35-43 N: 5-9 O: 5-9 Cl: 1-1

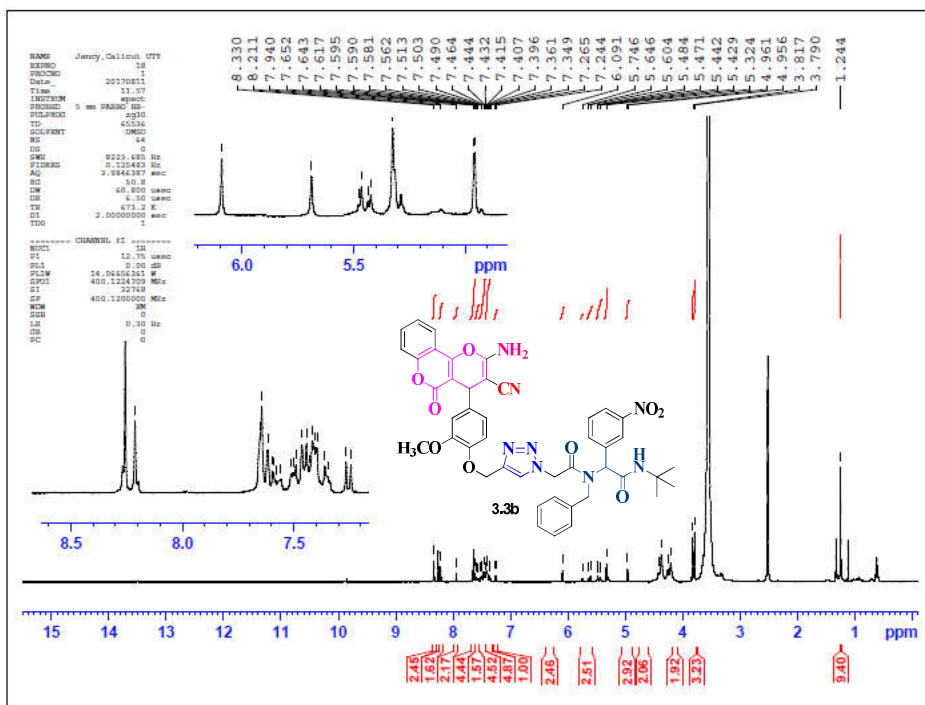
C41H42ClN7O7
 2 (0.064)



Page 1



Mass	Calc. Mass	mDa	PPM	DBE	i-FIT	i-FIT (Norm)	Formula
780.2941	780.2912	2.9	3.7	23.5	12.3	0.0	C41 H43 N7 O7 Cl

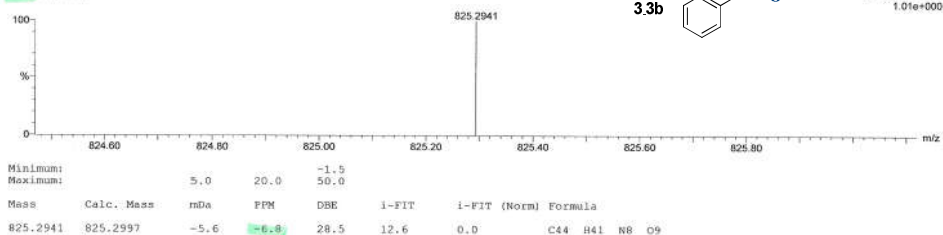
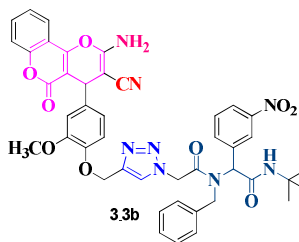


Elemental Composition Report

Single Mass Analysis

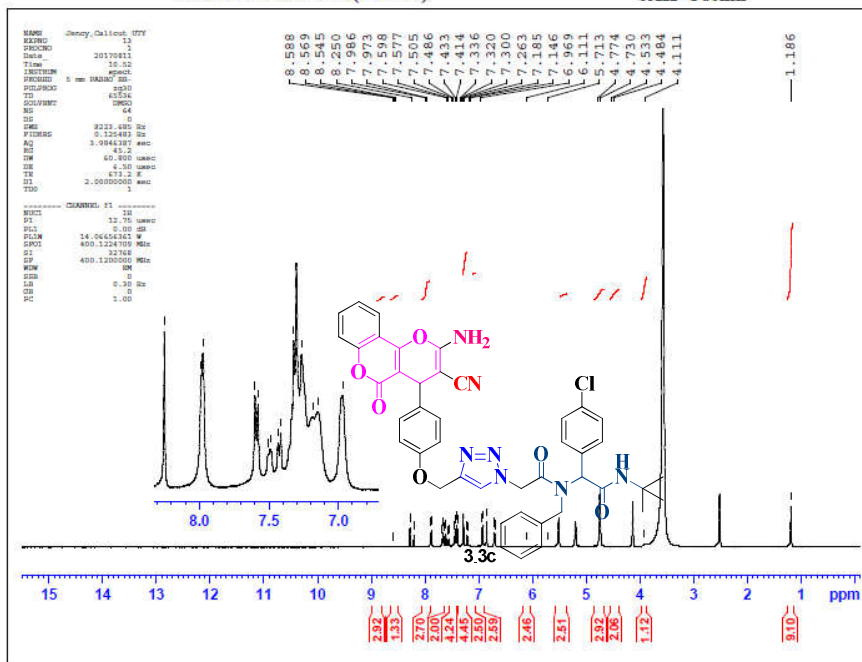
Tolerance = 20.0 PPM / DBE: min = -1.5, max = 50.0
 Element prediction: Off
 Number of isotope peaks used for I-FIT = 3

Monoisotopic Mass, Even Electron Ions
 5 formula(e) evaluated with 1 results within limits (up to 50 closest results for each mass)
 Elements Used:
 C: 43-44 H: 35-41 N: 5-9 O: 5-9
 C₄₄H₄₀N₈O₉
 C202.40 (0.874)



SAIFNML70801C-02(JM177)

SAIF Cochin



Elemental Composition Report

Single Mass Analysis

Tolerance = 20.0 PPM / DBE: min = -1.5, max = 50.0

Element prediction: Off

Number of isotope peaks used for i-FIT = 3

Monoisotopic Mass, Even Electron Ions

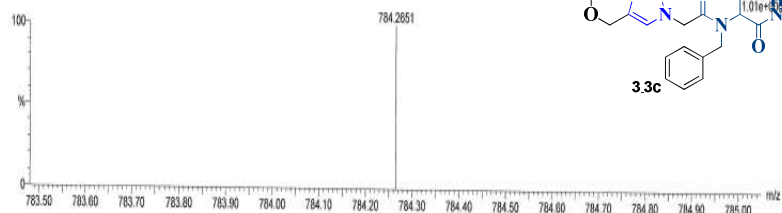
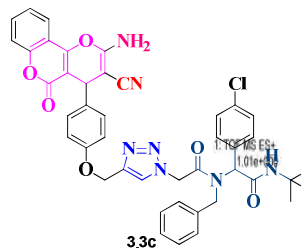
4 formula(e) evaluated with 1 result within limits (up to 50 closest results for each mass)

Elements Used:

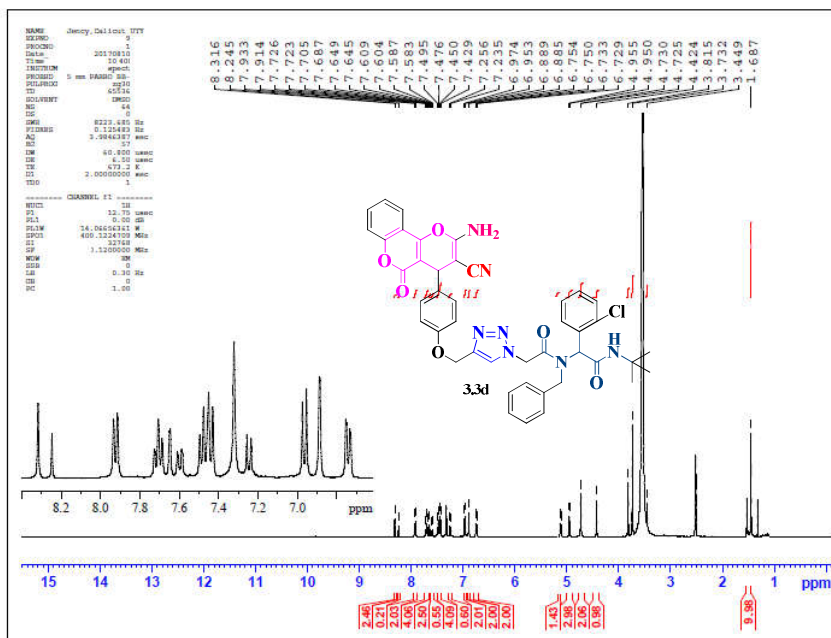
C: 43-43 H: 35-40 N: 5-8 O: 5-8 Cl: 1-1

C43H39ClN7O6

C177 187 (4.102)



Mass	Calc. Mass	mDa	PPM	DBE	i-FIT	i-FIT (Norm)	Formula
784.2651	784.2650	0.1	0.1	27.5	12.3	0.0	C43 H39 N7 O6 Cl

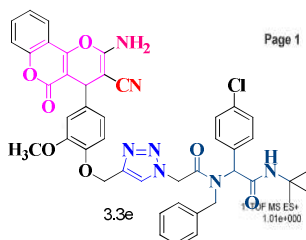


Elemental Composition Report

Single Mass Analysis

Tolerance = 20.0 PPM / DBE: min = -1.5, max = 50.0
 Element prediction: Off
 Number of isotope peaks used for i-FIT = 3

Monoisotopic Mass, Even Electron Ions
 4 formula(s) evaluated with 1 results within limits (up to 50 closest results for each mass)
 Elements Used:
 C: 44-44 H: 35-41 N: 5-9 O: 5-9 Cl: 1-1
 C44H40ClN7O7
 C205.259 (6.7%)

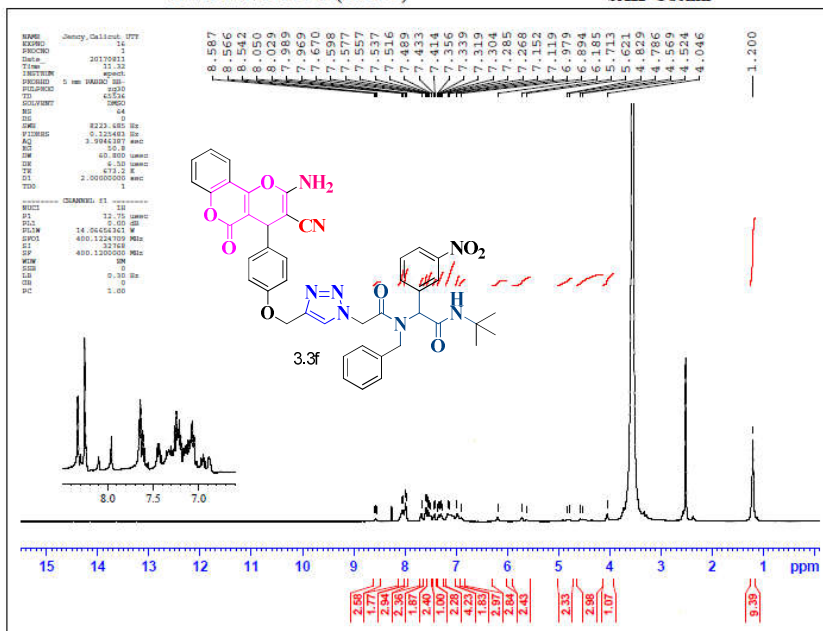


Mass	Calc. Mass	mDa	PPM	DBE	i-FIT	i-FIT (Norm)	Formula
814.2738	814.2756	-1.8	2.2	27.5	12.3	0.0	C44 H41 N7 O7 Cl

Minimum: -1.5
 Maximum: 5.0 20.0 50.0

SAIFNMI70801C-05(JM178)

SAIF Cochin



Elemental Composition Report

Single Mass Analysis

Tolerance = 20.0 PPM / DBE: min = -1.5, max = 50.0

Element prediction: Off

Number of isotope peaks used for i-FIT = 3

Monoisotopic Mass, Even Electron Ions

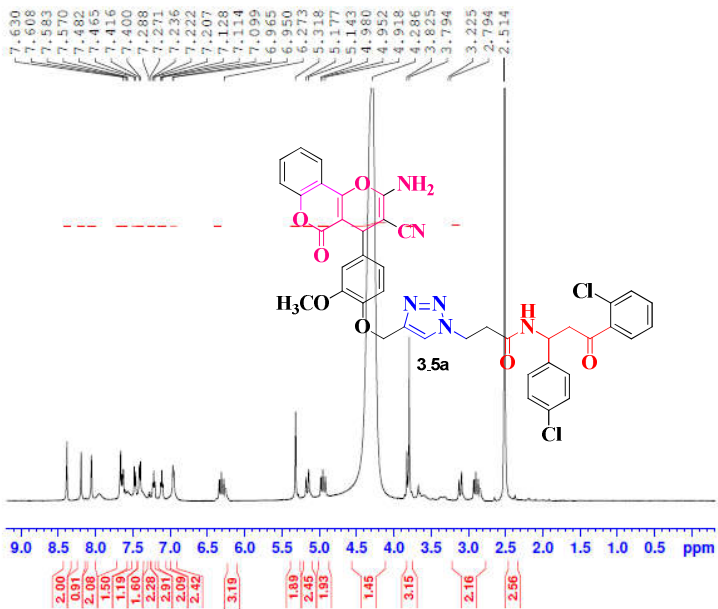
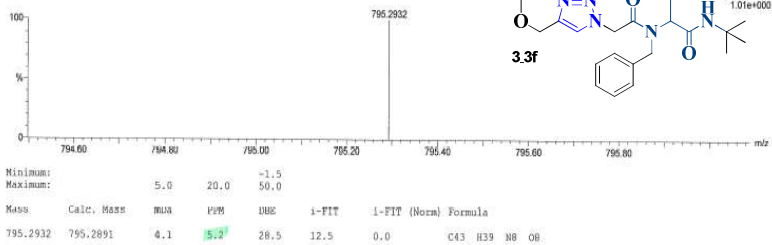
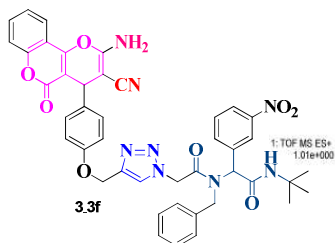
2 formula(e) evaluated with 1 results within limits (up to 50 closest results for each mass)

Elements Used:

C: 43-43 H: 35-40 N: 5-8 O: 5-8

C43H38NO8

C178.20 (0.450)

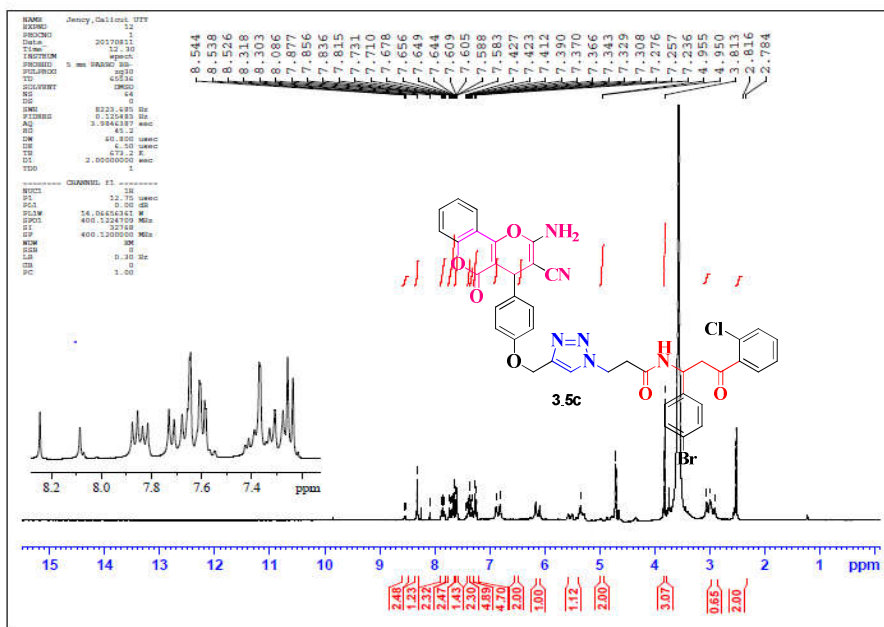
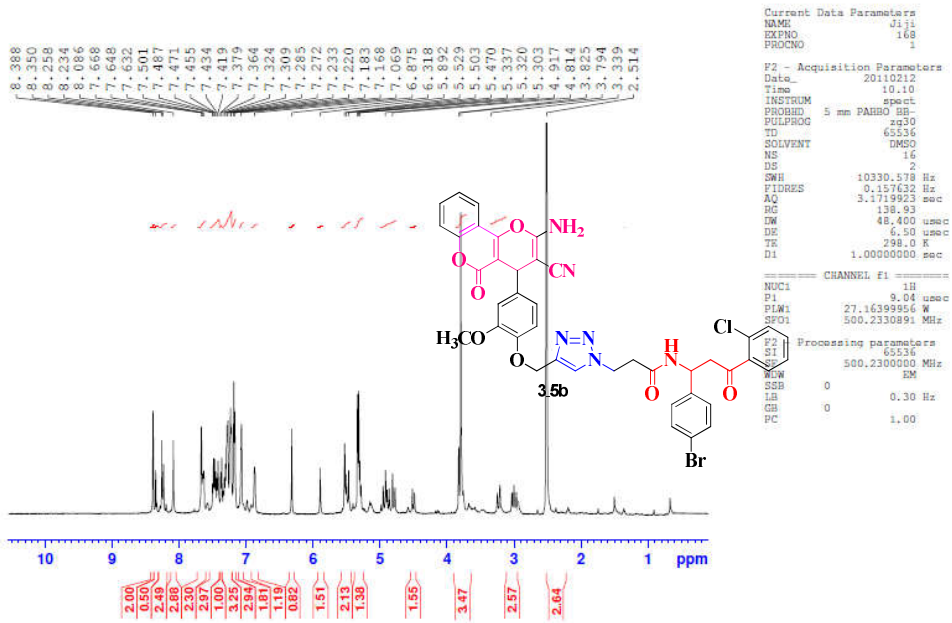


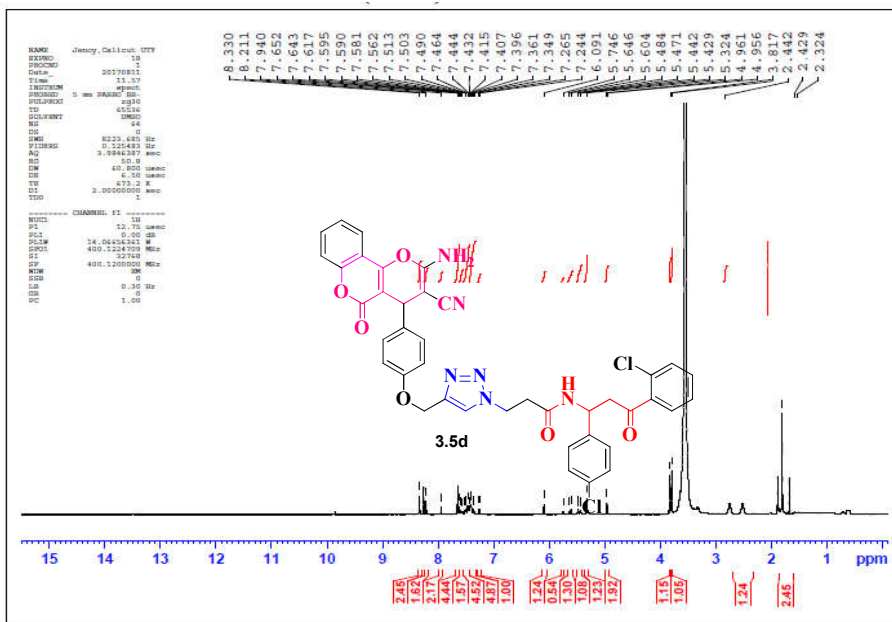
Current Data Parameters
 NAME: Jiji
 EXPNO: 169
 PROCNO: 1

F2 - Acquisition Parameters
 Date_ Time: 20160212 20:20
 INSTRUM: spect
 PROBRN: 5 mm PABBO BB-
 PULPROG: zg30
 TD: 65536
 SOLVENT: DMSO
 NS: 16
 DS: 2
 SWH: 10330.578 Hz
 FIDRES: 0.157632 Hz
 AQ: 3.1719923 sec
 RG: 138.93
 DW: 48.400 usec
 DE: 6.50 usec
 TE: 298.0 K
 D1: 1.00000000 sec

==== CHANNEL f1 =====
 NUC1: 1H
 P1: 9.04 usec
 PLW1: 27.16399956 W
 SFO1: 500.2330895 MHz

F2 - Processing parameters
 SI: 65536
 SF: 500.2300000 MHz
 WDW: EM
 SSB: 0
 LB: 0.30 Hz
 GB: 0
 PC: 1.00





Elemental Composition Report

Single Mass Analysis

Tolerance = 20.0 PPM / DBE: min = -1.5, max = 50.0
 Element prediction: Off
 Number of isotope peaks used for i-FIT = 3

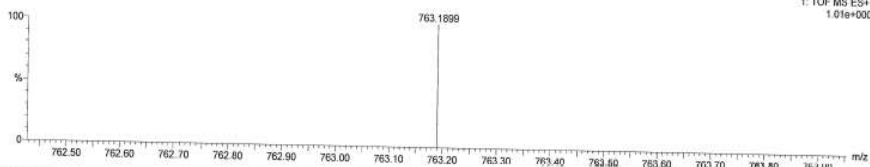
Monoisotopic Mass, Even Electron Ions

33 formula(e) evaluated with 1 results within limits (up to 50 closest results for each mass)

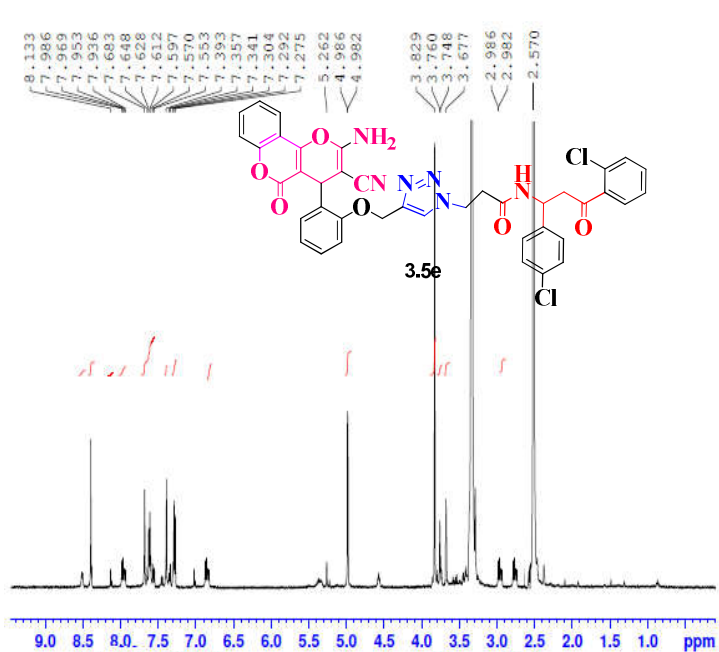
Elements Used:

C: 20-40 H: 15-33 N: 2-7 O: 2-6 Cl: 1-2

C40H33ClN6O6
 C153.64 (1.398)



Minimum:	5.0	20.0	-1.5				
Maximum:			50.0				
Mass	Calc. Mass	mDa	PPM	DBE	i-FIT	i-FIT (Norm)	Formula
763.1899	763.1839	6.0	7.9	26.5	12.7	0.0	C40 H33 N6 O6 Cl2

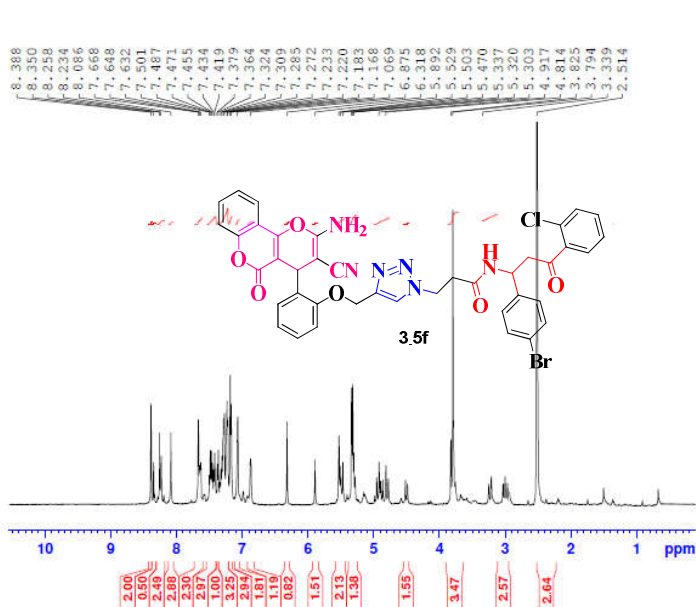


Current Data Parameters
 NAME J11
 EXPNO 166
 PROCNO 1

F2 - Acquisition Parameters
 Date_ 20140212
 Time 21.30
 INSTRUM spect
 PROBHD 5 mm PABBO BB-
 PULPROG zg30
 TD 65536
 SOLVENT DMSO
 NS 16
 DS 2
 SWH 10330.578 Hz
 FIDRES 0.157632 Hz
 AQ 3.1719923 sec
 RG 171.32
 DW 48.400 usec
 DE 6.50 usec
 TE 298.0 K
 D1 1.00000000 sec

==== CHANNEL f1 =====
 NUC1 1H
 P1 9.04 usec
 PLW1 27.16399956 W
 SFO1 500.2330891 MHz

F2 - Processing parameters
 SI 65536
 SF 500.2300000 MHz
 WDW EM
 SSB 0
 LB 0.30 Hz
 GB 0
 PC 1.00



Current Data Parameters
 NAME J11
 EXPNO 166
 PROCNO 1

F2 - Acquisition Parameters
 Date_ 20110212
 Time 10.10
 INSTRUM spect
 PROBHD 5 mm PABBO BB-
 PULPROG zg30
 TD 65536
 SOLVENT DMSO
 NS 16
 DS 2
 SWH 10330.578 Hz
 FIDRES 0.157632 Hz
 AQ 3.1719923 sec
 RG 138.93
 DW 48.400 usec
 DE 6.50 usec
 TE 298.0 K
 D1 1.00000000 sec

==== CHANNEL f1 =====
 NUC1 1H
 P1 9.04 usec
 PLW1 27.16399956 W
 SFO1 500.2330891 MHz

F2 - Processing parameters
 SI 65536
 SF 500.2300000 MHz
 WDW EM
 SSB 0
 LB 0.30 Hz
 GB 0
 PC 1.00

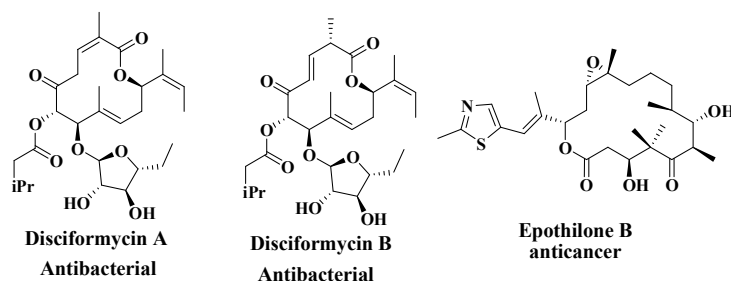
Chapter 4

**Furan tagged Bifunctional Macrocyclic
Peptidomimetic Fluorescent inhibitors via
Sequential Multicomponent reaction and Click
chemistry**

4.1 Introduction	188
4.2 Result and discussion	190
4.3 Photophysical properties	195
4.4 Biological studies	201
4.5 Structure identification	207
4.6 Experimental section	213
References	216
Supplementary data	218

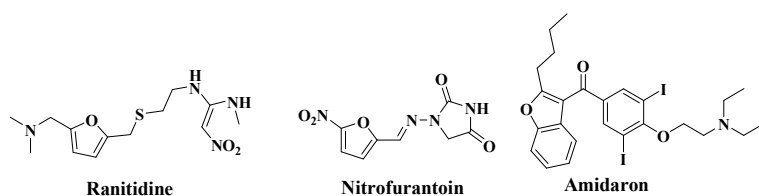
4.1 Introduction

In the previous two chapters we presented the carboxamide and acetamide modification of chromene heterocycle to obtain triazole fused linear peptidomimetics with anticancer activity and imaging properties. The promising results obtained from our work on linear peptidomimetics encouraged us to move on to the development of privileged scaffold functionalized macrocycles to explore these properties in such molecules. As briefly discussed in the first chapter, macrocycles are privileged ring systems with 12 or more atoms and are present in numerous natural products and pharmaceutical agents.¹ Unlike other small molecules, macrocycles offer enhanced conformational flexibility helpful for the selective binding of biological targets, high solubility, high lipophilicity, enhanced membrane permeability, improved metabolic stability and good oral bioavailability.² Macrocylic peptidomimetics are subclass of macrocycles which are designed to mimic the cyclic peptides or proteins with improved pharmacokinetic and physicochemical properties.³ Selected examples of privileged scaffold functionalized macrocyclic therapeutic agents are presented in scheme 4.1



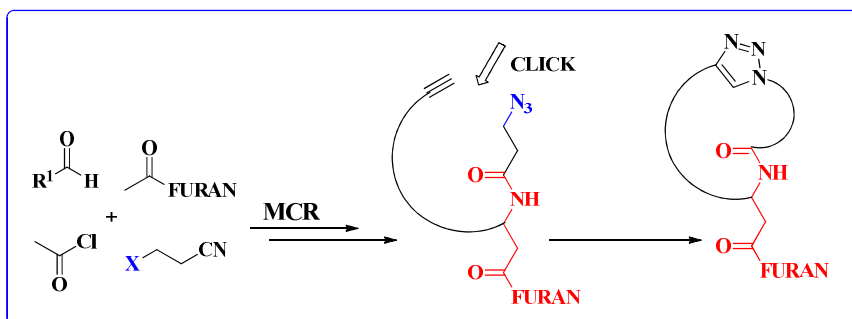
Scheme 4.1: Examples of privileged scaffold functionalized 12 membered macrocycles.

Furan heterocycle was selected as the secondary privileged scaffold to anchor with the macrocyclic scaffold. Furan derivative exhibit excellent pharmacological activities such as antidepressant, anti-anxiolytic, anti-inflammatory, analgesic, antihypertensive, antiglaucoma, antimicrobial, anticancer activities.⁴ In addition to the biological properties, furan incorporated molecules with conjugated double bonds and fused ring systems were also used in electronic devices such as semiconductors,⁵ OLEDs,⁶ and dye sensitized solar cells (DSSC).⁷ Furan containing macrocycles were also reported as ligands for binding various metal ions like Zn^{2+} , Ca^{2+} , Mg^{2+} , Mn^{2+} , Cu^{2+} , Cd^{2+} , La^{2+} and Gd^{3+} etc.⁸ They also exhibit excellent antimicrobial, antioxidant activities.⁹ Furan easily undergo oxidation under chemical and physiological conditions. The furan photo oxidation based click reactions is an important strategy in biological labelling.¹⁰ The incorporation of furan moiety into the biomolecules such as peptide, proteins and nucleic acids is an important method in site specific labelling. Recently furan incorporated peptides and proteins are used for bimolecular labelling.¹¹ Typical examples of commercial drug molecules with furan ring systems are presented in Scheme 4.2.



Scheme 4.2: Selected examples of commercial drug molecules with furan ring as core scaffold

Motivated from these interesting developments, we decided to integrate a furan heterocycle with a cyclic acetamide peptidomimetic with varying ring size based on the fusion of click chemistry with multicomponent coupling strategy as shown in scheme 4.3.

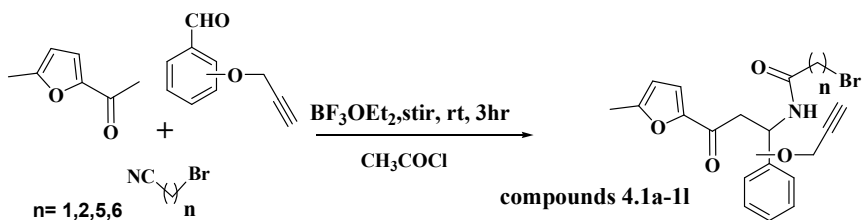


Scheme 4.3: An outline of methodology for the synthesis of furan tagged macrocyclic acetamide peptidomimetics.

4.2 Result and discussion

4.2.1. Synthesis of furan macrocycles

The studies were started with the synthesis of alkyne functionalized furan incorporated β -amido ketones **4.1a** via an alternative Mannich type four component reaction (4CR).¹² This 4CR involves reaction between 2-acetyl-5-methylfuran, bromoalkanenitrile and a propargylated aromatic aldehyde in the presence of slight amount of acetyl chloride and borontrifluoride diethyletherate ($\text{BF}_3 \cdot \text{OEt}_2$) to afford the bromo derivative as shown in the scheme 4.4. In a typical reactions, bromoalkanenitriles having different chain length such as 2-bromoacetonitrile, 3-bromopropionitrile, 6-bromohexanenitrile, and 7-bromoheptane nitrile were used. The synthesized compounds and their percentage yields are listed in table 4.1.

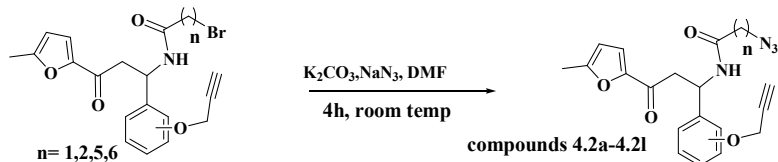


Scheme 4.4: Synthesis of furan amido alkynes

Table 4.1: Structure and percentage yield of furan amido alkynes.

entry	amidoalkyne	yield	entry	amidoalkyne	yield
1		73%	7		67%
2		69%	8		69%
3		70%	9		71%
4		71%	10		72%
5		67%	11		68%
6		65%	12		74%

In the subsequent step, the bromo derivatives were converted to corresponding azide derivatives by treating them with sodium azide under basic conditions in DMF at room temperature as shown in Scheme 4.5. The reactions gave furan azido alkynes **4.2a-4.2l** with good to excellent yields.

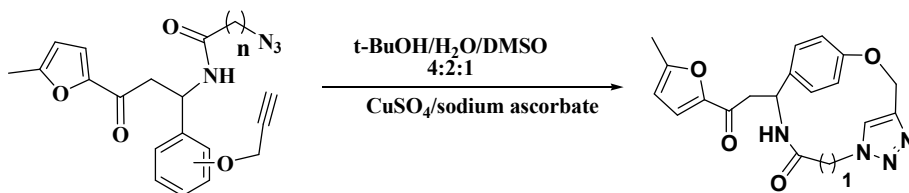


Scheme 4.5: synthesis of furan azido alkynes

Table 4.2: Structure and percentage yield of furan amido alkynes.

entry	azidoalkyne	yield	entry	azidoalkyne	yield
1		73%	7		67%
2		69%	8		69%
3		70%	9		71%
4		71%	10		72%
5		67%	11		68%
6		65%	12		74%

The acetamide derivatives thus functionalized with both alkyne and azide moieties were then subjected to macrocyclization via intramolecular copper catalyzed alkyne-azide click chemistry. The ring size were controlled by the selective use of the nitrile component with appropriate chain length. Accordingly, 11 membered furan tagged macrocycle **4.1a** was synthesized using 2-bromoacetonitrile as the nitrile component, propargylated salicylaldehyde as aldehyde component and 2-acetyl-5-methylfuran as ketone part. These substrates were undergone Mannich type reaction in minimum amount of acetylchloride and $\text{BF}_3 \cdot \text{OEt}_2$ as catalyst. The reaction mixture was stirred for 4 hours and the subsequent aqueous work up yielded furan incorporated Mannich type adduct with an alkyne functionality **4.1a**. The bromine present in **4.1a** was then replaced with an azide functional group by treating it with sodium azide in DMF under basic conditions at room temperature. Followed by this, macrocyclization was carried out via copper catalyzed alkyne-azide click chemistry under Sharpless conditions using copper sulphate (CuSO_4) as copper (II) source in presence of sodium ascorbate in a solvent system containing *t*-BuOH/ H_2O /DMSO in 4:2:1 ratio. The reaction yielded macrocycle **4.3a** with 72% yield after aqueous work up. Similar procedures were adopted for the synthesis of macrocycles **4.3b-4.3l** using various nitrile sources and propargylated aldehydes under same reaction conditions. Accordingly, the 11-18 membered macrocycles listed in table 4.3 were obtained in 65-76% yield.

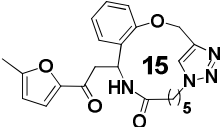
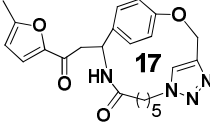
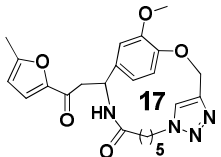
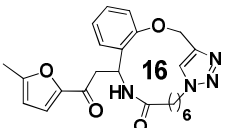
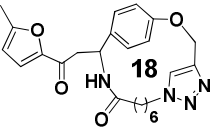
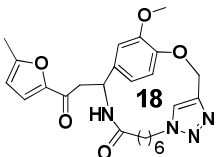


Scheme 4.6: Synthesis macrocycles

Table 4.3: Synthesized macrocycles.

Entry	Peptidomimetic	% yield	Abs _{max} (nm)	Em _{max} (nm)	Stokes shift (nm)
4.3a		72	312	512	200
4.3b		74	306	510	204
4.3c		76	306	510	200
4.3d		70	311	511	205
4.3e		69	300	505	204
4.3f		72	308	512	203

Table 4.3 contd.....

Entry	Peptidomimetic	Abs _{max} (nm)	Em _{max} (nm)	Stokes shift (nm)	
4.3g		73	312	515	203
4.3h		72	314	516	202
4.3i		70	316	515	199
4.3j		68	325	520	195
4.3k		69	328	520	192
4.3l		68	320	525	205

4.3 Photophysical properties

The photophysical properties of the synthesized furan amido alkynes **4.1a-4.1l**, furan azido alkynes **4.2a-4.2l** and the macrocycles **4.3a-4.3l** were studied by measuring the absorption and emission properties of the compound in 0-10 pH in DMSO solvent. The absorption, emission

and stokes shift values of all the compounds were listed in table 4.4, 4.5 and 4.6.

Table 4.4: Photophysical properties of furan amido alkynes.

Entry	Absorption max	Emission max	Stokes shift
4.1a	305	485	182
4.1b	310	485	175
4.1c	312	482	170
4.1d	306	485	179
4.1e	302	486	184
4.1f	307	483	176
4.1g	308	487	179
4.1h	319	488	169
4.1i	320	487	167
4.1j	318	485	167
4.1k	312	483	171
4.1l	306	483	177

Table 4.5: Photophysical properties of furan azido alkynes.

Entry	Absorption max	Emission max	Stokes shift
4.2a	285	468	183
4.2b	287	472	185
4.2c	287	475	188
4.2d	285	472	187
4.2e	284	472	188
4.2f	285	474	189
4.2g	288	474	186
4.2h	288	476	188
4.2i	288	475	187
4.2j	288	476	188
4.2k	288	476	188
4.2l	288	474	186

Table 4.6: Photophysical properties of furan tagged macrocyclic peptidomimetics

Entry	Absorption max	Emission max	Stokes shift
4.3a	312	512	200
4.3b	306	510	204
4.3c	306	510	204
4.3d	311	511	200
4.3e	300	505	205
4.3f	308	512	204
4.3g	312	515	203
4.3h	314	516	202
4.3i	316	515	199
4.3j	325	520	195
4.3k	328	520	192
4.3l	320	525	205

All the molecules showed exceptionally high Stokes shift in the range 167-205 nm. When comparing the absorption and emission properties of the linear precursors **4.1a-1l** and **4.2a-4.2l**, the macrocycles **4.3a-4.3l** were exhibited higher stokes shift values. The normalized absorption and emission spectra of typical compounds are shown in fig.4.1, 4.2 and 4.3.

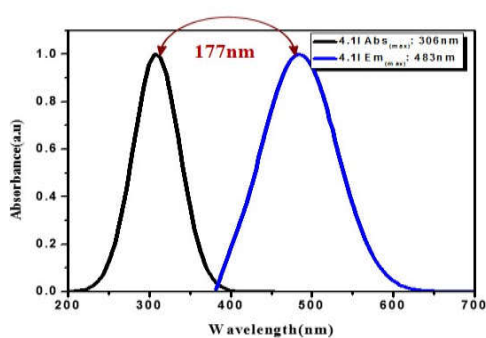


Fig. 4.1: The normalized absorption and emission spectra of 4.11

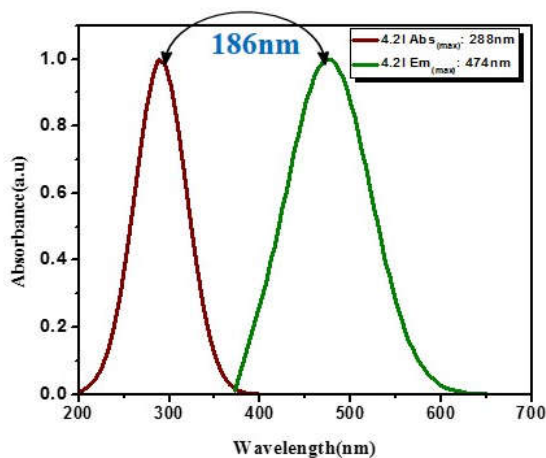


Fig.4. 2: The normalized absorption and emission spectra of 4.21

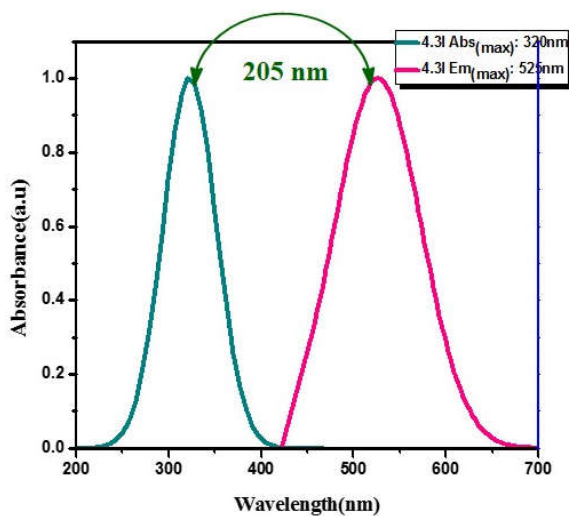


Fig. 4.3: The normalized absorption and emission spectra of 4.31

Fluorophores with large Stokes shifts are valuable tools for multicolour experiments to reduce the number of detection channels, to overcome cross-talk and simplifying the imaging scheme.¹³ However, only few of such bright and photo stable probes with large Stokes shift are commercially available and most of them are coumarin based small

molecules.¹⁴ The main drawback of these coumarin dyes are their moderate photo stability due to the excitation to the triplet state upon excitation and low fluorescence quantum yields in polar solvents restricts their use in optical microscopy/nanoscopy.¹⁵ The Stokes shift has a direct relation with the excited state and ground state dipole moment of the fluorophore.¹⁶ In most cases, the dipole moment of a fluorophore in the excited state differs from that in the ground state. Therefore, after excitation, the solvent dipoles that surround a molecule of the fluorophore may rearrange, to form a better stabilized excited state with lower energy.¹⁷ If the dipole moment of the dye molecule in the excited state is higher than the dipole moment of the same dye in the ground state and the solvent polarity increases, then the energy of the excited state becomes lower and the molecule will give a red shifted emission in more polar solvents.¹⁸ Geometrical relaxation in the excited state and rearrangement of the solvent dipoles are two photophysical processes responsible for the value of the Stokes shift.¹⁹ Thus, a potential strategy to increase the Stokes shift, is to design structures with large differences between the equilibrated geometries and dipole moments in the ground and excited states.

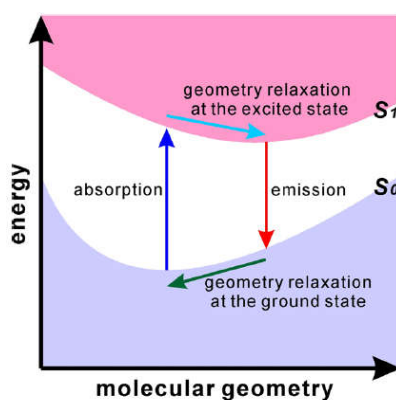


Fig.4.4 : An illustration of the light absorption and emission process leading to change in Stokes shift in fluorophore

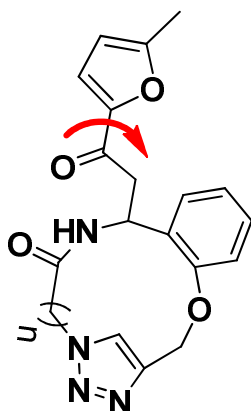


Fig.4.5: The design strategy for increasing the Stokes Shift of furan by introducing a rotational bulky substituent with steric hindrance.

One of such design strategy is the attachment of a rotational substituent to the furan frame work through a single bond. Such a substituent can cause steric hindrance leading it to bend out of the furan molecular plane imparting a non-planar geometry to it.²⁰ This creates a prerequisite for the substituent to rotate in the excited state during geometry relaxation. When the substituent rotates in the excited state, a strong interaction between the substituent and its neighbouring atoms ensures a large amount of torsional work which is then translated into the stokes shift. To enhance the resonance effect and produce a large rotation upon photoexcitation, the substituent should have a strong tendency to participate in the π - conjugated network of the main fluorophore. Similarly, a reasonably strong steric hindrance is required to impart a large amount of torsional work during the substituent rotation, such that a large stokes shift is afforded.

In addition to this, the rotating substituent to produce an observable effect on the optoelectronic properties of a compound, it must demonstrate a significant level of charge transfer between the

molecular orbitals that are associated with the $S_0 \rightarrow S_1$ transition. These molecular orbitals are typically, but not necessarily, HOMO and LUMO. The active participation of the substituent in this orbital charge transfer will impart a large change in electron density of the substituent drives its rotation in the excited state and also will introduce considerable changes to the energy levels of the S_0 and S_1 states, leading to a large amount of charge in the related molecular orbitals.

In the present case, the substituent is a macrocycle which can satisfy many of the criteria mentioned above to justify the large Stokes shift observed in the furan tagged macrocycles. However, high level DFT/TD-DFT calculations are required for a deeper understanding on the unusual Stokes shift observed in these molecules, especially when considering the fact that these macrocycles are not fully conjugated.

4.4 Biological studies

4.4.1 Primary drug property evaluation

The drug property descriptors of all the precursors as well as macrocycles were calculated using an online service, www.molinspiration.com. All the drug property descriptors of alkyne derivatives **4.1a-4.1l** (Table 4.7), the azido alkynes **4.2a-4.2l** (Table 4.8) and the macrocycles **4.3a-4.3l** (Table 4.9) were within the limit of Lipinski's rule of five. According to the Lipinski's rule of five, the drug-likeness of the molecules were assessed mainly based on molecular size, lipophilicity as well as polarity (topological polar surface area; tPSA): Drug like molecules usually have log P values between -0.4 and 5.6 and a molecular weight of <500. An orally bioavailable drug will have tPSA between 75 and 160. Usually

macrocycles occupy the position in between the small molecule therapeutics and large biomolecules. They do not obey the Lipinski's rule of five (Ro5) properties. But for the synthesized macrocycles **4.3a-4.3l** all the drug property descriptors including molecular weight, number of hydrogen bond donors and acceptors, lipohilicity as well as polarity (topological polar surface area; tPSA) are within the limit of Ro5 and indicating their potential for explorations on their biological activities.

Table 4.7: The drug property descriptors of furan amido alkynes

Entry	Number of violations	Number of atoms	Log p <5	Molecular weight <500	Number of ON <10	Number of OH NH <5	Number of rotatable of bonds <10	Topological surface area tPSA
4.1a	0	25	1.90	404.26	5	1	8	68.54
4.1b	0	25	1.95	404.26	5	1	8	68.54
4.1c	0	27	1.54	434.29	6	1	9	77.78
4.1d	0	26	2.17	418.29	5	1	9	68.54
4.1e	0	26	2.22	418.29	5	1	9	68.54
4.1f	0	28	1.81	448.31	6	1	10	77.78
4.1g	0	28	2.95	446.34	5	1	11	68.54
4.1h	0	28	3.00	446.34	5	1	11	68.54
4.1i	0	30	2.58	476.37	6	1	12	77.78
4.1j	0	29	3.45	460.37	5	1	12	68.54
4.1k	0	29	3.50	460.37	5	1	12	68.54
4.1l	0	31	3.09	490.39	6	1	13	77.78

Table 4.8: The drug property descriptors of azido alkynes

Entry	Number of violations	Number of atoms	Log p <5	Molecular weight <500	Number of ON <10	Number of OH NH <5	Number of rotatable of bonds <10	Topological surface area tPSA
4.2a	0	27	2.37	366.38	8	1	9	118.30
4.2b	0	27	2.42	366.38	8	1	9	118.30
4.2c	0	29	2.00	396.40	9	1	10	127.53
4.2d	0	28	2.14	380.40	8	1	10	118.30
4.2e	0	28	2.18	380.40	8	1	10	118.30
4.2f	0	30	1.77	410.43	9	1	11	127.53
4.2g	0	30	2.91	408.46	8	1	12	118.30
4.2h	0	30	2.96	408.46	8	1	12	118.30
4.2i	0	32	2.55	438.48	9	1	13	127.53
4.2j	0	31	3.42	422.49	8	1	13	118.30
4.2k	0	31	3.46	422.49	8	1	13	118.30
4.2l	0	33	3.06	452.51	9	1	14	127.53

Table 4.9: The drug property descriptors of furan tagged Macrocytic peptidomimetics

Entry	Number of violations	Number of atoms	Log p <5	Molecular weight <500	Number of ON <10	Number of OH NH <5	Number of rotatable of bonds <10	Topological surface area tPSA
4.3a	0	28	0.89	380.40	8	1	3	99.26
4.3b	0	27	0.66	366.38	8	1	3	99.26
4.3c	0	29	0.25	343.33	8	1	4	108.50
4.3d	0	28	0.93	380.40	8	1	3	99.26
4.3e	0	30	0.52	410.43	9	1	4	108.50
4.3f	0	28	1.24	380.40	8	2	3	110.12
4.3g	0	31	2.17	422.49	8	1	3	99.26
4.3h	0	31	2.21	422.49	8	1	3	99.26
4.3i	0	33	1.80	452.51	9	1	3	108.50
4.3j	0	32	2.67	436.51	8	1	3	99.26
4.3k	0	32	2.72	436.51	8	1	3	99.26
4.3l	0	34	2.31	466.54	9	1	4	108.50

4.4.2 In vitro anticancer activity

4.4.2 (A) Cell culture and maintenance

A representative compound **4.3i** were used for the cytotoxicity evaluation to study the potential of these molecules as anticancer agents. Human breast cancer MCF-7 cells were maintained in RPMI medium 1640 supplemented with 10% fetal bovine serum as well as 100 µg/mL streptomycin, 100 U/mL penicillin, 2 mM L-glutamine and Earle's BSS adjusted to contain 1.5 g/l Na bicarbonate, 0.1 mM

nonessential amino acids, and 1.0 mM of Na pyruvate in a humidified atmosphere containing 5% CO₂ at 37 °C.

4.4.2 (B): In vitro cytotoxicity of synthesized 4.3i

Cell viability was determined by MTT assay. MCF-7 cells were seeded in 96-well plates at a concentration of 1.0x10⁴ cells/well and incubated overnight at 37°C in a 5% CO₂ humidified environment. Then the cells were treated with different concentrations of the sample **4.3i** like 5, 10, 15, 20, 25, 30, 35, 40, 45 and 50 µM/mL (dissolved with RPMI medium 1640), respectively. Controls were cultivated under the same conditions without addition of sample **4.3i**. The treated cells were incubated for 48 h for MTT assay. The stock concentration (5 mg/mL) of MTT-(3-(4,5-Dimethylthiazol-2-yl)-2,5-diphenyltetrazolium bromide, a yellow tetrazole) was prepared and 100 µL of MTT was added in each wells and incubated for 4 h. Purple color formazan crystals were observed and these crystals were dissolved with 100 µL of dimethyl sulphoxide (DMSO), and read at 620 nm in a multi well ELISA plate reader (Thermo, Multiskan). The molecules showed excellent cytotoxicity against MCF-7 cell lines with an IC₅₀: 20 µM as shown in fig.4. 6

4.4.2 (C): In vitro imaging studies: *DAPI (4, 6-Diamidino-2-phenylindole, dihydrochloride) staining*

MCF-7 cells were treated with **4.3i** at its IC₅₀ concentration (20 µM/mL) for 48 h, and then fixed with methanol: acetic acid (3:1, v/v) prior to washing with PBS. The washed cells were then stained with 1mg/mL DAPI (4,6-Diamidino-2-phenylindole, dihydrochloride)

for 20 min in the dark atmosphere. Stained images were recorded with fluorescent microscope with appropriate excitation filter. The bright field and fluorescence microscopic images are shown in fig. 4.3i. The strong bluish fluorescence and cellular uptake observed in the imaging studies with 4.3i reveals that these molecules have potency to selectively locate malignant cell lines such as MCF-7.

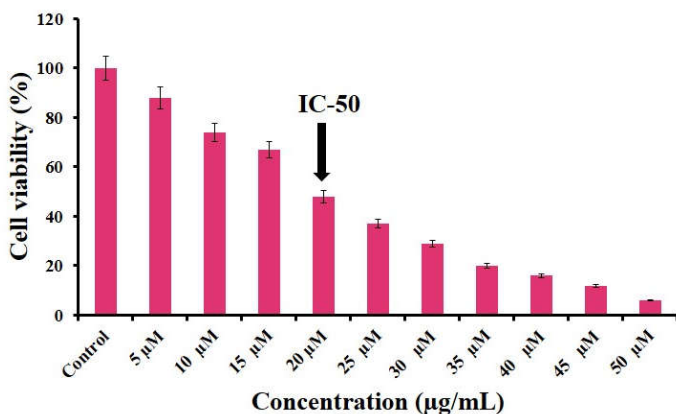


Fig. 4.6: MTT assay results confirming the in vitro cytotoxicity effect of 4.3i against the MCF-7 cells. The detected IC50 concentration was 20µM/mL.

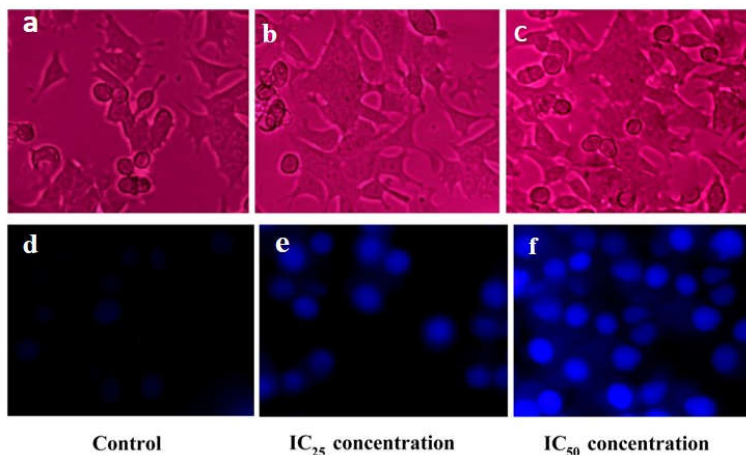


Fig.4.7: Bright field inverted light microscopy images (a) (cc), (b) (IC 25) and (c) (IC 50) and fluorescence microscopy images (d) (CC), (e) (ICC 25) and (f) (IC50) of 4.3i treated MCF-7 cells.

In summary, the chapter 4 presents an efficient protocol for the synthesis of furan tagged macrocycles with varying ring size from 11-18. All the macrocycles are fluorescent molecules with large Stokes shift and also having excellent cytotoxicity against human breast cancer cell lines MCF-7. Compared to the linear peptidomimetics described in chapters 2 and 3, the macrocyclic molecules showed enhanced Stokes shifted emission and enhanced cytotoxicity (IC50 20 μ M) pointing sufficient potency to merit further developments with these molecules.

4.5 Structure identification

4.5.1 Structure identification of 2-Bromo-N-(3-(5-methylfuran-2-yl)-3-oxo-1-(2-(prop-2-yn-1-yloxy)phenyl)propyl)acetamide 4.1a

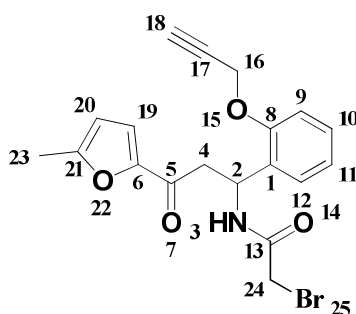


Fig. 4.7: structure of compound 4.1a

For the general discussion, the compound **4.1a** is taken as the representative for the alkyne derivative of furan β -amido ketones. The molecule is numbered as shown in Figure 4.7. The FT-IR spectrum of the compound **4.1a** (figure 4.7) gave major absorptions at 3463, 3292, 2926, 2132, 1693, 1614, 1509, 1470, 1369, 1269 and 1156 cm^{-1} . The NH stretching vibration band of the acetamido group occurs at 3463 cm^{-1} . The band at 3269 cm^{-1} confirmed the strong C-H stretching band of alkyl group. The weak band at 2132 cm^{-1}

¹correspond to the stretching vibration of C-C triple bond. The peak at 1693 cm⁻¹ corresponds to the amide I band, i.e., the band due to the C=O stretching vibration of (C2) and the amide II band which arises from the interaction between the N-H bending and the C-N stretching of the C-N-H group is obtained at 1614cm⁻¹.

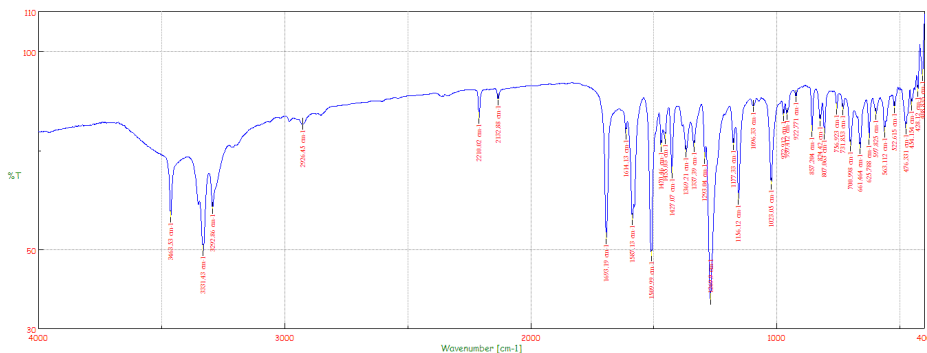


Fig. 4.8: FT-IR spectrum of 4.1a

The initial information obtained about the compound **4.1a** was further confirmed by the ¹H NMR spectrum (Figure 4.9). The singlet obtained at $\delta = 8.32$ is due to the amido bond (NH). The aromatic proton at position 19 of the furan ring appeared as a doublet at 7.933-7.914. Another doublet at 6.389-6.381 corresponds to the neighboring proton at position 20. Other downfield resonances such as a quartet at δ 7.75-7.67, the multiplet at δ 7.50-7.90 corresponds to the remaining aromatic protons. The CH proton at position 2 is obtained as a triplet δ 5.03 The CH₂ protons at position 4 are obtained as a doublet of doublet at δ 4.78-4.99 and 4.27-4.58 with approximately equal coupling constants. The singlet at 2.37 is due to the three protons of the methyl group at position 23.

2187 corresponds to the azide part. The weak band at 2161 cm^{-1} correspond to the stretching vibration of C-C triple bond. The peak at 1635 cm^{-1} corresponds to the amide I band, i.e., the band due to the C=O stretching vibration of (C2) and the amide II band which arises from the interaction between the N-H bending and the C-N stretching of the C-N-H group is obtained at 1614 cm^{-1} .

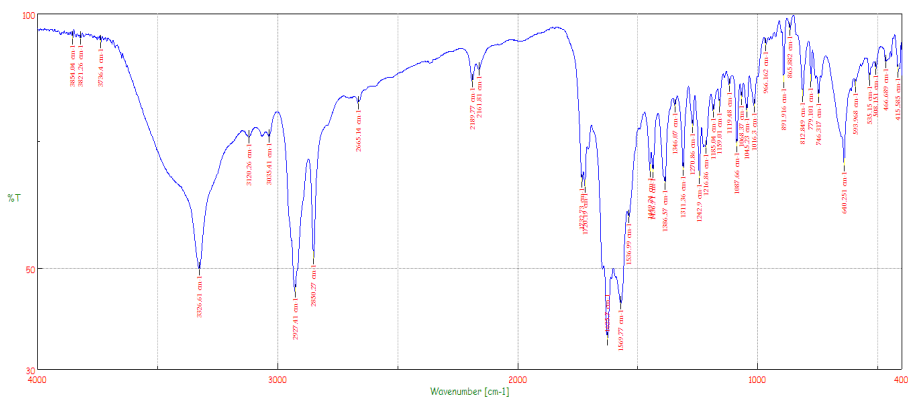


Fig. 4.10: FT-IR spectrum of compound 4.2a

The initial information obtained from the FT-IR spectrum was further confirmed by $^1\text{H-NMR}$ spectrum as shown in fig.4.11. The two proton singlet observed at δ 1.77 is attributed to the CH_2 proton at position 24. The two proton doublet at δ 3.78 corresponds to the CH_2 proton at position 4. The two proton singlet at δ 4.95 corresponds to the CH_2 proton at position 16. The one proton singlet at δ 5.31 corresponds to the CH proton at position 2. The aromatic protons observed at δ 6.83, δ 7.24-7.26, δ 7.59-7.65. the NH proton at position 3 is observed at δ 8.33.

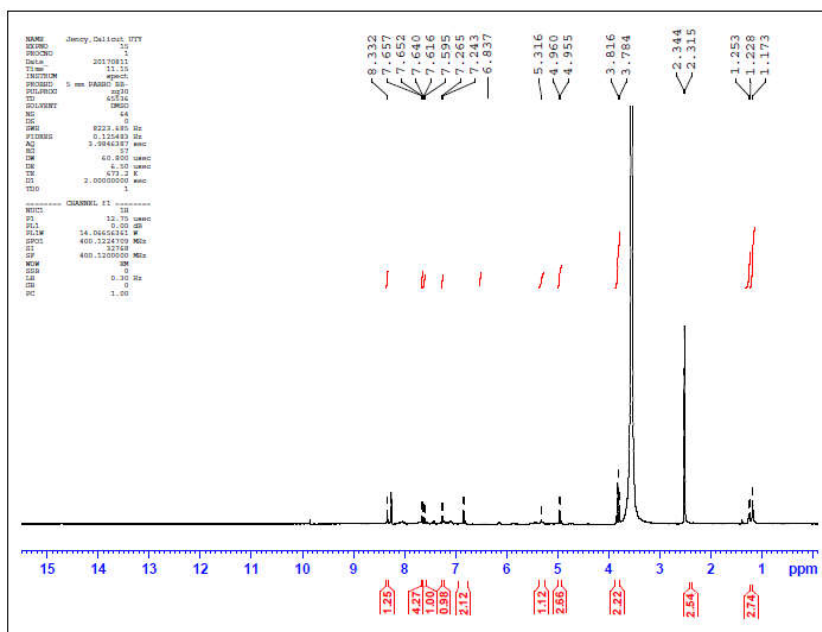


Fig. 4.11: ¹H-NMR spectrum of 4.2a

4.5.6 Structure identification of 10-(2-(5-Methylfuran-2-yl)-2-oxoethyl)-9,10-dihydro-2H-3,6-(metheno)benzo[k][1,4,5,6,9]oxatetraazacyclododecin-8(7H)-one 4.3a

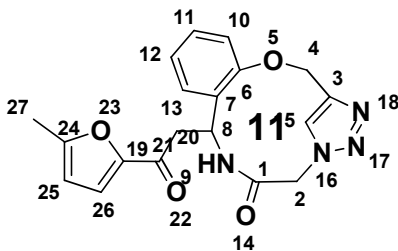


Fig. 4.12: structure of compound 4.3a

For the general discussion, the compound **4.3a** is taken as the representative for the furan tagged macrocycles. The molecule is numbered as shown in Figure **4.12**. The FT-IR spectrum of the compound **4.1a** (fig. **4.13**) gave major absorptions at 3419, 2921, 1698, 1614, 1509, 1487, 1369, 1269 and 1136 cm^{-1} . The NH stretching vibration band of the acetamido group occurs at

3419 cm^{-1} . The peak at 1698 cm^{-1} corresponds to the amide I band, i.e., the band due to the C=O stretching vibration of (C2) and the amide II band which arises from the interaction between the N-H bending and the C-N stretching of the C-N-H group is obtained at 1614 cm^{-1} .

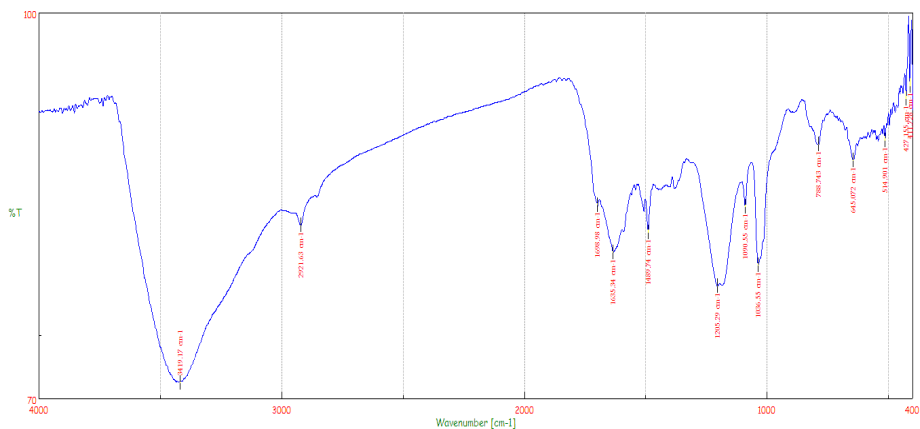


Fig. 4.13: FT-IR spectrum of compound 4.3a

The initial information obtained from the FT-IR spectrum is again confirmed by $^1\text{H-NMR}$ spectrum as shown in fig. 4.14. The three proton singlet at δ 2.58 corresponds to the CH_3 proton at position 27. The two proton doublet of doublet at δ 3.78 is attributed to the CH_2 proton at position 20. The two proton singlet at δ 4.96 corresponds to the CH_2 proton at position 2. The two proton singlet at δ 5.30 corresponds to the CH_2 proton at position 4. The one proton singlet at δ 6.29, δ 6.94 and multiplet between δ 7.05-7.45 corresponds to the aromatic protons. The one proton singlet at δ 7.50 corresponds to the triazole proton and singlet at δ 8.30 corresponds to the singlet NH proton at position 9.

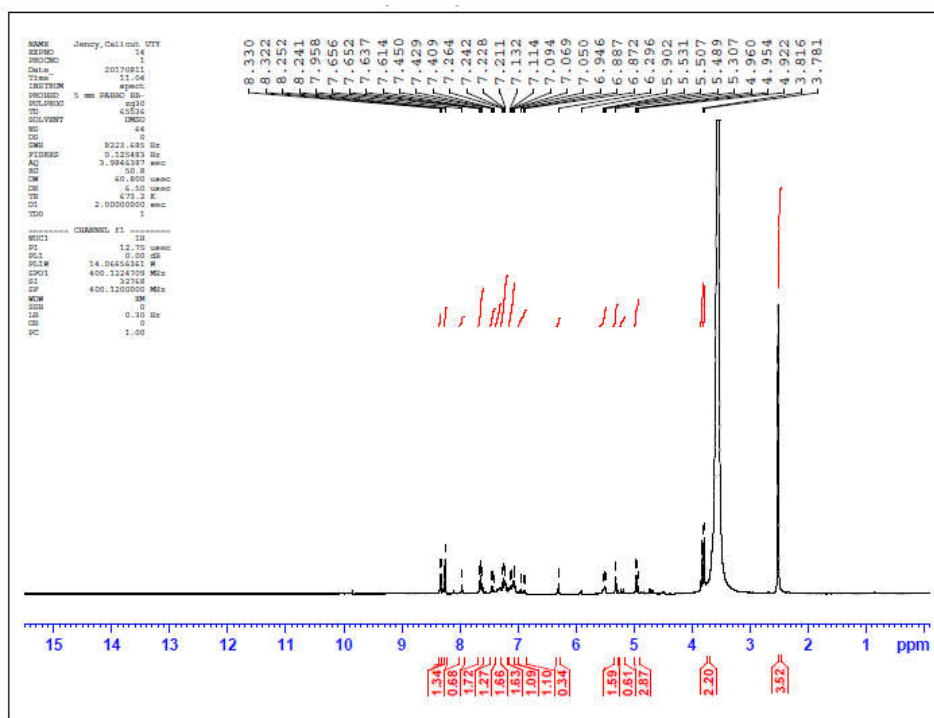


Fig.4.14: ^1H -NMR spectrum of 4.3a

4.6 Experimental section

4.6.1 General

IR spectra were recorded on a JASCO-FT/IR-4100 Fourier transform infrared spectrometer and measured as KBr pellets. ^1H were determined in DMSO or CDCl_3 with a Bruker amx 500 MHz spectrometer. The chemical shifts (δ) are given relative to tetramethylsilane (TMS) and the coupling constants (J) are reported in hertz (Hz).

4.6.2 Typical procedure for the synthesis of furan amido alkyne 4.1a :

In a typical reaction 1 equivalent of 2-Acetyl-5-methyl-furan (124mg), propargylated 4-Hydroxy benzaldehyde (160mg), 2-Bromoacetonitrile (119mg) were dissolved in minimum amount of acetyl chloride in an R.B

flask and added catalytic amount of $\text{BF}_3 \cdot \text{Et}_2\text{O}$. The reaction mixture is stirred for 4 hours. Aqueous work up of the reaction mixture followed by silica column chromatography yield 4.1a in 73% yield.

4.6.3. 2-Bromo-N-(3-(5-methylfuran-2-yl)-3-oxo-1-(2-(prop-2-yn-1-yloxy)phenyl)propyl)acetamide 4.1a: Brownish solid, 302mg, 75%, M.P. 153–154°C. $^1\text{H-NMR}$ (DMSO, 500 MHz): 2.37(s,2H), 4.27(s,1H), 4.78(dd,2H), 5.03(s,1H), 6.38(s,1H), 7.50-7.90(d,1H), 7.93-7.91(d,1H), 8.32(s,1H). IR (KBr) $\nu \text{ cm}^{-1}$: 3463, 3292, 2926, 2132, 1693, 1614, 1509, 1470, 1369, 1269 and 1156 cm^{-1}

4.6.4 3-Bromo-N-(3-(5-methylfuran-2-yl)-3-oxo-1-(4-(prop-2-yn-1-yloxy)phenyl)propyl)propanamide 4.1d: Brownish solid, 292mg, 80%, M.P. 170–172°C. $^1\text{H-NMR}$ (DMSO, 500 MHz), δH (ppm): 2.35(s,3H), 2.57(s,2H), 3.42(s,H), 3.52(s, 1H), 3.81(s,2H), 4.95(s,2H), 5.15(s,1H), 7.23-7.87(m,6H), 8.30(s,1H). IR (KBr) $\nu \text{ cm}^{-1}$: 3457, 3260, 2947, 2100, 1643, 1609, 1515, 1460, 1379, 1280 and 1164 cm^{-1}

4.6.5. Typical experimental procedure for the 2-Azido-N-(3-(5-methylfuran-2-yl)-3-oxo-1-(2-(prop-2-yn-1-yloxy)phenyl)propyl)acetamide 4.2a: one equivalent of 4.1a (0.404g) is dissolved in minimum amount of dimethylformamide and three equivalent of K_2CO_3 were added. The reaction mixture is stirred for 4 hours. Diluted with water. Filtered and dried to get 4.2a in 73% yield.

4.6.6 2-Azido-N-(3-(5-methylfuran-2-yl)-3-oxo-1-(2-(prop-2-yn-1-yloxy)phenyl)propyl)acetamide 4.2a: Brownish solid, 210mg, 70%, M.P. 180–182°C. $^1\text{H-NMR}$ (DMSO, 500 MHz), δH (ppm): 1.17(s,1H), 2.31(s,2H), 2.34(s,3H), 3.78(dd,2H), 4.95(s,2H), 5.31(s,2H), 6.83(s,1H), 7.24-7.65(m,6H), 8.03(s,1H). IR (KBr) $\nu \text{ cm}^{-1}$: 3423, 3326, 3292, 2927, 2187, 2161, 1635, 1614, 1569, 1536, 1449, 1436, 1386 and 1346 cm^{-1}

4.6.7 **3-Azido-N-(3-(5-methylfuran-2-yl)-3-oxo-1-(4-(prop-2-yn-1-yloxy)phenyl)propyl)propanamide 4.2e:** ¹H-NMR (DMSO, 500 MHz), δH (ppm): 1.17(s,1H), 2.51 (s,3H), 3.2(s, 1H), 3.25(s,2H), 3.99(s,2H), 5.16(s,1H), 6.07(s,1H), 7.49-7.96(m,6H), 8.30(s,1H). IR (KBr)v cm⁻¹: 3406,3316, 3201, 2921, 2104, 2100, 1648, 1608, 1575, 1538, 1450, 1487, 1380 and 1335cm⁻¹

4.6.8 **10-(2-(5-Methylfuran-2-yl)-2-oxoethyl)-9,10-dihydro-2H-3,6-(metheno)benzo[k][1,4,5,6,9]oxatetraazacyclododecin-8(7H)-one 4.3a:** ¹H-NMR (DMSO, 500 MHz), δH (ppm):2.58(s,3H), 3.78(dd,2H), 4.96(s,2H), 5.30(s,2H),6.29(s,1H), 6.94(s,1H), 7.05-7.45(m,5H), 7.50(s,1H), 8.30(s,NH). IR (KBr)v cm⁻¹: 3419, 2921, 1698, 1614, 1509, 1487, 1369,1269 and 1136cm⁻¹.

4.6.9 **10-(2-(5-Methylfuran-2-yl)-2-oxoethyl)-9,10-dihydro-2H-3,6-(metheno)benzo[k][1,4,5,6,8]oxatetraazacyclododecin-8(7H)-one** ¹H-NMR (DMSO, 500 MHz), δH (ppm):2.61(s,3H), 3.95(dd,2H), 4.83 (s,1H), 5.47(s,2H),6.27(s,1H), 7.09(s,1H), 7.47(s,1H), 7.54(s,1H),7.56(s,4H) 8.30(s,NH). IR (KBr)v cm⁻¹: 3471, 2934, 1681, 1613, 1508, 1488, 1324,1256 and 1126cm⁻¹.

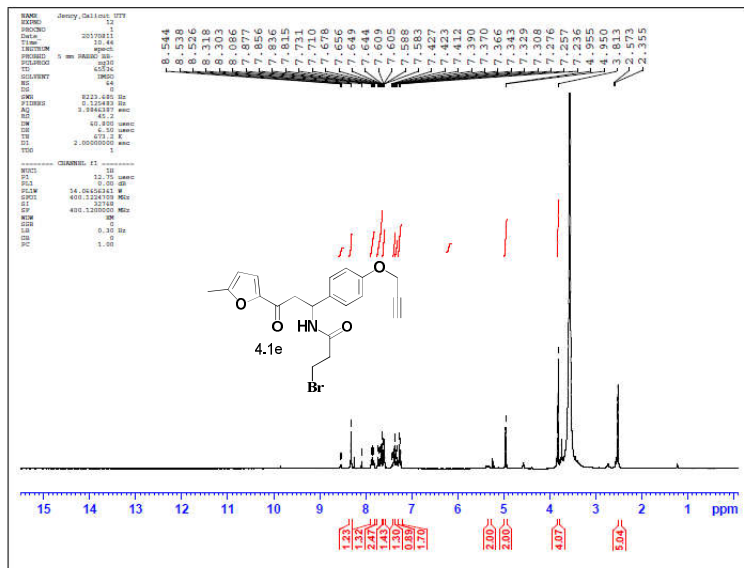
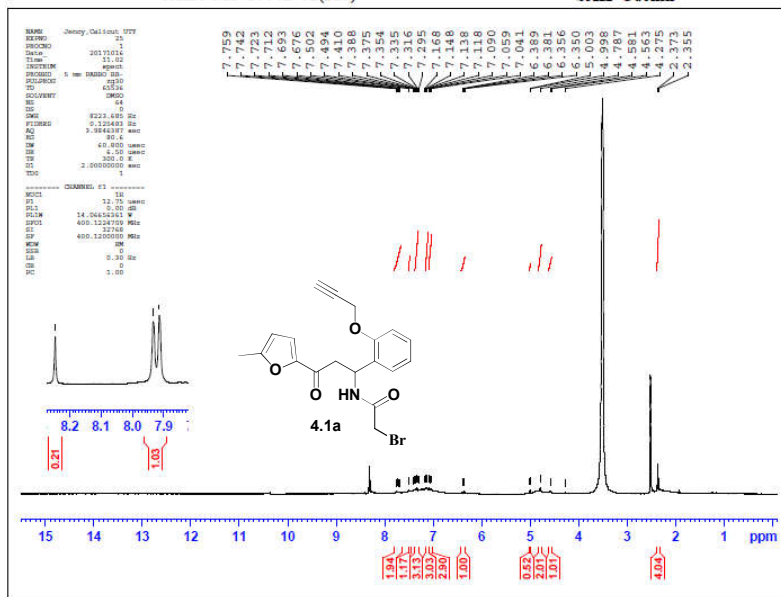
References

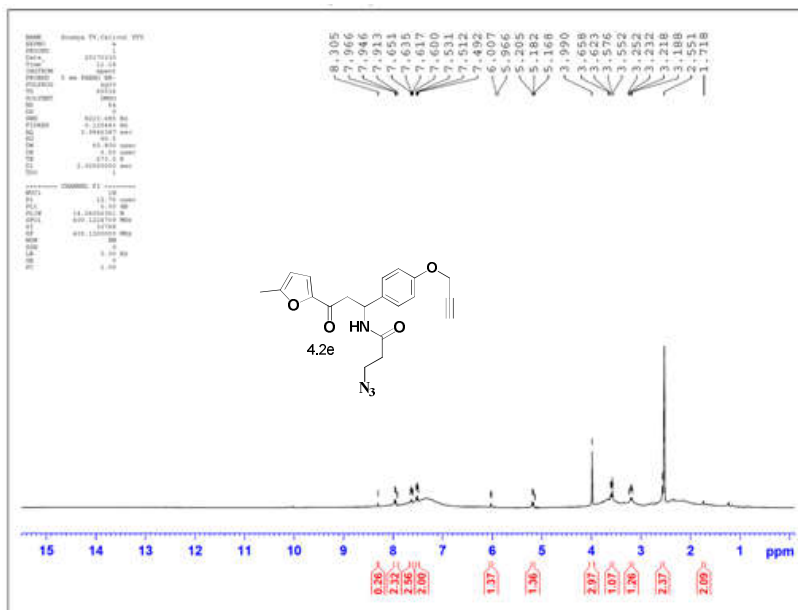
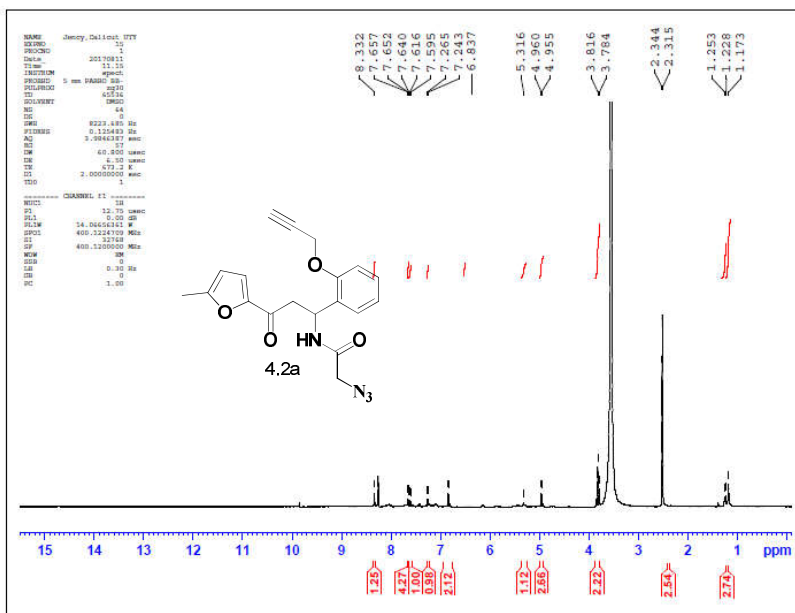
1. (a) Wisner, J.A. *Nature chemistry*, **2013**, 5, 646-647. (b) Yu, X.; Sun, D. *Molecules*, **2013**, 18, 6230-6268.
2. Mallinson J.; Collins, I. *Future Med. Chem.* **2012**, 4, 11, 1409–1438.
3. Galindo, F.; Burguete, M. I.; Vigarra, L.; Luis, S. V.; Kabir, N.; Gavrilovic, J.; Russell, D. A. *Angew. Chem.* **2005**, 117, 6662-6666.
4. Banerjee, R.; Kumar, H.K.S.; Banerjee, M. *Int. J. Rev. Life. Sci.* **2012**, 2, 1, 7-16.
5. (a) Anthony, J. E. *Chem. Rev.* **2006**, 106, 22, 5028-5048. (b) Jiang, W.; Li, Y.; Wang, Z. H. *Chem. Soc. Rev.* **2013**, 42, 6113-6127
6. (a) Yu, X.; Wang, M.; Qiao, X.; Li, J.; Li, H. *Tetrahedron*, **2015**, 71, 852-856.
7. Lin, J.T.; Chen, P.C.; Yen, Y.S.; Hsu, Y.C.; Chou, H.H.; Yeh, M.C.P. *Org. Lett.* **2009**, 11, 1, 97-100.
8. Rathi, P.; Singh, D.P. *J. Mol. Struct.* **2015**, 1093, 201–207.
9. Rothermel, G.L.; Miao, L.; Hill, A.L.; Jackels, S.C. *Inorg. Chem.* **1992**, 31, 4854-4859.
10. (a) Carrette, L.L.G.; Gyssels, E.; Madder, A. *Curr. Prot. Nucl. Acid Chem.* **2013**, 54, 5.12.1–5.12.16. (b) Stevens, K.; Madder, A. *Nucleic Acids Research*, **2009**, 37, 5, 1555-1565. (c) Op de Beeck, M.; Madder, A., *J. Am. Chem. Soc.* **2011**, 133, 4, 796–807 (c) Op de Beeck, M. Madder A. *J. Am. Chem. Soc.* **2012**, 134, 26, 10737–10740. (d) 4) Carrette, L.L.G.; Gyssels, E.; Loncke, J.; Madder, A. *Org. Biomol. Chem.* **2014**, 12, 6, 931-935. (e) Carrette, L.L.G.; Morii, T.; Madder, A. *Bioconj. Chem.* **2013**, 24, 12, 2008-2014. (f) Deceuninck, A.; Madder, A.; *Chem. Comm.* **2009**, 340-342. (e) 7) Hoogewijs, K.; Buyst, D.; Winne, J.M.; Martins, J.C.; Madder, A. *Chem. Comm.* **2012**, 49, 28, 2927. (f) Antonatou, E.; Hoogewijs, K.; Baudot, A.; Kalaitzakis, D.; Vassilikogiannakis, G.; Madder, A. *Chemistry*. **2016**, 22, 25, 8574-8461. Hoogewijs, K.; Buyst, D.; Winne, J.M.; Martins, J.C.; Madder, A. *Chem. Commun.* **2013**, 49, 2927-2929.
11. (a) Bahulayan, D.; Das, S.K.; Iqbal, J. *J. Org. chem.* **2003**, 68, 5733-5738 (b) Pandey, G.; Singh, R.P.; Garg, A.; Singh, V.K. *Tetrahedron Lett.* **2005**, 46, 2137-2140. (d) Arend, M.;

- Westermann, B.; Risch, N.; *Angew. Chem. Int. Ed.* **1998**, *37*, 1044 – 1070. (e) Chowdari, N.S.; Suri, J.T.; Barbas, C.F. *Org. Lett.* **2004**, *6*, 15, 2507–2510.
12. Gao, Z.; Hao, Y.; Zheng, M.; Chen, Y. *RSC Adv.*, **2017**, *7*, 7604-7609.
 13. Sednev, M. V.; Belov, V.N.; Hell, S.W.; *Methods Appl Fluoresc.* **2015**, *3*, 042004.
 14. Benniston, A.C.; Winstanley, T.P.; Lemmetyinen, H.; Tkachenko, N.V.; Harrington, R.W.; Wills, C. *Org. Lett.* **2012**, *14*, 1374–1377.
 15. Ravi, M.; Samanta, A.; Radhakrishnan, T. P. *J. Phys. Chem.* **1994**, *98*, *37*, 9133–9136.
 16. (a) Lakowicz, J. R. *Principles of Fluorescence Spectroscopy*, 2nd ed.; Kluwer Academic: New York, **1999**. (b) Valeur, B. *Molecular Fluorescence: Principles and Applications*; Wiley-VCH Verlag: Weinheim, **2001**.
 17. Chen, Y.; Zhao, J.; Guo, H.; Xie, L. *J. Org. Chem.* **2012**, *77*, 2192–2206
 18. Turro, N. J.; Ramamurthy, V.; Scaiano, J. C. *Principles of Molecular Photochemistry: An Introduction*; University Science Books: Sausalito, **2009**.
 19. Liu, X.; Xu, Z.; Cole, J.M. *J. Phys. Chem. C.* **2013**, *117*, 16584–16595.

SAIFNM171004B-02(225)

SAIF Cochlin





Chapter 5
Conclusion and Future Perspectives

As reflected in the title of the thesis, the work presented in this thesis is on the development of privileged scaffold functionalized peptidomimetics based on the combination of multicomponent coupling strategy with click chemistry. Two privileged heterocycles such as chromene and furan had been selected as the core scaffold. These core scaffolds were functionalized with synthetic equivalents of α -amino acids and β -amino acids such as carboxamide or acetamide moieties through a triazole linker to obtain linear or cyclic peptidomimetic structures and their biological and photophysical property evaluation is the topic investigated and presented in this thesis.

The chapter 1 gives a brief introduction on the importance of privileged scaffolds in medicinal chemistry and the discussion on the recently emerged synthetic methodology for the design of privileged scaffolds incorporating peptidomimetics by combining multicomponent reactions and click chemistry.

The chapter 2 describes the chemistry and chemical biology of two new series of chromene peptidomimetics with carboxamide and acetamide peptide residues based on Click with MCR synthetic strategy as shown in the graphical representation given as fig. 1

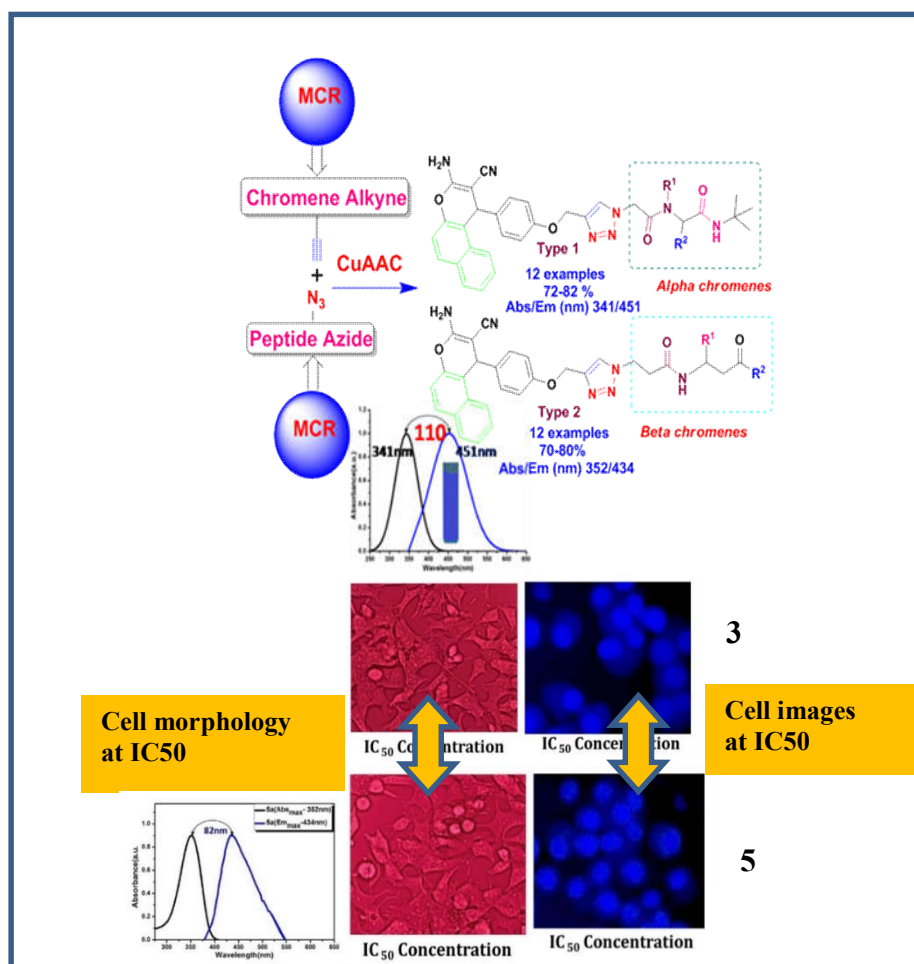


Fig. 5.1: Graphical representation of the peptide randomization studies discussed in chapter 2.

3 new alkynes, 10 new azides, and 24 new peptidomimetic fluorophores were synthesized and their fluorescence properties were evaluated. Spectroscopic studies indicated that the efficiency of the new compounds, especially the type 2 peptidomimetics are comparable with commercial Alexa Fluor® 405 and eFluor®450, extensively used in flow cytometry. Similarly, the drug property

descriptors were calculated and the data obtained revealed the possibility of these molecules for modulating difficult target classes that have large, flat, and groove-shaped binding sites. Selected molecules were subjected to cytotoxicity evaluation against human breast cancer cell lines MCF-7 and the results obtained are promising for further developments based on these molecules. The new compounds added to the chemical space are shown in figures 5.2 to 5.4 and their physicochemical and biological properties are listed in tables 5.1 and 5.2

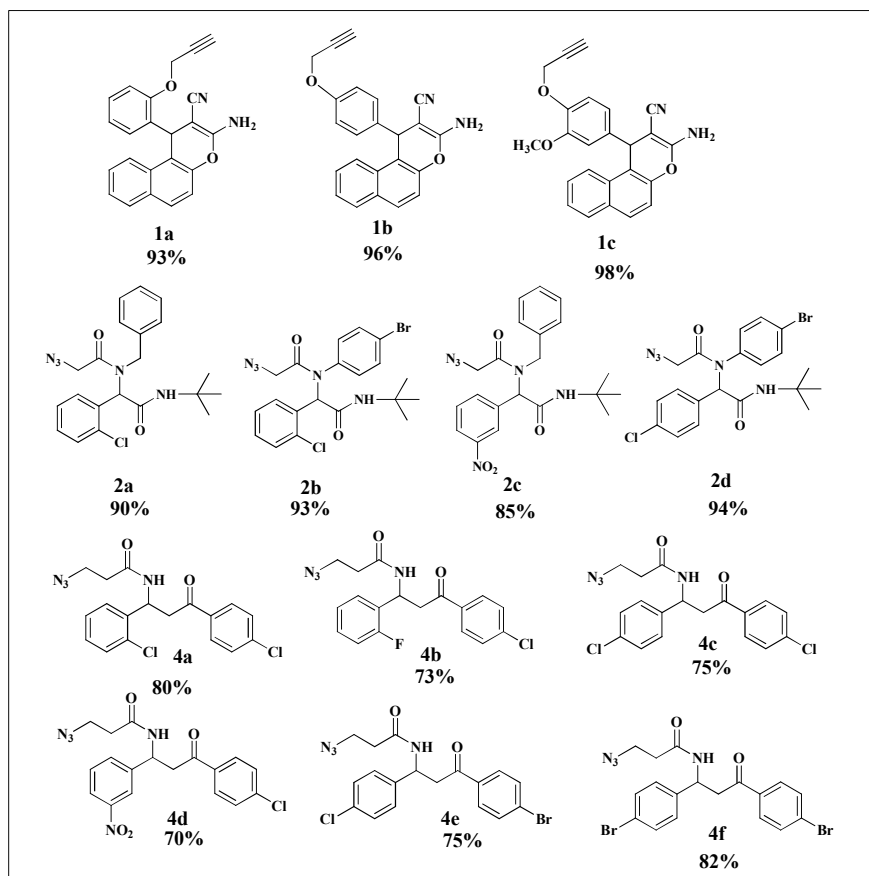


Fig.5.2: Alkyne and azido scaffold diversity reported in chapter 2

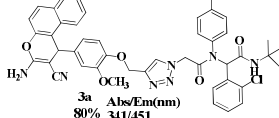
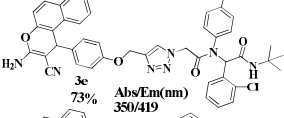
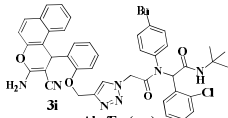
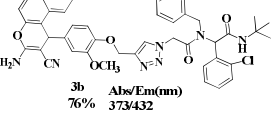
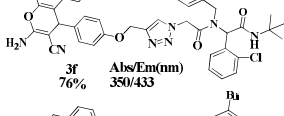
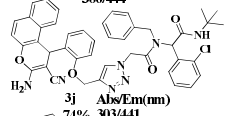
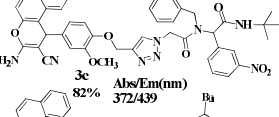
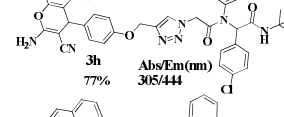
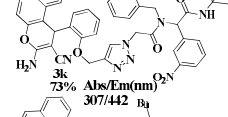
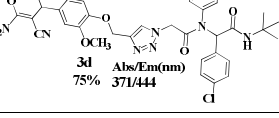
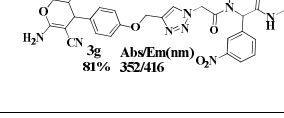
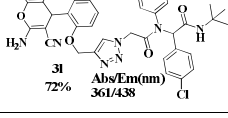
Entry	linear peptidomimetics	Entry	linear peptidomimetics	Entry	linear peptidomimetics
1.	 3a Abs/Em(nm) 80% 341/451	5.	 3e Abs/Em(nm) 73% 350/419	9.	 3i Abs/Em(nm) 75% 306/444
2.	 3b Abs/Em(nm) 76% 373/432	6.	 3f Abs/Em(nm) 76% 350/433	10.	 3j Abs/Em(nm) 74% 303/441
3.	 3c Abs/Em(nm) 82% 372/439	7.	 3h Abs/Em(nm) 77% 305/444	11.	 3k Abs/Em(nm) 73% 307/442
4.	 3d Abs/Em(nm) 75% 371/444	8.	 3g Abs/Em(nm) 81% 352/416	12.	 3l Abs/Em(nm) 72% 361/438

Fig. 5.3: List of new chromene -triazole -carboxamide peptidomimetics discussed in chapter 2.

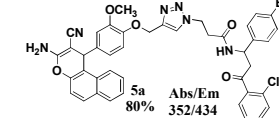
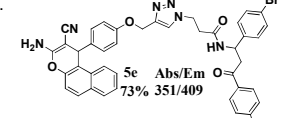
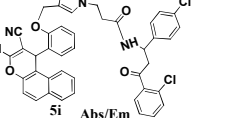
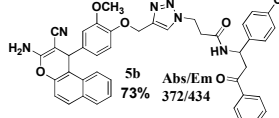
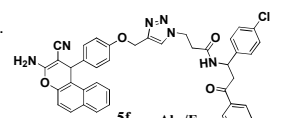
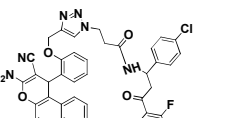
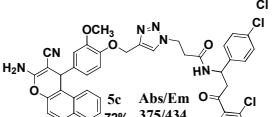
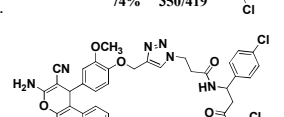
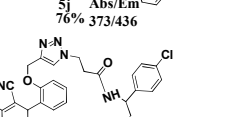
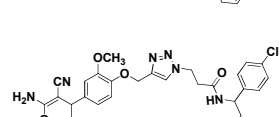
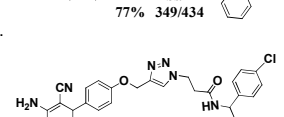
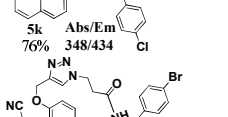
Entry	linear peptidomimetics	Entry	linear peptidomimetics	Entry	linear peptidomimetics
1.	 5a Abs/Em 80% 352/434	5.	 5e Abs/Em 73% 351/409	9.	 5i Abs/Em 70% 379/434
2.	 5b Abs/Em 73% 372/434	6.	 5f Abs/Em 74% 350/419	10.	 5j Abs/Em 76% 373/436
3.	 5c Abs/Em 72% 375/434	7.	 5g Abs/Em 77% 349/434	11.	 5k Abs/Em 76% 348/434
4.	 5d Abs/Em 76% 370/434	8.	 5h Abs/Em 80% 374/434	12.	 5l Abs/Em 78% 346/409

Fig. 5.4: List of new chromene -triazole -acetamide peptidomimetics discussed in chapter 2

Table 5.1: The structure and properties of type 1 peptidomimetics

Entry	Properties
1	Yield-80%, MW-859.19, noN-11, noHNNH-2, mi LogP-8.75, TPSA-154.87, Abs _{max} : 341nm, Em _{max} : 451nm, $\Delta\lambda$: 110nm, IC50: 40 μ M.
2	Yield: 76%, MW: 795.29, noN-11, noHNNH-3, mi LogP-8.07, TPSA-154.87, Abs _{max} : 373nm, Em _{max} : 432 nm, $\Delta\lambda$: 59 nm
3	Yield-82%, MW-806.32, noN-14, noHNNH-3, mi LogP-7.31, TPSA-154.87, Abs _{max} -372nm, Em _{max} -439nm, $\Delta\lambda$ -67nm
4	Yield-75%, MW-859.18, noN-11, noHNNH-3, mi LogP-8.77, TPSA-154.87, Abs _{max} -371nm, Em _{max} -444 nm, $\Delta\lambda$ -73nm
5	Yield-73%, MW-829.17, noN-10, noHNNH-3, mi LogP-8.76, TPSA-145.64, Abs _{max} -350nm, Em _{max} -419nm, $\Delta\lambda$ -69 nm
6	Yield-76%, MW-765.28, noN-10, noHNNH-3, mi LogP-8.02, TPSA-145.64, Abs _{max} -350 nm, Em _{max} -433 nm, $\Delta\lambda$ -83nm
7	Yield-81%, MW-776.30, noN-13, noHNNH-3, mi LogP-7.33, TPSA-145.64, Abs _{max} -352 nm, Em _{max} -416 nm, $\Delta\lambda$ -64nm
8	Yield-75%, MW-829.17, noN-10, noHNNH-3, mi LogP-8.78, TPSA-145.64, Abs _{max} -305 nm, Em _{max} -444 nm, $\Delta\lambda$ -139 nm.
9	Yield-75%, MW-829.17, noN-11, noHNNH-3, mi LogP-8.02, TPSA-145.64.45, Abs _{max} -306nm, Em _{max} -444nm, $\Delta\lambda$ -138nm.
10	Yield-82%, MW-765.28, noN-11, noHNNH-3, mi LogP-6.91, TPSA-197.45, Abs _{max} -303nm, Em _{max} -441 nm, $\Delta\lambda$ -138nm
11	Yield-75%, MW-776.30, noN-14, noHNNH-3, mi LogP-6.22, TPSA-197.45, Abs _{max} -307 nm, Em _{max} -442nm, $\Delta\lambda$ -135nm
12	Yield-73%, MW-829.17, noN-11, noHNNH-3, mi LogP-8.06, TPSA-145.64, Abs _{max} -361nm, Em _{max} -438nm, $\Delta\lambda$ -77nm

Table 5.2: The structure and properties of Type 2 peptidomimetics

Entry	Properties
1	Yield-80%, MW-818.09, noN-11, noHNNH-3, mi LogP-6.96, TPSA-151.63, Abs _{max} : 352nm, Em _{max} : 434nm, Δλ: 82nm, IC50 : 40 μM/mL
2	Yield: 73%, MW: 773.58, noN-11, noHNNH-3, mi LogP-6.88,TPSA-151.63, Abs _{max} : 372nm, Em _{max} : 434 nm, Δλ: 62 nm
3	Yield-72%, MW-773.58, noN-11,noHNNH-3, mi LogP-6.83,TPSA-151.63, Abs _{max} -375nm,Em _{max} -434nm,Δλ-59nm
4	Yield-76%, MW-757.17, noN-11, noHNNH-3, mi LogP-6.32, TPSA-151.63,Abs _{max} -370nm, Em _{max} -434 nm, Δλ-64nm
5	Yield-73%, MW-832.51, noN-10, noHNNH-3, mi LogP-7.55, TPSA-142.4, Abs _{max} -351nm,Em _{max} -409nm, Δλ-58nm
6	Yield-74%, MW-743.63,noN-10, noHNNH-3, mi LogP-7.29, TPSA-142.4 Abs _{max} -350 nm, Em _{max} -419 nm,Δλ-69nm
7	Yield-77%, MW-773.66, noN-10, noHNNH-3, mi LogP-7.24, TPSA-142.4, Abs _{max} -349 nm, Em _{max} -434 nm, Δλ-85nm
8	Yield-80%, MW-727.18,noN-10, noHNNH-3, mi LogP-6.73,TPSA-142.4 Abs _{max} -374nm, Em _{max} -434 nm,Δλ-60 nm
9	Yield-76%, MW-743.63, noN-10, noHNNH-3, mi LogP-6.44, TPSA-142.4, Abs _{max} -379nm,Em _{max} -436nm,Δλ-63nm
10	Yield-76%, MW-727.18, noN-10, noHNNH-3, mi LogP-5.93,TPSA-142.4 Abs _{max} -373nm, Em _{max} -434nm,Δλ-69nm
11	Yield-76%, MW-743.63, noN-10,noHNNH-3, mi LogP-6.49, TPSA-142.4 Abs _{max} -348nm, Em _{max} -434nm, Δλ-86nm
12	Yield-78%, MW-832.53, noN-10, noHNNH-3, mi LogP-6.75, TPSA-142.4, Abs _{max} -346 nm, Em _{max} -409 nm, Δλ-63 nm

Chapter 3 present the synthesis of a series of bifunctional pyranocoumarin peptidomimetics with inhibitory property towards human breast cancer cell lines MCF-7 and having excellent

fluorescence properties suitable for developing bioimaging agents based on these molecules. The graphical representation of the work presented in chapter 3 is given in fig.5.5

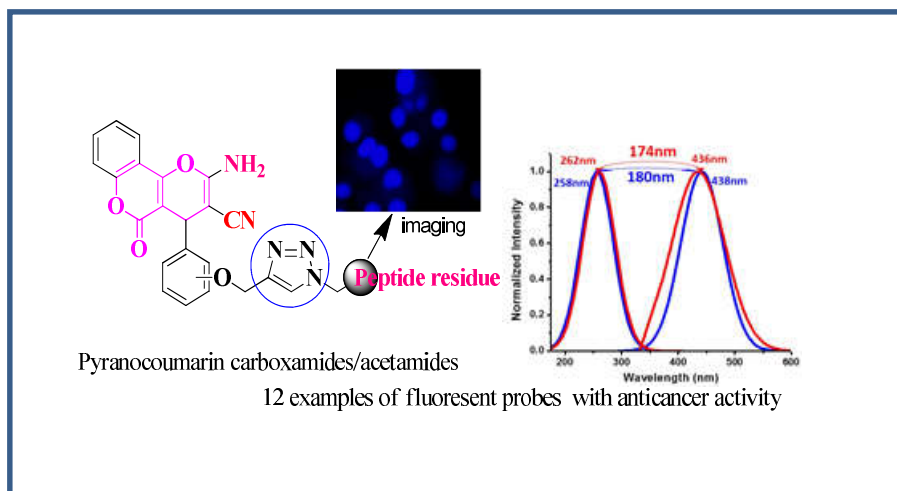
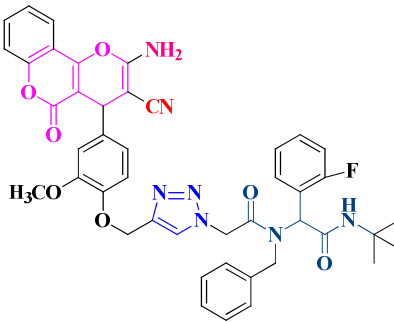
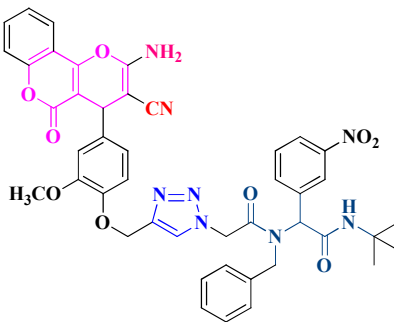
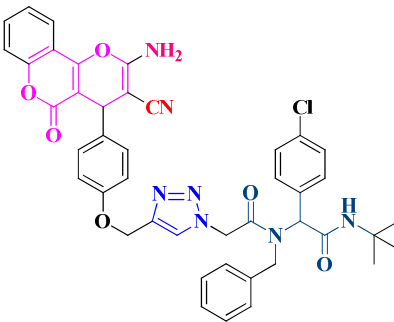


Fig.5.5: Graphical representation of the work presented in chapter 3 about the development of bioactive and fluorescent pyranocoumarin peptidomimetics.

The bandgap of selected molecules were calculated from DFT modelling using B3LYP/6-31G method basis set (Gaussian 09). And the molecules showed wide band gap above 2.2 eV. All the molecules showed large Stokes shifted fluorescence suitable for developing probes for cell imaging. The cytotoxicity evaluations were also showed excellent anticancer properties of these molecules against human breast cancer cell line MCF-7. The photophysical properties of all molecules and biological properties of selected molecules are listed in table 5.3

Table 5.3: pyranochromene-triazole-carboxamide peptidomimetics (PTC)

Entry	Structure	Properties
1		Yield-85% MW-797.30 noN-13 noHNNH-3 mi LogP-4.90 TPSA-181.17 Abs _{max} -262nm Em _{max} -436nm Δλ-174nm IC50:50μM/mL
2		Yield-84% MW-824.29 noN-13 noHNNH-3 mi LogP-5.03 TPSA-181.17 Abs _{max} -265nm Em _{max} -432nm Δλ-174nm
3		Yield-81% MW-784.26 noN-12 noHNNH-3 mi LogP-5.44 TPSA-171.94 Abs _{max} -259nm Em _{max} -430nm Δλ-171nm

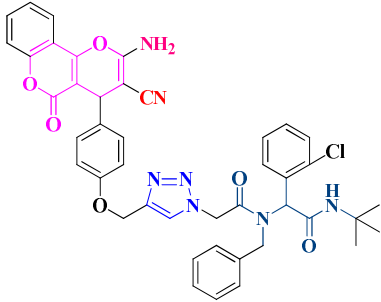
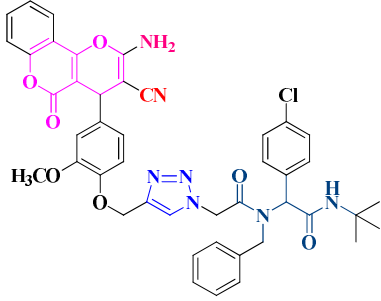
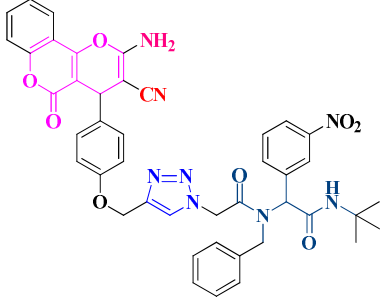
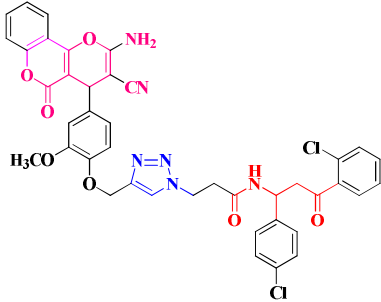
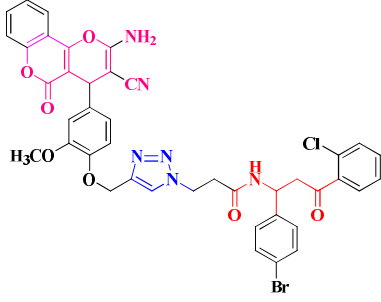
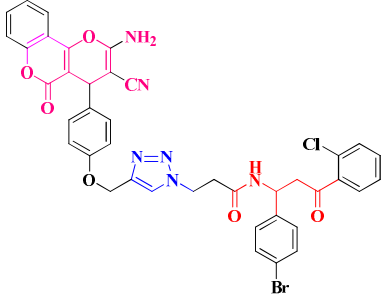
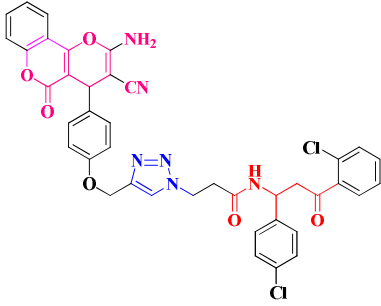
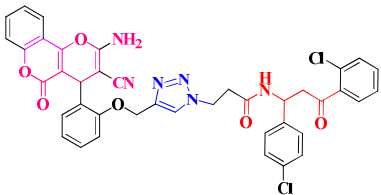
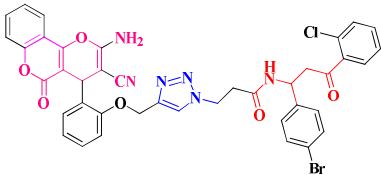
4		Yield-83% MW-784.26 noN-12 noHNNH-3 mi LogP-5.31 TPSA-171.94 Abs _{max} -264nm Em _{max} -435nm Δλ-171nm
5		Yield-83% MW-814.28 noN-12 noHNNH-3 mi LogP-5.26 TPSA-181.17 Abs _{max} -258nm Em _{max} -432nm Δλ-174nm
6		Yield-82% MW-794.81 noN-12 noHNNH-3 mi LogP-5.39 TPSA-1223.75 Abs _{max} -258nm Em _{max} -438nm Δλ-176nm

Table 5.4: pyranochromene-triazole-Ketoamide peptidomimetics (PTK)

Entry	Structure	Properties
1		<p>Yield-80% MW-791.63 noN-14 noHNNH-3 mi LogP-4.86 TPSA-177.93 Abs_{max}-265nm Em_{max}-431nm Δλ-166nm IC50:50μM/mL</p>
2		<p>Yield-82% MW-836.09 noN-17 noHNNH-3 mi LogP-4.67 TPSA-177.93 Abs_{max}-265nm Em_{max}-435nm Δλ-166nm</p>
3		<p>Yield-80% MW-806.06 noN-14 noHNNH-3 mi LogP-5.42 TPSA-168.7 Abs_{max}-266nm Em_{max}-435nm Δλ-165 nm</p>

4		Yield-83% MW-761.16 noN-13 noHNNH-3 mi LogP-5.68 TPSA-168.7 Abs _{max} -266nm Em _{max} -436nm Δλ-165nm
5		Yield-85% MW-761.61 noN-13 noHNNH-3 mi LogP-5.63 TPSA-168.7 Abs _{max} -265nm Em _{max} -430nm Δλ-165nm
6		Yield-81% MW-806.06 noN-16 noHNNH-3 mi LogP-5.04 TPSA-168.7 Abs _{max} -266nm Em _{max} -432nm Δλ-166nm

Chapter 4 presents the progress of the work from linear peptidomimetics to macrocyclic peptidomimetics based on the same MCR-Click strategy described in chapters 2 and 3. In this study, the chromene scaffold was replaced with a furan privileged scaffold and an intra-molecular MCR-Click strategy was adopted for the synthesis of the macrocycles as shown in Fig.5.6

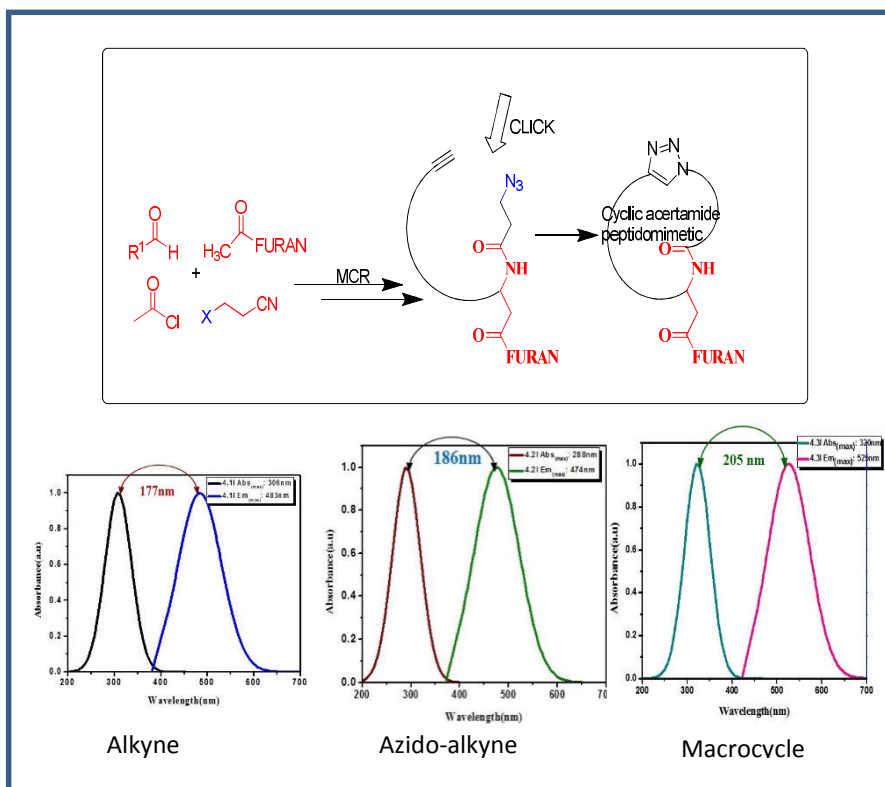


Fig.5.6: Graphical representation of the work presented chapter 4 about the synthesis of furan tagged macrocycles with varying ring size.

All the synthesized linear and Macrocyclic compounds were analyzed for their absorption and emission properties. The macrocycles showed large stokes shift values compared to their linear precursors as shown in fig.5.6. The cytotoxicity of the selected macrocyclic compound were also analyzed and the details was also discussed in chapter 4 as shown in fig.5.7. The structures of the macrocycles and the summary of their physicochemical details are presented in table 5.7.

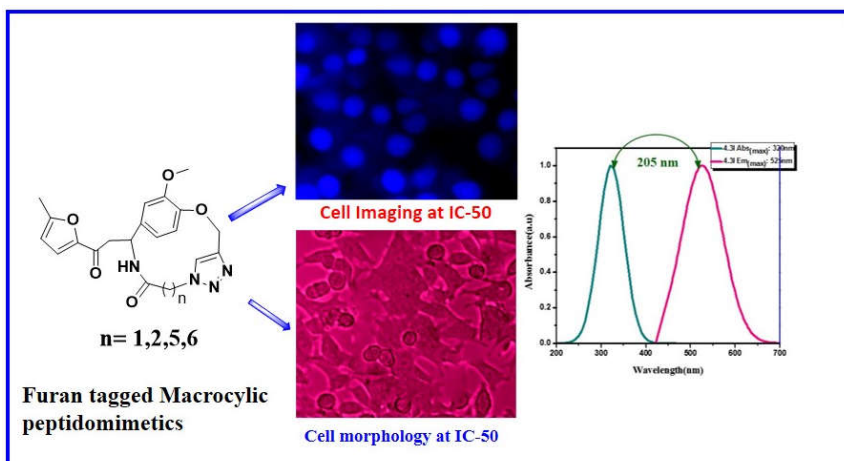
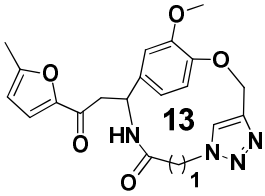
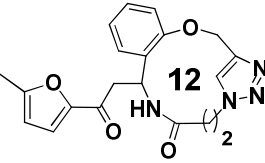
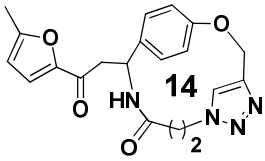
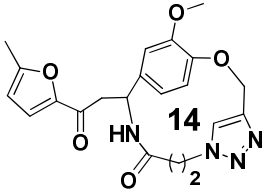
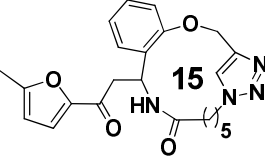


Fig. 5.7: graphical representation of work present in chapter 4 about the photophysical and cytotoxicity evaluation of furan tagged Macrocylic peptidomimetics.

Table 5.5. Summary of physicochemical properties of macrocycles discussed in chapter 4.

Entry	Structure	Properties
1		Yield-72% MW-380.40 noN-8 noHNH-1 mi LogP-0.89 TPSA-99.26 Abs _{max} : 312nm Em _{max} : 512nm Δλ: 200nm
2		Yield-74% MW-360.38 noN-8 noHNH-1 mi LogP-0.66 TPSA-99.26 Abs _{max} : 306nm Em _{max} : 510nm Δλ: 204nm

3		Yield-76% MW-343.33 noN-8 noHNH-1 mi LogP-0.25 TPSA-108.50 Abs _{max} : 311nm Em _{max} : 511nm Δλ: 200nm
4		Yield-70% MW-380.40 noN-8 noHNH-1 mi LogP-0.93 TPSA-99.26 Abs _{max} : 311nm Em _{max} : 511nm Δλ: 200nm
5		Yield-69% MW-410.43 noN-9 noHNH-1 mi LogP-0.52 TPSA-108.50 Abs _{max} : 300nm Em _{max} : 505nm Δλ: 205nm
6		Yield-72% MW-380.40 noN-8 noHNH-2 mi LogP-1.24 TPSA-110.12 Abs _{max} : 308nm Em _{max} : 512nm Δλ: 204nm
7		Yield-73% MW-422.46 noN-8 noHNH-1 mi LogP-2.17 TPSA-99.26 Abs _{max} : 312nm Em _{max} : 515nm Δλ: 203nm

8		Yield-72% MW-422.49 noN-8 noHNH-1 mi LogP-2.21 TPSA-99.26 Abs _{max} : 314nm Em _{max} : 516nm Δλ: 202nm
9		Yield-70% MW-452.51 noN-8 noHNH-1 mi LogP-1.80 TPSA-108.50 Abs _{max} : 316nm Em _{max} : 515nm Δλ: 199 nm IC50 : 20 μM/mL
10		Yield-68% MW-436.51 noN-9 noHNH-1 mi LogP-2.67 TPSA-99.26 Abs _{max} : 325nm Em _{max} : 520nm Δλ: 195nm
11		Yield-69% MW-436.51 noN-8 noHNH-1 mi LogP-2.72 TPSA-99.26 Abs _{max} : 325nm Em _{max} : 520nm Δλ: 192nm
12		Yield-68% MW-466.54 noN-9 noHNH-1 mi LogP-2.31 TPSA-108.50 Abs _{max} : 320nm Em _{max} : 525nm Δλ: 205nm

In summary, this thesis presents development of a series of privileged scaffold functionalized linear and macrocyclic peptidomimetics with 2-in-1 properties such as anticancer activities and fluorescence properties with large Stokes shifted emission suitable for developing probes for bioimaging. The step-economic synthetic strategy adopted for this work is close to green with the potential to develop cost effective therapeutic agents for curing as well as diagnosis. Available details up to this point are promising. However, further detailed investigations are essential to answer many questions related to this study. Especially,

1. The selectivity of these molecules towards malignant cell lines or toxicity of them towards normal cells.
2. The cytotoxicity of these molecules towards other cancer cell lines or targets.
3. The role of triazole in the observed cytotoxicity.
4. The reason for the observed large stokes shift especially the large Stokes shift observed in the furan tagged macrocyclic systems with respect to their possible conformations etc.

These studies will be undertaken as futuristic aspects to develop this area further ahead to achieve the goal of easy and cost effective synthesis of therapeutic agents.

Research paper published

T. Jency Mohan, D. Bahulayan. Design, synthesis and fluorescence property evaluation of blue emitting triazole-linked chromene peptidomimetics, *Mol Divers*, **2017**, 21:585–596.

Paper under evaluation:

T. Jency Mohan, D. Bahulayan. An expeditious protocol for the synthesis of multipurpose pyranocoumarin peptidomimetics with anticancer activity and intracellular imaging properties, *Chemistry Select*, Wiley-VCH.